UNIVERSITE DE LILLE I

U.F.R. DE BIOLOGIE

Année 1999 Thèse N°

Thèse

pour obtenir le grade de

DOCTEUR DE L'UNIVERSITE DE LILLE I

Mention : Sciences de la Vie et de la Santé

Présentée et soutenue publiquement

le 17 décembre 1999

par

Fabien VAN COPPENOLLE

Etude des mécanismes d'action de la prolactine dans les cellules de la prostate. Implications dans la prolifération et l'apoptose.

Jury

Mme Natalia PREVARSKAYA, Professeur à l'Université de Lille I	Président
Mr Henri COUSSE, Conseiller Scientifique, Pierre Fabre (Castres)	Rapporteur
Mr Bernard DUFY, Directeur de Recherches, C.N.R.S. (Bordeaux)	Rapporteur
Mr Jean-Claude BEAUVILLAIN, Professeur à l'Université de Lille II	Examinateur
Mr Jean-Paul DUPOUY, Professeur à l'Université de Lille I	Examinateur
Mme Halima OUADID, Maître de Conférences, Université de Lille I	Examinateur
Mr Jean-Pierre RAYNAUD, Professeur à l'Université P. et M. Curie (Paris)	Examinateur

A mes parents,

Le commencement de toutes les sciences, c'est l'étonnement de ce que les choses sont ce qu'elles sont.

Aristote. Métaphysique, I, 2.

AUX MEMBRES DU JURY.

Madame le Président :

Professeur Natalia PREVARSKAYA

Professeur à l'Université de Lille I

Messieurs les rapporteurs :

Docteur Henri COUSSE

Conseiller Scientifique, Pierre Fabre (Castres)

Docteur Bernard DUFY

Directeur de recherches, C.N.R.S. (Bordeaux)

Madame et Messieurs les examinateurs :

Professeur Jean-Claude BEAUVILLAIN

Professeur à l'Université de Lille II

Professeur Jean-Paul DUPOUY

Professeur à l'Université de Lille I

Docteur Halima OUADID-AHIDOUCH

Maître de Conférences à l'Université de Lille I

Professeur Jean-Pierre RAYNAUD

Professeur à l'Université Pierre et Marie Curie (Paris)

Je vous remercie très vivement d'avoir accepté de nous honorer de votre présence et de siéger dans ce jury. La lecture critique d'un travail n'est pas chose aisée et cela prend beaucoup de temps. J'espère néanmoins que vous avez trouvé intérêt à examiner cette thèse, fruit de trois années de travail au sein du laboratoire de Physiologie Cellulaire.

A MES TUTEURS.

Je tiens à remercier tout particulièrement le Professeur Natalia PREVARSKAYA et le Docteur Halima OUADID-AHIDOUCH pour leur grande disponibilité durant ces trois années de thèse. A votre contact, j'ai eu le privilège de bénéficier de votre enseignement et de partager votre enthousiasme. Vous m'avez donné tous les moyens, tous les conseils éclairés, nécessaires à la réalisation de ce manuscrit.

A TOUS CEUX QUI M'ONT AIDE DANS LA REALISATION DE CE TRAVAIL DE THESE.

J'ai cotoyé bon nombre de personnes. Je les remercie très sincèrement pour leur sympathie, leur aide précieuse, leur disponibilité, leur soutien et leur écoute.

SOMMAIRE

CANAUX IONIQUES ET PROLIFERATION CELLULAIRE

APOPTOSE, CALCIUM ET PATHOLOGIES PROSTATIQUES

DEUXIEME PARTIE

ETUDE DES MECANISMES D'ACTION DE LA PROLACTINE SUR LA PROLIFERATION ET L'APOPTOSE DES CELLULES DE LA PROSTATE

INTRODUCTION

ETAT DE LA QUESTION

Les hyperplasies bénignes et les cancers de la prostate sont des maladies des plus fréquentes. Le cancer de la prostate est la seconde cause de mortalité par cancer chez l'homme. Malgré les différentes approches thérapeutiques (hormonales ou non), l'efficacité des traitements reste médiocre.

Il est fermement établi que la croissance et le développement de la prostate sont placés sous contrôle hormonal (pour revue, voir Walsh, 1984; Geller, 1989; Horton, 1992). C'est la raison pour laquelle les traitements des hyperplasies bénignes et des cancers de la prostate consistent actuellement à supprimer au maximum les androgènes circulants au moyen d'anti-androgènes (flutamide), de thérapie aux analogues du Gn-RH ou d'inhibiteurs de la 5 α-reductase (Permixon, Finastéride). Bien que ces traitements soient très efficaces sur les taux d'androgènes, ils restent peu probants sur le processus prolifératif lui-même.

Les androgènes ont un rôle indiscutable dans la régulation du fonctionnement normal et pathologique de la prostate, mais **d'autres facteurs non encore clairement déterminés pourraient intervenir et notamment une hormone hypophysaire, la prolactine (PRL).** Les cellules normales et tumorales de la prostate possèdent des récepteurs de la PRL (Fekete *et al.*, 1989), dont l'activité mitogénique sur divers types de cellules est bien documentée. De plus, un certain nombre de travaux indique que la PRL favorise la croissance et la prolifération de la prostate seule (Wennbo *et al.*, 1997), ou en synergie avec la testostérone (T) (Lane *et al.*, 1997 ; Nevalainen *et al.*, 1997) et plus efficacement encore avec la dihydrotestostérone (DHT) (Prins, 1987). Par ailleurs, des données récentes stipulent que les cellules prostatiques synthétisent de la prolactine qui pourrait intervenir dans une boucle de stimulation autocrine/paracrine de la prolifération cellulaire (Nevalainen *et al.*, 1997). De

plus, la PRL joue un rôle important dans les tumeurs malignes et bénignes de la prostate (Van Poppel *et al.*, 1987).

OBJECTIFS

Les travaux faisant état des effets de la PRL sur la prostate abondent mais restent fragmentaires : aucun d'entre eux ne mentionne le mécanisme d'action propre de la PRL sur la prostate. Les renseignements sur le mode d'action de la PRL et sur son rôle dans la tumorisation sont quasi-inexistants. Cette carence a pour conséquence l'ignorance de la voie de la PRL en tant qu'hormonothérapie. Nous nous sommes donc lancés dans cette étude afin de caractériser les mécanismes d'action de la PRL sur la croissance et le développement de la prostate. Nous nous sommes attachés à développer cette étude par des approches *in vivo* (sur le rat) et *in vitro* (électrophysiologie, imagerie calcique, ...) dans le but de ne pas restreindre nos champs d'investigation et de répondre le plus largement possible aux question posées.

Dans un premier temps, nous nous sommes appliqués à caractériser l'action de la PRL *in vivo*. Ce type d'étude nous a permis de mettre en évidence l'effet trophique de la PRL sur la prostate de rat. Une analyse approfondie réalisée au moyen de techniques biochimiques a permis de démontrer que la PRL induit la surexpression de Bcl-2, une molécule anti-apoptotique. A ce niveau, la PRL peut agir selon deux voies : soit en augmentant la prolifération cellulaire, soit en diminuant l'apoptose. Afin de répondre à cette hypothèse, nous avons poursuivi nos recherches par des approches expérimentales *in vitro*. Cette deuxième série d'étude a été menée grâçe à l'emploi des techniques de patch-clamp et d'imagerie calcique principalement. Ces travaux, réalisés sur des cellules cancéreuses de prostate humaines et sur des cellules normales de prostate de rat , ont permis de démontrer que la PRL

stimule l'activité de canaux potassiques impliqués dans la prolifération cellulaire. Ce mécanisme constitue l'un des moyens par lequel la PRL stimule la prolifération cellulaire de cellules prostatiques. Nous avons par ailleurs démontré que la PRL inhibe les phénomènes apoptotiques en modulant le contenu des stocks calciques des cellules cancéreuses prostatiques humaines.

Ce manuscrit s'articule en deux parties. La première concerne les résultats obtenus *in vivo* et la seconde décrit les aspects *in vitro* de l'effet de la prolactine sur le développement de la prostate. Les travaux réalisés au cours des trois années de thèse, ont permis la réalisation des articles et manuscrits suivants :

* 2 articles publiés (Receptors and Channels ; Febs Letters) ;
* 2 articles sous presse (The Prostate) ;
* 5 articles soumis (Endocrinology ; Cancer Research ; B.B.R.C. ; Febs Letters ; J. Memb. Biol.).

Chaque article est accompagné d'une introduction situant l'intérêt et le contexte scientifique du travail effectué. Les conclusions et les perspectives soulignent les retombées possibles dans le cadre de nouvelles voies thérapeutiques et dans la meilleure compréhension des mécanismes qui interviennent dans la cancérogenèse de la prostate.

LA PROSTATE

La prostate (du grec « pro » : devant et « statis » : situé) est un organe complexe, principalement glandulaire, impair et médian, annexé à l'appareil génital mâle. Cette glande est située au-dessous de la vessie. La prostate intervient dans la reproduction et prévient les infections du tractus urogénital. Par ailleurs, la prostate est le siège de pathologies complexes dont les principales sont les hyperplasies bénignes (HBP) et les cancers. Avec l'accroissement de la longévité, les maladies prostatiques dont l'incidence et la gravité augmentent avec l'âge, constituent à l'heure actuelle l'une des causes principales de mortalité chez l'homme.

1- Anatomie de la prostate

La glande prostatique adulte pèse en moyenne 20 g et a la taille d'une noix. Cette glande est située au-dessous de la vessie, autour de la partie initiale de l'urètre, entre la symphyse pubienne et le rectum (figure 1).

Bien que la prostate normale humaine soit macroscopiquement homogène, il est possible de la diviser en plusieurs zones (figure 2) selon les travaux de Mc Neal (1981). La zone fibromusculaire antérieure est formée de tissu musculaire lisse. Elle correspond à environ 1/3 du volume de l'organe et est totalement dépourvue de structures glandulaires. La zone centrale représente environ 25 % du volume de la prostate glandulaire. Elle s'étend autour des canaux éjaculateurs qui la traversent verticalement. La zone centrale forme la base de la prostate. La zone périphérique est la plus étendue (70 %) des 3 zones glandulaires. Elle s'enroule autour de la zone centrale et se développe en-dessous d'elle pour former toute la

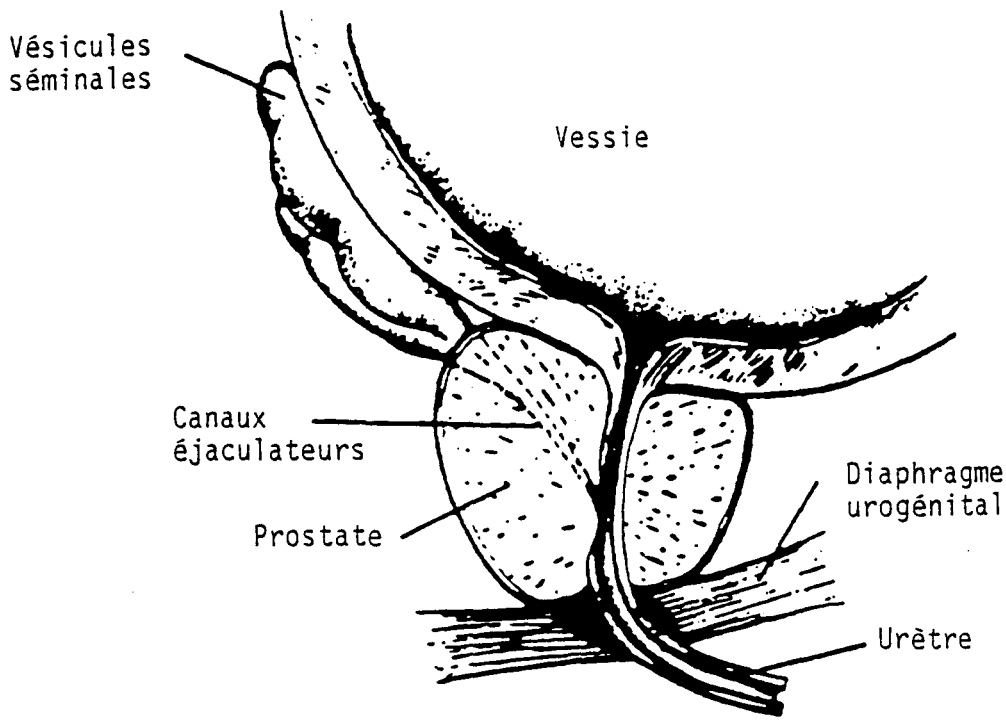

Figure 1 : Localisation schématique de la prostate chez l'homme(d'après Aronson et de Kemion, 1996).

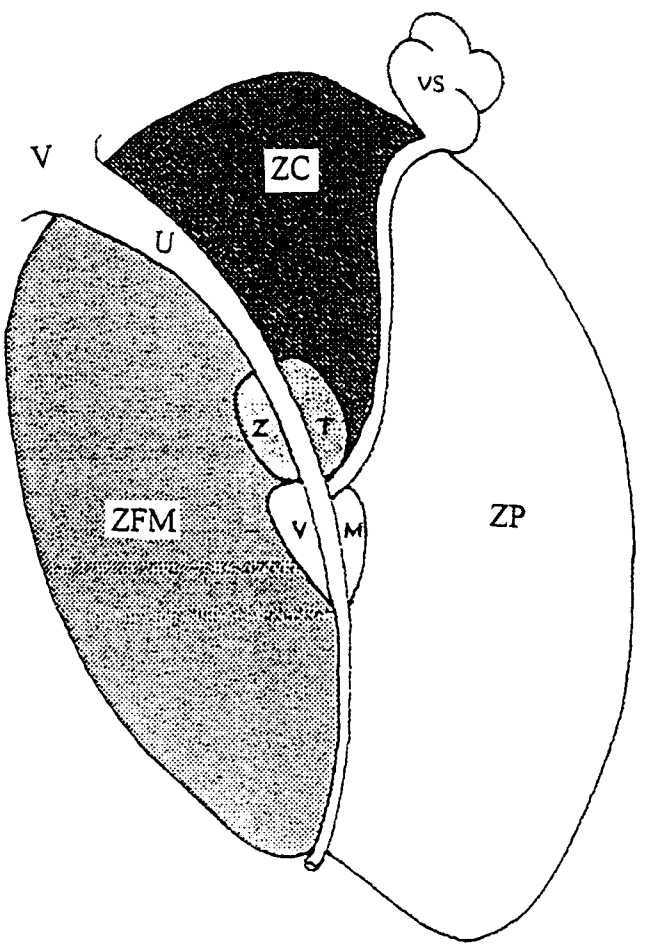

Figure 2: Représentation schématique de la prostate humaine selon McNeal (1981).

Légende :

V : Vessie	U : Urètre	VM : Veru montanum
VS : Vésicules séminales	ZP : Zone périphérique	ZT : Zone transitionnelle
ZC : Zone centrale	ZFM : Zone fibromusculaire	

face postérieure ou rectale de la prostate et la plus grande partie de ses faces latérales. C'est dans cette zone que surviennent la presque totalité des carcinomes. La région préprostatique est la zone la plus réduite de la prostate glandulaire (environ 5 %). Elle comprend les glandes périurétrales et la zone de transition située de part et d'autre du segment proximal de l'urètre. La zone de transition est séparée de la zone périphérique, qui la recouvre en partie, par un fin septum fibreux. Si la zone préprostatique est réduite, elle est en revanche d'une grande importance en pathologie, puisque selon Mc Neal, elle est le siège exclusif de l'hypertrophie bénigne de la prostate. La zone de transition peut être également le point de départ d'un carcinome (figure 2).

La prostate de rat possède une structure différente de la prostate humaine (figure 3). Elle est composée de deux lobes ventraux situés au niveau de la partie basse de la vessie. La prostate dorsolatérale entoure l'urètre et peut être disséquée, avec beaucoup de précision, en deux lobes latéraux et un lobe dorsal. Contrairement aux autres lobes, les prostates latérales de rat sont des zones homologues à la prostate humaine où les HBP se développent (Price, 1963). De ce fait les lobes latéraux constituent un bon modèle d'étude des HBP.

2- Histologie de la prostate

La prostate est constituée de plusieurs types cellulaires. Ainsi, l'on note la présence de cellules épithéliales, de cellules endothéliales, de fibroblastes et de fibres musculaires lisses (pour revue, voir Lobacarro *et al.*, 1997).

Les cellules épithéliales sont les plus étudiées. Ce type cellulaire forme le tissu glandulaire. Les fibroblastes, les cellules endothéliales et les fibres musculaires lisses composent le stroma prostatique. La prostate possède également des cellules neuroendocrines sécrétant des neuropeptides. Ces cellules n'expriment pas le récepteur aux androgènes. Cependant, un pourcentage élevé de cellules neuroendocrines est associé à un mauvais

pronostic clinique dans le cas des cancers de la prostate. En effet, les neuropeptides sécrétés agiraient, à la manière de facteurs de croissance, de façon autocrine et/ou paracrine. Aucunes données bibliographiques indiquent si la PRL est synthétisée et sécrétée par ce type de cellules.

Les relations entre les différentes catégories cellulaires sont capitales dans la physiologie de la prostate. En effet, il existe une véritable dépendance entre les cellules épithéliales et les cellules stromales. Selon des travaux récents (Lobaccaro *et al.*, 1997 ; Shabigh *et al.*, 1999). Les cellules épithéliales ne possèdent pas le récepteur aux androgènes, contrairement aux cellules endothéliales. L'hypothèse actuelle stipule que les cellules épithéliales, stimulées par les cellules endothéliales, sécrètent un facteur vasculaire (inconnu à ce jour). Cette molécule agirait sur les cellules endothéliales et entrainerait une augmentation du flux sanguin. En absence d'androgènes, les cellules endothéliales ne peuvent stimuler les cellules épithéliales. Il se produit alors une diminution du flux sanguin, une hypoxie et la mort des cellules épithéliales, endothéliales et stromales par apoptose (Shabigh *et al.*, 1999).

3- Rôle physiologique

La prostate intervient dans la reproduction et dans les processus de résistance aux infections. La prostate participe à 15 % du volume de l'éjaculât. Au moment de l'éjaculation, des fibres nerveuses sympathiques innervent les récepteurs α_1 adrénergiques des muscles lisses prostatiques et déclenchent l'expulsion du liquide prostatique dans l'urètre.

La glande prostatique produit de nombreuses substances déversées dans l'urètre. Cela inclut du zinc, de l'acide citrique, du calcium, de la phosphatase acide et du PSA (prostate specific antigen). Le fluide prostatique possède la plus haute concentration en zinc de tout

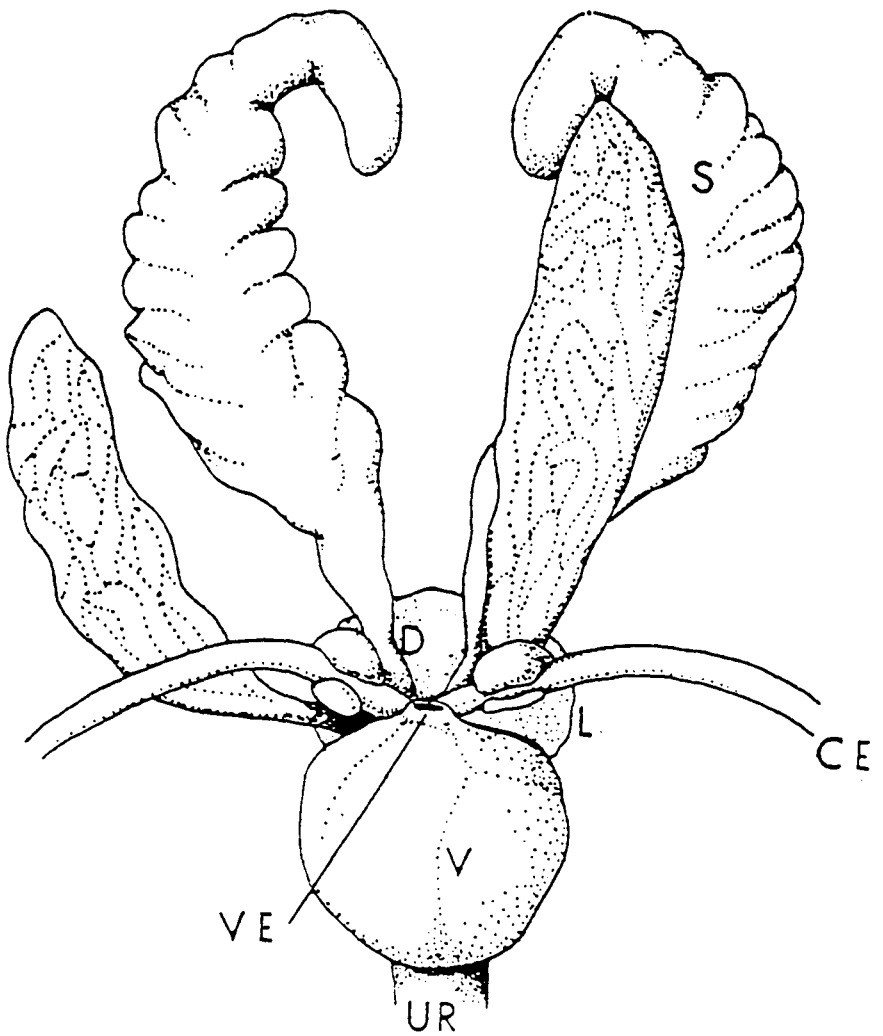

Figure 3 : Localisation schématique de la prostate de rat (d'après Price, 1963).
Légende :
UR : Urètre ;
VE : Vessie ;
V : Lobe prostatique ventral ;
L : Lobe prostatique latéral ;
D : Lobe prostatique dorsal ;
CE : Canaux éjaculateurs ;
S : Vésicules séminales.

l'organisme. Cet ion agit comme facteur antibactérien. Sa libération par la prostate joue un rôle préventif dans les infections du tractus urinaire.

4- Pathologies principales de la prostate

Les hyperplasies bénignes et les cancers de la prostate sont détaillés ci-dessous. Il existe également d'autres maladies prostatiques comme les prostatites (inflammation de la prostate d'origine bactérienne ou non) que nous ne mentionnons pas ici.

4.1- Hyperplasies bénignes

Les adénomes prostatiques (HBP) sont les tumeurs bénignes les plus répandues chez l'homme. Les symptômes apparaissent au cours de la croissance des compartiments stromal et glandulaire de la prostate. Ce phénomène physiologique débute pendant la puberté et se poursuit tout au long de la vie de l'individu. Souvent, des symptômes urinaires (difficultés de miction, obstruction de la vessie) se développent parallèlement avec la croissance de la prostate. Les HBP débutent vers la trentaine (figure 4). Après 50 ans, 50 % des hommes souffrent d'HBP (Berry *et al.*, 1984). Ce taux atteint environ 90 % vers 90 ans.

4.2- les cancers de la prostate

Les adénocarcinomes de la prostate représentent la seconde cause de mortalité par cancer chez l'homme après le cancer du poumon. Chaque année, environ 15 000 nouveaux cas sont diagnostiqués en France (Garnick, 1995). Les symptômes apparaissent quand la tumeur appuie sur la vessie ou sur l'urètre. Elle oblige le patient à se lever plusieurs fois par nuit pour uriner. Les cancers de la prostate se détectent également au cours d'analyses concernant une HBP.

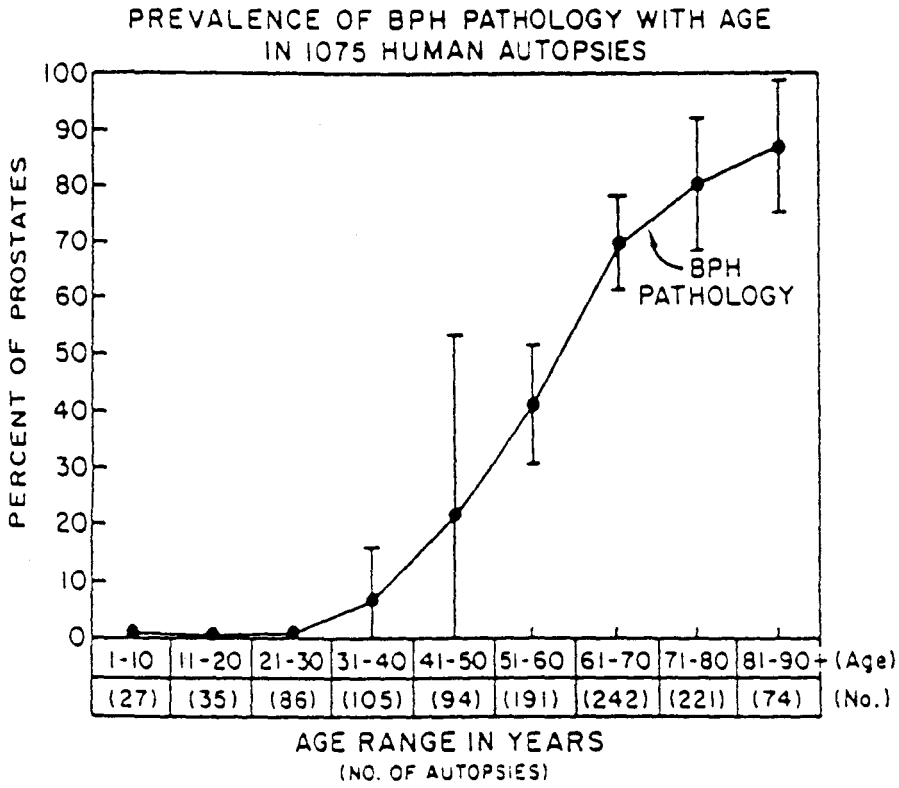

Figure 4: Evolution du pourcentage d'hyperplasies bénignes de la prostate en fonction de l'âge. Valeurs obtenues après autopsies (d'après Berry *et al.*, 1984).

5- Les traitements

5.1- Traitements hormonaux

Le développement des cancers de la prostate et des HBP survient avec l'âge et se trouve sous la dépendance des androgènes (Garnick, 1995) produits principalement par les testicules (Figure 5). La testostérone (T) est convertie en dihydrotestostérone (DHT), la forme la plus active des androgènes, par la 5α-reductase. La DHT se fixe ensuite sur des récepteurs prostatiques et induit la prolifération cellulaire. Les androgènes produits par les glandes surrénales jouent également un rôle, chez l'homme dans les pathologies prostatiques (Bruyninx *et al.*, 1998). Au contraire, chez le rat, les glandes surrénales ne sécrètent pas d'androgènes (Bruyninx *et al.*, 1998).

Les traitements actuels des HBP et des cancers de la prostate visent donc à diminuer au maximum l'action des hormones sexuelles masculines. Comme l'indique la figure 5, cela peut se réaliser à plusieurs niveaux, par inhibition de la 5α-reductase (Permixon, Finastéride) ou en empêchant la fixation de la DHT sur son récepteur (Flutamide). Certaines molécules peuvent être utilisées, lors de cas avancés de cancer, pour réduire la synthèse de T au niveau des testicules et des glandes surrénales (kétoconazole, aminoglutéthimide). Enfin, l'emploi d'analogues du GnRH (leuprolide, buséréline) induit un rétrocontrôle négatif sur la synthèse de l'hormone lutéinisante (LH) qui provoque une chute de la synthèse de T testiculaire.

Malheureusement, malgré des taux d'androgènes circulants très bas, les tumeurs régressent dans un premier temps et entrent à nouveau dans un cycle de prolifération actuellement incurable. C'est le phénomène dit « d'échappement » (Kozlowski *et al.*, 1991). Les tumeurs initialement hormono-dépendantes (c'est-à-dire nécessitant une stimulation androgénique pour proliférer) deviennent insensibles aux androgènes (hormono-

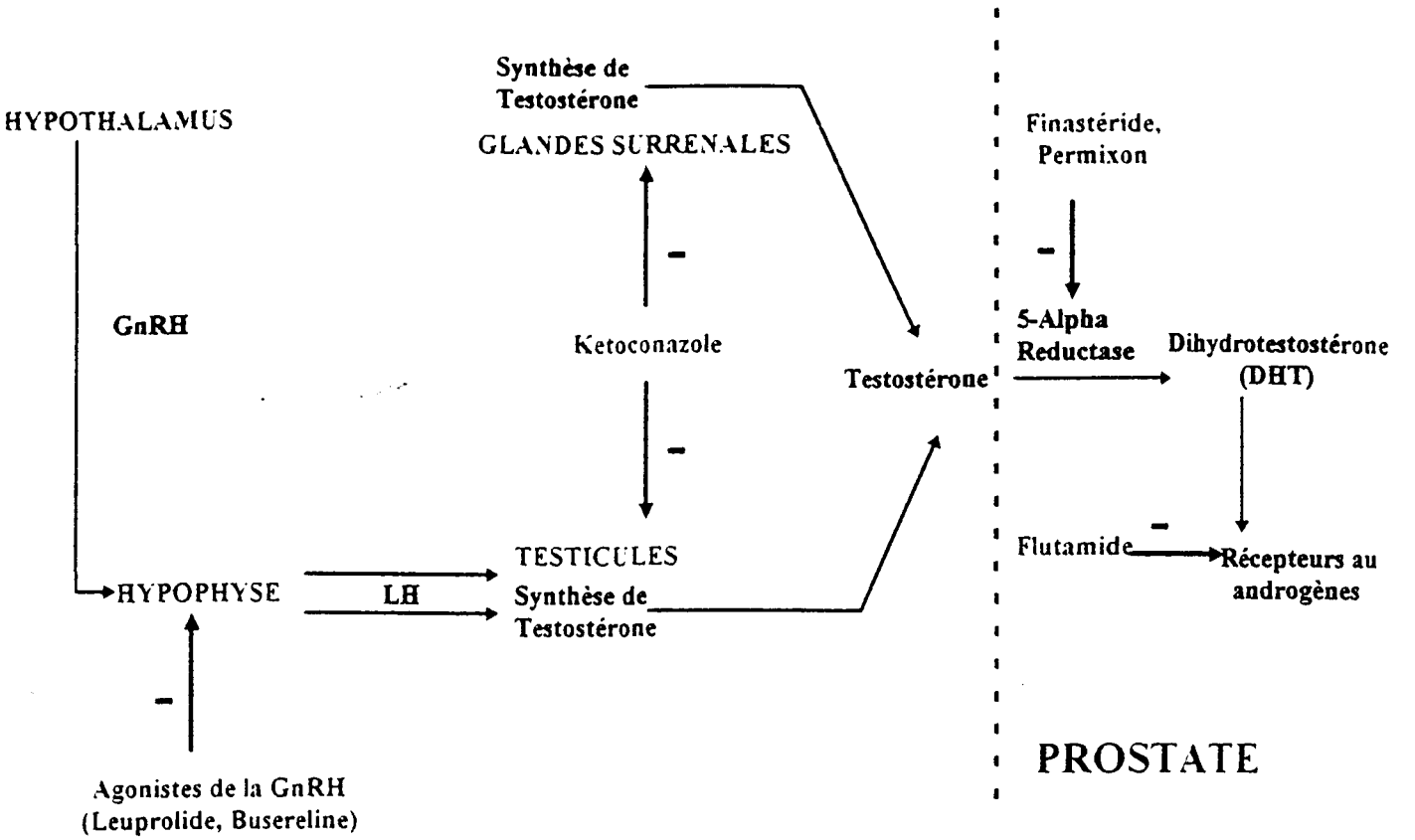

Figure 5 : Les divers traitements de l'hyperplasie et du cancer de la prostate ont pour but d'interrompre les voies biologiques qui déclenchent la synthèse de la testostérone ou qui régulent l'action de cette hormone sur les cellules de la prostate (à droite). Les agonistes de la GnRH (Leuprolide, Buséréline) bloquent la sécrétion de LH. Le Kétoconazole inhibe la sécrétion de testostérone au niveau des testicules et des glandes surrénales. Le Permixon et le Finastéride réduisent l'activité de la 5α-reductase qui converti la testostérone en DHT. Enfin, le Flutamide bloque la fixation de la DHT sur son récepteur.

indépendantes). Cela signifie que d'autres facteurs interviennent et notamment la PRL. En effet, les cellules prostatiques possèdent des récepteurs fonctionnels à la PRL (Nevalainen *et al.*, 1997). La même équipe a démontré que la prostate humaine et de rat sécrète de la PRL qui pourrait agir de manière autocrine/paracrine sur la prolifération cellulaire (Nevalainen *et al.*, 1997). Enfin, avec l'âge, le taux de T diminue chez l'homme (Davidson *et al.*, 1983), alors que la concentration plasmatique de la PRL suit une évolution inverse (Vekemans *et al.*, 1975). L'ensemble de ces phénomènes amène à penser que la PRL joue un rôle majeur dans les pathologies prostatiques et pourrait être prise en compte en hormonothérapie.

5.2- Inhibiteurs des récepteurs adrénergiques

Récemment, le tamsulosine a fait son apparition dans le cadre des traitements des HBP. Cette molécule est un antagoniste des récepteurs adrénergiques de type α_1, spécifiques de la prostate, des fibres musculaire lisses. Son emploi provoque un relâchement musculaire et donc une augmentation du diamètre urétral. Les symptômes caractéristiques des HBP sont de ce fait atténués, même si le volume de l'adénome reste inchangé.

5.3- Traitements chirurgicaux

Dans le cas des HBP, la chirurgie a pour but d'augmenter le diamètre de l'urètre. L'opération la plus courante est la résection transurétrale (RTU) pratiquée par endoscopie. Elle consiste à enlever une partie de la glande en périphérie de l'urètre à l'aide d'un bistouri électrique. D'autres techniques existent : la cryothérapie, l'emploi du laser et la nécrose des tissus par chauffage.

Les traitements chirurgicaux des cancers de la prostate conduisent à une prostatectomie radicale. En effet, l'ablation de la prostate est le dernier recours quand le

cancer est détecté à un stade avancé et lorsque les traitements pharmacologiques ne suffisent plus. Cette opération s'accompagne parfois d'une castration.

5.4- Radiothérapie et chimiothérapie

La radiothérapie est employée dans les cas de cancers localisés. Par contre, l'efficacité de la chimiothérapie dans le cadre des cancers de la prostate est très faible. En effet, ce type de cancer est caractérisé par un taux de prolifération très bas, ce qui lui confère sa résistance à cette voie thérapeutique.

6- Lignées cellulaires cancéreuses prostatiques principales utilisées en recherche

Le phénomène d'échappement constitue le problème majeur du traitement des cancers de la prostate. L'étude de l'évolution des cellules cancéreuses et de leur dépendance vis-à-vis des androgènes est possible, *in vitro*, grâce aux lignées cellulaires.

Les cellules LNCaP (Lymph Node Carcinoma Prostate) sont issues d'une biopsie à l'aiguille d'un ganglion supraclaviculaire chez un homme de 50 ans souffrant d'un cancer de la prostate (Horoszewicz *et al.*, 1983). Cette lignée est androgéno-dépendante et exprime des récepteurs aux androgènes (Brolin *et al.*, 1992), ainsi que les cytokératines 8 et 18 caractéristiques des cellules épithéliales luminales prostatiques (Lalani *et al.*, 1997).

Les cellules PC3 dérivent d'une métastase osseuse humaine. Ces cellules épithéliales n'expriment pas de récepteurs aux androgènes et sont de ce fait hormono-indépendantes (Kaighn *et al.*, 1979). Cette lignée semble être issue d'un stade plus avancé de cancer prostatique que la lignée LNCaP.

La lignée DU-145 provient d'une métastase prostatique humaine localisée dans le cerveau. Ces cellules sont hormono-indépendantes (Stone *et al.*, 1978), malgré l'expression de récepteurs aux androgènes.

LA PROLACTINE

La prolactine, classiquement décrite comme l'hormone de la lactation, présente de forte analogies structurales avec l'hormone de croissance. Actuellement, la PRL intervient dans plus de 85 actions biologiques.

L'activité lactogénique d'extraits d'hypophyse antérieure a été mise en évidence en 1928 (Stricker *et al*, 1928). En 1933, Riddle a démontré que des extraits purifiés d'hypophyse antérieure stimulent la croissance du jabot de pigeon, équivalent de la glande mammaire des mammifères. Ce test servit de dosage biologique avant l'utilisation des dosages radio-immunologiques. Le terme « prolactine » fut proposé par Riddle pour définir l'hormone responsable de ce phénomène. Il faudra attendre jusqu'en 1970 pour que Friesen réussisse à isoler la PRL de l'hormone de croissance (GH : growth hormon). Le premier dosage radio-immunologique de la PRL fut mis au point en 1971.

1- Structure de la PRL

La PRL est constituée par une chaîne de 199 acides aminés. Son poids moléculaire est de 23 kD (figure 6). La PRL présente respectivement 61 % et 77 % d'homologie avec la GH et l'hormone placentaire lactogène (Brue *et al.*, 1989). Dans le sang, la PRL est représentée essentiellement sous forme monomérique (« little » prolactine). Les autres formes, étant de polymères, sont nommées « big » (45 kD) et « big-big » (130 kD) prolactine. Ces deux formes oligomériques ne sont pas prises en compte dans les dosages radio-immunologiques tandis que leurs éventuelles activités biologiques ne sont pas connues. La « big-big » PRL possède moins de 15 % de l'affinité pour les récepteurs de la PRL elle-même (forme « little »). La

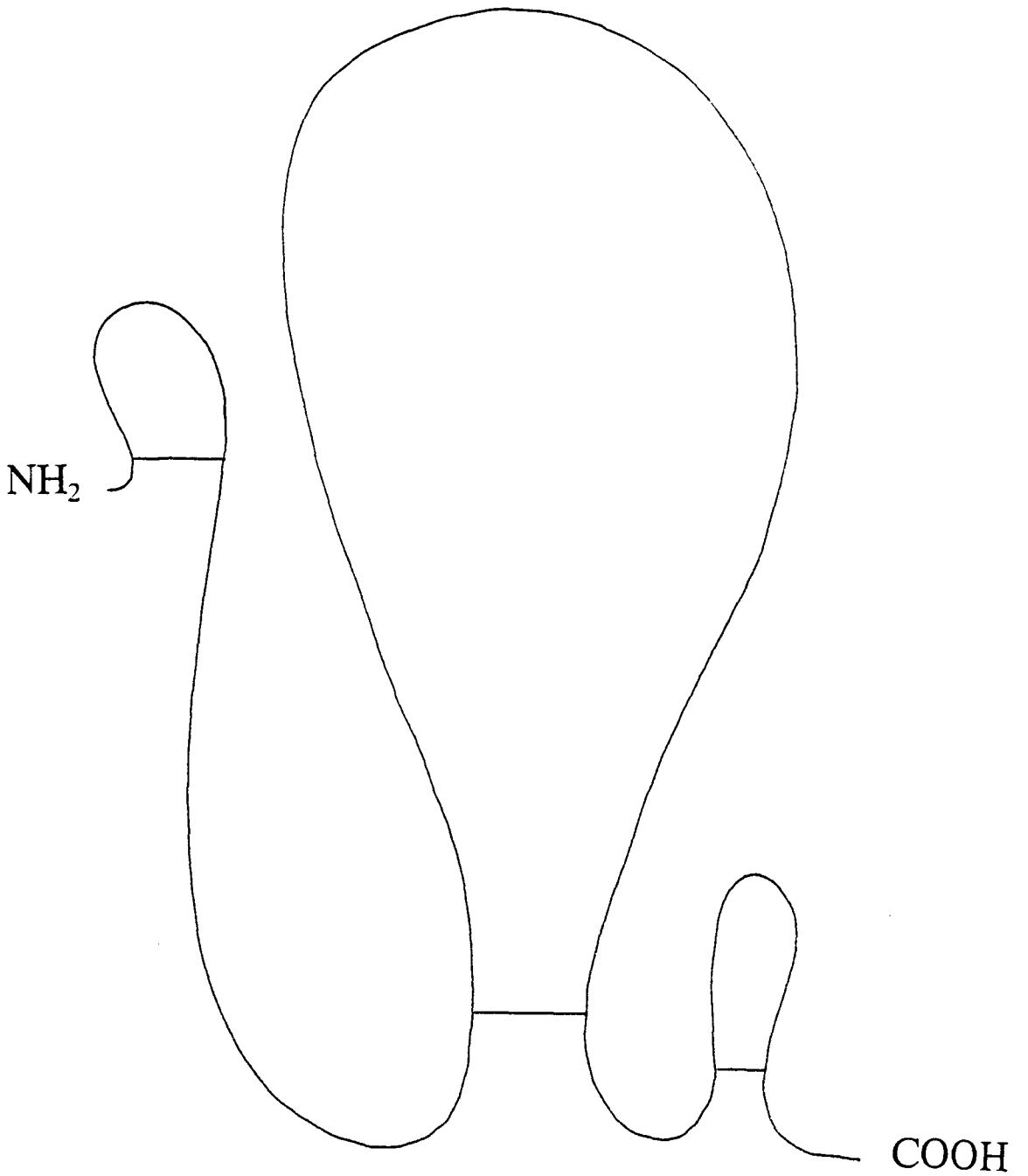

Figure 6 : Représentation schématique de la prolactine de 23 kD de poids moléculaire (« little prolactin »).

« little » PRL constitue 75 à 90 % environ de l'hormone circulante contre 8 à 20 % pour la « big » et 5 % pour la « big-big » PRL. D'autres formes de PRL résultent de modifications post-traductionnelles (Sinha *et al.*, 1995) de la chaîne protéique initialement synthétisée et non à une multiplicité génétique. Le gène de la PRL est situé chez l'homme sur le chromosome 6. Il possède 5 exons et 4 introns. Ainsi, il existe des formes clivées, glycosylées, phosphorylées, désamidées ou sulfatées. La plupart de ces formes sont moins actives que la « little » PRL.

2- Régulation de la synthèse et de la sécrétion de PRL

La PRL est principalement synthétisée par les cellules éosinophiles de l'hypophyse antérieure appelées cellules lactotropes. La PRL est également sécrétée par d'autres tissus tels que les cellules déciduales du placenta (Handwerger *et al.*, 1990), par l'endomètre (Masler *et al.*, 1979), par le cerveau (Schachter *et al.*, 1984 ; Emanuele *et al.* 1992 ; Wilson *et al.*, 1992 ; Valatx *et al.*, 1992), par certaines cellules du système immunitaire (Montgomery *et al.*, 1992 ; Pellegrini *et al.*, 1992) et par la prostate (Nevalainen *et al.*, 1997).

La biosynthèse et la sécrétion de la PRL hypophysaire sont soumises à l'influence de très nombreux facteurs, soit d'origine hypothalamique, soit d'origine périphérique (gonade, thyroïde).

La dopamine est l'inhibiteur hypothalamique physiologique de la PRL (Yazigi *et al.*, 1997) (figure 7). Cela explique que les médicaments comme les neuroleptiques (sulpiride, halopéridol) (Debeljuk *et al.*, 1975 ; Boucherle *et al.*, 1981) qui bloquent les récepteurs dopaminergiques peuvent entraîner une hyperprolactinémie. La bromocriptine, un agoniste dopaminergique est, au contraire, un traitement de choix pour lutter contre l'hyperprolactinémie (Lane *et al.*, 1997).

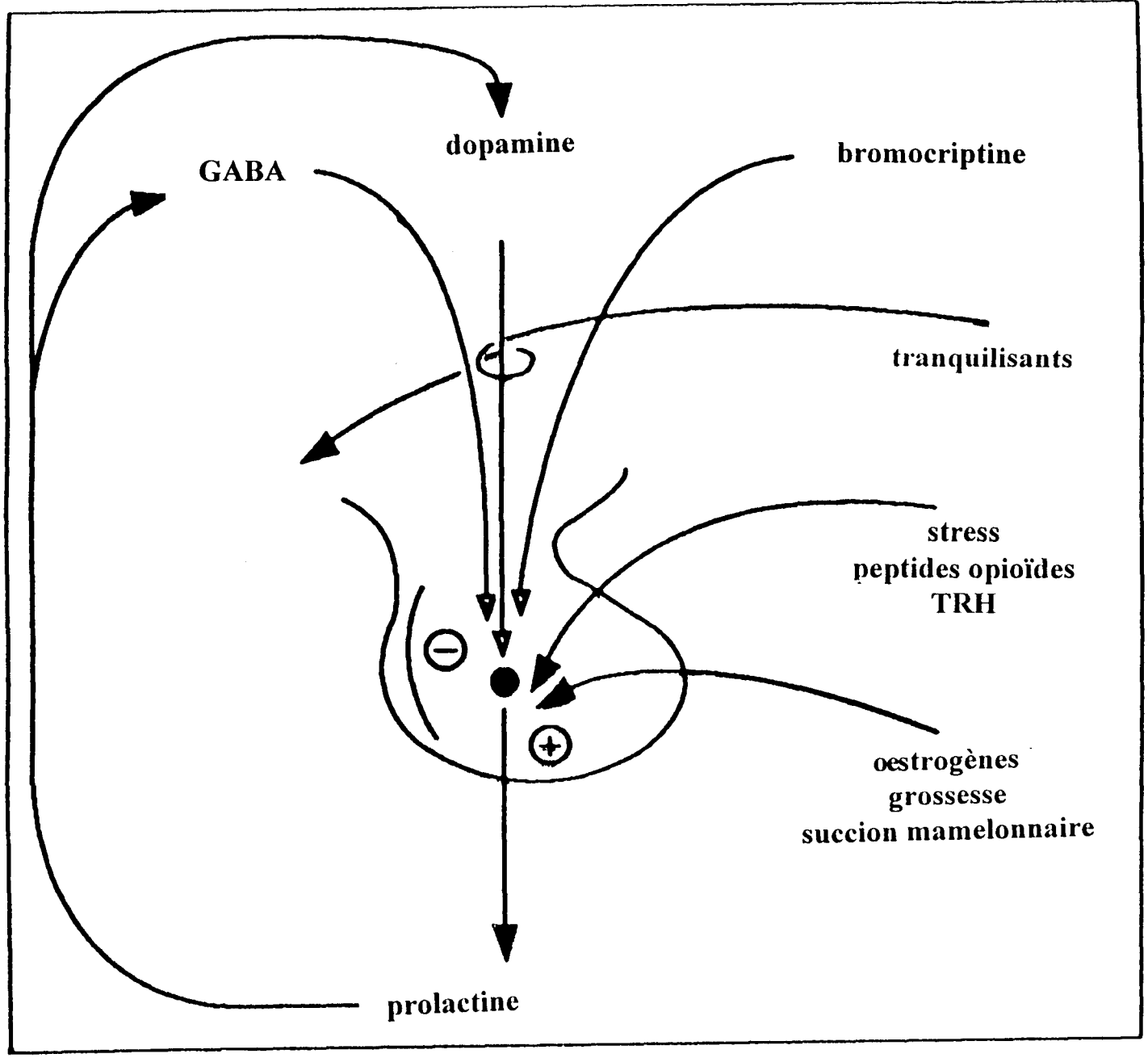

Figure 7: Régulation de la sécrétion de prolactine hypophysaire.

Le GABA (acide gamma-aminobutyrique), un autre facteur hypothalamique, a une action inhibitrice et indépendante de la dopamine sur la sécrétion de PRL (Schally *et al.*, 1977).

Le GAP (GnRH-associated), un peptide de 56 acides aminés libéré conjointement avec la GnRH agit en tant qu'inhibiteur de la production de PRL (Clarke *et al.*, 1987).

Parmi les facteurs stimulateurs de la synthèse et de la libération de PRL, aucun ne semble être dominant. Ainsi, la TRH (tyrolibérine), outre son action stimulatrice sur la TSH hypophysaire, augmente la sécrétion de PRL. L'effet de la TRH est plus important chez la femme que chez l'homme, probablement du fait de l'effet de potentialisation des œstrogènes chez la femme (Rackoff *et al.*, 1973).

Le VIP (vaso-intestinal peptide), un autre facteur hypothalamique stimule la sécrétion de PRL (Conti *et al.*, 1987 ; Kato *et al.*, 1978).

L'angiotensine II (Schramme *et al.*, 1983), l'ocytocine (Hyde *et al.*, 1989) exercent le même type d'action, mais leur importance physiologique est peu connue.

Les taux plasmatiques de PRL sont également contrôlés par l'œstradiol. Cette hormone stimule la sécrétion (Neill *et al.*, 1971 ; Shin *et al.*, 1979), la synthèse (Kaplan *et al.*, 1976 ; Maurer, 1982), le stockage (kiino *et al.*, 1981) de PRL et accroît la taille et le nombre de cellules lactotropes (Maurer *et al.*, 1977 ; Boockfor *et al.*, 1986). Il est bon de noter que l'œstradiol induit un inflammation de la prostate latérale chez le rat (Paubert-Braquet, 1996) via la voie prolactinique (Lane *et al.*, 1997).

A l'inverse de la plupart des hormones de l'antéhypophyse, la PRL a de multiples organes cibles (glande mammaire, foie, surrénales, gonades, prostate). La PRL n'est pas, de ce fait, sous le joug d'une hormone unique assurant le rétrocontrôle de sa sécrétion. C'est la PRL qui assure cet autocontrôle négatif (Kledzik *et al.*, 1976).

3- Variations des taux de PRL plasmatiques

La concentration plasmatique de PRL oscille entre 5 et 10 ng/ml chez l'homme et 5 à 15 ng/ml chez la femme. La libération de PRL par l'hypophyse se déroule de façon pulsatile selon un rythme de 90 minutes environ. Au cours de la journée, on note un cycle nycthéméral avec un pic nocturne de PRL. *In utero*, le taux de PRL croît au cours de la période foetale jusque 200 ng/ml environ, puis chute dans la semaine qui suit la naissance (Aubert, 1982) et reste stable jusqu'à la puberté. Chez les adolescents, une augmentation de la sécrétion de PRL est constatée chez la jeune fille, parallèle au développement mammaire et contemporaine à la sécrétion d'oestradiol (Borson-Chazot, 1988). Il existe des fluctuations du taux de PRL notamment chez la femme, à partir de la puberté, lors du cycle menstruel, avec des taux bas au cours de la phase folliculaire et une valeur maximale au moment du pic ovulatoire (Marshall *et al.*, 1988). Le taux de PRL croît au cours de la grossesse et pendant les périodes d'allaitement. D'autres facteurs augmentent la sécrétion de PRL comme le stress (Jahn *et al.*, 1986), le sommeil (Parker *et al.*, 1974) et l'alimentation (Carlson *et al.*, 1983). Chez l'homme, le taux de PRL augmente avec l'âge (Vekemans *et al.*, 1975), contrairement à celui des androgènes (Davidson *et al.*, 1983).

4- Distribution et régulation des récepteurs de la PRL

Les récepteurs de la PRL (R-PRL) sont présents dans un grand nombre de tissus comme la glande mammaire, le rein, l'ovaire et le foie. Les organes lymphoïdes comme le thymus , la rate, les ganglions et la moelle osseuse en sont aussi pourvus. Récemment,

Nevalainen et ses collaborateurs ont mis en évidence la présence de R-PRL dans la prostate humaine et dans la prostate de rat (1997).

4.1- Structure du récepteur de la PRL

La grande homologie existant entre la PRL et la GH appartenant toutes deux à la famille des cytokines, se retrouve sur leurs récepteurs respectifs. Actuellement, 3 types de R-PRL ont été caractérisés chez le rat : une forme courte (291 acides aminés) (Boutin *et al.*, 1988), une forme longue (519 acides aminés) (Shirota *et al.*1990) et une forme intermédiaire (393 acides aminés) (Ali *et al.*, 1991). La forme intermédiaire a été mise en évidence uniquement dans la lignée Nb2 issue d'un lymphome de rat. Ces récepteurs se distinguent par la longueur de leur région cytoplasmique. Les domaines extracellulaires et transmembranaires sont identiques (figure 8).

L'homodimérisation de la forme longue et intermédiaire du R-PRL se produit lors de la fixation de la PRL et entraîne l'activation d'une tyrosine kinase JAK2 (Rui *et al.*, 1994). JAK2 phosphoryle probablement le récepteur. Il s'ensuit la phosphorylation du facteur de transcription Stat 5 (Goupille *et al.*, 1994). Cette molécule forme ensuite un homodimère qui se fixe sur des régions spécifiques de l'ADN et régule la transcription des gènes (figure 9). La région extracellulaire du R-PRL possède une séquence conservée Trp-Ser-X-Trp-Ser qui pourrait agir dans les interactions récepteur/récepteur ou hormone/récepteur (DeVos *et al.*, 1992). La région box1 contient un domaine permettant l'interaction entre le R-PRL et JAK2 (O'Neal *et al.*, 1993 ; Kelly *et al.*, 1993). Box2 est indispensable pour l'activation de Stat 5 (Goupille *et al.*, 1997).

La phosphorylation de la forme courte du R-PRL ne peut physiquement pas se produire (Lebrun *et al.*, 1995). Néanmoins, des études sur des cellules NIH 3T3 indiquent que

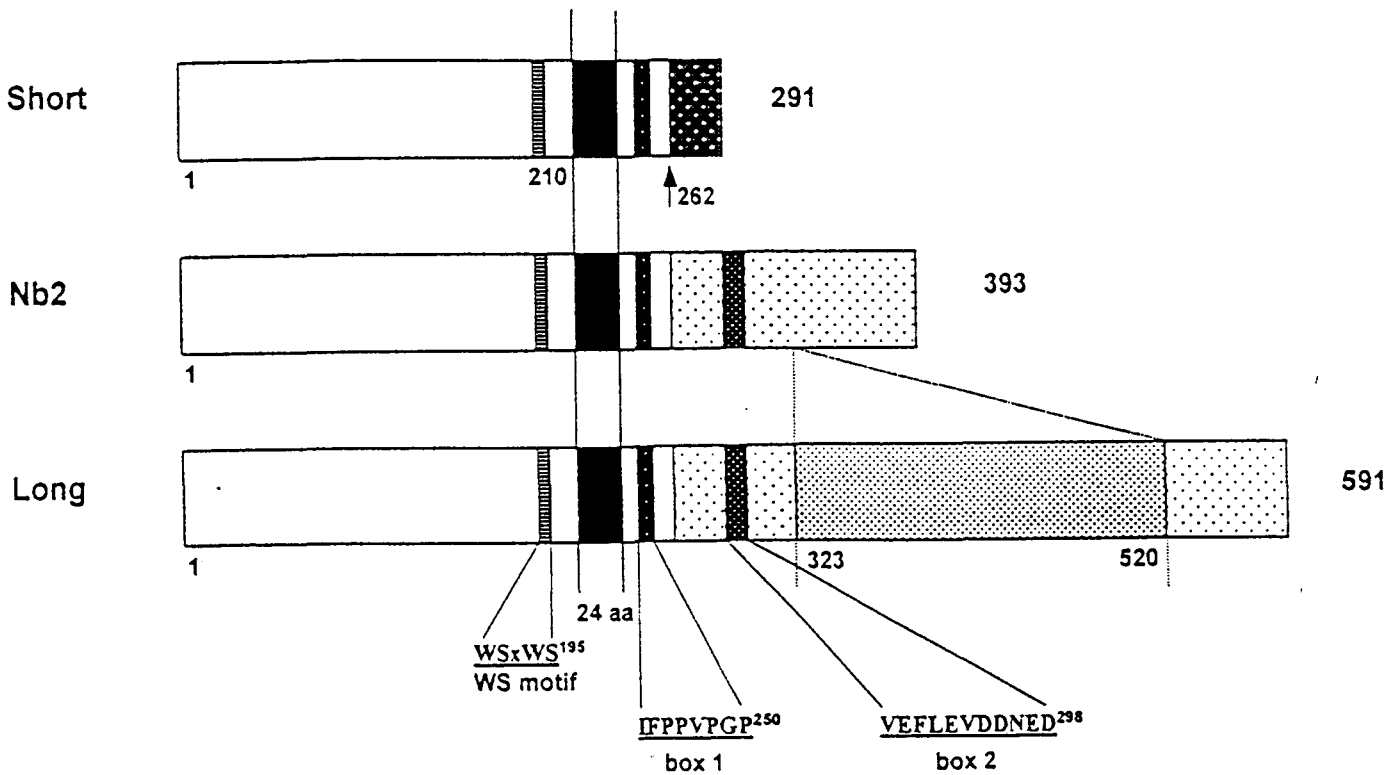

Figure 8: Structures schématiques des différentes formes de récepteurs de la prolactine découverts chez le rat. On distingue la forme courte (« short »), la forme intermédiaire (« Nb2 » d'après la lignée de lymphome à partir de laquelle ce récepteur a été caractérisé) et la forme longue (« long »). Le domaine extracellulaire se situe à droite. Le segment transmembranaire est composé de 24 acides aminés (en noir). Le domaine intracellulaire se place à la droite de ce dernier. Les régions homologues sont hachurées de la même manière. Le repère 262 de la forme courte représente la zone où se produit un épissage alternatif menant à la formation d'un domaine intracellulaire spécifique. La région en pointillé (de 323 à 520 acides aminés) est la zone de la forme longue absente sur la forme intermédiaire. Les séquences nommées « WS », « box 1 » et « box 2 » sont caractéristiques des récepteurs de la famille des cytokines (d'après Kuo *et al.*, 1998).

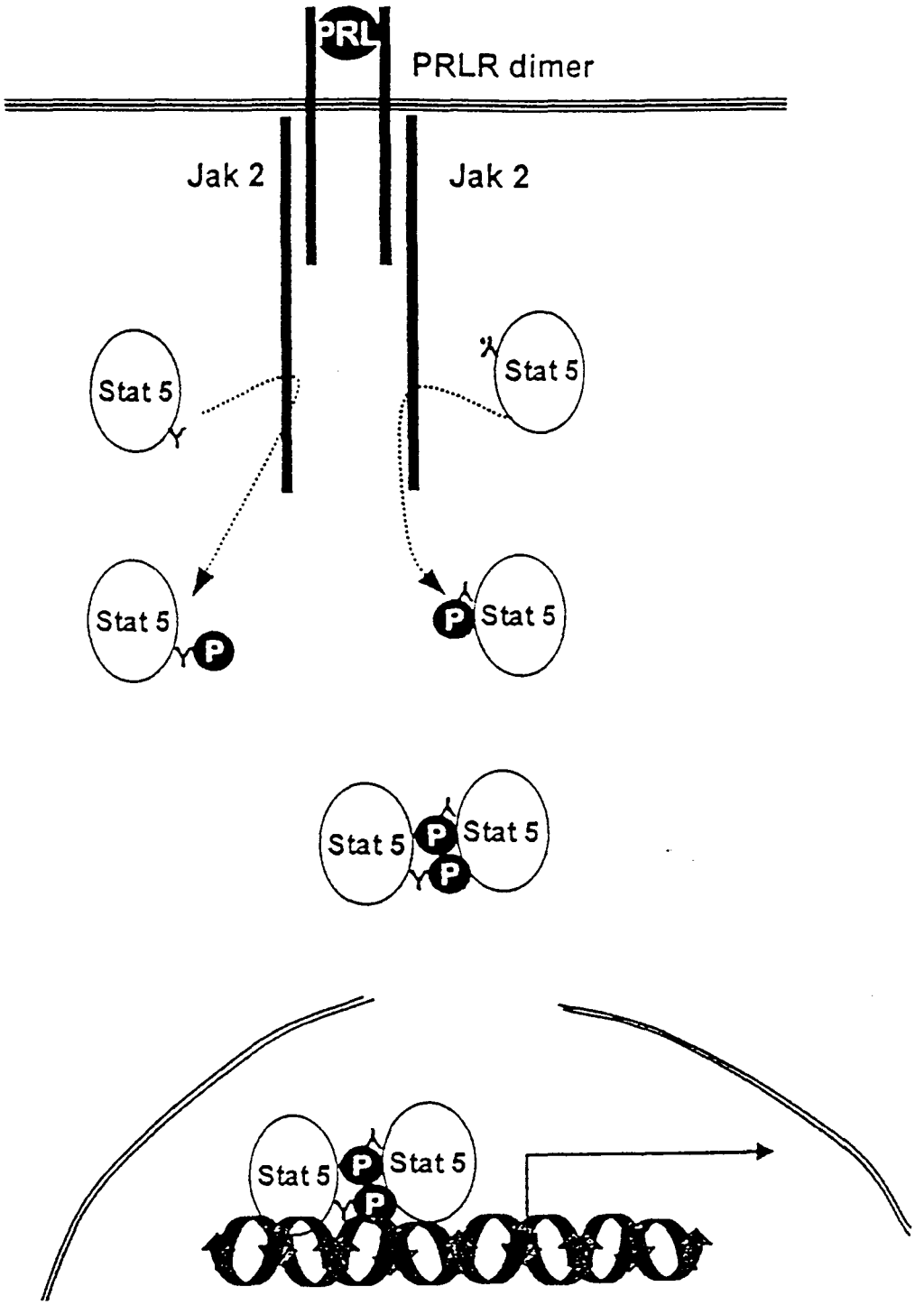

Figure 9: La dimérisation des récepteurs entraîne la phosphorylation de JAK 2. La phosphorylation des récepteurs, probablement par JAK 2 provoque la phosphorylation, puis la dimérisation de Stat 5. Ce dimère, véhiculé jusqu'au noyau se lie à des régions spécifiques de l'ADN et régule la transcription de gènes (d'après Kuo *et al.*, 1998).

la forme courte du R-PRL est capable d'induire la division cellulaire (Das et Vonderhaar, 1995).

5- Actions de la PRL

La PRL possède un large spectre d'action. En effet, plus de 85 effets biologiques, pouvant être classés en sept catégories, ont été décrits : les actions associées à l'équilibre hydro-électrolytique ; les effets sur la croissance et le développement ; une action sur les fonctions de reproduction ; des effets métaboliques ; les effets sur le comportement ; un rôle immuno-modulateur et une action sur la peau. Dans l'espèce humaine, l'action la mieux connue est celle exercée sur le développement de la glande mammaire et la lactogénèse.

Outre son action sur la glande mammaire, la PRL intervient dans la physiologie et dans les pathologies de la prostate. Les cellules prostatiques humaines et de rat expriment des récepteurs fonctionnels à la PRL (Nevalainen *et al.*, 1997). La PRL provoque la différenciation et la prolifération des cellules sur des cultures organotypiques de prostate (Nevalainen *et al.*, 1996). La surexpression du gène de la PRL chez des souris transgéniques provoque une hyperplasie prostatique (Wennbo *et al.*, 1997). En outre, la prostate elle-même sécrète de la PRL qui pourrait agir de manière autocrine/paracrine (Nevalainen *et al.*, 1997). Malheureusement, les mécanismes d'action de la PRL sont peu connus. Des travaux stipulent que la PRL induit la croissance et la prolifération prostatique en synergie avec les androgènes (Prins, 1987), ou augmente la concentration intracellulaire en testostérone dans les cellules de la prostate (Farnsworth, 1988). A l'inverse, d'autres études ont caractérisé une action indépendante de la PRL sur la prostate vis-à-vis des androgènes (Reiter *et al.*, 1995 ; Smith *et al.*, 1985 ; Price, 1963).

6- Substances antiprolactiniques

La sécrétion de PRL est principalement régulée négativement par la PRL. Ainsi, les agonistes dopaminergiques jouent un rôle prépondérant en terme de substances antiprolactiniques. La bromocriptine, un agoniste des récepteurs de type D2, est utilisée dans le cadre des problèmes de stérilité chez l'homme et la femme, des aménorrhées et du traitement de fond des prolactinomes (tumeur hypophysaire). Des études cliniques ont démontré l'effet bénéfique de traitements à la bromocriptine de patients souffrant d'un cancer (Rana *et al.*, 1995 ; Jeromin, 1982) ou d'une hyperplasie bénigne de la prostate (Van Poppel *et al.*, 1987 ; Matos-Ferreira *et al.*, 1987).

CANAUX IONIQUES ET PROLIFERATION CELLULAIRE

La membrane plasmique joue un rôle essentiel dans la physiologie cellulaire. En effet, elle constitue la seule zone de contact et d'échange de la cellule avec le milieu extérieur. La membrane plasmique permet le maintien de gradients électrochimiques entre les milieux intracellulaires et extracellulaires, principalement portés par les ions Ca^{2+}, K^+, Na^+, Cl^- et H^+. Les différences de potentiel ainsi formées interviennent dans nombre de processus physiologiques et physiopathologiques. C'est au niveau de la membrane plasmique que s'établissent les mécanismes biochimiques de transduction des signaux entraînant une réponse physiologique de la cellule. Les mécanismes de transduction sont pour la plupart provoqués par des phénomènes électriques engendrés par le mouvement d'ions véhiculés par des protéines transmembranaires dont les principales sont les canaux ioniques.

Les canaux ioniques sont impliqués dans les mécanismes précoces de transduction des signaux entraînant la cellule vers des processus physiologiques (mitose, exocytose, contraction, apoptose, « multi drug resistance », ...) ou pathologiques (tumorisation, hypertrophie, ...). L'étude des canaux ioniques, et par extension, des mouvements ioniques revêt donc une importance capitale dans la compréhension de la physiologie et de la physiopathologie cellulaire.

1- Les grandes familles de canaux potassiques

Il existe une grande variété de canaux potassiques caractérisés par des propriétés et des structures moléculaires différentes. Malgré cette diversité, il est possible de proposer une classification basée sur la modulation de ces canaux par le voltage, par des ions et par d'autres facteurs.

1.1 Canaux potassiques activés par le voltage

Nous avons adopté la classification de Chandy, (1991). Cette nomenclature se base sur les différents gènes qui codent pour les protéines homologues des canaux potassiques identifiés d'abord chez la drosophile et retrouvés ensuite chez les mammifères. Quatre familles ont été caractérisées : shaker, shaw, shab et shal :

- la famille « shaker » qui correspond à la famille Kv1. Elle comprend 8 types de canaux, de Kv1.1 à Kv1.8. La majorité de ces canaux s'inactive plus ou moins rapidement.
- la famille « shaw » qui comprend 4 types de canaux (de Kv3.1à Kv3.4). Ces canaux ne s'inactivent pas et sont classiquement dénommés de « type retardé ».
- la famille « shab » qui comprend Kv2.1et Kv2.2.
- la famille « shal » qui comprend (Kv4.1 et Kv4.2).

Les deux dernières familles (shab et shal) ont des propriétés intermédiaires des canaux de type shaker et shaw.

Ces différents types et sous-types de canaux potassiques activés par le voltage présentent des sensibilités différentes aux inhibiteurs classiques des canaux potassiques comme la 4-aminopyridine (4-AP) et le tetraéthylammonium (TEA). La purification des fractions des neurotoxines, a contribué à la classification de ces canaux. En effet, certaines neurotoxines inhibent, à des doses de l'ordre de la nanomole, spécifiquement un type de canal. Ainsi, la

margatoxine (MgTX) inhibe spécifiquement le canal potassique de type Kv1.3, alors que la dentrotoxine (DTX) inhibe le Kv1.1 et Kv1.2.

1.2 Canaux potassiques modulés par les ions et l'ATP

L'activité de certains types de canaux est modulée par des ions intracellulaires. Parmi ces canaux, les plus répandus sont les canaux activés par le calcium (K_{Ca}), les canaux activés par le sodium (K_{Na}) et les canaux inhibés par l'ATP (K_{ATP}).

1.2.1 Canaux potassiques activés par le calcium

Il existe différents sous-types de canaux potassiques sensibles au potentiel et activés par le calcium (K_{Ca}^{2+}). Ils sont classés en trois grandes catégories selon leur conductance unitaire et leur pharmacologie :

- les canaux potassiques de grande conductance « BK » ou « maxi K » (100-300 pS) : leur ouverture se produit après fixation de plusieurs molécules de calcium .

Ces canaux sont sensibles au TEA et à la charybdotoxine (ChTX) et sont spécifiquement inhibés par l'ibériotoxine (IBTX) ;

- les canaux potassiques de conductance intermédiaire (40-100 pS). Ces canaux sont inhibés par la charybdotoxine et par le Cetiedil ;
- les canaux potassiques de faible conductance « SK » (10-35 pS) sont peu ou pas sensibles au potentiel. Leur activité est réduite par la charybdotoxine et par l'apamine.

En plus de ces 3 types de canaux potassiques, s'ajoute un autre type de canal de grande conductance, activé par le calcium, et appartenant à la famille des « Kv » : c'est le canal « Slowpoke » (Slo).

Le calcium peut également inhiber l'activité de certains canaux potassiques. C'est le cas du canal potassique des cellules de la prostate humaine LNCaP (Skryma et al., 1999). Ce canal n'a pas encore été classé.

1.2.2 Canaux potassiques activés par le sodium

Ces canaux potassiques sont activés par le sodium intracellulaire. Ils sont sensibles à la 4-AP et insensibles au TEA. Les canaux K_{Na+} sont inhibés par le magnésium et le barium intracellulaires.

1.2.3 Canaux potassiques inhibés par l'ATP

Les canaux K_{ATP} sont inhibés par une augmentation de l'ATP intracellulaire. L'inhibiteur classique de ces canaux est la glibenclamide, de la famille des sulphonylurées. La cromakaline et le pinacidil ouvrent ces canaux.

1.3 Canaux potassiques modulés par le volume

Ces canaux, dits mécanosensibles, répondent aux modifications de pression et d'étirement de la membrane plasmique. Il existe des canaux activés (« strecth-activated ») ou inactivés (« stretch-inactivated ») par l'étirement. Leur sensibilité envers la pression se ferait soit via la membrane plasmique (par modification de la conformation du canal inséré dans la bicouche de phospholipides), soit par des éléments du cytosquelette (transmission de la tension par l'intermédiaire d'une structure élastique).

2- Implication des canaux potassiques dans la prolifération cellulaire

De nombreuses études ont mis à jour la fonction déterminante de l'activité des canaux potassiques dans la prolifération cellulaire (Deutsch, 1990 ; Dubois et Rouzaire-Dubois, 1993 ; Wonderlin et Strobl, 1996). Ces travaux s'appuient sur le fait que d'une part, les inhibiteurs des canaux potassiques inhibent la prolifération cellulaire et que d'autre part, les agents mitogènes stimulent l'expression et/ou l'activité des canaux potassiques. Récemment, plusieurs études suggèrent un rôle clé des canaux potassiques dans le cycle cellulaire, plus particulièrement dans la progression dans la phase G1. Cependant, le lien entre l'activité des canaux potassiques et la synthèse de l'ADN n'est pas encore clairement établi.

Plusieurs hypothèses ont été émises pour pouvoir expliquer le rôle des canaux potassiques dans le contrôle de la prolifération.

2.1- Modulation de l'influx de calcium par les canaux K^+

L'équipe de Nilius (1992, 1993) a étudié les liens unissant les canaux potassiques, le potentiel de repos, les flux calciques et la prolifération des cellules de mélanomes humains. Leurs travaux aboutissent aux conclusions suivantes : l'activation des canaux potassiques induit une hyperpolarisation et favorise donc une entrée de calcium selon son gradient de concentration. Cette augmentation de la concentration intracellulaire en calcium induit la progression des cellules dans la phase S.

Outre l'influx calcique, les canaux potassiques peuvent moduler la concentration intracellulaire en calcium par l'intermédiaire des stocks intracellulaires. En effet, Lee *et al.* (1994) ont démontré que sur des cellules de neuroblastomes humains, l'activation de canaux

potassiques sensibles à l'ATP provoque une diminution de la mobilisation du calcium intracellulaire et donc de la prolifération qui en découle.

2.2- Régulation du pH intracellulaire par les canaux potassiques

Le pH intracellulaire (pHi) intervient dans le contrôle de la prolifération cellulaire. Une étude sur des astrocytes a révélé que l'emploi d'inhibiteurs de canaux potassiques provoque une augmentation du pHi et une diminution de la prolifération cellulaire (Pappas *et al.*, 1994). Néanmoins, l'un des inhibiteurs utilisé est la 4-AP, une base faible, qui pourrait induire des variations de pHi indépendamment de son effet sur les canaux potassiques. La compréhension des mécanismes précis de régulation du pHi par les canaux potassiques nécessite des travaux complémentaires.

2.3- Modulation de l'influx de sodium par les canaux potassiques

Une étude unique (Cone et Cone, 1976) a démontré qu'un neurone du système nerveux central, soumis à une dépolarisation développe un influx de sodium. Ce phénomène est suivi par une division du noyau, sans que la mitose n'aille à son terme. Cette mitose avortée donne naissance à une cellule binucléée. Il semblerait donc que, dans ce type cellulaire, le sodium soit impliqué dans la régulation des processus de réplication et par extension dans la division cellulaire. Ce lien de cause à effet nécessite d'autres investigations afin de corroborer le rôle des variations intracellulaires de sodium dans la prolifération cellulaire.

2.4- Régulation du volume cellulaire par les canaux potassiques

L'hypothèse de régulation de la prolifération cellulaire par le volume cellulaire s'appuie sur les observations suivantes : (i) le potentiel de repos des cellules de neuroblastome est très peu sensible à l'inhibition des canaux potassique (Rouzaire-Dubois et Dubois, 1991);

(ii) la relation entre le potentiel de repos et le calcium intracellulaire n'est pas claire (Lee et al., 1993) et (iii) la prolifération des cellules tumorales est peu dépendante du calcium extracellulaire (Durham and walton, 1982). Rouzaire-Dubois et Dubois ont émis cette hypothèse en 1991. Le TEA induit simultanément une augmentation du volume des cellules et une réduction de la prolifération cellulaire. Une augmentation du volume cellulaire de 25 % induit une inhibition complète de la prolifération des cellules de neuroblastome (Rouzaire-Dubois et Dubois, 1998).

Deux propositions tentent d'expliquer la manière dont la variation du volume de la cellule influence la prolifération : (i) la déformation de la membrane peut modifier l'organisation des éléments du cytosquelette ; (ii) le changement du volume de la cellule peut altérer la composition et la concentration ionique intracellulaire. Les conséquences de l'une ou l'autre de ces propositions pourraient modifier l'expression ou l'activité des protéines régulatrices du cycle cellulaire (Rouzaire-Dubois et Dubois 1998). Des observations similaires ont été rapportées par Xu et al., (1996) sur les cellules humaines myeloblastiques (ML-1). En effet, l'application de la 4-AP (inhibiteur des canaux potassiques) induit l'arrêt des cellules en phase G1 et une augmentation du volume cellulaire. De même, le canal potassique de type Kv1.3 est impliqué dans la régulation du volume dans les lymphocytes T (Deutsch et chen, 1993).

3- Canaux potassiques impliqués dans la prolifération des cellules de la prostate

L'expression de canaux ioniques et leurs rôles dans la physiologie et la physiopathologie sont très peu étudiés dans les cellules de la prostate, qu'elles soient normales

ou malignes. Skryma *et al.*. (1997) ont caractérisé un canal potassique sur la lignée cancéreuse prostatique humaine LNCaP. Ce canal est impliqué dans la prolifération cellulaire. L'activité des canaux, régulée par le voltage, est également sous la dépendance du taux de calcium intracellulaire : toute augmentation de la concentration en calcium cytosolique inhibe l'activité des canaux potassiques. Par ailleurs, les cellules LNCaP ne disposent pas de canaux calciques dépendants du voltage (Skryma *et al.*, 1997). L'augmentation du taux de calcium pourrait avoir comme origine des canaux calciques non dépendants du voltage et/ou la mobilisation des stocks intracellulaires. Il est connu que des facteurs de croissance et des hormones agissent de la sorte sur le taux de calcium intracellulaire et provoquent la prolifération des cellules (Munaron *et al.*, 1997). De telles variations de calcium pourraient inhiber les canaux K^+ des LNCaP, induire une dépolarisation membranaire et donc, réduire l'influx de calcium. Ce mécanisme pourrait expliquer le rôle de ces canaux potassiques dans la prolifération des cellules cancéreuses tumorales de la prostate humaine.

Un autre type de canal potassique dépendant du voltage a été mis en évidence sur des cellules normales de prostate de rat (Ouadid-Ahidouch *et al.*, 1999). Ce canal diffère de celui présent à la surface des cellules LNCaP. Il est possible que le type de canal potassique soit représentatif du caractère tumoral des cellules prostatiques. Si cette hypothèse s'avère exacte, les canaux potassiques pourraient constituer des cibles pharmacologiques privilégiées dans le cadre des traitements des pathologies de la prostate.

4- Autres types de canaux ioniques impliqués dans la cancérisation de la prostate

La première étude impliquant les canaux sodiques dans le développement du pouvoir invasif des cellules prostatiques, a été entreprise sur le modèle de cancer de la prostate de rat de souche Dunning. Deux lignées cellulaires cancéreuses ont été obtenues chez le rat Dunning (Grimes *et al.*, 1995) :

- la lignée MAT-LyLu qui possède un haut pouvoir métastatique ;
- la lignée AT-2, moins invasive que la précédente lorsqu'elle est injectée dans une prostate de rat Dunning.

Contrairement aux cellules AT-2, la lignée MAT-LyLu exprime des canaux sodiques dépendants du voltage (Laniado *et al.*, 1997). Un traitement à la tétrodotoxine (TTX : une toxine inhibitrice de canaux sodiques) réduit significativement la capacité métastatique des cellules MAT-LyLu (Grimes *et al.*, 1995). Des expériences similaires ont été réalisées sur des lignées cancéreuses prostatiques humaines LNCaP et PC-3. Les cellules PC-3 expriment des canaux sodiques dépendants du voltage contrairement aux cellules LNCaP. La TTX inhibe spécifiquement le caractère invasif des PC-3. Cette toxine est sans effet sur les cellules LNCaP (Laniado *et al.*, 1997).

Il semblerait donc que les canaux sodiques jouent un rôle important dans la dissémination des cellules cancéreuses prostatiques. Les mécanismes exacts impliquant les canaux Na^+ et la formation de métastases restent à définir.

APOPTOSE, CALCIUM ET PATHOLOGIES PROSTATIQUES

La croissance de tous tissus, qu'ils soient normaux ou malins, est déterminée par la modulation de l'équilibre entre la prolifération et la mort cellulaire. Au sein d'un organisme adulte, ces taux sont tels que ni une involution, ni une croissance anormale des tissus ne se produit. Cependant, une cellule peut acquérir un phénotype malin suite au contact avec des agents extérieurs ou à des traitements perturbant la balance prolifération/apoptose. En effet, certaines molécules carcinogènes, plutôt que de stimuler la division cellulaire, provoquent une diminution de la mort cellulaire programmée (Isaacs, 1993). Ce phénomène est maintenant admis dans le cas des cancers de la prostate (Bruyninx *et al.*, 1998). L'apparition de cellules malignes, leur survie, leur accumulation, puis leur dissémination produit, à terme, des cancers malheureusement létaux pour la plupart.

1- L'apoptose

L'apoptose, encore appelée « mort cellulaire programmée », est un terme défini pour la première fois en 1972 par Kerr *et al.* Etymologiquement, ce mot d'origine grecque signifie « chute des feuilles en automne ». Une cellule, entrant dans ce processus, subit de nombreux bouleversements physiologiques et structuraux. La cellule apoptotique se détache et sera finalement détruite par les macrophages. En revanche, les processus de nécrose sont différents. En effet, suite à des stimuli externes, la nécrose conduit à des modifications des influx ioniques, un gonflement et éventuellement un éclatement de la cellule. Au cours de la

nécrose, la cellule joue un rôle passif, alors que l'apoptose est un processus qui requiert une dépense énergétique. Concrètement, l'apoptose se traduit par des bouleversements biochimiques et morphologiques qui aboutissent à une dégradation irréversible de l'ADN et à sa fragmentation par des endonucléases. L'agrégation des fragments d'ADN donne naissance à des corps apoptotiques caractéristiques, visibles après coloration de l'ADN, en microscopie optique (figure 10).

L'apoptose est un phénomène répandu, se produisant normalement à différentes étapes de la morphogenèse, de la croissance et du développement. L'apoptose est induite par différents types de signaux endogènes (généralement des hormones ou des facteurs de croissance) ou exogènes (radiations, virus ou médicaments). L'absence de facteurs de survie est également à l'origine de processus apoptotiques. C'est le cas de l'ablation des androgènes, par castration chimique ou physique, qui induit la mort cellulaire programmée des cellules prostatiques de l'épithélium glandulaire (Kyprianou et Isaacs, 1988). L'élimination des cellules prostatiques consécutive à la castration est la voie principale de traitement des pathologies prostatiques par hormonothérapie.

De nombreuses enzymes, dont certaines sont activées par le calcium, participent à l'apoptose. Les effets du calcium sont en effet relayés par des protéines qui fixent cet ion. Les variations du taux de calcium intracellulaire interviennent dans la régulation de l'activité de facteurs de transcription, ainsi que dans l'activation d'enzymes dépendantes du calcium. C'est le cas de la transglutaminase, de la calmoduline, de la calcineurine, de la calréticuline, des caspases et des endonucléases.

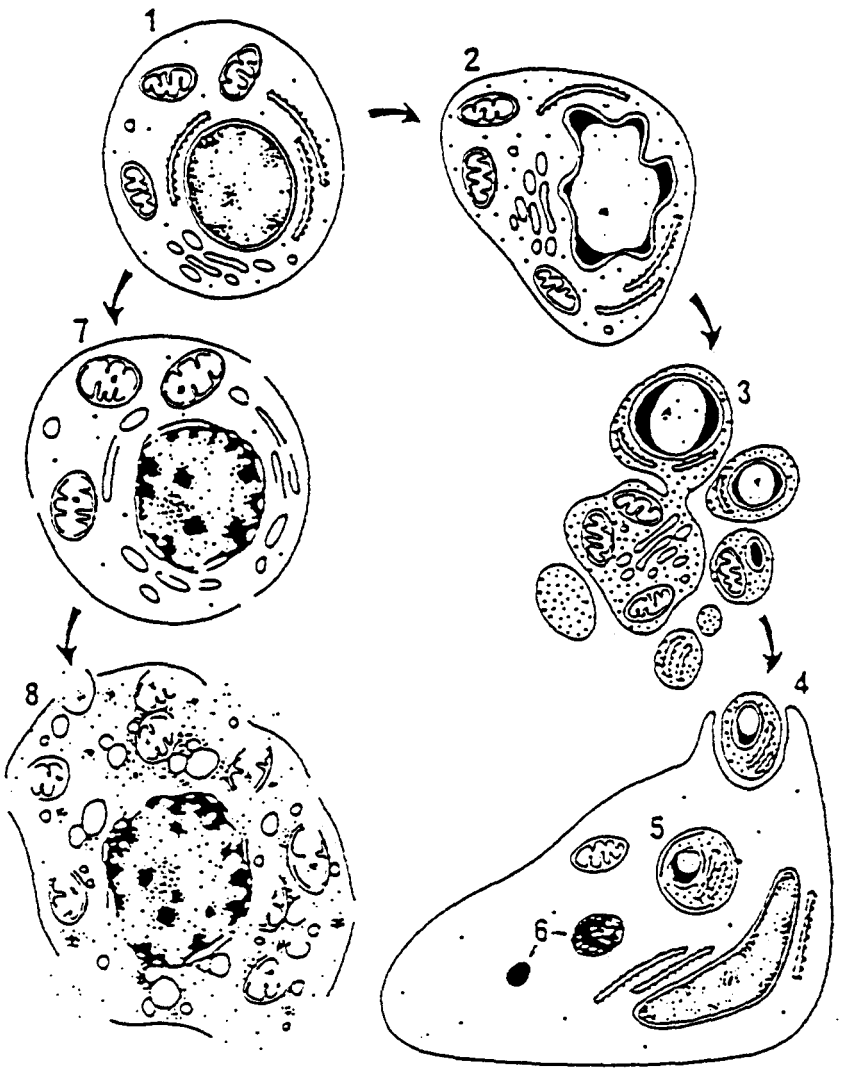

Figure 10: Changements morphologiques principaux dans l'apoptose, à droite et la nécrose, à gauche (d'après Wyllie *et al.*, 1980).

1- Cellule normale

2- Condensation de la chromatine et du cytoplasme d'une cellule en début d'apoptose

3- Fragmentation nucléaire et cellulaire

4- Phagocytose d'un corps apoptotique

5- Corps apoptotique phagocyté

6- Résidus apoptotiques (apoptose terminale)

7- Gonflement d'une cellule en nécrose

8- Eclatement cellulaire

2- Modulation de la mort cellulaire programmée dans la prostate

2.1- Rôle des androgènes

Comme décrit précédemment, la prostate est composée de cellules épithéliales (basales et apicales) qui bordent les acini, de cellules stromales et de cellules endothéliales (formant les vaisseaux sanguins). Dans le tissu prostatique, l'apoptose des cellules épithéliales apicales est induite après la déprivation en androgènes. Ce processus est décrit par certains auteurs comme spécifique aux cellules épithéliales apicales (English *et al.*, 1989). Les cellules stromales et basales de l'épithélium seraient androgeno-indépendantes et n'entreraient pas en apoptose. Néanmoins, des travaux stipulent que même ces cellules sont impliquées par les processus apoptotiques (Shabigh *et al.*, 1999). La castration, chez le rat, stopperait la libération d'un facteur de régulation vasculaire, sécrété par les cellules épithéliales et agissant sur les cellules endothéliales. En retour, les cellules endothéliales entraînent une diminution du flux sanguin (Shabsigh *et al.*, 1998), provoquant ainsi une hypoxie qui conduit à l'apoptose des cellules épithéliales, endothéliales et stromales dans une moindre mesure.

Les cellules épithéliales glandulaires (basales et apicales) constituent 80 % du total des cellules des lobes de prostate de rat. Environ 70 % d'entre elles disparaissent 7 jours après la castration. Le lobe ventral a été longtemps un modèle d'étude des phénomènes apoptotiques, d'une part pour sa sensibilité aux androgènes et d'autre part pour sa dissection relativement aisée. Le lobe latéral s'avère néanmoins plus proche du modèle humain. En effet, la prostate latérale développe un forte sensibilité vis-à-vis des hormones. De plus, histologiquement, ce lobe est homologue à la zone transitionnelle de la prostate humaine où se développent les HBP (Price, 1963).

Après la castration, le taux de testostérone chute à 1.2 % de sa valeur initiale au bout de 6 heures (Kyprianou et Isaacs, 1988). Le taux de DHT (la forme active des androgènes) chute de 55 % 12 heures après la castration. La diminution des androgènes, considérés comme des facteurs de survie, provoque l'entrée des cellules prostatiques en apoptose.

2.2- Modulation de la transcription et de la transduction au cours de l'apoptose

La transcription et la transduction de certains gènes sont stoppées après la castration. C'est le cas de l'ornithine décarboxylase, de l'histone H4 et de la p53 (Furuya et Isaacs, 1993). D'autres gènes, par contre, sont rapidement transcrits et traduits : c-myc (Quarmby *et al.*, 1987), TRPM-2 (testosterone repressed prostatic message) (Montpetit *et al.*, 1986), H-ras (Furuya et Isaacs, 1993), calmoduline (Furuya et Isaacs, 1993) et TGF-β1 (Kyprianou et Isaacs, 1988). Notons que nombre de ces gènes (c-myc, H-ras) sont impliqués dans la prolifération cellulaire.

3- Régulation de l'apoptose par le calcium

Le calcium est un second messager ubiquitaire participant à des fonctions physiologiques multiples: division cellulaire, différenciation, sécrétion, apoptose et nombre de signaux de transduction. Au sein même du processus apoptotique, il apparaît que le calcium agit au cours de nombreuses étapes.

3.1- Homéostasie calcique

Au sein d'une cellule, la concentration moyenne en calcium est maintenue entre 0.05 et 0.2 μM. La cellule baigne dans un milieu extracellulaire contenant environ 1 mM de calcium. De nombreux organites, comme le réticulum endoplasmique (RE), les mitochondries

et le noyau accumulent de grandes quantités de calcium. Cette compartimentation est assurée par nombre de transporteurs (comme les pompes Ca^{2+} ATPases présentes sur la membrane des organites intracellulaires) et de canaux calciques. L'ouverture des canaux calciques, qui induit une entrée de calcium, peut être dépendante du voltage (« voltage gated calcium channel ») ou de la fixation d'un ligand (« ligand-gated calcium channel ») (figure 11). Il existe également des canaux calciques dont l'ouverture est indépendante du voltage. Ce sont les canaux dits CCE pour « calcium channel entry ».

La mobilisation du calcium intracellulaire (c'est-à-dire la vidange des réserves calciques) peut se faire par l'activation des récepteurs à l'IP3 (inositol triphosphate) et/ou celle des récepteurs à la ryanodine. Ces deux récepteurs canaux sont présents sur la membrane du réticulum endoplasmique. L'activation de ces récepteurs est également régulée par le calcium lui-même. Ainsi, une élévation préalable du taux de calcium induit l'ouverture de ces récepteurs et permet la dépletion des réserves intracellulaires en calcium. Ce phénomène est appelé « calcium-induced calcium release » (CICR).

La vidange des stocks calciques induit une augmentation transitoire de calcium. Cette dernière induit « l'entrée capacitative » conduisant à une augmentation soutenue du taux de calcium cytosolique (figure 12). Le calcium, libéré du réticulum endoplasmique, déclenche un signal qui provoque un influx de calcium par des canaux de type CRAC (« calcium release activated calcium channel »). Ce signal n'est pas encore clairement défini. Il pourrait être dû :

- à une modification conformationnelle du récepteur de l'IP3 (Kiselyov *et al.*, 1998) ;
- à un composant diffusible (nommé « CIF » : calcium influx factor) libéré en même temps que le calcium (Putney *et al.*, 1993).

D'autre part, l'influx de calcium survenant au cours de l'entrée capacitative semble être également régulée par la calmoduline (une enzyme dépendante du calcium et intervenant

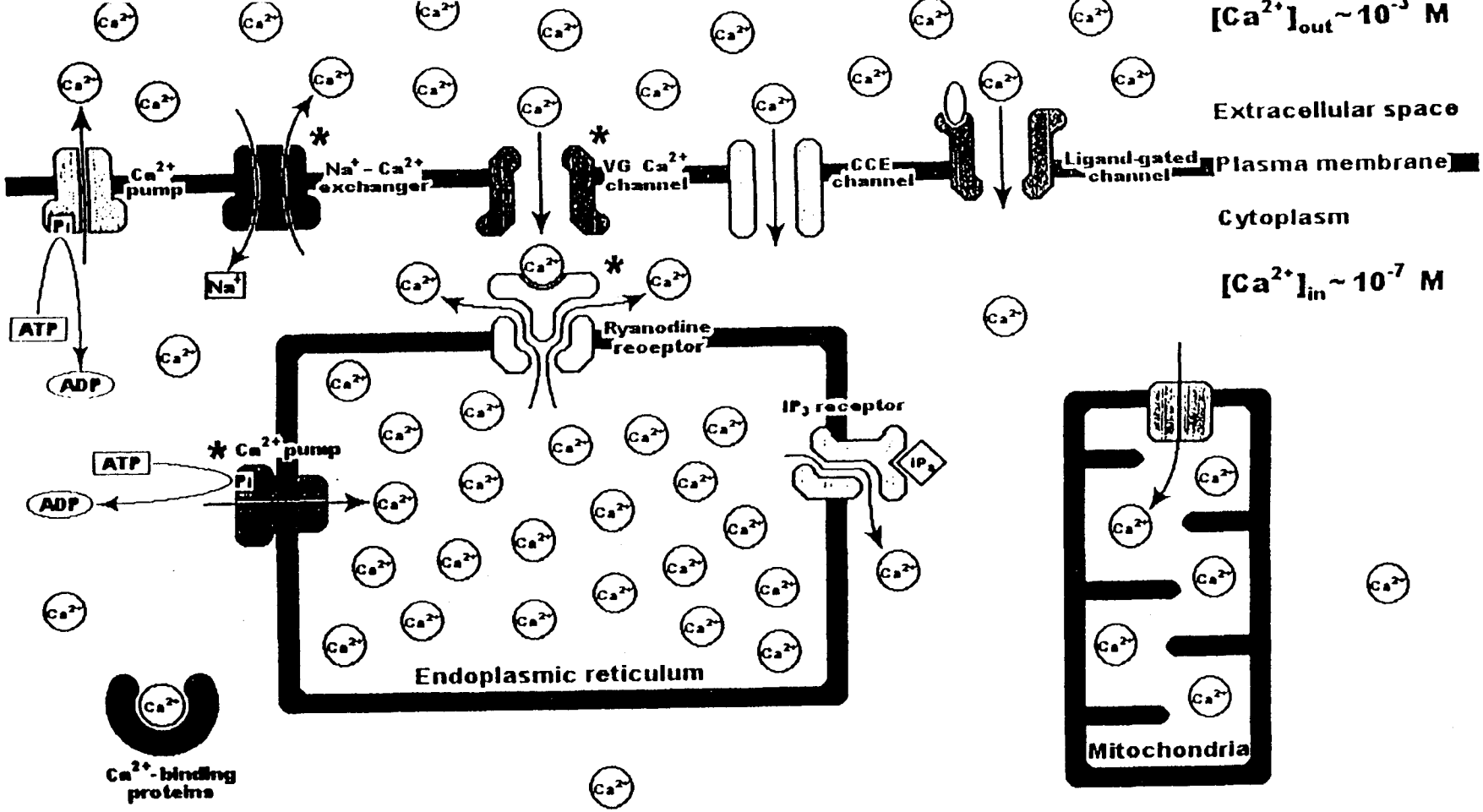

Figure 11 : Contrôle de l'homéostasie calcique intracellulaire.

Légende :

Ca^{2+} pump : pompe calcique

Na^+-Ca^{2+} exchanger : échangeur Na^+-Ca^{2+}

VG Ca^{2+} channel : canal calcique dépendant du voltage

CCE channel : « Calcium Channel Entry » ou canal calcique indépendant du voltage

Ligand-gated channel : canal activé par un ligand

Ryanodine receptor : récepteur à la ryanodine

IP_3 receptor : récepteur à l' IP_3

Ca^{2+}-binding proteins : protéines liant le calcium

Extracellular space : espace extracellulaire

Plasma membrane : membrane plasmique

Cytoplasm : cytoplasme

endoplasmic reticulum : réticulum endoplasmique

Mitochondria : mitochondrie

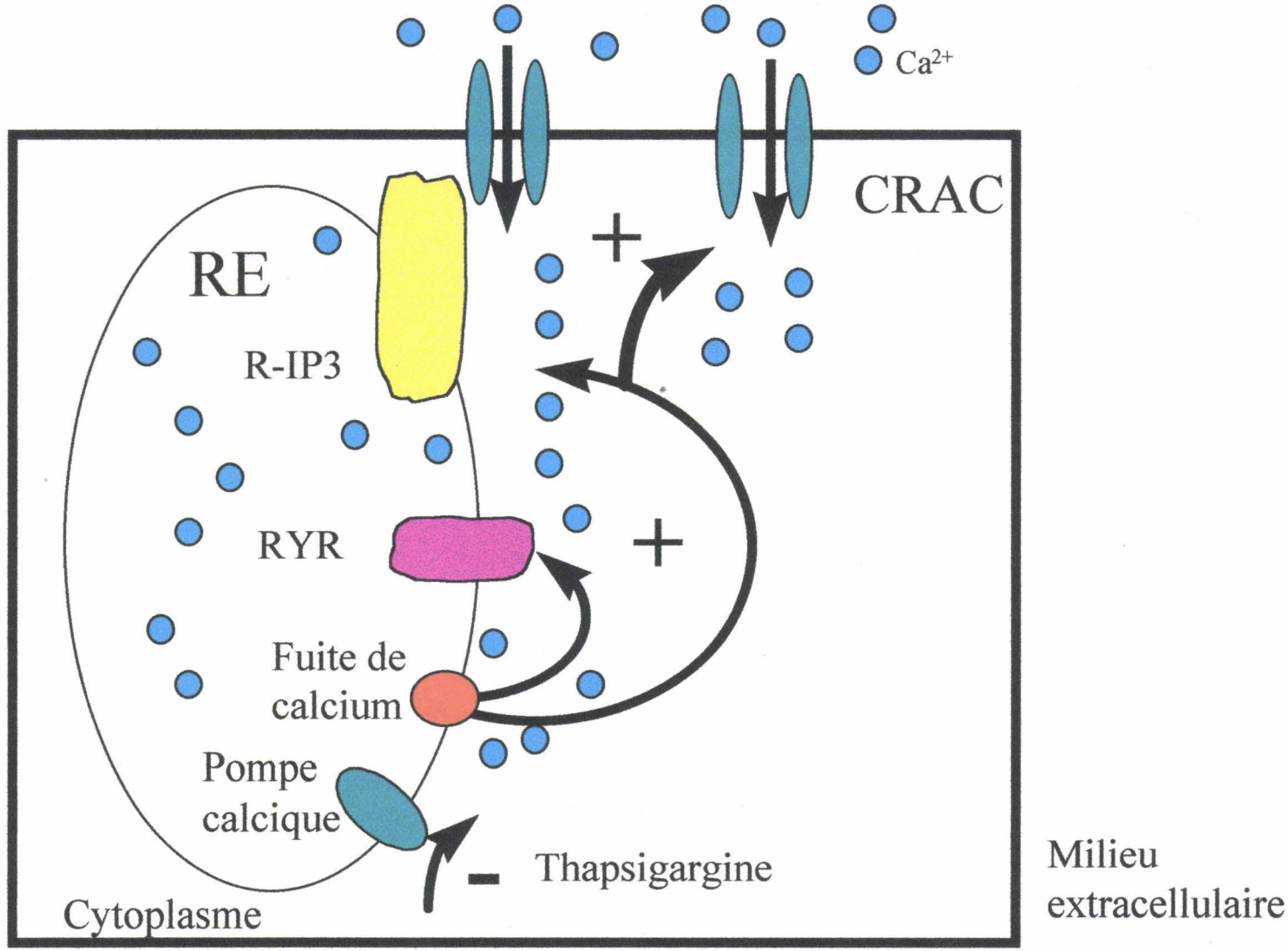

Figure 12: Modélisation de l'entrée capacitative induite par la thapsigargine. La thapsigargine inhibe les pompes calciques. La fuite de calcium stimule les récepteurs a la ryanodine (RYR) et les récepteurs à l'IP3 (R-IP3). Le changement de conformation du R-IP3 active les canaux de type CRAC. Il se produit alors une augmentation soutenue de la concentration en calcium cytosolique.

dans les processus apoptotiques (Dowd *et al.*, 1991). Des inhibiteurs de la calmoduline bloquent l'entrée capacitative (Haverstick *et al.*, 1993).

L'étude du rôle de l'homéostasie calcique requiert l'emploi de toute une gamme d'outils pharmacologiques tels que la thapsigargine (molécule extraite de la plante *Thapsia garganica* ; inhibiteur des pompes Ca^{2+}-ATPases du réticulum endoplasmique qui servent à remplir en continu les stocks. Leur inhibition se traduit par une augmentation du taux de calcium cytoplasmique), des ionophores calciques (comme le « A 23187 »), la ionomycine (qui forme des pores), des inhibiteurs des canaux CRAC (Ni^{2+}, La^{3+}), des inhibiteurs des canaux calciques dépendants du voltage (dihydropyridines, vérapamil), des chélateurs du calcium (EGTA, BAPTA), ainsi que des sondes calciques fluorescentes (fura-2).

3.2- Flux de calcium au cours de l'apoptose

Au cours de l'apoptose, il se produit généralement des modifications de la concentration intracellulaire en calcium. C'est le cas dans certaines cellules prostatiques normales (Kyprianou *et al.*, 1988) ou cancéreuses (Martikainen *et al.*, 1991) ainsi que dans d'autres modèles cellulaires (Putney *et al.*, 1993).

La hausse de la concentration cytosolique en calcium peut être la conséquence d'un influx de calcium extracellulaire et/ou d'une mobilisation des réserves intracellulaires. Actuellement, deux théories s'opposent pour expliquer le rôle du calcium dans l'apoptose :

- une augmentation soutenue de la concentration en calcium intracellulaire par la vidange des stocks et/ou par un influx de calcium extracellulaire agirait comme un signal apoptotique (activation d'enzymes dépendantes du calcium) (He *et al.*, 1997). Ce processus est illustré par la figure 13. L'élévation de la concentration en calcium pourrait avoir pour cible des enzymes intermédiaires des signaux de transduction, par exemple des protéines kinases ou des phosphatases. Le calcium peut également activer des protéases

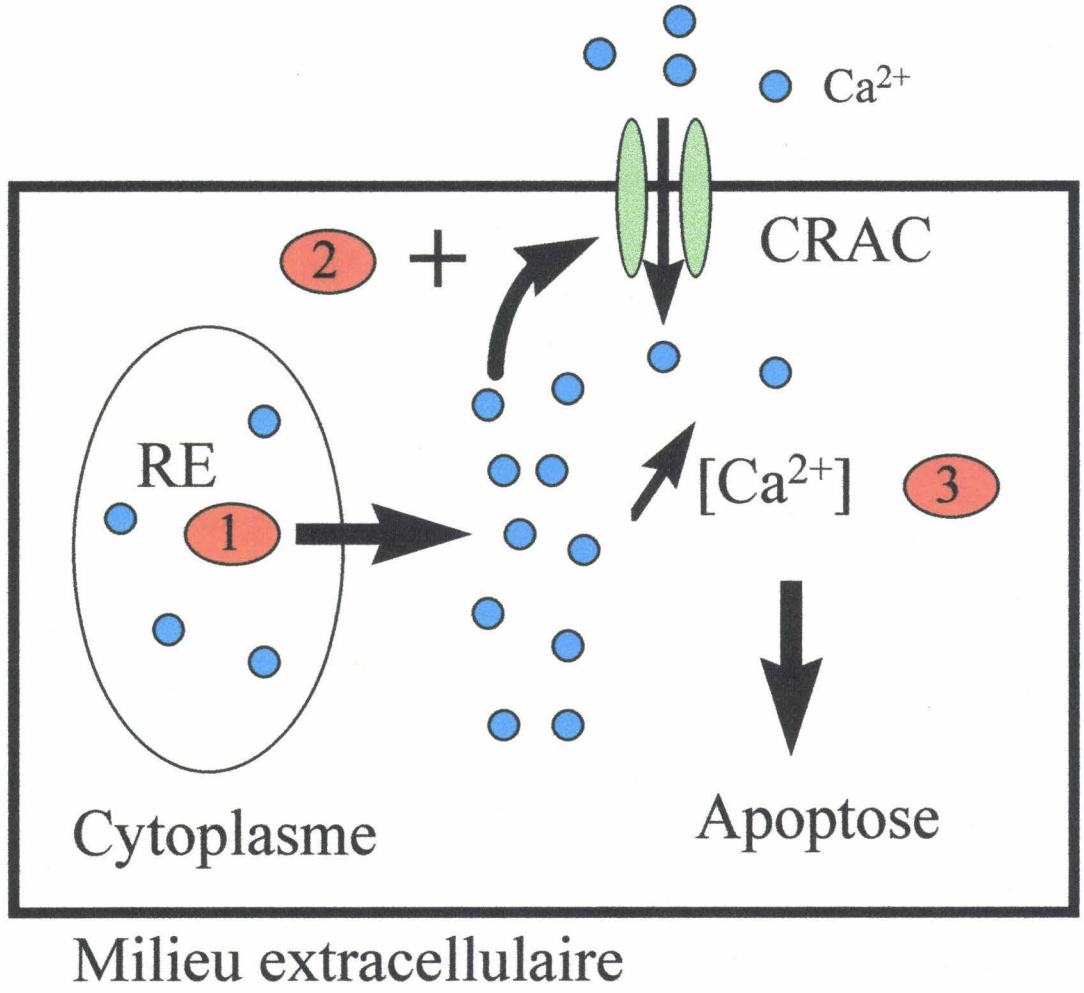

Figure 13: Apoptose provoquée par l'augmentation soutenue de calcium suite aux événements suivants:
1- Vidange du réticulum endoplasmique (RE);
2- Activation de l'entrée capacitative
3- Apoptose

comme les caspases, la transglutaminase (qui forme des liaisons protéiques maintenant l'intégrité de la cellule avant qu'elle ne soit phagocytée) ou des endonucléases qui mènent au clivage de l'ADN. Des taux élevés de calcium provoquent également la migration de protéines membranaires (mouvements de phosphatidylsérine de la face interne vers la face externe de la membrane plasmique) reconnues par les macrophages.

- l'action de vidanger les réserves calciques intracellulaires, plutôt que l'augmentation du calcium cytosolique déclencherait l'apoptose (Putney *et al.*, 1993) (figure 14). Il est possible que la vidange du calcium soit accompagnée de la libération d'une molécule proapoptotique comme une endonucléase. La déplétion des stocks pourrait également déstabiliser le réseau « calcium-protéines » ainsi que les portions de membrane qui lui sont associées conduisant à la formation de vésicules et de corps apoptotiques.

3.2.1- Entrée de calcium extracellulaire au cours de l'apoptose

Dans de nombreux modèles, les phénomènes apoptotiques s'accompagnent d'une augmentation de la concentration intracellulaire en calcium (Spielberg *et al.*, 1991 ; Kaiser *et al.*, 1977 ; Connor *et al.*, 1988). C'est le cas de cellules de prostate ventrale de rat après suppression des androgènes (Connor *et al.*, 1988 ; Kyprianou *et al.*, 1988). L'apparition de l'apoptose de ces cellules est inhibée par la nifédipine qui bloque des canaux calciques. Cela signifie que le flux calcique serait une cause et non une conséquence de l'apoptose. D'autres études, où un ionophore calcique (ionomycine) induit l'apoptose de cellules cancéreuses prostatiques de rat Dunning R-3327, vont dans ce sens (Martikainen *et al.*, 1991). Les auteurs de cette étude suggèrent qu'une augmentation soutenue du taux de calcium déclenche l'apoptose.

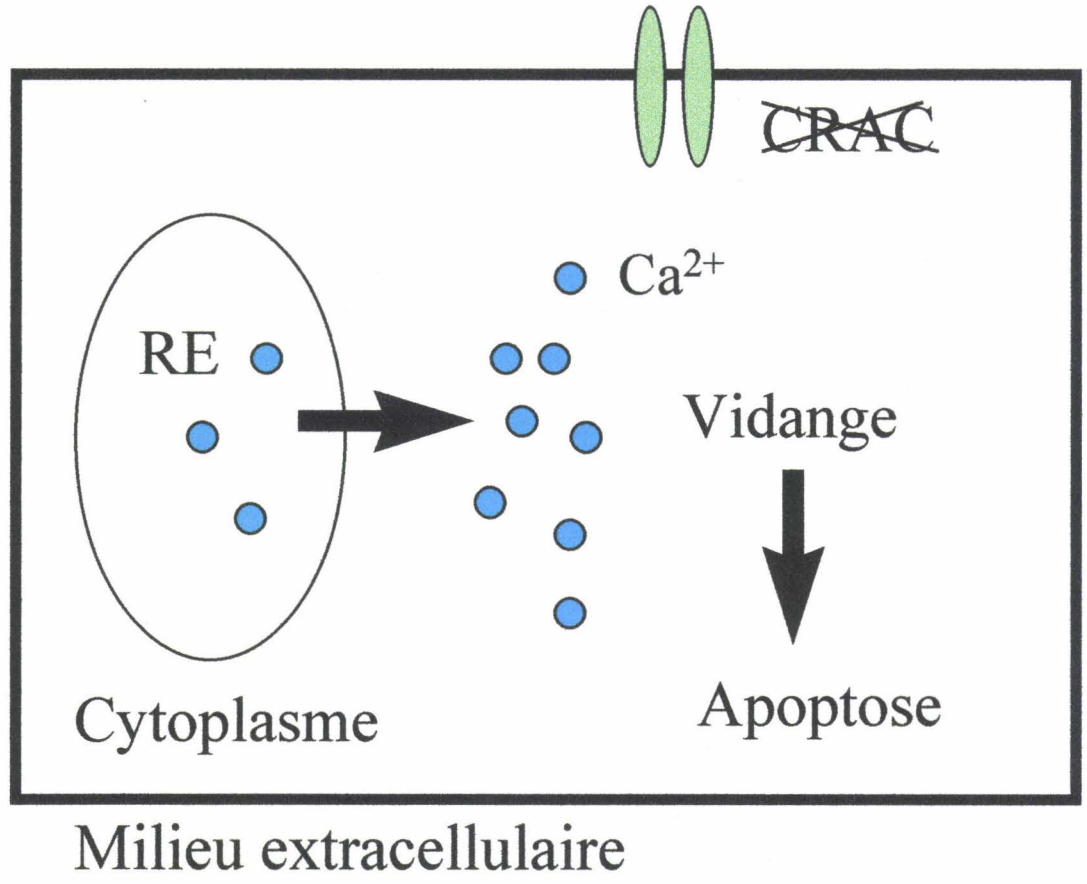

Figure 14: Apoptose provoquée par la vidange du réticulum endoplasmique (RE).

3.2.2- Mobilisation des réserves calciques et apoptose

La mobilisation du calcium (c'est-à-dire sa libération) joue également un rôle clé dans l'apoptose. Dans certains types cellulaires, la vidange des stocks entraîne l'apoptose. En effet, Lam *et al.* (1994) ont mesuré le taux de calcium cytosolique au cours de l'induction de l'apoptose, par les glucocorticoïdes, de deux lignées cellulaires de lymphocytes T murins. Ces lymphomes, contrairement aux lymphocytes normaux en culture primaire, ne développent pas un influx calcique au cours des processus apoptotiques (McConkey *et al.*, 1989). Les glucocorticoïdes provoquent une mobilisation du calcium et vidangent les stocks intracellulaires. L'emploi de la thapsigargine induit une libération de calcium par les stocks calciques par inhibition des calcium ATPases du réticulum endoplasmique. La libération du calcium cytosolique par la thapsigargine permet d'évaluer le contenu des stocks intracellulaires (figure 12). Il apparaît donc que la quantité de calcium conservée dans les stocks calciques intracellulaires est un facteur important dans l'induction de l'apoptose. La diminution du calcium luminal stimule l'apoptose. A l'inverse, toute augmentation du contenu des réserves calciques prévient les processus apoptotiques.

4- Régulation des flux calciques par les protéines de la famille de Bcl-2

L'oncoprotéine Bcl-2 (B cell lymphocyte type 2) a été identifiée comme un facteur inhibiteur de l'apoptose (Sentman *et al.*, 1991). Les cellules B qui surexpriment Bcl-2 résistent à l'apoptose lorsqu'elles sont soumises à une augmentation du calcium intracellulaire par un ionophore calcique (Liu *et al.*, 1991). De même, les cellules cancéreuses humaines LNCaP, initialement androgeno-dépendantes (Horoszewicz *et al.*, 1983) résistent au retrait des androgènes du milieu de culture quand elles surexpriment Bcl-2 (Raffo *et al.*, 1995). La surexpression de Bcl-2 rend donc les cellules de la prostate hormono-indépendantes.

Bcl-2 est une protéine intracellulaire associée à la membrane interne des mitochondries, à celle du noyau et du réticulum endoplasmique. Plusieurs molécules apparentées à Bcl-2 ont été caractérisées : des protéines antiapoptotiques comme Bcl-xl, MCL-1 et A1 (White, 1996), ainsi que des protéines proapoptotiques comme Bax, Bad et Bak (Abastado, 1996). L'hypothèse actuelle postule qu'il se formerait des homodimères comme Bcl-2-Bcl-2 ou Bax-Bax ou encore Bcl-2-Bax. En présence d'une excès de Bax, par rapport à Bcl-2, il se produirait plus d'appariement Bax-Bax, ce qui induirait l'apoptose (White *et al.*, 1996). Cette hypothèse peut être schématisée de la manière suivante :

Bcl2- Bcl-2 : **survie** ; Bcl-2-Bax : **survie** ; Bax-Bax : **mort**.

Cette hypothèse expliquerait le développement de l'hormonorésistance des cellules LNCaP transfectées avec le gène codant pour Bcl-2 (Raffo *et al.*, 1995).

L'oncoprotéine Bcl-2, transmembranaire, est capable de provoquer l'entrée de calcium dans le réticulum endoplasmique. La concentration en calcium luminale augmente et préviendrait l'apoptose (Abastado, 1996). Les travaux de He *et al.* (1997) ont mis en évidence le rôle de Bcl-2 sur la régulation du contenu des stocks calciques. Cette étude a été réalisée sur deux lignées de lymphome de rat. L'une d'entre elles surexprime Bcl-2. Ces auteurs ont démontré que Bcl-2 inhibe l'apoptose des cellules traitées à la thapsigargine grâce à la régulation des flux calciques dans le réticulum endoplasmique. La figure 15 modélise les variations des taux de calcium du réticulum mesurées dans les cellules de lymphomes.

- En présence d'un taux normal de calcium extracellulaire :

Les pompes Ca^{2+}ATPase et Bcl-2 maintiennent une concentration élevée en calcium luminal (A et B). En présence de thapsigargine, les organites qui n'expriment pas Bcl-2 sont vides (C). Ces cellules entrent en apoptose à l'inverse de celles qui peuvent maintenir un taux suffisant de calcium grâce à Bcl-2 (D).

- Dans un milieu appauvri en calcium :

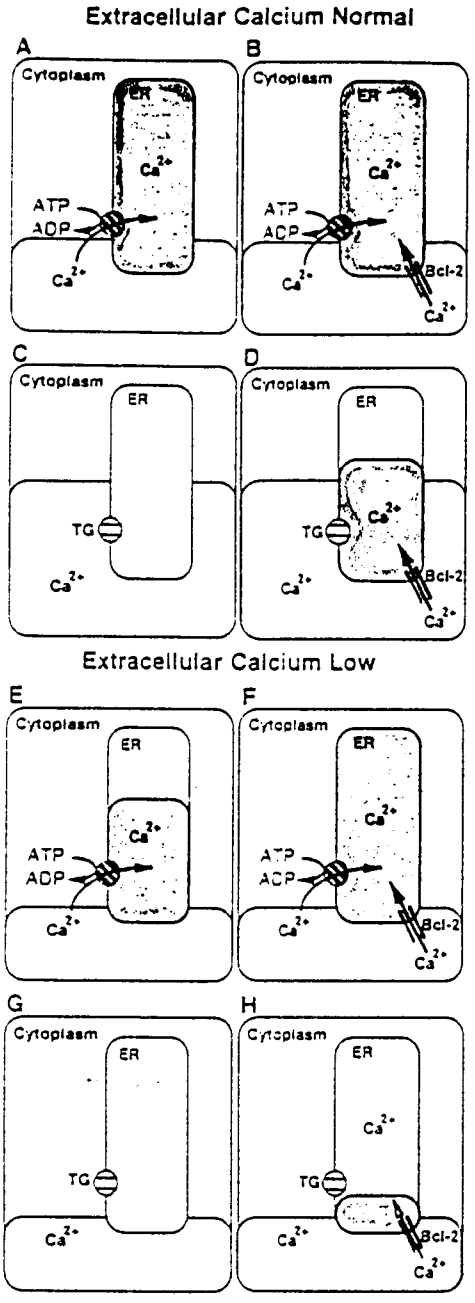

Figure 15 : Modèle de régulation de l'homéostasie calcique par Bcl-2 dans le réticulum endoplasmique (RE) (d'après He *et al.*, 1997).A-D : cellules cultivées dans un milieu contenant des concentrations physiologiques en calcium (1.3 mM). E-H : cellules cultivées dans un milieu contenant une faible concentration en calcium (0.13 mM). A, C, E et G représentent des cellules dépourvues de Bcl-2. B, D, F et H représentent des cellules qui expriment Bcl-2. A, B, E et F ne sont pas traitées à la thapsigargine (TG) contrairement aux cellules C, D, G et H. Bcl-2 est présente dans sur les cellules de la colonne de droite.

il se produit une baisse du contenu des stocks en absence de Bcl-2 (E). Ce n'est pas le cas des organites des cellules exprimant Bcl-2 (F). L'application de thapsigargine vidange les stocks en G, alors qu'en H, Bcl-2 parvient à la prévenir partiellement et, de ce fait, inhibe l'apoptose.

5- Autres protéines impliquées dans la régulation de l'apoptose et dépendantes du calcium

5.1- La calmoduline

La calmoduline est une protéine multifonctionnelle dont l'activation dépend du calcium (Klee *et al.*, 1982 ; Means, 1988). Des travaux ont démontré que le calcium agit en conjonction avec la calmoduline dans la cascade de transduction qui mène à l'apoptose. Par exemple, l'expression de la calmoduline est augmentée lors de l'induction de la mort cellulaire programmée de lymphocytes par les glucocorticoïdes (Dowd *et al.*, 1991). Au contraire, l'inhibition de la calmoduline par le calmidazolium la prévient (McConkey *et al.*, 1989).

5.2- La calcineurine

La calcineurine, encore appelée phosphatase 2B, est activée par la calmoduline et le calcium. Une étude récente sur des cellules cancéreuses prostatiques androgeno-indépendantes (Wang *et al.*, 1999) clarifie le rôle de cette protéine dans la régulation de la mort cellulaire programmée. L'augmentation du calcium cytosolique active la calcineurine. Celle-ci déphosphoryle la protéine proapoptotique Bad et la libère de la protéine 14.3.3. La protéine Bad, sous sa forme active, provoque la mort de la cellule par apoptose.

5.3- La calréticuline

La calréticuline, protéine dépendante du calcium, est présente dans le réticulum endoplasmique et concourt au maintien de l'homéostasie calcique en chélatant le calcium. Son expression, au sein des cellules de la prostate ventrale de rat, est régulée par les androgènes (Zhu *et al.*, 1998). Par ailleurs, la calréticuline régule l'induction de la mort des cellules cancéreuses prostatiques androgéno-sensibles (Zhu *et al.*, 1999).

MATERIELS

ET

METHODES

Etudes *in vivo*

1- Traitement des animaux de laboratoire

Les rats mâles adultes de souche Wistar (200-220 g) proviennent d'IFFA CREDO (Lyon, France) et du Centre d'Elevage DEPRE (Saint Doulchard, France).

NB : des expériences similaires ont été menées conjointement sur des animaux issus de ces deux centres d'élevage. Nous avons obtenu des résultats équivalents. La provenance des rats n'est donc pas un facteur à prendre en compte dans la suite de nos expérimentations.

Les animaux sont maintenus en l'état durant une semaine avant le début des expérimentations. Ils sont disposés, de manière aléatoire, à cinq par cage où ils reçoivent 12 h de lumière par jour. L'eau, ainsi que la nourriture sous forme de granulés, sont disponibles à volonté.

L'ensemble des travaux concernant l'utilisation d'animaux suit les règles formulées par le Conseil de la Communauté Européenne, le 24 novembre 1986 (86/609/EEC).

1.1- Préparation des animaux

Les opérations chirurgicales sont réalisées sous anesthésie complète de l'animal à l'aide d'injection intrapéritonéales d'hydrate de chloral (400 mg/kg ; Sigma). Aux animaux traités chirurgicalement sont administrés des antibiotiques (pénicilline 22 000 UI/kg, Sigma) pour prévenir les risques d'infection.

1.1.1- Castrations

Les castrations sont pratiquées via le scrotum, en éliminant l'épididyme en même temps que les testicules. Les rats dits « pseudo-castrès » sont opérés de la même manière, mais

sans que les testicules et l'épididymes ne soient ôtés. Après suture, le champ opératoire est désinfecté avec une solution de bétadine (Vetoquinol, France). Une autre technique de castration a été testée. Au cours de cette dernière l'épididyme n'a pas été enlevé. Nous n'avons noté aucunes différences significatives du point de vue des poids et de l'histologie de la prostate.

1.1.2- Pose et préparation des implants

Dans le but d'administrer une quantité voulue d'androgènes exogènes par rapport aux animaux témoins, nous avons réalisé des implants sous-cutanés (Silastic medical-grade silicone tubing : 0.078 i.d. X 0.125 o.d. ; Dow Corning Corp., Midland, MI), d'une longueur de 1 cm, remplis de testostérone (Sigma) ou de dihydrotestostérone (Sigma) et placés au niveau de l'omoplate des animaux (Robaire *et al.*, 1979). La préparation des implants est la suivante : après avoir collé l'une des extrémités du tube (Silastic Medical Adhesive : Dow Corning Corp.), celui-ci est rempli avec l'hormone en poudre. La seconde extrémité du tube est scellée à son tour avec de la colle. Les implants sont immergés 12 h dans de l'eau distillée avant leur pose sur l'animal afin d'hydrater la matrice de silicone et de laver tout excédent d'hormone. Il a été démontré qu'un implant de 2.5 cm délivre une quantité de testostérone (T) équivalente à celle que fourniraient les testicules (Robaire *et al.*, 1979). Nous avons choisi des implants de 1 cm de long afin de diminuer de moitié la quantité d'androgène administrée et dans le but de recréer un environnement hormonal le plus proche possible d'un organisme âgé où le taux de T est réduit de 50% (Davidson *et al.*, 1983). Les implants sont posés le 1er jour ou le 8ème jour, selon de mode expérimental choisi, après avoir pratiqué une « boutonnière » au niveau de la zone dorsale proche de l'omoplate de l'animal. La région incisée est recousue et désinfectée.

1.1.3- Induction de l'hyperprolactinémie

L'hyperprolactinémie est provoquée par des injections intrapéritonéales et journalières de 40 mg/kg de sulpiride (± sulpiride, Sigma), une molécule connue pour ses effets inhibiteurs des récepteurs dopaminergiques de type II (Debeljuk *et al.*, 1975). Les animaux servant de contrôle ne reçoivent que des injections intrapéritonéales de sérum physiologique (NaCl 0.9%).

1.1.4- Gavages des animaux de Lipido-stérolique extract of *Serenoa repens* et de Finastéride

L'extrait lipido-stérolique de *Serenoa repens* (Permixon® ; Pierre Fabre Médicaments ; lots 708 et 712) a été administré par gavages quotidiens, à heure fixe aux doses suivantes : 100, 320 ou 640 mg/kg. 5% d'éthanol est ajouté au mélange pour augmenter sa fluidité.

Le finastéride (Chibro-Proscar® ; Merck ; lot 974214) a été administré *per os* de manière journalière, à la même heure, à la dose de 5 mg/kg. Tout comme pour l'E.L.S.S.R., un adjuvant de 5% d'éthanol accroît la fluidité de la solution de gavage.

1.2- Sacrifice des animaux

Le sacrifice des animaux est réalisé sous anesthésie à l'hydrate de chloral (400 mg/kg, Sigma). Les animaux sont décapités à l'aide d'une guillotine. Le sang est récupéré dans des tubes préalablement traités à l'EDTA (5%, Sigma) et est stocké dans de la glace. Le sang est alors centrifugé à 3000 rpm pendant 10 mn. Les échantillons de sérum obtenus sont congelés et conservés à -80°C en vue des dosages radioimmunologiques. Les lobes prostatiques composés de 2 lobes ventraux, 2 lobes latéraux et d'un lobe dorsal (voir figure 3) sont disséqués avec soin et pesés séparément. Ils sont alors rapidement fixés dans 10 % de formol

neutre (Dislab, France), pour les études histologiques ou dans 2.5% de glutaraldéhyde (Sigma) pour les analyses immunohistologiques. Enfin, d'autres lobes sont congelés dans du « tissu tek » (Poly Labo, France).

2 - Dosages radioimmunologiques

2.1- Principe

Le principe de ce dosage repose sur la compétition entre un antigène froid (Ag) (substance à doser) et un antigène marqué (Ag^*) pour la fixation à un anticorps spécifique (Ac) selon la réaction :

$$Ag^* + Ag + Ac \rightleftharpoons Ag\text{-}Ac + Ag^*\text{-}Ac$$

Cette réaction étant en équilibre et les quantités d'Ag^* et d'Ac connues et constantes, toute variation de la quantité d'Ag froid entraîne une modification de l'équilibre et donc une variation de la quantité de complexe Ag^*-Ac formé. Dans de telles conditions, la quantité d'Ag froid contenue dans l'échantillon à doser peut être déterminée par référence à une courbe étalon.

2.2- Application aux dosages hormonaux :

Les dosages hormonaux de PRL, de T, de DHT et de « Luteinizing Hormon » (LH) des échantillons de sérum de rat ont été réalisés en collaboration avec le Professeur J-C BEAUVILLAIN et le Docteur D. CROIX (Laboratoire de Neuroendocrinologie et Physiopathologie Neuronale, INSERM U 422, Lille), ainsi qu'en collaboration avec le Professeur J-P. DUPOUY (Laboratoire de Neuroendocrinologie du Développement, Bâtiment SN4, U.S.T.L.).

3 - Etudes histologiques

Les tissus prostatiques, fixés dans du formol neutre à 10%, sont paraffinés et coupés. Les coupes obtenues sont ensuite colorées à l'hematoxylin-erythrosin-saffron (HES ; Sigma).

Les études histologiques ont été réalisées en collaboration avec le Docteur F. CARPENTIER (Service d'Anatomo-Pathologie, C.H.R. V. Pruvost, Roubaix) et le Docteur X. LEBOURHIS (Laboratoire de Biologie du Développement, Bâtiment SN3, U.S.T.L.).

4 - Etudes immunohistochimiques

Cette étude consiste en la détection de la protéine antiapoptotique Bcl-2 (White *et al.*, 1996) sur des coupes de prostates latérales de rat. Cette approche a été réalisée en collaboration avec le Docteur C. SLOMIANNY et Monsieur E. DEWAILLY du Laboratoire de Physiologie Cellulaire.

Immédiatement après la dissection des prostates latérales, des pièces de 1 mm x 1 mm sont fixées par immersion dans du paraformaldéhyde (Sigma ; 1.5% dilué dans du tampon phosphate (PBS)) pendant 1h30 à 4°C. Après plusieurs lavages, les blocs sont infusés durant 24h dans un mélange de sucrose (2.5 M ; Sigma) et de polyvinyl pyrrolidone (20% ; Sigma). Par la suite, les échantillons sont congelés dans de l'azote liquide. Des sections de 0.2 µm sont coupées et déposées sur des lames de verre. Une solution de 1.2% de gélatine (Sigma) diluée dans du PBS (PBSG), agissant pendant 30 mn, inhibe la possibilité de toute fixation non spécifique de l'anticorps. L'incubation avec l'anticorps primaire anti Bcl-2 (anticorps polyclonal anti lapin IgG, Calbiochem) est réalisée à 4 °C pendant 12 h. Après plusieurs rinçages au PBSG, les lames sont incubées pendant 1 h à 37 °C avec l'anticorps secondaire

(anticorps de singe anti lapin, IgG marquée avec au FITC, Jackson), puis lavées au PBS. Les coupes sont observées grâce à un microscope Zeiss Axiophot à épifluorescence (excitation : 450-490 nm ; émission : 520 nm). Les contrôles négatifs sont réalisés de la même manière, mais sans incubation avec l'anticorps primaire.

5 - Analyses statistiques

Les masses relatives des prostates de rat sont exprimées par rapport à la masse relative du corps de l'animal d'après les travaux de Robinette *et al.* (Robinette, 1988). Nous avons également analysé les valeurs obtenues lors des dosages hormonaux. Les degrés de significativité sont établis grâce à l'emploi du test de Tukey. Les degrés de significativité sont fixés aux niveaux suivants : $p<0.05$; $p<0.01$ et $p<0.001$.

Etudes *in vitro*

1 - Culture cellulaire

Au cours de nos expériences, nous avons employé principalement deux types de lignées cellulaires :

- des cellules cancéreuses prostatiques humaines LNCaP (Lymph Node Carcinoma Prostate) ;
- des cellules prostatiques de rat de souche Wistar en culture primaire.

1.1- La lignée cellulaire LNCaP

Cette lignée de cellule prostatique humaine est issue d'une biopsie à l'aiguille d'un ganglion axillaire pratiquée chez un homme de 50 ans atteint d'un carcinome prostatique (Horoszewicz *et al.*, 1983). La lignée LNCaP (clone FGC ; CRL 1740) provient de l'« American Type Cell Collection » (A.T.C.C., USA). La caractéristique et l'intérêt principal de cette lignée réside dans le fait qu'elles sont hormono-dépendantes. En effet, ces cellules nécessitent la présence d'androgènes pour maintenir leur prolifération.

Les cellules LNCaP sont cultivées dans du milieu RPMI 1640 (ICN, France) enrichi en sérum de veau foetal (ICN, USA) décomplémenté (30 mn à 56°C), en L-glutamine 2 mM (ICN, USA) et en antibiotiques (pénicilline 50 UI/ml et streptomycine 50 µg/ml, ICN, USA).

Les cellules sont ensemencées sur différents supports en fonction de leur utilisation ultérieure :

- des flacons de culture de 25 cm^2 ou de 75 cm^2 de surface (Greiner, Allemagne) pour le stockage et l'entretien ;
- des boîtes de pétri de 35 mm de diamètre (Greiner, Allemagne), sans lamelles de verre pour les expériences de patch-clamp. Une lamelle de verre de 22 mm (Greiner, Allemagne) de diamètre est disposée dans chaque boîte pour les expérimentations en microspectrofluorimétrie et en imagerie cellulaire.

Les cellules en culture sont stockées à 37 °C dans un incubateur dont l'atmosphère, saturée en eau, est enrichie en CO_2 (95% d'air et 5% de CO_2). Le milieu de culture est renouvelé deux fois par semaine.

Arrivées à confluence, les cellules sont détachées de leur support par une brève action de la trypsine-EDTA (ICN, USA). Les cellules décollées, la trypsine est inhibée par

l'adjonction de milieu de culture complet contenant du sérum de veau foetal. Il est alors possible d'ensemencer de nouveaux flacons de culture et de nouvelles boîtes de pétri.

1.2- Les cellules primaires de prostate de rat

Ces cellules sont issues de biopsies de rats mâles adultes de souche Wistar. La technique de prélèvement est similaire à celle employée lors des études *in vivo*.

Les prostates sont récupérées dans du milieu de culture contenant des antibiotiques (pénicilline 50 UI/ml et streptomycine 50 µg/ml). Sous une hotte à flux laminaire, les lobes prostatiques sont découpés en fragments de 1 mm x 1 mm, puis placés en incubation, à 37 °C pendant 2h, dans un milieu contenant de la collagénase de type XI (450 UI/ml, Sigma), de la hyaluronidase (250 UI/ml, Sigma) et de la DNase de type I (0.01%, Boehringer Mannheim, France). La digestion enzymatique terminée, les cellules sont centrifugées à 1300 rpm pendant 10 mn, puis rincées avec du milieu de culture (RPMI 1640 ; 5% sérum de veau foetal, 2 mM de L-glutamine, pénicilline 50 UI/ml et streptomycine 50 µg/ml). L'opération est répétée 3 fois afin d'éliminer toutes traces d'enzymes.

L'entretien des cellules primaires est similaire à celui des cellules LNCaP.

1.3- Maintien en culture des cellules

Les cellules LNCaP subissent un repiquage (encore appelé « passage ») par semaine. Nous cessons de les utiliser au bout de 10 passages afin qu'elles ne puissent subir de dérive génétique. Il est alors indispensable de démarrer une nouvelle culture à partir de cellules LNCaP congelées lors des premiers repiquages.

La survie des cellules primaires de prostate de rat est plus brève. Nous estimons que le temps d'utilisation de telles cultures ne doit pas excéder 2 semaines, dans le but d'éviter tous phénomènes de dégénérescence.

Avant chaque expérimentation, les cellules sont rincées plusieurs fois avec de l'H.B.S.S. (Hank's Buffer Salt Solution) dont la composition est donnée en fin de chapitre.

2 - Enregistrements électrophysiologiques

Les variations de potentiel de membrane ou de courants ioniques transmembranaires sont mesurées grâce à la technique de « patch-clamp » (Neher *et al.*, 1976) dans la configuration « cellule entière » (« whole cell recording », WCR) (Hamill *et al.*, 1981).

2.1- Pipettes d'enregistrement

Les pipettes d'enregistrement sont obtenues par étirement de tubes de verre en borosilicate à paroi fine sans microcapillaire (Clark Electromedical Instruments, USA) à l'aide d'une étireuse verticale. Le diamètre interne des pipettes de patch-clamp est de l'ordre de 1µm. Leur résistance moyenne s'étend de 2 à 4 MΩ. Les pipettes de patch-clamp sont remplies d'une solution appelée « milieu interne » dont la composition est détaillée en fin de chapitre.

2.2- Principe de mesure ; configuration du « fast whole-cell recording » (FWCR)

La pointe de la pipette de patch est délicatement posée sur la cellule à l'aide de micromanipulateurs (Narishige, Japon). Une faible aspiration conduit à une jonction, entre la pipette et la membrane, de haute résistance électrique nommée « seal » (résistance de 13 à 30 GΩ. Cette configuration se nomme « cellule attachée » (figure 16). Le passage en configuration « cellule entière » requiert une aspiration supplémentaire, cassant le fragment de membrane situé dans la lumière de la pipette et mettant ainsi en contact le milieu intrapipette

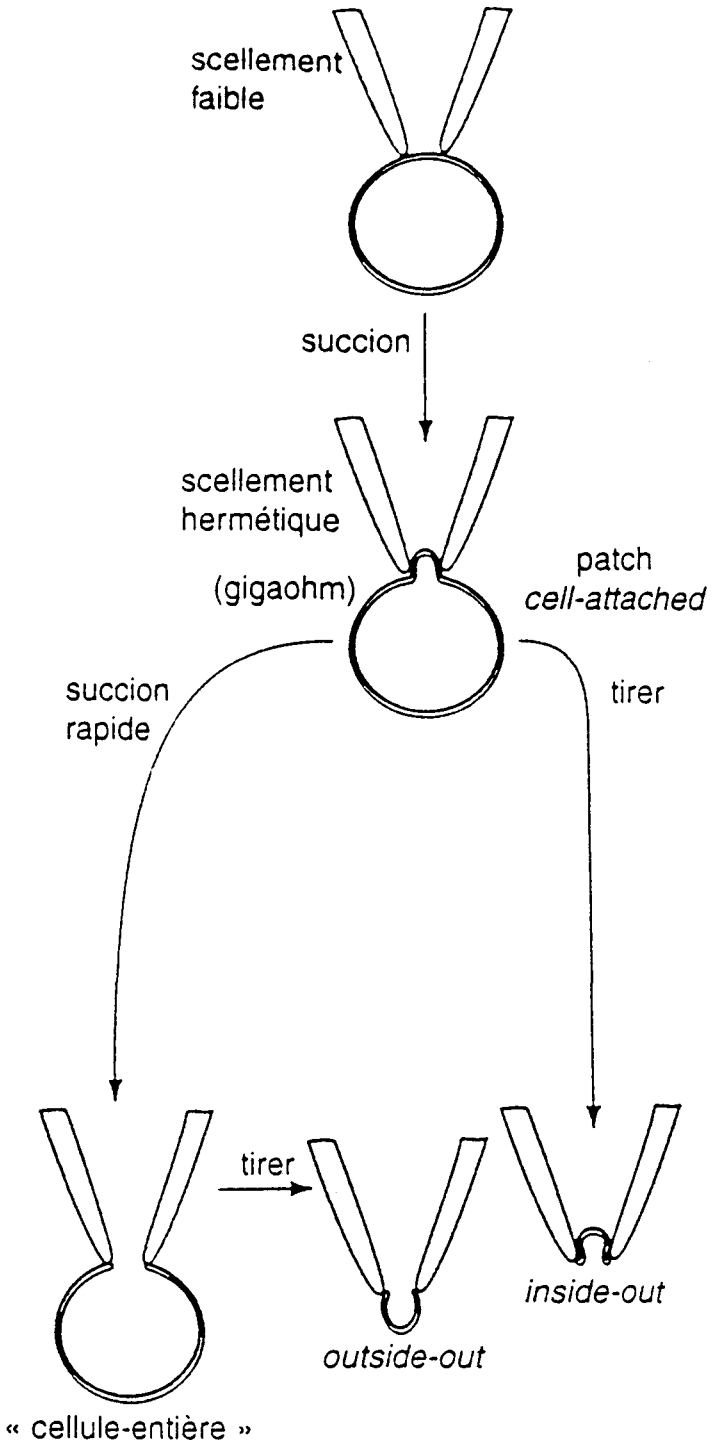

Figure 16 : Différentes configurations d'enregistrement en patch-clamp. Schéma indiquant les étapes successives menant aux différentes configurations.

et le milieu intracellulaire (figure 16). Cette configuration du WCR présente l'avantage de permettre l'accès au milieu intracellulaire par la pipette de patch et de maintenir constante la composition du cytosol (dialyse possible de composés contenus dans la pipette).

2.3- Configurations « inside-out » et « outside-out »

Les configurations « inside-out » et « outside-out » sont obtenues après excision d'un morceau de membrane plasmique par la pipette de patch. La face interne de la membrane est orientée vers l'extérieur de la pipette en configuration « inside-out ». A l'inverse, la face externe de la membrane baigne dans le milieu extracellulaire en configuration « outside-out » (figure 16). Ces deux configurations permettent d'enregistrer l'activité d'un ou de quelques canaux ioniques présents sur la portion de membrane excisée.

Les courants ioniques, en condition de potentiel imposé, ont été enregistrés à l'aide d'un amplificateur de patch-clamp Axopatch-1D (Axon Instruments, USA). Le contrôle de stimuli et l'acquisition des données ont été réalisés grâce à un ordinateur IBM-PC (USA) couplé à un convertisseur analogique/digital (Labmaster TL-1 interface, Axon Instruments, USA). L'enregistrement et l'analyse des données s'effectuent grâce au logiciel Pclamp 5.5.1 (Axon Instruments, USA).

3 - Mesures de la concentration cytosolique en calcium par fluorescence

L'utilisation de sondes fluorescentes permet de quantifier le Ca^{2+} libre dans des cellules vivantes, de mesurer le pH et de visualiser les changements intracellulaires d'un ion considéré. Le principe de mesure de la concentration intracellulaire en ions Ca^{2+} libres

($[Ca^{2+}]_i$) se base sur la capacité de molécules (appelées sondes) de voir leurs propriétés fluorescentes se modifier quand elles se lient au calcium.

Les sondes fluorescentes possèdent une haute affinité pour un ion spécifique. Ainsi, le fura 2, que nous employons, est spécifique de l'ion Ca^{2+} .

3.1- Structure et propriétés physico-chimiques du fura 2

Le fura 2 est une sonde calcique dite « à double excitation » dérivée du fluorophore stilbène possédant 4 fonctions carboxyliques ayant un arrangement spatial octacoordonné caractéristique des chélateurs calciques comme l'EGTA ou le BAPTA (figure 17). Lors d'une augmentation en calcium, le pic du spectre d'excitation est déplacé de 380 nm (λ=380 nm pour le fura 2 libre de calcium) vers des valeurs proches de 340 nm (λ=340 nm pour le fura 2 saturé en calcium) (figure 18). Le spectre d'émission possède un seul pic centré à une longueur d'onde de 510 nm (Grynkiewiecz *et al.*, 1985). Les mesures des rapports d'intensité de fluorescence (R= F340/F380), permettant de déterminer les variations de la $[Ca^{2+}]_i$ dont la valeur réelle est calculée, après calibration, grâce à l'équation de Grynkiewicz :

$[Ca^{2+}]_i = Kd\ \beta\ (R-Rmin) / (Rmax-R)$ où :

- Kd : constante de dissociation du fura 2 (d'après Grynkiewicz *et al.*, 1985) ;
- β : rapport du signal de fluorescence pour λ=380 nm en absence de calcium et à saturation en calcium ;
- R= F340/F380 mesuré après correction de l'autofluorescence ;
- Rmax : rapport maximum enregistré quand le fura 2 est saturé en calcium ;
- Rmin : rapport de fluorescence minimum du fura 2 en absence de calcium.

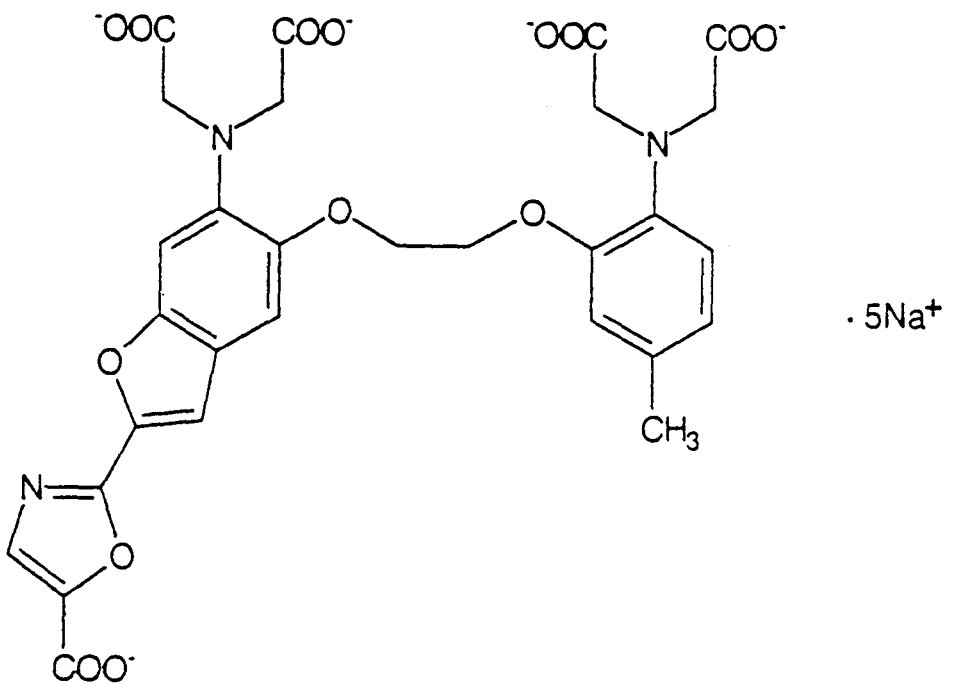

Figure 17 : Structure de la sonde calcique fluorescente fura 2 (forme acide + 5 cations d'accompagnement).

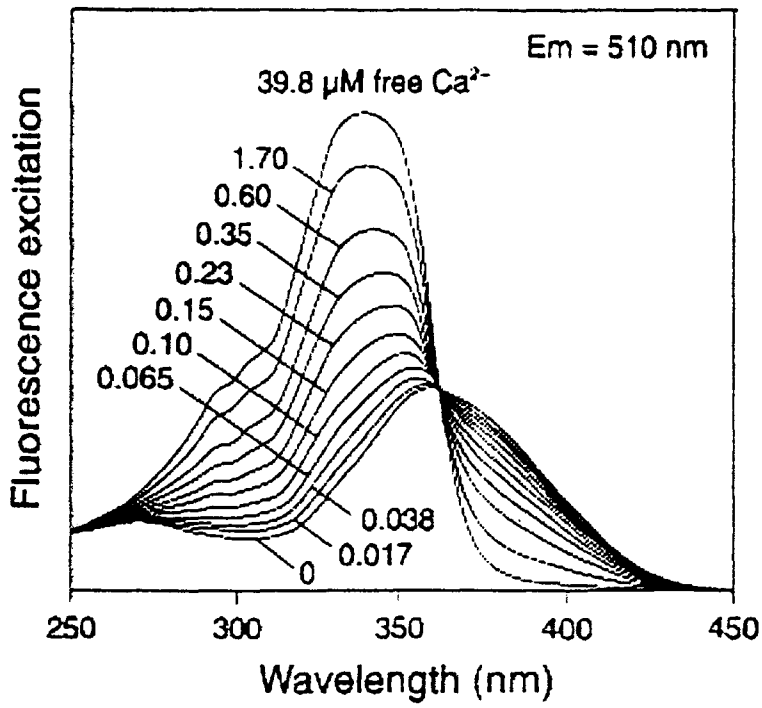

Figure 18: Spectre d'émission de la sonde fura 2 en fonction de la concentration de calcium.

3.2- Charge des cellules en fura 2

Le fura 2 existe sous deux formes :

- la forme libre, acide et non perméante : le fura 2 proprement dit. Cette molécule est hydrophile et sa fluorescence dépend du calcium ;
- la forme estérifiée, lipophile, non chargée et perméante : le fura 2 acétométhyl ester (fura 2/AM). Cette molécule pénètre de façon passive dans les cellules. Les estérases cytosoliques endogènes vont libérer la forme acide, par hydrolyse, qui sera alors piégée dans les cellules.

La charge des cellules correspond à l'incorporation du fura 2. Le protocole utilisé est différent selon la forme de fura 2 employée.

3.2.1- Charge par la forme acide

Le fura 2 acide (Calbiochem, France) pénètre dans la cellule grâce à la technique de patch-clamp en configuration « cellule entière » par dialyse passive à partir de la pipette d'enregistrement. En effet, le fura 2 est ajouté à la solution interne qui remplit la pipette de patch (concentration 50 à 100 µM). La charge de la cellule s'effectue durant 2 à 3 mn jusqu'à l'obtention d'u

n équilibre entre le compartiment cytosolique et le compartiment intrapipette.

3.2.2- Charge par la forme AM

Les cellules sont incubées durant 45 mn à 37°C, dans une solution d'HBSS contenant 2.5 µM de fura 2/AM (Calbiochem, France). Ce laps de temps permet l'obtention d'une charge homogène. Les cellules sont rincées trois fois avec de l'HBSS afin d'éliminer toutes traces de sonde résiduelle du milieu extracellulaire.

3.3- Calibration du signal de fluorescence

3.3.1- Calibration *in vitro*

La valeur du rapport Rmax est mesurée *in vitro* en employant du fura 2 acide (2 µM) dans de l'HBSS contenant 10 mM de $CaCl_2$. Le valeur Rmin est mesurée dans de l'HBSS dépourvu de $CaCl_2$ et en présence de 10 mM d'EGTA. Nous mesurons d'autre part le rapport de fluorescence pour une concentration intermédiaire en calcium : 500 nM Ca^{2+}. La valeur de Kd.β est calculée grâce au rapport F340/F380 déterminé pour cette concentration intermédiaire en Ca^{2+} en connaissant Rmax et Rmin. La courbe de calibration obtenue indique la gamme de concentration calcique que nous pouvons mesurer avec le fura 2, allant de quelques nM à quelques µM.

La calibration *in vitro* est la plus communément employée au cours de nos expériences.

Il est nécessaire de réaliser une calibration spécifique pour chaque système optique utilisé.

3.3.2- Calibration *in vivo*

Il est possible d'effectuer également une calibration *in vivo* (avec du fura 2/AM ou du fura acide chargé grâce à une électrode de patch). Nous utilisons la ionomycine (5 µM), formant des pores, afin que le calcium s'équilibre de part et d'autre de la membrane plasmique. Nous mesurons les valeurs des rapport F340/F380 pour les mêmes concentrations en calcium extracellulaire que lors des calibrations *in vivo* et *in vitro*. Les valeurs obtenues lors des calibrations *in vitro* et *in vivo* ne sont pas strictement identiques. En effet, la fluorescence de la sonde dépend de l'environnement dans lequel elle baigne et peut être

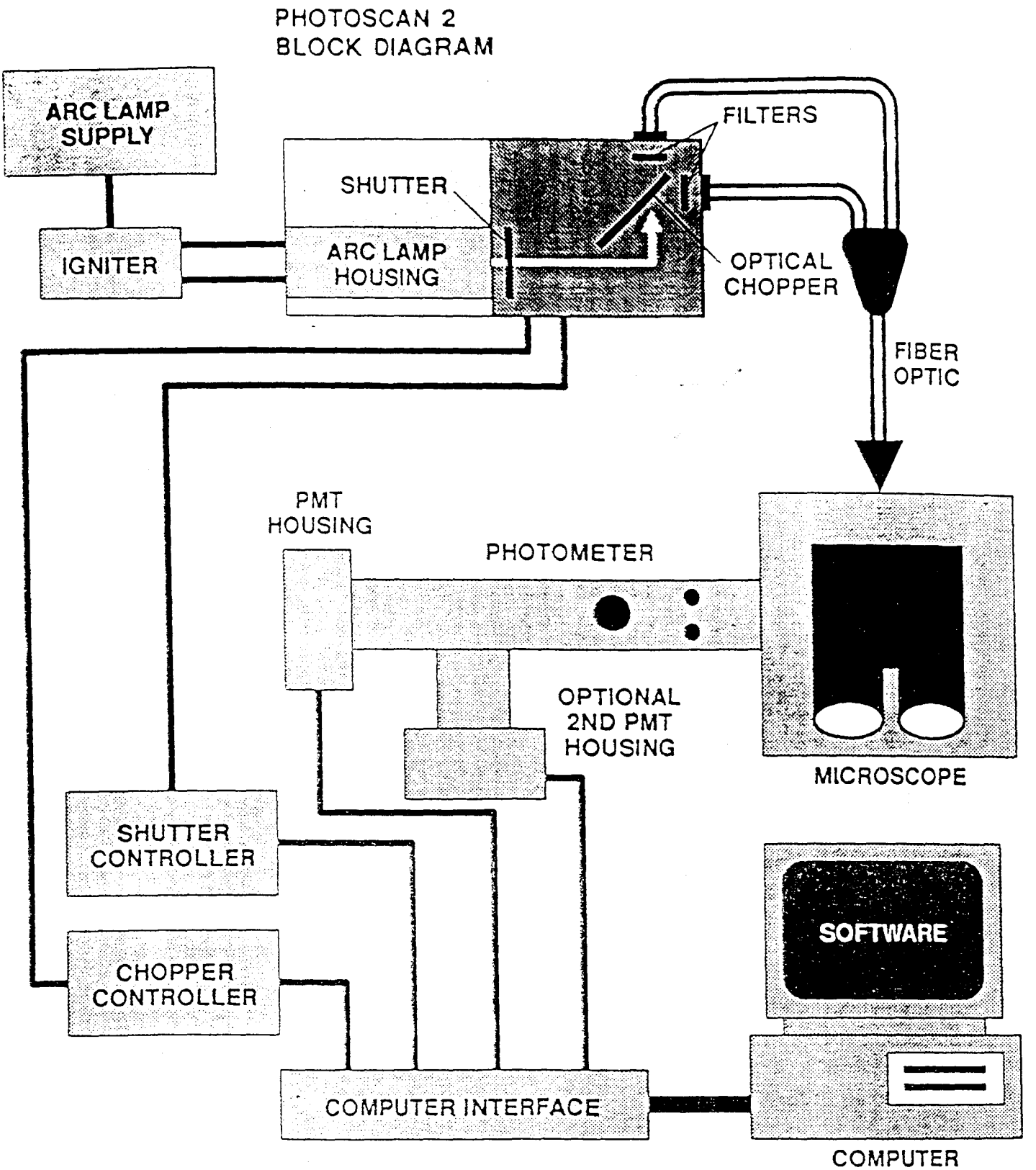

Figure 19 : Schéma du système de photométrie.

attribuée principalement à la viscosité du cytoplasme (Williams *et al.*, 1990 ; Poenie, 1990). Par ailleurs, il est à noter que les valeurs de fluorescence mesurées *in vivo* sont inférieures de 15 % en moyenne en comparaison à celles mesurées *in vitro* (Moore *et al.*, 1990).

3.4- Equipement optique

L'équipement optique diffère selon que l'on utilise l'approche photométrique ou l'imagerie calcique pour la mesure des variations de calcium cytosolique.

3.4.1- en photométrie

Le dispositif de mesure est schématisé dans la figure 19. L'équipement est composé d'un microscope inversé à épifluorescence (Nikon, Diaphot TMD/100, Japon) et d'un système adapté aux mesures utilisant la sonde fura 2 (PTI, USA). La source lumineuse provient d'une lampe au xénon (Osram, 75 W). L'obturateur règle le passage de la lumière en fonction de la fréquence d'échantillonnage. La lumière est transmise au travers d'un iris (qui ne laisse passer que les photons ayant des longueurs d'ondes inférieures à 550 nm). Un filtre UV sélectionne les longueurs d'ondes ultraviolettes comprises entre 300 et 400 nm. Les UV se dirigent ensuite vers un miroir dont la position peut être modifiée très rapidement par un galvanomètre. Ce miroir reflète alternativement la lumière à une longueur d'onde de 340 nm et 380 nm. La lumière, véhiculée par des fibres optiques, sera alors reflétée vers la préparation par un miroir dichroïque à 400 nm. Une partie de la fluorescence émise est captée par l'objectif (UV, X20), retraverse le miroir dichroïque à 400 nm (λ émission = 510 nm), puis arrive sur un filtre interférentiel (λ=510±20 nm) puis est dirigée vers un photomètre. Cet appareil transforme les variations d'intensité de fluorescence en variation de potentiel. Les signaux sont recueillis par une interface reliée à un ordinateur. Le signal est alors traité selon l'équation de Grynkiewicz en concentration de calcium intracellulaire grâce au logiciel Felix

(PTI, USA). La fréquence d'échantillonnage employée est d'une valeur du rapport F340/F380 par seconde.

3.4.2- en imagerie calcique

L'équipement (Applied Imaging, GB) est composé d'un microscope à épifluorescence (Nikon Diaphot 300), d'une lampe au xénon, d'une caméra CCD (12 bits), d'un ordinateur dont le logiciel « quanticell 900 » permet la stimulation, l'acquisition et l'analyse des images.

La lampe au xénon émet de la lumière dont la longueur d'onde est réglée à l'aide d'un monochromateur. Les UV cheminent via une fibre optique et traversent les miroirs dichroïques, spécifiques de l'utilisation du fura 2 et ayant les mêmes propriétés physiques que ceux employés en photométrie. Les images à 510 nm sont capturées par la caméra CCD et visualisées en fausse couleur en fonction de leur intensité lumineuse sur l'écran de l'ordinateur (gamme allant du bleu au rouge, respectivement pour des concentrations basses à élevées en calcium intracellulaire). La fréquence d'échantillonnage moyenne utilisée est d'une image toutes les 4 secondes.

3.5- Composition des milieux d'enregistrement et substances pharmacologiques utilisées

3.5.1- Milieux de remplissage des pipettes : milieux « internes »

La composition des solutions intrapipettes utilisées varie en fonction de la nature du courant que l'on désire observer et selon la technique électrophysiologique employée.

- En configuration « whole cell »

La solution intrapipette est la suivante (en mM) :KCl 150 ; $MgCl_2$ 2 ; EGTA 1.1 ;

Hepes 5 (pH=7.3 ; 290 mosmol.l^{-1}).

- En patch perforé

KCl 55 ; K_2SO_4 70 ; $MgCl_2$ 7 ; $CaCl_2$ 1 ; D-glucose 5 ; Hepes 10 ; nystatin 200µg/ml (pH=7.3 ; 290 mosmol.l^{-1}).

- En configurations « inside-out » et « outside-out »

« Outside-out » : KCl 150 ; $MgCl_2$ 2 ; EGTA 1.1 ; Hepes 5 (pH=7.3 ; 290 mosmol.l^{-1}).

« Inside-out » : NaCl 140 ; KCl 5 ; $CaCl_2$ 2 ; MgCl2 2 ; Na_2HPO_4 0.3 ; KH_2PO_4 0.4 ; $NaHCO_3$ 4 ; D-glucose 5 ; Hepes 10 (pH= 7.3 ; 300-310 mosmol.l^{-1}).

3.5.2- Milieux extracellulaires

Le milieu extracellulaire est l'HBSS (Hank's Buffer Salt Solution). Nous l'employons en électrophysiologie, en microspectrofluorimétrie et en imagerie calcique. Sa composition est la suivante (en mM) : NaCl 140 ; KCl 5 ; $CaCl_2$ 2 ; MgCl2 2 ; Na_2HPO_4 0.3 ; KH_2PO_4 0.4 ; $NaHCO_3$ 4 ; D-glucose 5 ; Hepes 10 (pH= 7.3 ; 300-310 mosmol.l^{-1}) ; en configuration « whole cell » et « outside-out ». En configuration « inside-out », le milieu extracellulaire est le suivant : KCl 150 ; $MgCl_2$ 2 ; EGTA 1.1 ; Hepes 5 (pH=7.3 ; 290 mosmol.l^{-1}).

3.5.3- Substances pharmacologiques employées

- Hormones

- Prolactine ovine (5 nM ; National Hormon Pituitary Program ; Torrance ; USA) ;
- 5α-dihydrotestosterone (Sigma) ;
- Testostérone (Sigma).

- Inhibiteurs de canaux potassiques

- TEACl (chlorure de tetraéthylammonium Composition des milieux d'enregistrement et substances pharmacologiques; 200 µM ; Sigma) ;

- α dendrotoxine (DTX ; 5 nM ; Sigma);
- Mast Cell Degranulated Peptide (MCDP ; 80 nM ; Sigma);
- 4 amino-pyridine (4 A-P ; 1 mM ; Sigma) ;
- charybdotoxine (CTX ; 30 nM ; Latoxan) bloque les canaux potassiques activés par le calcium et les canaux potassiques de type Kv1.3 ;
- iberiotoxine (IBTX ; 10 nM ; Latoxan);
- quinidine (1 μM ; Sigma);
- margatoxine (MGTX ; 1 mM ; Latoxan) bloque les canaux potassiques de type Kv1.3 et Kv1.6;
- vérapamil (concentration 10 μM ; Sigma) inhibiteur de canaux potassiques, calciques de type et d'une p glycoprotéine impliquée dans les phénomènes de « Multi Drug Resistance ».

- Substances agissant sur le métabolisme calcique

- Thapsigargine (10 μM ; Sigma) : inhibiteur des pompes calciques présentes sur la membrane du réticulum endoplasmique ;
- Ionomycine (5 μM ; Sigma) : forme des pores dans la membrane calcique et permet d'équilibrer les concentrations en calcium intra et extracellulaire ;
- Ryanodine (Calbiochem) : agoniste (pour des concentrations inférieures à 10 μM) ou antagoniste (pour des concentrations supérieures à 10 μM) aux récepteurs à la ryanodine présents sur la membrane du réticulum endoplasmique ;
- 4 chloro-m-crésol (10 μM, Calbiochem) : agoniste des récepteurs à la ryanodine.

- Autre substance utilisée

- génistéine (10 μM, Sigma) : inhibiteur des tyrosine kinases.

4- Mesures de l'apoptose

Les mesures du nombre de cellules apoptotiques ont été réalisées par le docteur Xuefen LE BOURHIS du Laboratoire de Biologie du Développement (U.S.T.L., Villeneuve d'Ascq).

Le bisbenzimide (Hoescht 33528 Sigma) est un agent intercalant de l'ADN permettant la visualisation de la chromatine en microscopie à fluorescence. Les cellules, cultivées sur des lamelles de verre traitées au collagène, sont fixées au méthanol (-20°C) pendant 10 minutes. Après 3 rinçages au PBS 1X (phosphate Buffered Saline), les cellules sont incubées à l'obscurité avec la solution de Hoescht (1 mg/ml), pendant 30 minutes, à température ambiante. Par la suite, les cellules sont rincées 2 fois au PBS 1X. Les lamelles sont montées sur lame (au glycergel) et conservées à l'obscurité. Les différentes morphologies des noyaux apoptotiques telles que la condensation périnucléaire de la chromatine, l'hyper-condensation de la chromatine et la formation de vésicules apoptotiques sont observées au microscope à épifluorescence Olympus BH2 (λ excitation = 435 nm).

5- Mesures de la prolifération cellulaire

Les mesures de prolifération cellulaire ont été réalisées par le docteur Xuefen LE BOURHIS du Laboratoire de Biologie du Développement (U.S.T.L., Villeneuve d'Ascq). L'évaluation de la prolifération cellulaire a été faite par comptage du nombre de cellules et par incorporation de thymidine tritiée dans l'ADN des cellules en culture. Les cellules sont incubées en présence de thymidine tritiée (1 μCi/ml) pendant 2 heures. Après 2 lavages au PBS 1X, les acides nucléiques sont précipités grâce à une solution d'acide trichloroacétique à 10% (Sigma, France). La radioactivité est par comptage dans du liquide de scintillation.

RESULTATS

ET

DISCUSSION

PREMIERE PARTIE

ETUDE DES EFFETS DE LA PROLACTINE, *IN VIVO*, SUR LA CROISSANCE DE LA PROSTATE

De fortes présomptions existent quant à l'influence de la PRL sur la croissance de la prostate :

- les cellules prostatiques possèdent des récepteurs à la prolactine (Nevalainen *et al.*, 1997) ;
- la prostate humaine et la prostate de rat synthétisent de la PRL qui pourrait agir de manière autocrine/paracrine sur la prolifération des cellules épithéliales (Nevalainen *et al.*, 1997) ;
- le taux de PRL augmente avec l'âge chez l'homme et le rat (Vekemans*et al.*, 1975), alors que la testostérone suit une évolution inverse (Davidson *et al.*, 1983). Ce phénomène se développe parallèlement à la croissance des HBP ;
- les cancers de la prostate sont souvent associés à des taux élevés de PRL plasmatique (Yatani *et al.*, 1987 ; Tasar *et al.*, 1986).

Malgré toutes ces données, la PRL n'est pas prise en compte dans les traitements hormonaux des HBP et des cancers de la prostate. Il est donc capital de connaître la manière dont la PRL agit sur la physiologie et la physiopathologie prostatique.

1- Effets de l'hyperprolactinémie sur la prostate de rat

Afin d'étudier les effets de la PRL sur la prostate, nous avons développé un modèle animal sur lequel nous avons induit une augmentation du taux de PRL dans le sang. Au cours de cette étude, nous avons caractérisé d'une part, les effets directs de l'hyperprolactinémie sur la croissance de la prostate de rat et d'autre part, la dépendance éventuelle des effets de la PRL vis-à-vis des androgènes. Des rats mâles adultes de souche Wistar ont été traités avec du sulpiride, un inhibiteur des récepteurs dopaminergiques de type 2 qui contrôlent la sécrétion de PRL par les cellules lactotropes de l'hypophyse antérieure. Ainsi, le sulpiride provoque une augmentation de la sécrétion de PRL hypophysaire (Debeljuk *et al.*, 1975; Nakagawa *et al.*, 1982). Nous avons établi plusieurs lots d'animaux (30 lots de 5 rats): animaux témoins, castrés, castrés-surrénalectomisés, castrés ayant reçu un implant de T ou de DHT et leurs contrôles négatifs respectifs.

Cette étude a conduit à la rédaction du manuscrit suivant, actuellement soumis au journal « Endocrinology ».

CONCLUSION

Cette étude a permis de démontrer les points suivants :

- **une augmentation par 6 du taux de PRL induit spécifiquement une hyperplasie et une hypertrophie glandulaire de la prostate latérale de rat. Ce résultat est fondamental, car le lobe latéral de la prostate de rat est homologue à la région de la prostate humaine où les HBP se développent (Price, 1963) ;**

EFFECTS OF HYPERPROLACTINEMIA ON THE RAT PROSTATE GROWTH: EVIDENCE OF ANDROGENO-DEPENDENCE.

Abbreviated title : Effects of hyperprolactinemia on the rat prostate growth.

Key words : prolactin, testosterone, dihydrotestosterone, rat prostate growth.

Fabien VAN COPPENOLLE, Christian SLOMIANNY, Françoise CARPENTIER*, Xuefen LE BOURHISΥ, Ahmed AHIDOUCH, Dominique CROIX #, Guillaume LEGRAND, Sarah FOURNIER, Henri COUSSE§, Dominique AUTHIE‡, Jean-Pierre RAYNAUD∅, Jean-Claude BEAUVILLAIN#, Jean-Paul DUPOUY⊗ and Natalia PREVARSKAYA.

Laboratoire de Physiologie Cellulaire; USTL; INSERM EPI-9938; Bâtiment SN3; 59655 Villeneuve d'Ascq Cedex; FRANCE.

*Service d'Anatomo-pathologie; Centre Hospitalier de Roubaix; Bd Lacordaire; 59056 Roubaix Cedex1; FRANCE.

ΥLaboratoire deBiologie du Développement; USTL; Bâtiment SN3; 59655 Villeneuve d'Ascq Cedex; FRANCE.

#Laboratoire de Neuroendocrinologie et de Physiopathologie neuronale; INSERM U422; Place de Verdun; 59045 Lille Cedex; FRANCE.

⊗Laboratoire de Neuroendocrinologie du Développement; USTL; Bâtiment SN4; 59655 Villeneuve d'Ascq Cedex; FRANCE.

§Laboratoire Pierre Fabre; La Chartreuse; 81106 Castres; FRANCE.

‡ Laboratoire Pierre Fabre Médicaments ; 81106 Castres Cedex; FRANCE

∅Université Pierre et Marie Curie, 75006 Paris; FRANCE.

Corresponding author's Address : Fabien VAN COPPENOLLE ; Laboratoire de Physiologie Cellulaire ; Centre de Biologie Cellulaire ; U.S.T.L. ; INSERM EPI 9938 ; Bâtiment SN3 ; 59655 Villeneuve d'Ascq Cedex ; France ; Tel : (33) 3 20 43 40 77 ; Fax : (33) 3 20 43 40 66 ; E-mail : fvancopp@pop.univ-lille1.fr

ABSTRACT:

The polypeptide hormone prolactin (PRL) is one of the non-steroid factors assumed to be involved in the proliferation of prostate cells and in the development and regulation of BPH and prostate cancer . However, PRL mechanisms and their effects on the prostate are not very well-known.

This study characterizes the action of PRL, alone or associated with androgens (testosterone (T) or dihydrotestosterone (DHT)), on the rat prostate gland. The effects of PRL and androgens were investigated over a period of 30 and 60 days in 22 groups of 5 Wistar rats: control, castrated, castrated with a substitutive implant of T or DHT, and sham operated. Hyperprolactinemia was induced with chronic injections of sulpiride (40 mg/kg/day), which enhances pituitary PRL release.

Of the three prostate lobes (ventral, dorsal and lateral), the lateral lobe was the most sensitive to an increase in plasma PRL level. Hyperprolactinemia increased the weight of the lateral prostate (LP) after 30 and 60 days in control (by factors of 4.1 and 2, respectively), in castrated-T implanted (by factors of 2.4 and 3, respectively) and in castrated-DHT implanted rats (by factors of 1.6 and 3.2, respectively). Hyperprolactinemia was ineffective without androgens. Sulpiride produced a glandular hyperplasia in the LP associated with inflammation. Furthermore, sulpiride treatment induced a rise in bcl-2 expression in prostate cells, which may have inhibited the level of apoptosis.

These results show that the growth of the rat prostate is under PRL control in synergy with androgens. We demonstrated that PRL may inhibit LP epithelial cell apoptosis by overexpressing bcl-2. This model could be a useful *in vivo* approach for studying the hormonal regulation of normal and pathological prostate development.

INTRODUCTION:

Benign prostatic hyperplasia (BPH) and prostate cancer have become a major health problem for men, due to the constant increase in human life expectancy: BPH is the most common benign tumor and prostate cancer is the second cause of cancer-related death in the western world in men (1).

It has now been clearly established that the growth, differentiation (2-4), and programmed cell death (5) of prostate cells are regulated by androgens. For this reason, the main treatment for prostate tumors consists of inhibiting cell growth by suppressing the action or production of endogenous androgens (6). However, in spite of this treatment, almost all tumors, and especially malignant tumors, continue to progress. The background of this clinical phenomenon is poorly understood. However, it has become obvious that other, non-androgenic factors, such as peptide hormones (7-9) and growth factors (10), are involved in prostate cell growth regulation.

The polypeptide hormone prolactin (PRL) is one of the non-steroïdal factors assumed to be involved in the proliferation of prostate cells (11) and in the development and regulation of BPH and prostate cancer (12-15).

PRL levels increase with age (10,16); while testosterone levels decrease (17,18), indicating that the role of PRL in the development of prostate hyperplasia becomes increasingly important with age. Using organ cultures, Nevalainen *et al.* (15) have shown, that PRL induces differentiation and proliferation in rat and human prostate. These PRL actions are mediated through the signal transduction pathways triggered by both the short and long forms of PRL receptors. Furthermore they showed that the rat prostatic epithelial cells express prolactin mRNA and protein and demonstrated an overall distribution of prolactin mRNA in the dorsal and lateral prostate (14). Some works have suggested that PRL promotes the growth and proliferation of prostate cells in synergism with androgens (19). It was also proposed that PRL

could increase free steroid concentrations in the blood, as well as the uptake of testosterone (T) in prostate cells (20). On the other hand, it has been suggested that PRL has an independent action on prostatic growth and metabolism (21-23). However, PRL mechanisms and their effects on the prostate are not very well-known. Some *in vitro* models of the prostate have been developed to investigate these problems, but an analysis of the independent and combined *in vivo* actions of these hormones is lacking. The interest of such an approach was shown by a study of PRL-transgenic mice (24), demonstrating a dramatic prostate enlargement.

The aim of the present study was to investigate the long-term effects of increased PRL levels in combination with androgens on the different lobes of rat prostate gland by creating a new *in vivo* model. Hyperprolactinemia was induced by daily injection of 40mg/kg of sulpiride, an antagonist of the type 2 dopamine receptor (D2) by which dopamine inhibits PRL secretion (25,26). In order to study the possible synergism between PRL and androgens (T or DHT), castrated groups of animals were formed, including some groups with subcutaneous implants of T and DHT. We now report the chronic effects of PRL-induced enlargement and inflammation of the lateral rat prostate without any histological changes on ventral and dorsal lobes.

MATERIALS AND METHODS:

Animals:

110 male Wistar rats (200-220 g) from IFFA CREDO, France, were used. These animals were conditioned for one week prior to experimentation. Rats were randomized and housed five per cage on a 12h light- 12h dark cycle. They were provided *ad libitum* with water and a standard laboratory chow.

During this work, all animal studies were conducted in accordance with the European Communities Council ruling of 24 November 1986 (86/609/EEC).

Methods:

- Surgical procedures:

All surgeries were performed on day 1 under ether anesthesia and strict sanitized conditions. The operated animals were treated with antibiotics (penicillin) to prevent infections.

Castrations were performed on day 1 via scrotal route by removing epididymal fat pads with the testes. The sham castrated rats were opened and their testes were dissected but not removed. Operated animals were then sutured and the injured areas were disinfected with betadine solution and sprayed with aluspray (Vetoquinol).

In order to add the desired quantity of exogenous androgens for comparison with control animals, we implanted silastic medical-grade silicone tubing (0.078 i.d. X 0.125 o.d.: Dow Corning Corp., Midland, MI) (1 cm length), filled with either testosterone (Sigma) or dihydrotestosterone (Sigma), subcutaneously over the scapula. One end of the tubing was sealed with adhesive (Silastic Medical Adhesive: Dow Corning) according to Robaire *et al* (27). After loading with the hormone, the unsealed end was sealed with adhesive. After the adhesive had hardened, the implants were put overnight in distilled water. It has been found that a 2.5 cm implant mimics physiological testosterone level (27). The choice of a 1 cm implant was to produce a subnormal testosterone release.

The implants were inserted on day 8 in pockets formed over the dorsal area of the scapula. The incised area was disinfected, then sutured.

- Hyperprolactinemia induction:

Hyperprolactinemia was induced by daily intraperitoneal injections of a 40 mg/kg aqueous sulpiride solution (± sulpiride, Sigma). Control animals were intraperitoneally injected daily with the carrier alone (NaCl 0.9 %).

Sampling:

Since previous reports (28-30) indicated an increase of PRL during stress, sham castrated and solvent-injected groups were also evaluated. It had previously been shown that empty tubing implants had no effect on rat prostate growth (27,31,32).

Table 1 gives the surgical event (castrations, sham castrations, and implants) and treatment (daily intraperitoneal injections of sulpiride or NaCl 0.9%) schedule for the various experimental groups.

On the sacrifice's day, blood samples were collected in EDTA-coated capillaries and stored immediately on ice. Blood was centrifuged at 3000 rpm for 10 minutes. Plasma samples were frozen at -80°C until the hormonal assay was performed. The prostate lobes were dissected, weighed and treated for light microscopy, by fixing in 10 % neutral buffered formalin, dehydration and embedding in paraffin.

- Hormonal assays:

Plasma levels of PRL and Luteinizing Hormone (LH) were measured by RIA with materials supplied by the NIDDK rat pituitary hormone distribution program (Torrance, CA, USA) using rat RP3-PRL and rat RP3-LH as reference preparations. T and DHT levels were measured by RIA with TRK 600 kit (Amersham, UK) according to a protocol from the manufacturer.

- Histology:

Tissue pieces were fixed in 10% neutral buffered formalin and embedded in paraffin. Histological analysis were performed on serial sections obtained from prostatic samples stained by hematoxylin-erythrosin-saffron (HES).

-Bcl-2 labeling:

Immediately after dissection of the lateral prostate, pieces approximately 1 mm x 1 mm were fixed by immersion in paraformaldehyde (1.5 % in phosphate buffer saline, PBS) for 1.5 h

at 4 C. After several washes (the final wash lasted all night), the blocks were infused for the next 24 h in a mixture of sucrose (2.5 M) and polyvinyl pyrrolidone (20 %) then frozen in liquid nitrogen. 0.2 µm sections were cut and positioned on glass slides. The sections were blocked with 1.2 % gelatin in PBS (PBSG) for 30 min to avoid nonspecific binding, and subsequently incubated overnight at 4 C in 100 % humidity with the primary antibodies for Bcl2 (polyclonal rabbit IgG, Calbiochem). After several washes in PBSG, the slides were incubated for 1 hour at 37 C with secondary antibodies (donkey anti-rabbit IgG labeled with FITC, Jackson), washed in PBS and mounted in Mowiol. The sections were observed under a Zeiss Axiophot microscope equipped with epifluorescence (excitation : 450-490 nm, emission : 520 nm). Negative controls consisted of the omission of the primary antibody.

- Statistical analysis:

We expressed prostate weight relative to body weight, according to Robinette (31). Variations in both prostate weight and plasma hormone levels were studied. The Tukey test was used to establish significant differences. Significance was established at levels of $p<0.05$; $p<0.01$ and $p<0.001$.

RESULTS

The prostate is divided in three parts: the ventral lobe (VP), the lateral lobe (LP) and the dorsal lobe (DP).

Hormonal assays : Induction of chronic hyperprolactinemia in rats treated by sulpiride:

1) PRL level : As shown in table 2, sulpiride induced a rise in basal plasma PRL levels in all groups of animals treated. Sulpiride enhanced the basal PRL level by a factor of 6.2 under control conditions and 3.6 in castrated animals. In castrated DHT-implanted rats, sulpiride injections increased the basal PRL level by a factor of 12. PRL levels in solvent-injected animals were not significantly different from those in controls.

2) In non-castrated animals, hyperprolactinemia induced a decrease of 55.68% in LH levels and 30.83% in T levels. As anticipated, hyperprolactinemia did not modify T and DHT levels in castrated and castrated T- or DHT-implanted groups.

3) Orchidectomy induced a dramatic decrease in T and DHT levels as compared to control. T (1 cm) and DHT (1cm) implants restored T levels to 45.78% and DHT to 336.60 % of control, respectively.

4) We also studied castrated-adrenalectomized, castrated-adrenalectomized-sulpiride-injected, sham castrated-sham adrenalectomized, and sham castrated-sham adrenalectomized solvent-injected groups in order to assess the role of adrenals in prostate growth. We did not notice any significant differences between T or DHT levels in castrated and castrated-adrenalectomized animals (data not shown).

The effects of hyperprolactinemia on the wet weight of prostate lobes:

The wet weight of the prostate was examined when the animals were killed after 30 and 60 days of treatment with sulpiride, respectively.

Figure 1 illustrates the wet weight of the LP after 30 days of sulpiride treatment under various experimental conditions. In castrated and implanted animals, T and DHT induced an increase in the wet weight of the lateral lobe by factors of 3.8 and 5.1, respectively, compared to castrated rats.

Sulpiride injections enhanced the weight of lateral lobes in non castrated animals 4.1 times compared to control. In castrated, T implanted animals, sulpiride induced a 2.4-fold increase in the lateral lobe weight, compared with non-injected rats. In castrated, DHT-implanted animals, hyperprolactinemia in those treated with sulpiride enhanced the growth of the LP by a factor of 1.6 compared to non-injected rats. There were no measurable differences between the lateral lobes of castrated and castrated, sulpiride-injected groups. No enlargement of the LP was observed after sham surgery and/or solvent injections.

Similarly, after 60 days, T and DHT enhanced the weight of the LP in castrated rats implanted with T or DHT by factors of 5.3 and by 3.6, respectively, compared to castrated animals, as shown in figure 1. Sulpiride injections induced a 2-fold increase in the LP wet weight in non-castrated animals, as compared to control, and a 3-fold increase in those of castrated, T-implanted and sulpiride injected animals compared to non-injected rats. In the castrated, DHT-implanted and sulpiride injected group, PRL enhanced the wet weight of the LP by a factor of 3.2 compared to non-injected animals.

No significant differences were observed between the LP of castrated and castrated-sulpiride-injected groups after 30 and 60 days. No enlargement of the LP occurred after sham surgery and solvent injections.

We also measured the relative weights of the VP and the DP after all the types of treatment described in table 1. The analysis of these data showed that hyperprolactinemia only have a little or any effects on the growth of the VP and DP after 30 or 60 days of treatment. PRL enhances the growth of the VP only in control conditions after 30 days by a factor 1.4 and after 60 days by a factor 1.2 (Fig.2). We did not notice a significant difference between the wet weight of the DP after 30 days in the rats treated with sulpiride (Fig.3). On the contrary, in control conditions and after 60 days, sulpiride treatment induced a 1.8-fold increase in the DP weight (Fig. 3).

The weights of the LP, VP and DP in castrated, adrenalectomized, sulpiride-injected animals were similar to those of castrated-adrenalectomized and castrated rats (data not shown).

Induction of glandular hyperplasia of lateral prostate in sulpiride-treated rats:

Similar histological aspects were observed after 30 and 60 days of experimentation. Sulpiride had no effect on ventral and dorsal prostate morphology.

The lateral prostate of normal (Fig. 4A), sham-castrated and solvent injected rats (data not shown) were most frequently composed of nearly the same proportion of small and large glands, both limited by columnar epithelial cells. The lateral prostate lobes of castrated rats without any substitutive treatment presented atrophy with a large majority of small glands (Figure 4B). The LP atrophy of castrated animals receiving a substitutive treatment with T (Figure 4C) or with DHT (data not shown) was particularly attenuated compared to LP of sham-castrated rats (Figure 4B).

Lateral prostates from castrated, T- implanted rats (Figure4D) and normal (data not shown) receiving additional sulpiride treatment showed an increased proportion of large glands, some containing numerous intra-luminal neutrophils (Figure 4E). Similar histological aspects were observed in the LP of castrated, DHT-implanted animals receiving additional sulpiride treatment (data not shown). The connective tissue surrounding these inflamed glands was focally infiltrated by lymphocytes, a few neutrophils and macrophages, and thickened by a discrete fibroblastic and collagenic fibrosis, sometimes associated with a slight muscular hyperplasia (Figure 4F).

Thus, in the presence of androgenic activity, sulpiride treatment seems to induce lateral prostatic glandular hyperplasia, and, to a lesser extent, a fibromuscular hyperplasia, focally associated with non-specific, acute, chronic inflammation.

Overexpression of Bcl-2 in the LP of control and sulpiride-treated rats:

The control LP sections showed a spotted cytoplasmic labeling (organelles, except the nucleus) on the whole epithelial cells (Fig. 5A). In control and sulpiride-treated LP, the labeling was intensified in the epithelial cells bordering the acini, giving target-like images, brighter at the periphery of the acini (Fig. 5B). The infiltrated cells were only faintly labeled. In the VP, the labeling observed under control and control-sulpiride treated conditions was similar to that shown in the control LP sections (data not shown).

DISCUSSION

In this study, we demonstrate the effects of chronic hyperprolactinemia on rat prostate growth. A particularly significant alteration in the rats with chronic hyperprolactinemia was a dramatic enlargement of the lateral lobe. This lateral prostate hyperplasia was focally associated with acute, chronic inflammation.

In order to induce a chronic hyperprolactinemia, we used a model of long-term (30 and 60 days) androgen treatment associated with daily sulpiride injections. Sulpiride, a specific dopaminergic type-2 receptor inhibitor, is known to stimulate PRL secretion from the pituitary (25,26). It also has two actions on PRL plasma level: sulpiride initially induces a peak of prolactinemia in approximately 30 minutes (26 times the initial value), then, over the next two hours, PRL decreases, while remaining higher than the initial value (6 times the basal level) (25). Thus, a chronic (60-day) treatment with sulpiride causes a significant increase in plasma PRL level (62.54 ± 26.77 ng/ml) as compared with control (10.16 ± 2.57 ng/ml) or solvent-injected (18.9 ± 9.03 ng/ml) animals. In our experiments, the rats were sacrificed on the day after the last sulpiride injection, so the prolactinemia measured does not represent the PRL peak, but the chronic PRL level after 60 days treatment with sulpiride. There are other ways besides using dopaminergic antagonists to produce artificial hyperprolactinemia, e.g. alzet pumps containing PRL or transplanted pituitaries. However, these experiments are stressful for the animals and secondary PRL levels are stress-dependent. Furthermore, in the case of transplanted pituitaries, several other pituitary hormones are secreted. Thus, sulpiride treatment is the most convenient way of inducing hyperprolactinemia in rats.

Our experiments in castrated-adrenalectomized rats show that the contribution of the adrenals to endogenous androgen level support is negligible. Thus, the adrenals do not interfere with rat prostate growth. These results are in agreement with van Weerden *et al.* (33):

the authors measured a very low level of androstenedione and no detectable plasma concentrations of dehydroepiandrosterone in rat adrenal gland cell suspensions. On the contrary, in humans, the adrenals significantly contribute to the control of the androgen level (34).

The effects of hypeprolactinemia were only observed in the lateral lobe of the rat prostate, affecting wet weight, histological structure, and Bcl-2 expression. The dorsal and ventral lobes were insensitive to the rise in PRL. The lateral lobe is considered the most hormonosensitive part of the prostate (31,35,36). It has been shown that the dorsolateral lobes are the parts of the rat prostate that give rise to spontaneous and experimental tumors (37-39) with varied hormone responsiveness. Moreover, the lateral and dorsal lobes are considered to be the most homologous to the human prostate (23), where it has been suggested that PRL plays an important role in BHP and prostate cancer development (12-15).

Hyperprolactinemia, stimulated by daily sulpiride injections, induced a marked enlargement of the lateral prostate in non-castrated animals (4.1 times control after 30 days and 2 times control after 60 days). PRL had no effect on castrated animals. However, in castrated, T-implanted and castrated, DHT-implanted rats, the rise in PRL levels also increased the weight of the lateral prostate (by a factor of 2.4 for T- and 1.6 for DHT-, respectively, after 30 days and by a factor of 3 for T- and 3.2 for DHT-, respectively, after 60 days), suggesting that PRL acts in synergy with the androgens.

In our experiments, T (1 cm) implants partially restored (45 %) normal T level. Robaire *et al.* (27) showed that T (2.5 cm) implants are needed to restore the physiological T level in the rat. However, DHT (1 cm) implants increased the DHT level by 336 % as compared with the physiological level in non-castrated rats. This difference in T and DHT level recovery by using 1 cm implants is explained by the fact that the physiological level of DHT (formed by 5α-reductase from T) was lower (0.183 ± 0.032 ng/ml) than the T level (2.087 ± 0.272 ng/ml).

In non-injected rats, the T level was higher than in animals treated with sulpiride (Tab. 2). As it has been shown that hyperprolactinemia decreases the number of pituitary GnRH receptors and LH secretion (40,41), the T level, controlled by LH is, therefore, also reduced. Thus, in our experiments, the rise in the wet weight of the lateral prostate in the non-castrated sulpiride-injected animals could be explained by the rise in PRL level.

In men, the PRL level increases (10,16) and the T level diminishes with age (17,18). Some research has demonstrated the same changes in rat PRL (42) and T (43) levels. In our study, in castrated, T-implanted groups, the T level was 55 % less than control. We used 1 cm T implants (which deliver half a physiological T level) in order to mimic the T level of aging rats. In our work, the hyperprolactinemia induced by sulpiride produced LP hyperplasia. Thus, in old rats and in aging men, a rise in prolactinemia could be sufficient to induce prostate hyperplasia, even with lower T levels. In this *in vivo* model, it is possible to develop a hormonal environment similar to that of aging rats and elderly men.

Our histological studies demonstrate that hyperprolactinemia induces glandular hyperplasia in the lateral (but not the dorsal and ventral) prostate in the rats with increased PRL levels. An increase was observed in the proportion of large glands associated with inflammation. This was not the case in the lateral prostate of animals not injected with sulpiride. Robinette *et al.* (31) reported that estradiol-17β had a specific action on lateral prostate growth. Estradiol-17β causes inflammation in dorsolateral (36) and lateral rat prostates (44) that can be reduced by treatment with bromocriptine (a dopaminergic agonist, known to decrease PRL levels). So, the potent involvement of estradiol-17β in prostate dysplasia and inflammation implies PRL action. Moreover, an enlargement of the dorsolateral prostate was shown (24) in transgenic mice with an overexpressed PRL receptor, suggesting the implication of PRL in the growth of the prostate gland.

The mechanism by which PRL affects prostate growth is not yet known. In our study, we noticed synergistic effects between PRL and androgens. This phenomenon could be due to the fact that PRL is considered to be enhance the T effect (20), as well as increasing cytosol and nuclear androgen receptor levels in rats (19). Furthermore, androgens (19,45) and PRL (45,46) up-regulate PRL receptor levels in the rat prostate. Moreover, hyperprolactinemia induces the turnover of tissue DHT content in the lateral prostate (35,47,48). Some *in vitro* studies have demonstrated an independent action of PRL in prostate cells (21-23). PRL also has an androgeno-independent proliferative effect in the lateral rat prostate in organ culture (49). PRL receptors have been identified in the ventral prostate (50), as well as in both lateral and dorsal rat and human prostates (15). Some of these receptors are located on the basal and lateral surfaces of the epithelial cells (15). These receptors may fix circulatory PRL and induce the growth of the lateral prostate lobe in rats. Nevertheless, PRL receptors are also located on the apical surfaces of the secretory epithelial cells of prostatic acini (15). As the epithelial prostatic cells are joined by tight junctions, PRL receptors located on the apical surface of these cells are not accessible to circulatory PRL, unlike basolateral cell membrane receptors. However, in recent experiments, Nevalainen *et al.* (14,15) clearly demonstrated that prostatic epithelial cells were able to produce prolactin. They used *in situ* hybridization to show that the epithelium of dorsal and lateral rat prostates expressed prolactin mRNA and protein. Thus, prostatic PRL may act in an autocrine/paracrine manner in the prostate through apical receptors, where it may mediate some androgen actions. The incidence of serum hyperprolactinemia on prostatic PRL synthesis is unknown.

Interestingly, the experiments carried out by Nevalainen *et al.* (14) demonstrated that the expression pattern of PRL protein was different in the dorsal and lateral prostate. In the dorsal prostate, the cytoplasm of sparsely located, single epithelial cells was very strongly stained. In contrast, in the lateral lobe, the majority of the epithelial cells were stained but the

staining was less intense than in the dorsal prostate. These results probably explain the fact that, in our experiments, we did not observe the effect of PRL on the dorsal prostate.

In addition, for the first time, we observed a rise in the expression of the antiapoptotic protein Bcl-2 in the LP epithelial cells of non castrated animals treated with sulpiride. We did not notice this phenomenon in the VP. Bcl-2 is known to down-regulate apoptosis in prostate cells (51-54) as in other models (55-58). Bcl-2 also provides resistance to androgen depletion in androgen-sensitive human prostate cancer cells LNCaP (51). Thus, in this *in vivo* model of hyperprolactinemia, the overexpression of Bcl-2 in non castrated animals led to a decrease in the apoptosis level in the epithelial cells of the LP. This modifies the balance between proliferation and apoptosis, eventually causing the LP hyperplasia shown in the histological study. In the NB2 rat lymphoma cell line, PRL induced a 15-fold increase in the level of bcl-2 mRNA within 3 hours (59). The authors suggest that the trophic action of PRL results from suppression of the cell death induced by the rise in the expression of Bcl-2 (59,60). So, in our study, the enhancement of the LP weight may be explained by PRL-induced inhibition of apoptosis. Furthermore, the tissue-specific modulation of Bcl-2 expression by PRL in the rat prostate may explain the lack of sensitivity of the VP to PRL, even if each rat prostate lobe has PRL receptors (46, 61-63). The antiapoptotic action of PRL on prostate cells requires further investigation and may be useful in developing treatment.

In conclusion, the chronic hyperplasia model proposed in this work may serve as a useful approach for studying the development mechanism of prostate hyperplasia. This model, representing PRL-dependent hyperplasia, is probably close to the human pathology, where the implication of PRL is uncontested.

ACKNOWLEDGMENTS:

We would like to thank Etienne Dewailly, Ariane Bouteillier, Claudine Carbon and Christelle Milluy for carrying out the histological and immunohistochemical technical procedures. This work was supported by grants from A.R.T.P. (Association pour la Recherche sur les Tumeurs de la Prostate, FRANCE), Pierre Fabre Médicaments (FRANCE), the I.N.S.E.R.M. (Institut National de la Santé et de la Recherche Médicale; FRANCE), the A.R.C. (Association pour la Recherche sur le Cancer; FRANCE) and the Ligue Nationale contre le Cancer (FRANCE). We also thank the NIDDK and the National Hormone Pituitary Program (Torrance, CA, USA) for the gift of PRL and LH materials.

REFERENCES:

1. **Woolf SH** 1995 Screening for prostate cancer with prostate specific antigen. An examination of the evidence. Engl. J. Med. 333: 1401-1405
2. **Walsh PC** 1984 Benign prostatic hyperplasia: etiological considerations. Prog. Clin. Biol. Res. 145: 1-25
3. **Geller J** 1989 Pathogenesis and pathological treatment of benign prostatic hyperplasia. The Prostate suppl. 2: 95-104
4. **Horton R** 1992 Benign prostatic hyperplasia/ New Insights. J. Clin. Endocrinol. Metab. 74: 504A-504C
5. **Isaacs JT** 1984 Antagonistic effect of androgen on prostatic cell death. The Prostate. 5: 545-557
6. **Carraro JC, Raynaud JP, Koch G, Chisholm GD, Di Silverio F, Teillac P, Da Silva FC, Cauquil J, Chopin DK, Hamdy FC, Hanus M, Hauri D, Kalinteris A, Marencak J, Perier A, Perrin P** 1996 Comparison of phytotherapy (Permixon) with finasteride in the

treatment of benign prostate hyperplasia : a randomized international study of 1 098 patients. The Prostate. 29(4) : 231-240

7. **Abrahamsson PA, Wadström LB, Alumets J, Falkmer S, Grimelius L** 1986 Peptide-hormone and serotonin-immunoreactive cells in normal and hyperplastic prostate glands. Path. Res. Pract. 181: 675-683

8. **di Sant'Agnese PA** 1992 Neuroendocrine differentiation in carcinoma of the prostate. Diagnostic, prognostic, and therapeutic implications. Cancer. 70(1): 254-268

9. **Shah GV, Rayford W, Noble MJ, Austenfeld M, Weigel J, Vamos S and Mebust WK** 1994 Calcitonin stimulates growth of human prostate cancer cells through receptor mediated increase in cyclic 3',5'-monophosphate and cytoplasmic Ca^{2+} transients. Endocrinology. 134: 596-602

10. **Hammond GL, Kontturi M, Maattala P, Puukka M, Vihko R** 1977 Serum FSH, LH and prolactin in normal males and patients with prostatic diseases. Clin. Endocrinol. (Oxf) 7: 129-135

11. **Costello LC, Franklin RB** 1994 Effect of prolactin on the prostate. The Prostate 24: 162-166

12. **Kadar T, Ben-David M, Pontes JE, Fekete M, Schally AV** 1988 Prolactin and luteinizing hormone receptors in human benign prostatic hyperplasia and prostate cancer. The Prostate. 12(4): 299-307

13. **Janssen T, Kiss R, Schulman C** 1995 Organ culture of human tissue model of hormonal and pharmacological regulation of benign prostatic hyperplasia and of prostate cancer. Acta Urol. Belg. 14(3): 7-14

14. **Nevalainen MT, Valve EM, Ahonen T, Yagi A, Paranko J and Harkonen PL** 1997 Androgen-dependent expression of prolactin in rat prostate epithelium *in vivo* and in organ culture. FASEB J. 11: 1297-1307

15. **Nevalainen MT, Valve EM, Ingleton PM, Nurmi M, Martikainen PM and Harkonen PL** 1997 Prolactin and prolactin receptors are expressed and functioning in human prostate. J. Clin. Invest. 99: 618-627

16. **Vekemans M, Robyn C** 1975 Influence of age in serum prolactin levels in women and men. Br. Med. J. 4: 738-739

17. **Davidson JM, Chen JJ, Crapo L, Gray GD, Greenleaf WJ, Catania JA** 1983 Hormonal changes and sexual function in aging men. J. Clin. Endocrinol. Metab. 57: 71-77

18. **Nankin HR, Calkins JH** 1986 Decrease bioavailable testosterone in aging normal and impotent men. J. Clin. Endocrinol.Metab. 63: 1418-1420

19. **Prins GS** 1987 Prolactin influence of cytosol and nuclear androgen receptors in the ventral, dorsal and lateral lobes of the rat prostate. Endocrinology 120: 1457-1464

20. **Farnsworth WE** 1988 Prolactin effect on the permeability of human benign hyperplastic prostate to testosterone. Prostate 12 (3): 221-229

21. **Reiter E, Lardinois S, Klug M, Sente B, Hennuy B, Bruyninx M, Closset J and Hennen G** 1995 Androgen-independent effects of prolactin on the differents lobes of the immature rat prostate. Mol. Cell. Endocrinol. 112: 113-122

22. **Smith C, Assimos D, Lee C and Grayhack JT** 1985 Metabolic action of prolactin in regressing prostate: independent of androgen action. Prostate 6: 49-59

23. **Price D** 1963 Comparative aspects of development and structure in the prostate. Natl. Cancer Inst. Monogr. 12: 351-369

24. **Wennbo H, Kindblom J, Isaksson OGP and Tornell J** 1997 Transgenic mice overexpressing the prolactin gene develop dramatic enlargement of the prostate gland. Endocrinology 138: 4410-4415

25. **Debeljuk L, Rozados R, Daskal H, Velez V and Mancini AM** 1975 Acute and chronic effects of sulpiride on serum prolactin and gonadotropin levels in castrated male rats (38581). Proc. Soc. Biol. Med. 148 (2): 550-552

26. **Nakagawa K, Obara T, Matsubara M and Kubo M** 1982 Relationship of changes in serum concentrations of prolactin and testosterone during dopaminergic modulation in males. Clin. Endocrinol. 17: 345-352

27. **Robaire B, Ewing LL, Irby DC, Desjardins C** 1979 Interactions of testosterone and estradiol-17β on the reproductive tract of the male rat. Biol. Reprod. 21: 455-463

28. **Jahn GA, Deis RP** 1986 Stress-induced prolactin release in female, male and androgenized rats: influence of progesterone treatment. Endocrinology 110 (3): 423-428

29. **Donnerer J, Lembeck F** 1990 Different control of the adrenocorticotropin-corticosterone response and of prolactin secretion during cold stress, anesthesia, surgery, and nicotine injection in the rat: involvement of capsaicin-sensitive sensory neurons. Endocrinology 126 (2): 921-926

30. **Fujikawa T, Soya H, Yoshizato H, Sakaguchi K, Doh-Ura K, Tanaka M, Nakashima K** 1995 Restraint stress enhances the gene expression of prolactin receptor long form at the choroid plexus. Endocrinology 136(12): 5608-5613

31. **Robinette C** 1988 Sex-hormone-induced inflammation and fibromuscular proliferation in the rat lateral prostate. The Prostate 12: 271-286

32. **Paubert-Braquet M** 1996 Effect of *Serenoa repens* extract (Permixon) on estradiol/testosterone-induced experimental prostate enlargment in th rat. Pharmacol. Res. 34 (3-4): 171-9

33. **van Weerden WM, Bierings HG, van Steenbrugge GJ, de Jong FN, Schröder FH** 1992 Adrenal glands of mouse and rat do not synthesize androgens. Life Sci. 50(12): 857-861

34. **Mason JI, Bird IM, Rainey WE** 1995 Adrenal androgen biosynthesis with special attention to P450c17. Ann. NY Acad. Sci. 774: 47-58

35. **Schacht MJ, Niederberger CS, Garnett JE Sensibar JA, Lee C and Grayhack JT** 1992 A local direct effect of pituitary graft on growth of the lateral prostate in rats. The Prostate 20: 51-58

36. **Lane KE, Leav I, Ziar J, Bridges RS, Rand WM and Ho SM** 1997 Suppression of testosterone and estradiol-17β-induced dysplasia in the dorsolateral prostate of Noble rats by bromocriptine. Carcinogenesis 18(8): 1505-1510

37. **Pollard M** 1998 Lobund-Wistar rat model of prostate cancer in man. The Prostate 37(1): 1-4

38. **Pollard M** 1998 Dihydrotestosterone prevents spontaneous adenocarcinomas in the prostate-seminal vesicle in aging L-W rats. The Prostate 36(3): 168-171

39. **Pollard M** 1992 The lobund-Wistar rat model of prostate cancer. J. Cell. Biochem. Suppl. 16H: 84-88

40. **Park SK, Selmanoff M** 1993 Hyperprolactinemia suppresses the luteinizing hormone responses to N-methyl-D- aspartate, epinephrine, and neuropeptide-Y in male rats. Endocrinology 133 (5): 2091-2097

41. **de Greef WJ, Ooms MP, Vreeburg JT, Weber RF** 1995 Plasma levels of luteinizing hormone during hyperprolactinemia: response to central administration of antagonists of corticotropin-release factor. Neuroendocrinology 61 (1): 19-26

42. **Console GM, Gomez Dumm CL, Brown OA, Ferese C, Goya RG** 1997 Sexual dimorphism in the age changes of the pituitary lactotrophs in rats. Mech. Aging Dev. 95(3): 157-166

43. **Banerjee PP, Banerjee S, Lai JM, Strandberg JD, Zirkin BR, Brown TR** 1998 Age-dependent and lobe-specific spontaneous hyperplasia in the brown norway rat prostate. Biol. Reprod. 59(5): 1163-1170

44. **Tangbanluekal L, Robinette CL** 1993 Prolactin mediates estradiol-induced inflammation in the lateral prostate of wistar rats. Endocrinology 132(6): 2407-2416

45. **Nevalainen MT, Valve EM, Makela SI, Blauer M, Tuohimaa PJ, Harkonen PL** 1991 Estrogen and prolactin regulation of rat dorsal and lateral prostate in organ culture. Endocrinology. 129: 612-622

46. **Nevalainen MT, Valve EM, Ingleton PM, Harkonen PL** 1996 Expression and hormone regulation of prolactin receptors in rat dorsal and lateral prostate. Endocrinology 137(7) : 3078-3088

47. **Blankenstein MA, Bolt-de Vries J, Coert A, Nievelstein H, Schroder FH** 1985 Effect of long-term hyperprolactinemia on the prolactin receptor content of the ventral prostate. The Prostate 6(3) : 277-283

48. **Prins GS, Lee C** 1982 Influence of prolactin-producing pituitary grafts on the *in vivo* uptake, distribution and disappearance of [^{3}H] testosterone and [^{3}H] dihydrotestosterone by the rat prostate lobes. Endocrinology 110: 920-925

49. **Lee C, Hopkins D, Holland J** 1985 Reduction in prostatic concentration of endogenous dihydrotestosterone in rats by hyperprolactinemia. The Prostate 6: 361-367

50. **Perez-Villamil B, Bordiu E, Puente-Cueva M** 1992 Involvement of physiological prolactin levels in growth and prolactin receptor content of prostate glands and testes in developing male rats. J. Endocrinol. 132(3) : 449-459

51. **Raffo JA, Perlman H, Chen MW, Day ML, Streitman JS, Buttyan R** 1995 Overexpression of bcl-2 protects prostate cancer cells from apoptosis *in vitro* and confers resistance to androgen depletion *in vivo*. Cancer Research. 55 :4438-4445

52. **Perlman H, Zhang X, Chen MW, Walsh K, Buttyan R** 1999 An elevated bax/bcl-2 ratio corresponds with the onset of prostate epithelial cell apoptosis. Cell Death and Differentiation. 6 :48-54

53. **Kyprianou N, Tu H, Jacobs SC** 1996 Apoptotic versus proliferative activities in human benign prostatic hyperplasia. Hum. Pathol. 27(7) :668-675

54. **Colombel M, Vacherot F, Diez SG, Fontaine E, Buttyan R, Chopin D** 1998 Zonal variation of apoptosis and proliferation in the normal prostate and benign prostatic hyperplasia. Br. J. Urol. 82(3) : 380-385

55. **Ibrado AM, Huang Y, Fang G, Liu L, Bhalla K** 1996 Overexpression of Bcl-2 and Bcl-xL inhibits Ara-C-induced CPP323/Yama protease activity and apoptosis of human acute myelogenous leukemia HL-60 cells. Cancer research. 56(20) :4743-4748

56. **Hayashi R, Luk H, Horio D, Dashwood R** 1996 Inhibition of apoptosis in colon tumors induced in the rat by 2-amino-3-methylimidazo[4,5-f]quinoline. Cancer Research. 56(19) :4307-4310

57. **Wada M, Doi R, Hosotani R, Lee JU, Fujimoto K, Koshiba T, Miyamoto Y, Fukuoka S, Imamura M** 1997 Expression of Bcl-2 and PCNA in duct cells after pancreatic duct ligation in rat. Pancreas. 15(2) :176-182

58. **Wei H, Wei W, Bredesen DE, Perry DC** 1998 Bcl-2 protects against apoptosis in neural cell line caused by thapsigargin-induced depletion of intracellular calcium stores. J. Neurochem. 70 : 2305-2314

59. **Leff MA, Buckley DJ, Krumenacker JS, Reed JC, Miyashita T, Buckley AR** 1996 Rapid modulation of the apoptosis regulatory genes, bcl-2 and bax by prolactin in rat Nb2 lymphoma cells. Endocrinology. 137(12) : 5456-5462

60. **Krumenacker JS, Buckley DJ, Leff MA, McCormack JT, de Jong G, Gout PW, reed JC, Miyashita T, Magnuson NS, Buckley AR** 1998 Prolactin-regulated apoptosis of Nb2 lymphoma cells : pim-1, bcl-2, and bax expression. Endocrine. 9(2) : 163-170

61. **Hanlin M, Yount AP** 1975 Prolactin binding in the rat ventral prostate. Endocr. Res. Commun. 2(8) : 489-502

62. **Aragona C, Friesen HG** 1975 Specific prolactin binding sites in the prostate and testis of rats. Endocrinology. 97(3) : 677-84

63. **Kledzik GS, Marshall S, Campbell GA, Gelato M, Meites J** 1976 Effects of castration, testosterone, estradiol on specific prolactin-binding activity in ventral prostate of male rats. Endocrinology. 98(2) : 373-379

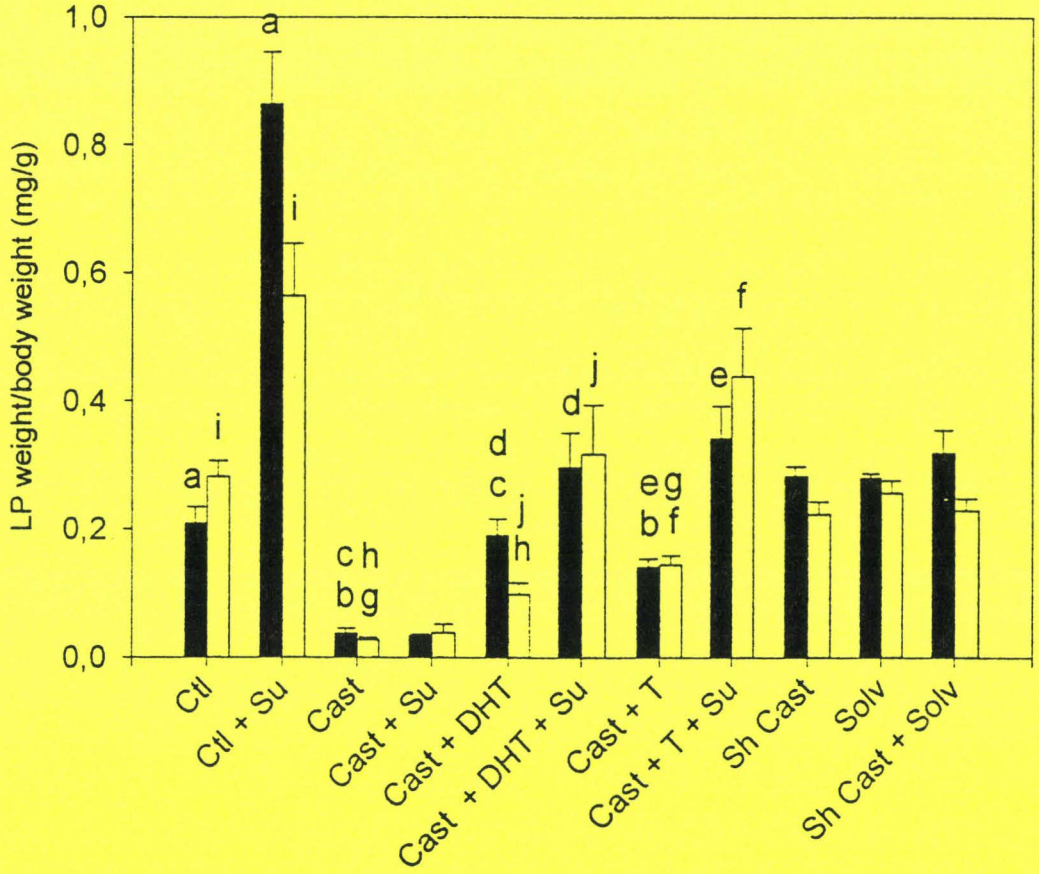

Fig. 1. Histogram showing total lateral prostate weight (mg) divided by total body weight (g). Animals received treatment described in Tab.1. Values are means and bars indicate SEM; n=5 ; black columns : 30 days of treatments ; gray columns : 60 days of treatment. The values of the following treatments are significantly different: $P<0.001$: a, b, f; $P<0.01$: c, g, h, i; $P<0.05$: d, e, j. (Ctl : control animals ; Su : sulpiride treated ; Cast : castrated ; DHT : DHT implanted ; T : T implanted ; Sh Cast : sham castrated ; Solv : solvent injected).

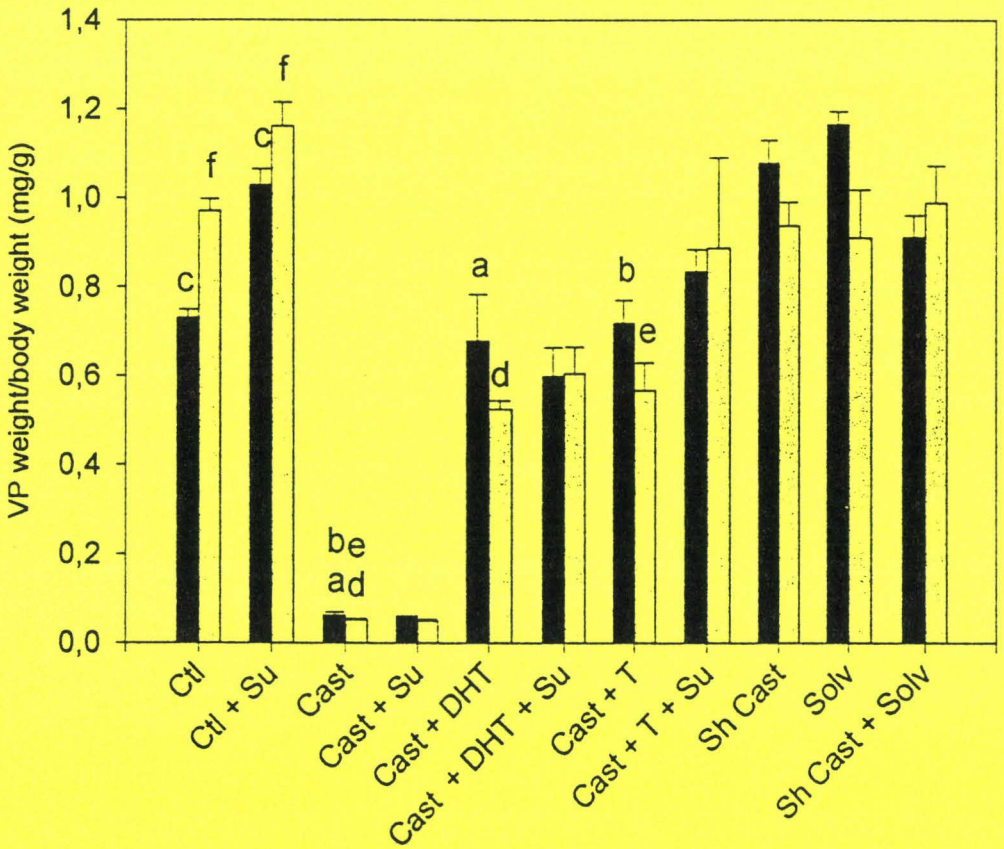

Fig. 2. Histogram showing total ventral prostate weight (mg) divided by total body weight (g). Animals received treatment described in Tab.1. Values are means and bars indicate SEM; n=5 ; black columns : 30 days of treatments ; gray columns : 60 days of treatment. The values of the following treatments are significantly different: $P<0.001$: a, b, d, e ; $P<0.05$: c, f. (Ctl : control animals ; Su : sulpiride treated ; Cast : castrated ; DHT : DHT implanted ; T : T implanted ; Sh Cast : sham castrated ; Solv : solvent injected).

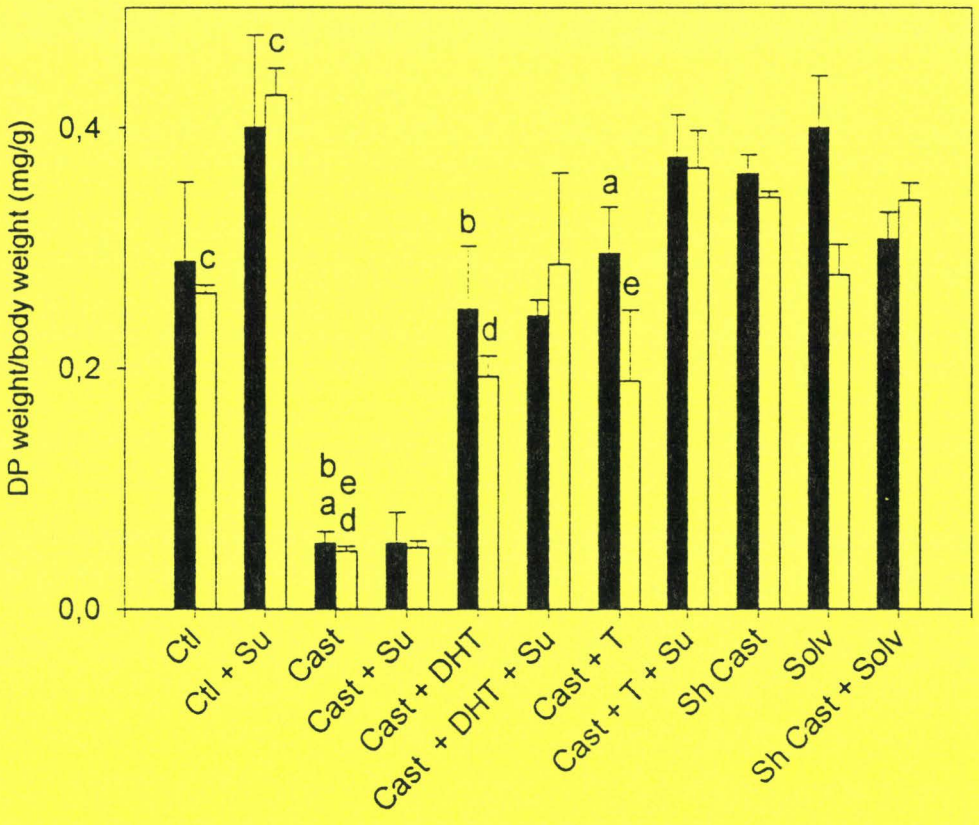

Fig. 3. Histogram showing total dorsal prostate weight (mg) divided by total body weight (g). Animals received treatment described in Tab. 1. Values are means and bars indicate SEM; n=5 ; black columns : 30 days of treatments ; gray columns : 60 days of treatment. The values of the following treatments are significantly different: $P<0.01$: a, c, d ; $P<0.05$: b, e. (Ctl : control animals ; Su : sulpiride treated ; Cast : castrated ; DHT : DHT implanted ; T : T implanted ; Sh Cast : sham castrated ; Solv : solvent injected).

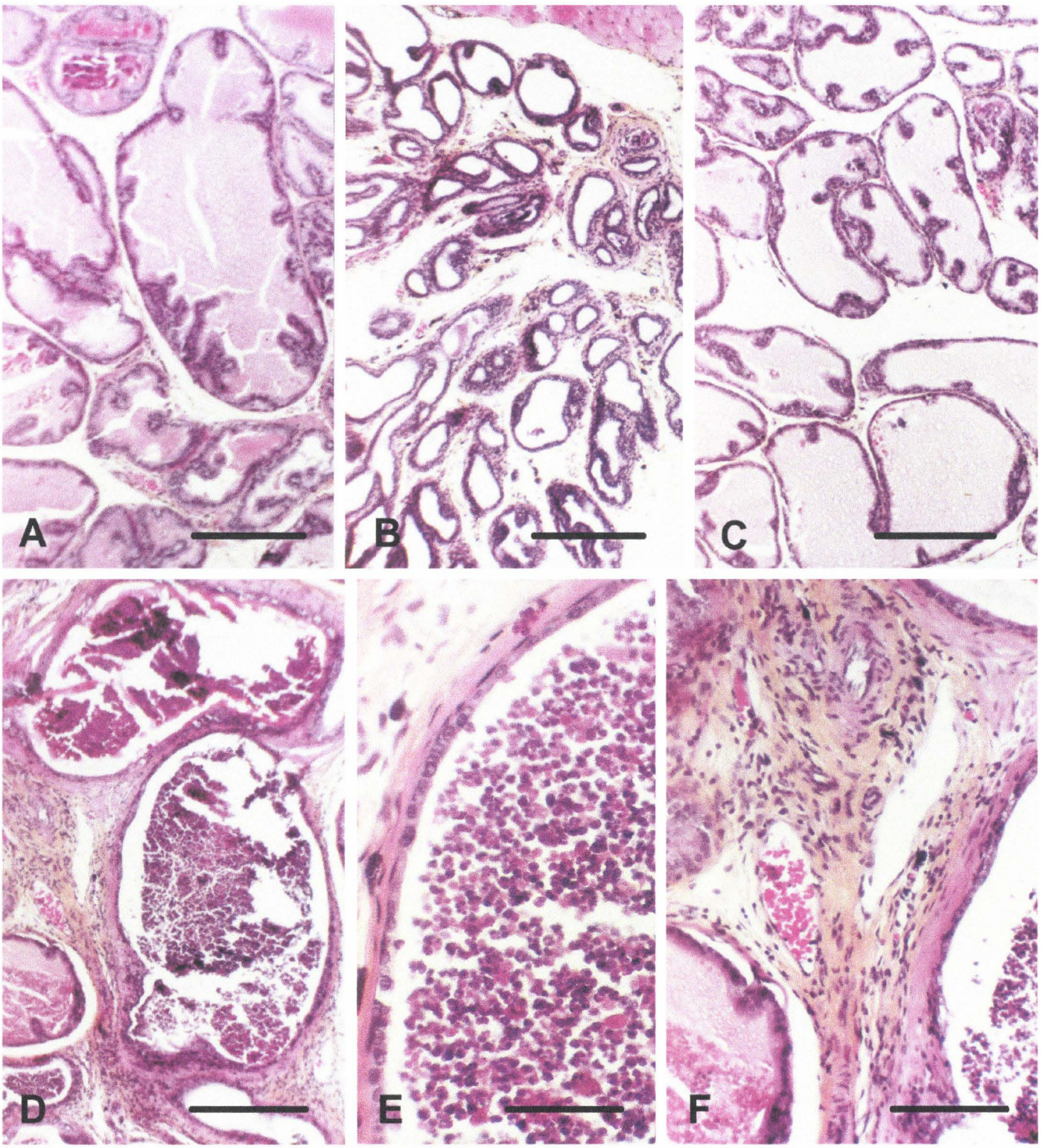
A
B
C
D
E
F

Fig. 4. Histological aspects of lateral prostate of rats. Animals received treatments for 60 days as described in Tab. 1. A, non treated rat. Admixture of small and large glands in similar proportions. Bar, 500 µm. B, castrated rat. Predominance of tiny glands. Bar, 500 µm. C, castrated and T-implanted rat. Gland volumes are intermediate of that of control and castrated rats. Bar, 500 µm. D, castrated, T-implanted and sulpiride treated rat. Presence of very large glands, some of which containing numerous neutrophils. Bar, 500 µm. E, castrated, T-implanted and sulpiried treated rat. infiltration of neutrophils in one gland. Bar, 50 µM. F, castrated, T-implanted and sulpiride treated rat. Interglandular hyperplasis with lymphocytic infiltrates. Bar, 200 µm.

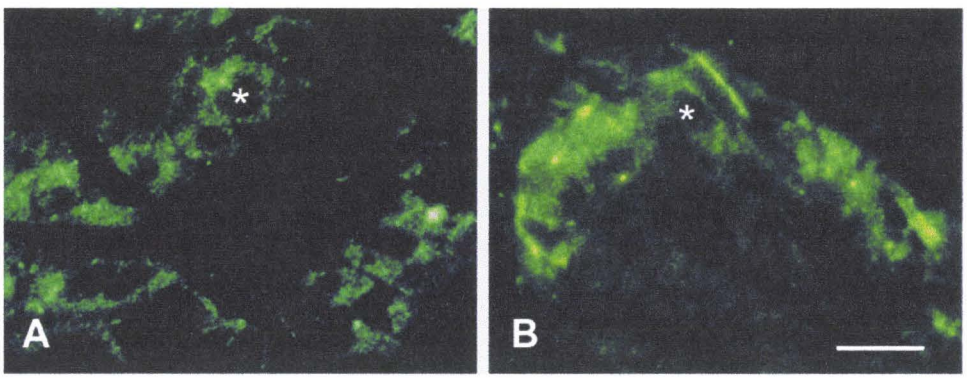
A
B

Fig. 5. Immunofluorescence of anti-Bcl-2 treated thin sections (0.2 μm) of rat lateral prostate. Control rat (A) and 30-day control and sulpiride-treated rat (B). Note the spotted labeling of the cytoplasm, avoiding the nuclei (*). Compare the basal expression in control rat versus the overexpression of Bcl-2 in the control and sulpiride-treated rat. Magnification : x400. Bar represents 30 μm.

Scheme of experimental procedures for 30 days and 60 days sulpiride treatment

Experimental groups	Surgery on day 1	Surgery on day 8	Treatments from day 8 to the sacrifice day
I- control	-	-	-
II- control+sulpiride	-	-	sulpiride
III- castrated	castration	-	-
IV- castrated+sulpiride	castration	-	sulpiride
V- castrated+DHT	castration	DHT implant	-
VI- castrated+DHT+sulpiride	castration	DHT implant	sulpiride
VII- castrated+T	castration	T implant	-
VIII- castrated+T+sulpiride	castration	T implant	sulpiride
IX- sham castrated	sham castration	-	-
X- solvant injected	-	-	solvant
XI- sham castrated; solvant injected	sham castration	-	solvant
XII- control	-	-	-
XIII- control+sulpiride	-	-	sulpiride
XIV- castrated	castration	-	-
XV- castrated+sulpiride	castration	-	sulpiride
XVI- castrated+DHT	castration	DHT implant	
XVII- castrated+DHT+sulpiride	castration	DHT implant	sulpiride
XVIII- castrated+T	castration	T implant	-
XIX- castrated+T+sulpiride	castration	T implant	sulpiride
XX- sham castrated	sham castration	-	-
XXI- solvant injected	-	-	solvant
XXII- sham castrated; solvant injected	sham castration	-	solvant

Tab. 1. At the end of the study, the animals were sacrificed (on day 39 for groups I to XI and day 69 for groups XII to XXII). The ventral, lateral and dorsal prostate lobes were excised and weighed. Trunk blood was collected for hormone level measurements and one

plasma levels of rat prolactin, testosterone, DHT and LH after 60 days of treatment

	Prolactine (ng/ml)	Testosterone (pg/ml)	DHT (pg/ml)	LH (ng/ml)
control	10.16±2.57 c	2087±272	183±32	0.728±0.096 a
control, sulpiride	62.54±26.77 c	1444±184	181±12	0.323±0.019 a
castrated	25.40±72.01 a	ND	ND	13.572±1.348
castrated, sulpiride	91.50±18.98 a	ND	ND	15.525±2.927
castrated, DHT	5.840±1.678 d	202±62	617±95	0.170±0.027
castrated, DHT, sulpiride	70.60±44.20 d	219±25	439±27	0.372±0.187
castrated, T	25.87±60.36 b	955±75	203±47	4.603±0.834
castrated, T, sulpiride	68.60±15.01 b	971±232	154±18	3.044±1.124

Tab. 2. Plasma PRL, T, DHT and LH levels. Trunk blood was collected from Wistar rats after long-term treatment (60 days) and analyzed by RIA. Data are expressed as group means ± SEM (pg/ml) (n=5). ND: non detected values. $P<0.01$: a, b; $P<0.05$: c, d.

- **la PRL agit en synergie avec les androgènes et pourrait donc être un cofacteur majeur influençant la croissance de la prostate;**

- **une surexpression de la protéine antiapoptotique Bcl-2 est observée sur les membranes des organites intracellulaires des cellules épithéliales de prostates latérales de rats traités au sulpiride. Ce phénomène est spécifique au lobe latéral. Cela suppose que la prolactine pourrait agir par inhibition de la mort cellulaire programmée.**

2 - Etude cinétique des effets de la prolactine sur la croissance de la prostate de rat

Lors de la première étude, nous avons mis en évidence le rôle trophique de la PRL après 30 et 60 jours de traitement. Dans le cadre de cette seconde étude, nous nous sommes appliqués à analyser la cinétique des modifications pondérales engendrées par les traitements au sulpiride et aux androgènes.

2.1- Protocole expérimental

Au cours de cette seconde étude *in vivo*, nous avons utilisé 192 rats mâles adultes de souche Wistar. La pose des implants sous-cutanés de testostérone (T) s'est déroulée le jour de la castration. De cette manière, la perte des androgènes endogènes est partiellement compensée par l'apport de T de l'implant. Des implants de 1 cm ou de 0.5 cm de long ont été utilisés. Ces tailles correspondent à la restauration de 50% et de 25% respectivement du taux normal de T circulant. De ce fait, l'apoptose induite par l'ablation des testicules devrait être freinée par les implants. De plus, la moitié des rats ont été traités au sulpiride afin de réaliser une étude cinétique des effets de la PRL sur l'évolution du poids prostatique et le

déclenchement de l'apoptose. La durée des traitements s'est étendue sur 4 jours, 9 jours, 14 jours, 21 jours, 30 jours et 60 jours.

2.2- Résultats

Nous obtenons les résultats pondéraux suivants qui traduisent l'évolution du poids de la prostate latérale au cours du temps et selon les divers traitements hormonaux.

Les différents lots d'animaux employés sont décrits ci-dessous :

Durée du traitement	4 jours	9 jours	14 jours	21 jours	30 jours	60 jours
Traitements	**Moyenne Poids des lobes latéraux (mg)/ Poids total de l'animal (g) ± S.E.M. (n=4).**					
Contrôle	0.31755 ± 0.062	0.2806 ±0.006	0.2785 ± 0.033	0.2330 ±0.024	0.2091 ±0.0179	0.2821 ±0.0243
Contrôle + sulpiride	0.3034 ±0.067	0.2956 ±0.04	0.2423 ±0.042	0.2806 ±0.031	0.8643 ±0.082	0.5645 ±0.0818
Castrés	0.1589 ±0.012	0.0645 ±0.006	0.0464 ±0.008	0.0345 ±0.003	0.0374 ±0.007	0.0273 ±0.003
Castrés + sulpiride	0.1145 ±0.025	0.0841 ±0.003	0.0662 ±0.007	0.0486 ±0.011	0.0343 ±0.004	0.0381 ±0.038
Castrés + T (1 cm)	0.3683 ±0.016	0.3518 ±0.036	0.281 ±0.023	0.2019 ±0.008	0.1417 ±0.012	0.1449 ±0.015
Castrés + T (1 cm) + sulpiride	0.4357 ±0.121	0.2752 ±0.026	0.3660 ±0.029	0.3036 ±0.023	0.3423 ±0.05	0.4392 ±0.076
Castrés + DHT (1 cm)	0.302 ±0.032	0.2088 ±0.001	0.2169 ±0.018	0.165 ±0.022	0.1903 ±0.026	0.0985 ±0.017
Castrés+ DHT (1 cm) + sulpiride	0.2522 ±0.078	0.3202 ±0.078	0.3617 ±0.52	0.3183 ±0.02	0.2972 ±0.053	0.317 ±0.077

Tableau 1 : Récapitulatif des lots de rats Wistar (4 animaux par lot) et des valeurs obtenues après le sacrifice des animaux.

Nous avons ainsi réalisé 48 lots de 4 animaux.

A l'issu du traitement, les animaux ont été sacrifiés. Les prostates ont été disséquées, pesées et fixées selon le protocole détaillé dans le chapitre « Matériel et Méthodes ».

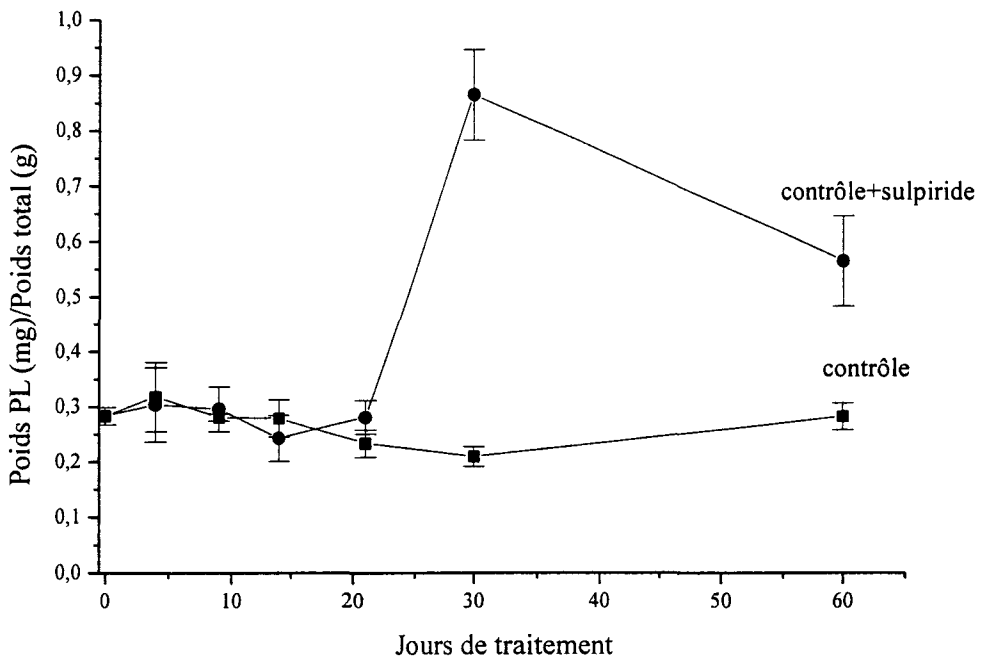

Figure 20 : Evolution du rapport poids de la prostate latérale (mg)/ poids total de l'animal (g). Les mesures ont été réalisées sur des rats non castrés (avec ou sans sulpiride). Ces rapports sont représentés sous forme de moyenne accompagnée de l'erreur standard.

Chez les animaux contrôle, (figure 20), le poids de la prostate latérale est relativement stable tout au cours de l'expérience. Chez les animaux traités au sulpiride, l'augmentation du poids de la prostate débute, de façon significative, à partir du 30ème jours et se poursuit jusqu'à la fin des traitements.

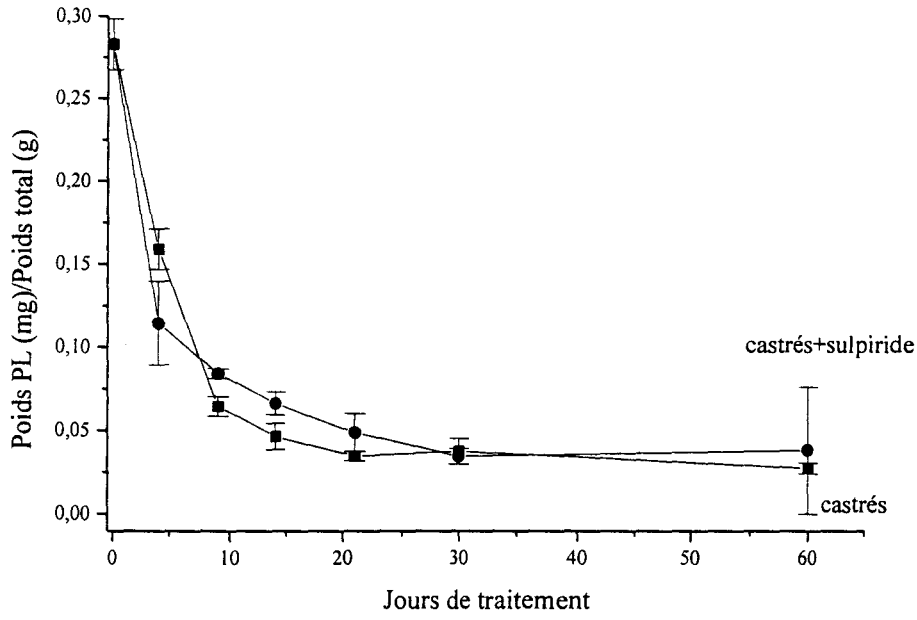

Figure 21: Evolution du rapport poids de la prostate latérale (mg)/ poids total de l'animal (g) chez des rats castrés, injectés ou non de sulpiride. Ces rapports sont représentés sous forme de moyenne accompagnée de l'erreur standard.

Dans le cas des animaux castrés, recevant ou non du sulpiride, la diminution du poids des prostates est achevée en 9 jours. Les prostates latérales ont perdu 86 % de leur poids initial. Après cette période, les valeurs restent stables. Nous n'observons pas de différences significatives entre les deux catégories de traitement.

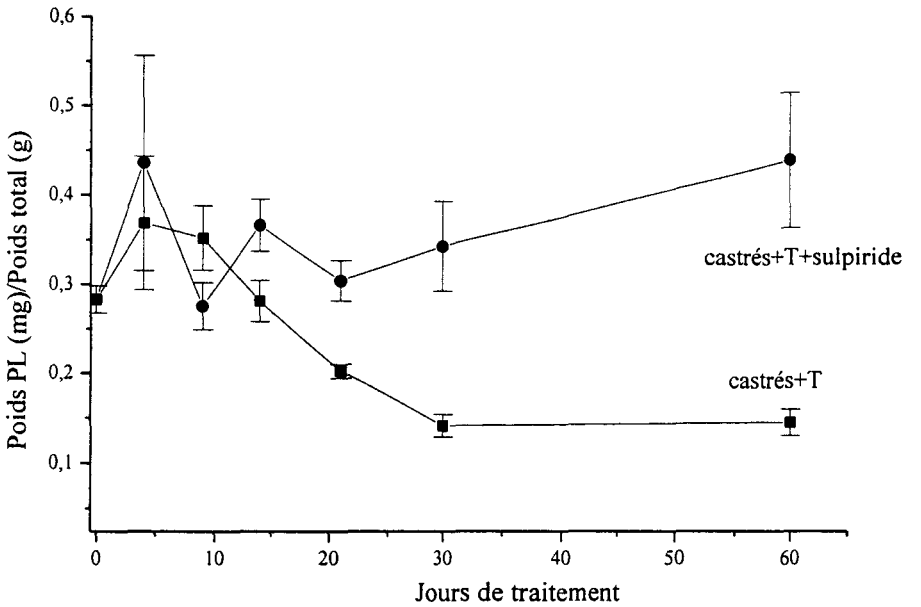

Figure 22: Evolution du rapport poids de la prostate latérale (mg)/ poids total de l'animal (g) (mesures réalisées sur des animaux castrés, ayant reçu un implant de testostérone, injectés ou non de sulpiride). Ces rapports sont représentés sous forme de moyenne accompagnée de l'erreur standard.

Chez les rats ayant reçu un implant de 1 cm de T, les poids prostatiques chutent de 46% en 30 jours. Au contraire, chez des animaux traités au sulpiride, nous observons une augmentation des poids des lobes latéraux à partir du 14ème jour de traitement. Au bout de 60 jours de stimulation par le sulpiride, les prostates latérales sont plus lourdes de 50 % par rapport aux valeurs de départ.

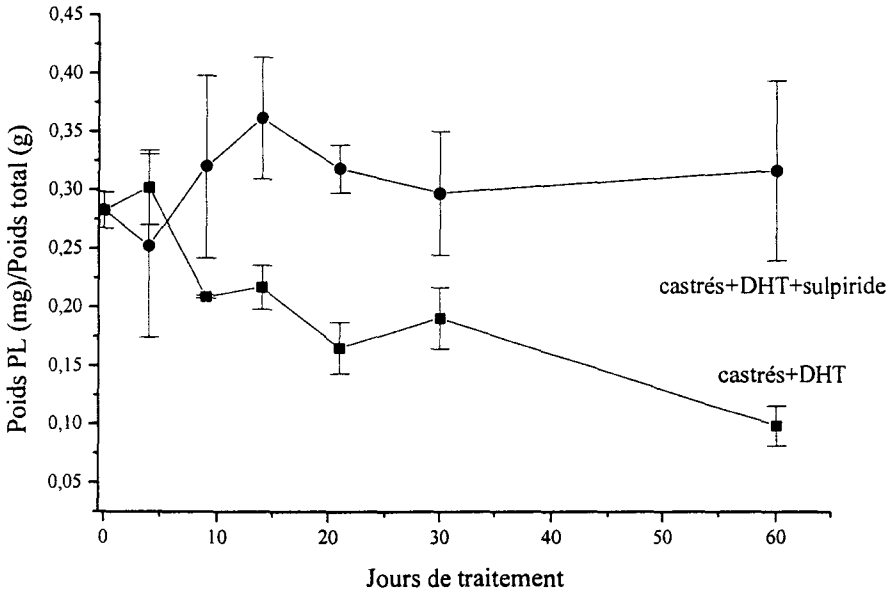

Figure 23: Evolution du rapport poids de la prostate latérale (mg)/ poids total de l'animal (g). Les rats sont castrés, portent un implant de DHT et reçoivent ou non du sulpiride. Ces rapports sont représentés sous forme de moyenne accompagnée de l'erreur standard.

Sur des animaux castrés possédant un implant de 1 cm de DHT, la régression du poids prostatique est lente (57 %) après 60 jours. Le sulpiride déclenche la croissance de la prostate à partir du 9ème jour par rapport aux valeurs obtenues chez des rats castrés et implantés de DHT. Au bout de 60 jours, les lobes latéraux des rats ayant subit une hyperprolactinémie sont trois fois plus lourds que ceux des animaux non injectés de sulpiride.

2.3- Discussion et conclusion

Ces résultats indiquent, dans un premier temps, la cinétique d'action de la PRL. Son effet est déjà visible après 30 jours de traitement chez les rats contrôle et 14 jours chez des rats castrés et implantés de T (1 cm) et 9 jours chez des animaux castrés et traités à la DHT (1 cm). Le sulpiride et donc la PRL ne modifient pas l'involution de la

glande des animaux castrés. Ces résultats étayent les conclusions précédentes, à savoir que la PRL nécessite la présence d'androgènes pour induire une croissance de la prostate. Des études antérieures démontrent que la PRL stimule l'effet de la T (Farnsworth, 1988) et augmente le nombre de récepteurs cytosoliques et nucléaires aux androgènes chez le rat (Prins, 1987). De plus, l'hyperprolactinémie induit un renouvellement rapide du contenu en DHT dans la prostate latérale de rat (Schacht *et al.* , 1992).

Nous poursuivons ce travail de recherche en mesurant le taux de prolifération cellulaire et l'index apoptotique. La prolifération cellulaire sera déterminée par immunohistochimie, en utilisant un anticorps anti KI-67 (Euromedex, France) qui interagit avec un antigène nucléaire lors du cycle cellulaire (en phases G1, S, G2 et M et non en phase G0). Cette nouvelle étude devrait nous permettre de vérifier les modalités d'action de la PRL et de détecter son implication dans la régulation de la prolifération et de l'apoptose des cellules de la prostate latérale.

Connaître les mécanismes de régulation de l'apoptose des cellules prostatiques est capital. En effet, les cancers de la prostate sont caractérisés par un taux de prolifération faible. Il est maintenant clairement établi que ces cancers résultent d'une inhibition de l'apoptose plutôt que d'une augmentation de la prolifération cellulaire (Bruyninx *et al.*, 1998).

3- Effets de l'extrait lipido-stérolique de *Serenoa repens* (Permixon®) et du finastéride® chez des rats subissant une hyperprolactinémie

Actuellement, les seules thérapies existant pour traiter les cancers hormono-dépendants de la prostate et les HBP se basent sur l'inhibition de l'action des androgènes. La voie de la PRL n'est pas prise en compte lors de tels traitements. Le but de cette troisième étude est d'inhiber les effets de la PRL observés *in vivo* lors de la première phase de notre recherche.

Nous avons choisi de tester le Permixon®, un extrait obtenu à partir du palmier scie. Le Permixon, où extrait lipidostérolique de *Serenoa repens* (E.L.S.S.R.) est couramment utilisé en clinique humaine pour traiter les HBP. Ce médicament est constitué de plusieurs molécules dont les principales sont des acides gras (acide palmitique, acide oléique, acide myristique, ...). L'E.L.S.S.R. possède un spectre d'action très large, ce qui lui confère une grande efficacité. Cet extrait inhibe les deux isoformes de la 5α-reductase et diminue de ce fait le taux d'androgènes circulants. L'E.L.S.S.R. inhibe également le développement des inflammations, spécifiques à la prostate latérale de rat, induite par l'oestradiol (Paubert-Braquet, 1996). Or, il est connu que l'oestradiol stimule la synthèse (Kaplan *et al.*, 1976), le stockage (Kiino *et al.*, 1981) et la sécrétion (Neill *et al.*, 1971) de la PRL dans les cellules lactotropes. Par ailleurs, les effets de l'oestradiol sont absents chez des rats traités à la bromocriptine (agoniste dopaminergique) qui inhibe la sécrétion de PRL. L'ensembles de ces données nous amène à penser que l'action bénéfique de l'E.L.S.S.R. peut se produire via l'inhibition de l'effet trophique de la PRL sur la prostate. La difficulté principale de cette étude résulte du fait que l'E.L.S.S.R. possède également une activité anti 5α-réductase importante. Afin de séparer les effets anti 5α-réductase et l'action antiprolactinique possible

de l'E.L.S.S.R., nous avons eu recours à de nombreux lots d'animaux et notamment à des rats castrés et implantés de DHT. Chez ces derniers, l'action anti 5α-réductase de l'E.L.S.S.R. ne peut plus s'exercer. Par ailleurs, des expériences similaires ont été entreprises sur des rats traités au finastéride. Cette molécule synthétique, utilisée en clinique humaine, possède une activité spécifiquement anti 5α-réductase.

La combinaison des résultats obtenus grâce à ces différents lots a permis l'écriture du manuscrit suivant, actuellement sous presse dans le journal « The Prostate ».

CONCLUSION

Cette étude nous a permis d'établir les conclusions suivantes :

- **l'E.L.S.S.R., outre son action anti 5α-reductase est capable d'inhiber l'effet trophique de la PRL sur la prostate latérale de rat ;**
- **le finastéride, n'a pas d'action antagoniste vis-à-vis de la PRL. Cette molécule inhibe spécifiquement la 5α-reductase.**

Les multiples activités de l'E.L.S.S.R. sont dues, très vraisemblablement aux nombreuses fractions qui le composent. Il serait intéressant de tester des sous-fractions de l'E.L.S.S.R. afin de caractériser le principe actif ayant une action anti prolactinique.

The Prostate 43:000–000 (2000)

Pharmacological Effects of the Lipidosterolic Extract of *Serenoa repens* (Permixon®) on Rat Prostate Hyperplasia Induced by Hyperprolactinemia: Comparison With Finasteride

Fabien Van Coppenolle,[1]* Xuefen Le Bourhis,[2] Françoise Carpentier,[3] Geoffrey Delaby,[1] Henri Cousse,[4] Jean-Pierre Raynaud,[5] Jean-Paul Dupouy,[6] and Natalia Prevarskaya[1]

[1]*Laboratoire de Physiologie Cellulaire, USTL, INSERM EPI 9938, Villeneuve d'Ascq, France*
[2]*Laboratoire de Biologie du Développement, UPRES 1033, USTL, Villeneuve d'Ascq, France*
[3]*Service d'Anatomo-Pathologie, Centre Hospitalier de Roubaix, Roubaix, France*
[4]*Laboratoire Pierre Fabre, La Chartreuse, Castres, France*
[5]*Université Pierre et Marie Curie, Paris, France*
[6]*Laboratorie de Neuroendocrinologie du Développement, USTL, Villeneuve d'Ascq, France*

BACKGROUND. The growth of the prostate gland is mainly dependent on androgens. Other hormones, like prolactin (PRL), also influence prostate development. Our purpose was to analyze and compare the effects of two drugs (5α-reductase inhibitor) used in the therapy of benign prostatic hyperplasia: lipidosterolic extract of *Serenoa repens* (LSESR), and finasteride in an in vivo model of rat prostate hyperplasia induced by hyperprolactinemia.
METHODS. Hyperprolactinemia was induced by 30 daily injections of sulpiride. Wistar rats received daily gavages of LSESR or finasteride. We used the following groups: control, castrated, castrated with a substitute testosterone (T), or 5α-dihydrotestosterone (DHT) implant.
RESULTS. Hyperprolactinemia increases the wet weight and induces hyperplasia in the lateral prostate (LP). Unlike finasteride, LSESR significantly reduced LP growth and hyperplasia in castrated, DHT-implanted, and sulpiride-treated rats.
CONCLUSIONS. Finasteride was only capable of inhibiting the effect of androgens on rat prostate enlargement. LSESR inhibited not only the androgenic but also the trophic effect of PRL in rat LP hyperplasia. *Prostate 43:00–00, 2000.* © 2000 Wiley-Liss, Inc.

KEY WORDS: **rat prostate hyperplasia; prolactin; androgens; LSESR; finasteride**

INTRODUCTION

Benign prostate hyperplasia (BPH) and prostate cancer are very common diseases among elderly men. Fifty percent of men over 50 years old suffer from BPH. Furthermore, prostate cancer is the second leading cause of death by cancer [1].

Prostate development and growth are controlled by androgens [2,3]. Treatments currently used in hor-

Grant sponsor: Pierre Fabre Médicament; Grant sponsor: Association pour la Recherche sur le Cancer; Grant sponsor: Association pour la Recherche sur les Tumews de la Prostate; Grant sponsor: Institut National de la santé de la Recherche Médicale; Grant sponsor: Ligue Nationale contre le Cancer.

*Correspondence to: Fabien Van Coppenolle, Laboratoire de Physiologie Cellulaire, Centre de Biologie Cellulaire, USTL, INSERM EPI 9938, Bâtiment SN3, 59655 Villeneuve d'Ascq Cedex, France. E-mail: fvancopp@pop.univ-lille1.fr

Received 23 August 1999;Accepted 17 November 1999

monotherapy for prostate diseases are only aimed at inhibiting the effect of androgens on prostate cell growth [4]. They are based on reducing androgen levels in the following ways: (1) Drugs such as the lipidosterolic extract of *Serenoa repens* (LSESR) [5] or finasteride [6] are used to inhibit the enzyme 5α-reductase, which converts testosterone (T) to 5α-dihydrotestosterone (DHT), the most active androgen in the stimulation of prostate-cell proliferation [7], in the prostate. (2) Flutamide inhibits the fixation of androgens to their receptors [8]. (3) Another approach, using chronic administrations of GnRH agonists [9,10], is also employed to induce an inhibition of androgenic synthesis.

In men, T levels decrease with age [11,12], while prolactin (PRL) concentrations increase [13,14]. It is becoming increasingly clear that PRL is implicated in prostate growth [15–19]. It has been suggested that PRL acts in synergy with androgens, either by enhancing the T effect [20] or by increasing the number of cytosolic and nuclear androgen receptors [21]. Furthermore, some in vitro experiments have shown that PRL can also act directly on prostate cells [22,23], as they possess PRL receptors [19,24–26]. In addition, Nevalainen et al. [19,20] demonstrated that human and rat prostate cells synthesize PRL. Thus, this hormone may regulate prostate growth in an autocrine/paracrine loop. However, the PRL pathway has not yet been taken into account in hormonotherapy for prostate diseases.

In this work, we studied the effects of LSESR and finasteride on rat prostate hyperplasia induced by hyperprolactinemia. We now report that LSESR inhibits the effects of PRL and androgens on prostate growth. On the other hand, finasteride (a specific 5α-reductase inhibitor) only antagonizes the action of T on rat lateral prostate growth.

MATERIALS AND METHODS

Animals

One hundred forty-five male Wistar rats (200–220 g) from Dépré Breeding Center (Saint Doulchard, France) were used. These animals were conditioned for 1 week prior to experimentation. Rats were randomized and housed 5 per cage on a 12-hr light-12-hr dark cycle. They were provided *ad libitum* with water and standard laboratory chow.

During this work, all animal studies were conducted in accordance with the European Communities Council ruling of November 24, 1986 (86/609/EEC).

Surgical Procedures

All surgeries were performed on day 1 under ether anesthesia and strict sanitized conditions. The operated animals were treated with antibiotics (penicillin) to prevent infections.

Castrations were performed on day 1 via the scrotal route by removing epididymal fat pads with the testes. Operated animals were then sutured, and the injured areas were disinfected with betadine solution and sprayed with aluspray (Vetoquinol, France).

In order to add the desired quantity of exogenous androgens for comparison with control animals, we implanted silastic medical-grade silicone tubing (0.078 i.d. × 0.125 o.d., Dow Corning Corp., Midland, MI) (1 cm length), filled with either testosterone (Sigma, France) or 5α-dihydrotestosterone (Sigma), subcutaneously over the scapula. One end of the tubing was sealed with adhesive (Silastic Medical Adhesive, Dow Corning Corp.) according to Robaire *et al.* [28]. After loading with the hormone, the unsealed end was sealed with adhesive. After the adhesive had hardened, the implants were stored overnight in distilled water. It has been found that a 2.5-cm implant mimics the physiological testosterone level [29]. The choice of a 1-cm implant was to produce a subnormal testosterone release.

The implants were inserted on day 8, in pockets formed over the dorsal area of the scapula. The incised area was disinfected, and then sutured.

Hyperprolactinemia Induction

Hyperprolactinemia was induced by daily intraperitoneal injections of a 40 mg/kg aqueous sulpiride solution (± sulpiride, Sigma).

LSESR (Permixon®) Gavages

The lipidosterolic extract of *Serenoa repens* (batch numbers 708 and 712) was from Pierre Fabre Médicament (Labège, France). The animals received daily gavages of LSESR plus carrier (2.5% ethanol) or carrier alone. The doses used were: 100 mg/kg/day; 320 mg/kg/day; or 640 mg/kg/day.

Finasteride Gavages (Chibro-Proscar®)

Finasteride (Merck, Whitehouse Station, NJ) compounds were dissolved in 2.5% ethanol. The animals received daily gavages of 5 mg/kg of finasteride (batch number 974214) or carrier alone.

Sampling

Since previous reports [30–32] indicated an increase in PRL during stress, sham castrated, solvent-injected groups and animals receiving carrier alone (2.5% ethanol in aqueous solution) were also evaluated. It was

TABLE I. Scheme of Experimental Procedures for 30 Days of Sulpiride, Permixon, and Finasteride Treatment

Experimental groups	Surgery on day 1	Surgery on day 8	Treatments from day 8 to sacrifice day
I, control			
II, control + sulpiride			Sulpiride
III, control + LSESR 100			LSESR 100 mg/kg
IV, control + LSESR 320			LSESR 320 mg/kg
V, control + Fin5			Finasteride 5 mg/kg
VI, control + sulpiride + LSESR 100			Sulpiride + LSESR 100 mg/kg
VII, control + sulpiride + LSESR 320			Sulpiride + LSESR 320 mg/kg
VIII, control + sulpiride + Fin5			Sulpiride + Finasteride 5 mg/kg
IX, castrated	Castration		
X, castrated + T	Castration	T implant	
XI, castrated + T + LSESR 100	Castration	T implant	LSESR 100 mg/kg
XII, castrated + T + LSESR 320	Castration	T implant	LSESR 320 mg/kg
XIII, castrated + T + Fin5	Castration	T implant	Finasteride 5 mg/kg
XIV, castrated + DHT	Castration	DHT implant	
XV, castrated + DHT + LSESR 100	Castration	DHT implant	LSESR 100 mg/kg
XVI, castrated + DHT + LSESR 320	Castration	DHT implant	LSESR 320 mg/kg
XVII, castrated + DHT + Fin5	Castration	DHT implant	Finasteride 5 mg/kg
XVIII, castrated + T + sulpiride	Castration	T implant	Sulpiride
XIX, castrated + T + sulpiride + LSESR 100	Castration	T implant	Sulpiride + LSESR 100 mg/kg
XX, castrated + T + sulpiride + LSESR 320	Castration	T implant	Sulpiride + LSESR 320 mg/kg
XXI, castrated + T + sulpiride + LSESR 640	Castration	DHT implant	Sulpiride + LSESR 640 mg/kg
XXII, castrated + T + sulpiride + Fin5	Castration	DHT implant	Sulpiride + Finasteride 5 mg/kg
XXIII, castrated + DHT + sulpiride	Castration	DHT implant	Sulpiride
XXIV, castrated + DHT + sulpiride + LSESR 100	Castration	DHT implant	Sulpiride + LSESR 100 mg/kg
XXV, castrated + DHT + sulpiride + LSESR 320	Castration	DHT implant	Sulpiride + LSESR 320 mg/kg
XXVI, castrated + DHT + sulpiride + Fin5	Castration	DHT implant	Sulpiride + Finasteride 5 mg/kg
XXVII, sham castrated	Sham-castration		
XXVIII, solvent-injected			NaCl 0.9%
XXIX, carrier-gavaged			2.5% ethanol in aqueous solution

previously shown that empty tubing implants have no effect on rat prostate growth [28,33,34].

Table I lists the surgical events (castrations and implants) and treatments (daily intraperitoneal injections of sulpiride and gavages of LSESR or finasteride) for the various experimental groups.

Immediately after sacrifice, the prostate lobes were dissected, weighed, and treated for light microscopy, as described below.

Histology

Tissue pieces were fixed in 10% neutral-buffered formalin and embedded in paraffin. Histological analyses were performed on serial sections obtained from prostatic samples stained with hematoxylin-erythrosin-saffron (HES).

Hormonal Assays

Plasma levels of PRL were measured by radioimmunoassay (RIA) with materials supplied by the NIDDK rat pituitary hormone distribution program (NIDDK, Torrance, CA), using rat RP3-PRL in reference preparations. In our experiments, the rats were sacrificed on the day after the last sulpiride injection, so that the prolactinemia measured represented the chronic PRL level after 30 days of treatment with sulpiride.

Statistical Analysis

We expressed the prostate weight relative to the body weight according to Robinette [33]. The Tukey test was used to establish the presence of significant differences. Significance was established at levels of $P < 0.05$, $P < 0.01$, and $P < 0.001$.

RESULTS

After 30 days of treatment, the rats were sacrificed. Rat prostates consist of three parts: ventral lobes, lat-

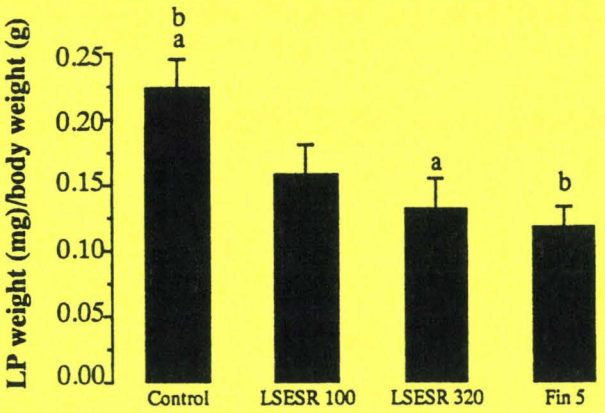

Fig. 1 Histogram showing total lateral prostate weight (mg) divided by total body weight (g). Animals received treatment as described in Table I. Values are means, and bars indicate SEM; n = 5. The values of the following treatments were significantly different: $P < 0.05$, a, b. Control, control animals; LSESR 100, animals receiving LSESR at 100 mg/kg/day *per os*; LSESR 320, animals receiving LSESR at 320 mg/kg/day *per os*; Fin 5, animals receiving finasteride at 5 mg/kg/day *per os*.

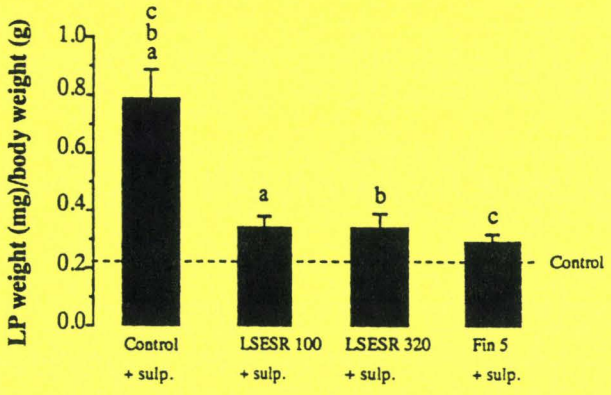

Fig. 2 Histogram showing total lateral prostate weight (mg) divided by total body weight (g). Animals received treatment as described in Table I. Values are means, and bars indicate SEM; n = 5. The values of the following treatments were significantly different: $P < 0.01$, a, b, c. Control, control animals; sulp., animals receiving intraperitoneal sulpiride injections (40 mg/kg/day); LSESR 100, animals receiving LSESR at 100 mg/kg/day *per os*; LSESR 320, animals receiving LSESR at 320 mg/kg/day *per os*; Fin 5, animals receiving finasteride at 5 mg/kg/day *per os*.

eral lobes, and dorsal lobes. Each lobe was dissected and weighed separately.

Only the lateral prostate (LP) is sensitive to hyperprolactinemia (data not shown). For this reason, only changes in the wet weight of the lateral lobes were analyzed in order to define the effects of LSESR and finasteride on LP enlargement induced by hyperprolactinemia.

Effects of LSESR and Finasteride on the Wet Weight of the LP

LSESR and finasteride were tolerated by all animals, and no side effects were observed. Sulpiride injections did not modify the weight of LP in castrated and in castrated-adrenalectomized rats (data not shown) after 30 days. LSESR and finasteride did not reduce the weight of these LP (sulpiride-treated or not; data not shown).

Figure 1 illustrates the wet weight of the LP in intact animals after 30 days of treatment.

LSESR at 100 mg/kg daily was ineffective, as the LP weight was not significantly reduced. On the contrary, LSESR at 320 mg/kg and finasteride at 5 mg/kg induced a significant decrease of 41% and 47%, respectively.

As shown in Figure 2, sulpiride induced a 3.5-fold increase in lateral lobe weight. In control animals treated with sulpiride, we noticed a significant decrease in LP weight with LSESR at 100 mg/kg (−56%), LSESR at 320 mg/kg (−57%), and finasteride at 5 mg/kg (−63%).

As shown in Figure 3, castration induced an 83% decrease in LP weight. T implants restored 78% of the LP weight in castrated animals. Gavages with LSESR (at 100 and 320 mg/kg) were ineffective in inducing a decrease in LP weight. On the contrary, finasteride at 5 mg/kg induced a decrease (−41%) in the LP weight in castrated, T-implanted rats compared to untreated castrated, T-implanted rats.

In Figure 4, as shown previously, castration decreased the LP weight. DHT implants restored 82% of the LP weight compared to noncastrated animals. In castrated rats implanted with DHT, neither LSESR at 100 and 320 mg/kg nor finasteride at 5 mg/kg reduced LP wet weight compared to castrated, DHT-implanted rats.

As shown in Figure 5, in castrated, T-implanted animals, sulpiride induced a 2.4-fold increase in lateral lobe weight compared with noninjected rats. LSESR at 100 mg/kg and at 320 mg/kg did not decrease the LP weight. On the contrary, LSESR at 640 mg/kg and finasteride at 5 mg/kg decreased the wet weight of the lateral lobes by 59% and 67%, respectively, under these experimental conditions.

As shown in Figure 6, daily sulpiride injections induced an 87% increase in LP weight in castrated and DHT-implanted rats. LSESR at 100 mg/kg did not reduce the LP weight in castrated, DHT-implanted, and sulpiride-treated animals. On the other hand, LSESR at 320 mg/kg significantly inhibited LP growth by 40%. However, finasteride at 5 mg/kg did not reduce the wet weight of the LP.

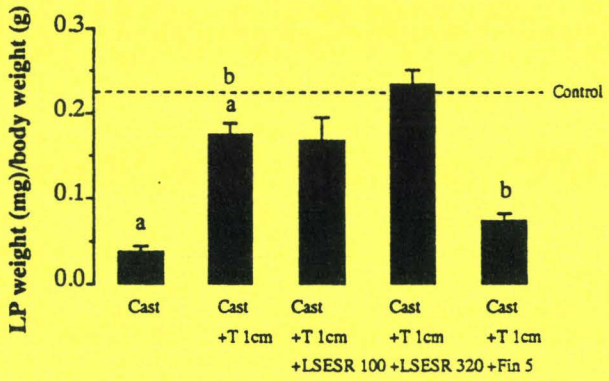

Fig. 3 Histogram showing total lateral prostate weight (mg) divided by total body weight (g). Animals received treatment as described in Table I. Values are means, and bars indicate SEM; n = 5. The values of the following treatments were significantly different: $P < 0.001$, a; $P < 0.01$, b. Cast, castrated animals; T 1 cm, animals receiving 1 cm subcutaneous T implant; LSESR 100, animals receiving LSESR at 100 mg/kg/day *per os*; LSESR 320, animals receiving LSESR at 320 mg/kg/day *per os*; Fin 5, animals receiving finasteride at 5 mg/kg/day *per os*.

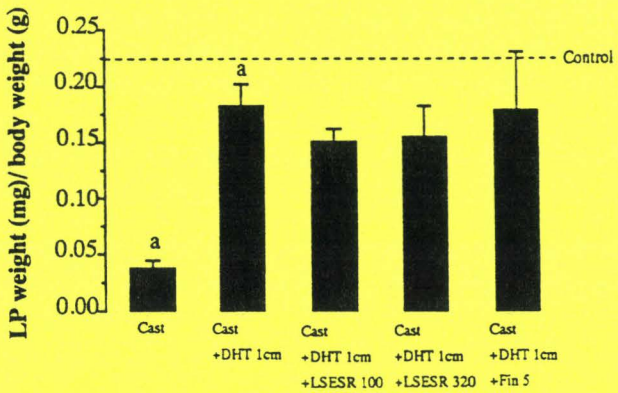

Fig. 4 Histogram showing total lateral prostate weight (mg) divided by total body weight (g). Animals received treatment as described in Table I. Values are means, and bars indicate SEM; n = 5. The values of the following treatments were significantly different: $P < 0.001$, a. Cast, castrated animals; DHT 1 cm, animals receiving 1 cm subcutaneous DHT implant; LSESR 100, animals receiving LSESR at 100 mg/kg/day *per os*; LSESR 320, animals receiving LSESR at 320 mg/kg/day *per os*; Fin 5, animals receiving finasteride at 5 mg/kg/day *per os*.

LP Histology Following Different Treatments

The LP of castrated, T-implanted rats contained similar proportions of small and large glands (Fig. 7A). In castrated, T-implanted, and sulpiride-treated rats, volumes of LP glands were generally larger than those of castrated, T-implanted rats, with the presence of very large glands (Fig. 7B). In castrated, T-implant, sulpiride- and LSESR-treated rats (Fig. 7C), gland volume was smaller than in castrated, T-implanted, and

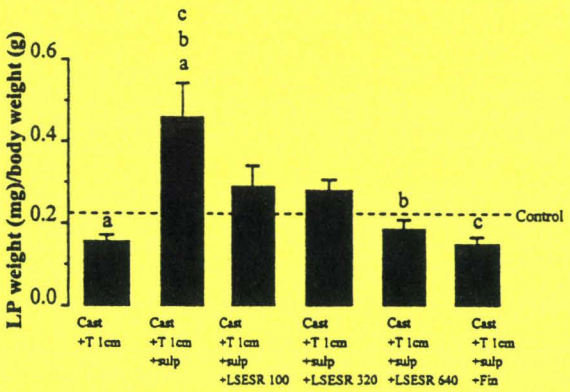

Fig. 5 Histogram showing total lateral prostate weight (mg) divided by total body weight (g). Animals received treatment as described in Table I. Values are means, and bars indicate SEM; n = 5. The values of the following treatments were significantly different: $P < 0.001$, a, c; $P < 0.01$, b. Cast, castrated animals; sulp., animals receiving intraperitoneal sulpiride injections (40 mg/kg/day); T 1 cm, animals receiving 1 cm subcutaneous T implant; LSESR 100, animals receiving LSESR at 100 mg/kg/day *per os*; LSESR 320, animals receiving LSESR at 320 mg/kg/day *per os*; LSESR 640, animals receiving LSESR at 640 mg/kg/day *per os*; Fin 5, animals receiving finasteride at 5 mg/kg/day *per os*.

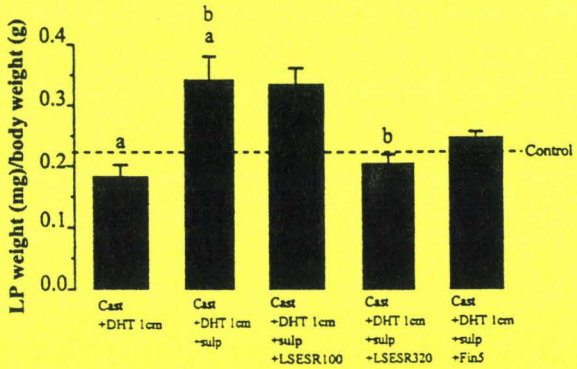

Fig. 6 Histogram showing total lateral prostate weight (mg) divided by total body weight (g). Animals received treatment as described in Table I. Values are means, and bars indicate SEM; n = 5. The values of the following treatments were significantly different: $P < 0.001$, a; $P < 0.01$, b. Cast, castrated animals; sulp., animals receiving intraperitoneal sulpiride injections (40 mg/kg/day); DHT 1 cm, animals receiving 1 cm subcutaneous DHT implant; LSESR 100, animals receiving LSESR at 100 mg/kg/day *per os*; LSESR 320, animals receiving LSESR at 320 mg/kg/day *per os*; Fin 5, animals receiving finasteride at 5 mg/kg/day *per os*.

sulpiride-treated rats. In castrated, T-implanted, sulpiride- and finasteride-treated rats (Fig. 7D), gland volume was similar to that of castrated and T-implanted rats, with neutrophil infiltration in some glands.

In castrated and DHT-implanted rats, the lateral prostate contained a similar proportion of small and large glands (Fig. 8A). In castrated, DHT-implanted, and sulpiride-treated rats, LP gland volume was gen-

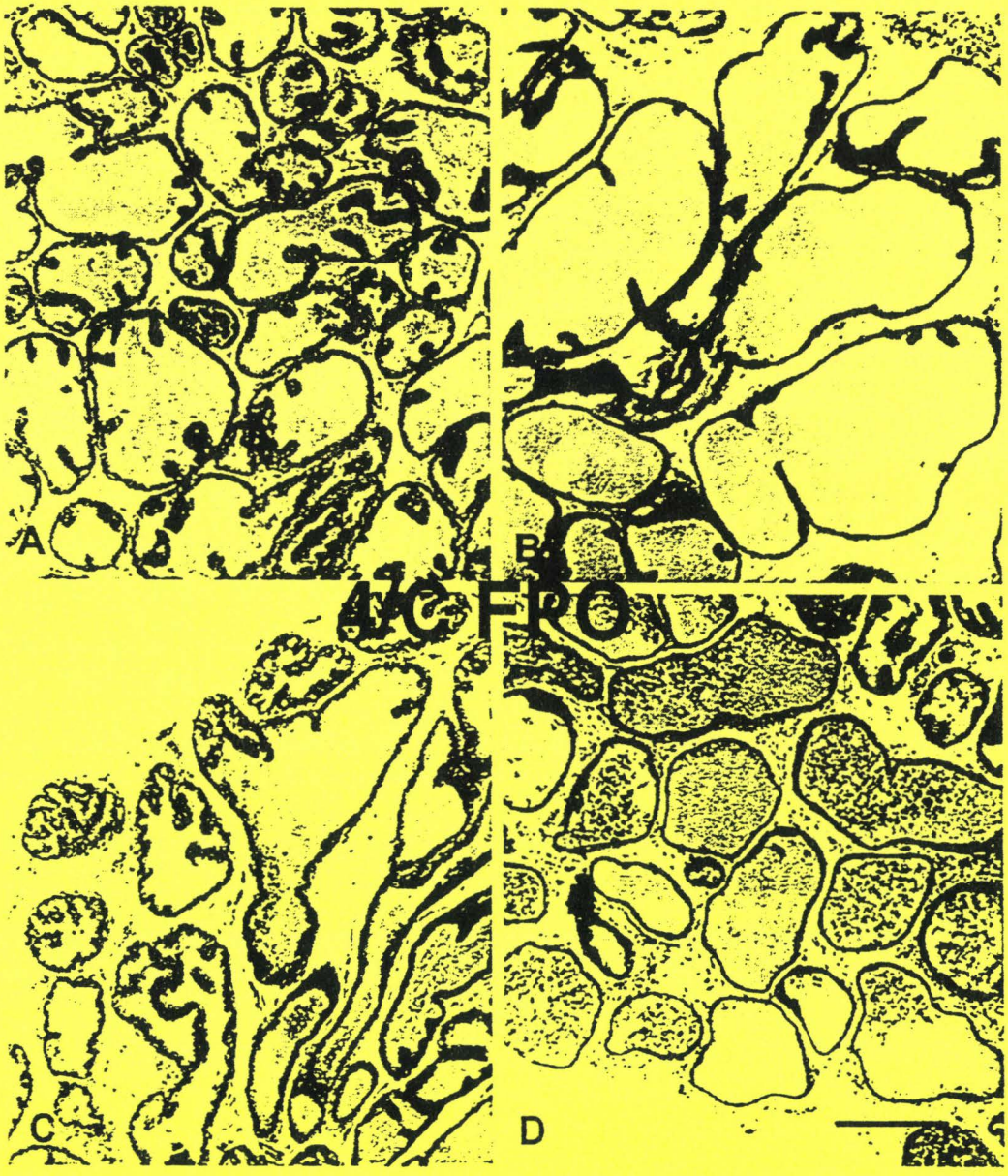

Fig. 7 Histological details of lateral prostate of castrated and T-implanted rats. Castrated and T-implanted animals received additional treatments for 30 days, as described in Table I. **A:** Castrated and T-implanted rat. Note the admixture of small and large glands. **B:** Castrated, T-implanted, and sulpiride-treated rat. Presence of very large glands. **C:** Castrated, T-implanted, sulpiride- and LSESR-treated rat. Glands are smaller than those of castrated, T-implanted, and sulpiride-treated rat. **D:** Castrated, T-implanted, sulpiride- and finasteride-treated rat. Gland volumes are similar to those of castrated and T-implanted rats, with neutrophil infiltration in some glands. Bar, 500 μm.

erally larger than in castrated, DHT-implanted rats. Moreover, some glands contained numerous neutrophils (Fig. 8B). In castrated, DHT-implanted, sulpiride- and LSESR-treated rats, the histological findings were similar to those from castrated and DHT-implanted rats, with similar proportions of small and large glands but no neutrophil infiltration (Fig. 8C). On the other hand, in castrated, DHT-implanted, sulpiride- and finasteride-treated rats, the histological findings were similar to those from castrated, DHT-implanted, and sulpiride-treated rats, with the presence of very large glands, some of which contained numerous neutrophils (Fig. 8D).

DISCUSSION

The purpose of this study was to examine and compare the effects of LSESR and finasteride in an animal model: rat prostate hyperplasia induced by hyperprolactinemia. LSESR is extracted from saw palmetto fruit (*Serenoa repens*). This extract is a mixture of many fatty acids (mainly palmitic, oleic, lauric, and myristic ac-

Fig. 8 Histological details of lateral prostate of castrated and DHT-implanted rats. Castrated and DHT-implanted animals received additional treatments for 30 days, as described in Table I. **A:** Castrated and DHT-implanted rat. Note mixture of small and large glands. **B:** Castrated, DHT-implanted, and sulpiride-treated rat. Presence of very large glands, some containing numerous neutrophils. **C:** Castrated, DHT-implanted, sulpiride- and LSESR-treated rat. Histological aspects are similar to those of castrated and DHT-implanted rats, with a mixture of large and small glands and no neutrophil infiltration. **D:** Castrated, DHT-implanted, sulpiride- and finasteride-treated rats, with the presence of very large glands, some containing numerous neutrophils. Bar, 500 μm.

ids) [35]. Thus, LSESR may have a pleiotropic action on prostate growth, first via its inhibition of 5α-reductase isoforms [35–37], and second, through its direct antiandrogenic activity [38]. LSESR therefore exerts an antiproliferative [35] and antiinflammatory [34,39] effect, but is unable to modify T secretion [40]. In this study, we demonstrated the antiprolactinic activity of LSESR for the first time. Finasteride is a specific inhibitor of the type-II 5α-reductase isoform. It was shown to inhibit LP hyperplasia and to reduce the wet weight of the LP under all conditions, except in castrated, DHT-implanted animals, irrespective of whether they were treated with sulpiride. Unlike LSESR, finasteride did not show any antiprolactinic activity. We have shown that among the three rat prostate lobes (ventral, lateral, and dorsal), only the LP is sensitive to hyperprolactinemia. In humans, the dosage of LSESR is 320 mg per day (2 doses of 160 mg) *per os*. The dosage of finasteride is 5 mg daily *per os*. In pharmacological studies [34,41], such as this work, the doses used are usually based on the human dosage per 1 kg of rat. This is why the animals received daily

gavages of 320 mg/kg of LSESR (or alternatively, 100 mg/kg and 640 mg/kg) or 5 mg/kg of finasteride. This *in vivo* model of prostate hyperplasia may be important for pharmacological studies because the LP is considered to be homologous to the transitional zone where human benign prostate hyperplasia occurs [42].

In our study, the animals received 30 daily injections of sulpiride in order to induce chronic hyperprolactinemia [43,44]. Sulpiride is a specific dopamine type-2 receptor inhibitor known to stimulate PRL secretion from the pituitary gland. This molecule affects PRL levels in two ways. Firstly, sulpiride induces a peak of prolactinemia after 30 min (up to 26 times the initial level). Secondly, the PRL concentration decreases over the next 2 hr, but still remains six times higher than the basal values [43]. In our experiments, we measured a 615% increase in PRL levels in control animals treated with sulpiride. Both LSESR (100 and 320 mg/kg) and finasteride (5 mg/kg/day) caused a significant decrease in LP weight in noncastrated animals. These results were mainly due to androgenic inhibition. Finasteride is known to be a specific inhibitor of 5α-reductase isoforms (especially the type-II isoform [45]) and to induce apoptosis in the rat ventral prostate [46]. On the contrary, as LSESR is a mixture of many fatty acids [33], it may interfere with other mechanisms that stimulate rat prostate growth. In control animals treated with sulpiride, PRL induced a significant increase in LP weight. This rise in LP weight was abolished by both LSESR (100 and 320 mg/kg/day) and finasteride (5 mg/kg/day). Thus, under hyperprolactinemia conditions, these two drugs may act by inhibiting the action of androgen. They may also diminish the direct or indirect effect of PRL on LP enlargement.

In order to distinguish between the antiandrogenic and antiprolactinic effects of LSESR and finasteride, we carried out experiments with castrated rats receiving a substitute androgen treatment via subcutaneous implants 1 cm long filled with T or DHT. A 1-cm T implant supplies half the normal T level [28,29]. Hyperprolactinemia did not enhance LP weight in castrated and in castrated-adrenalectomized rats (data not shown). In castrated rats, T implants partly restored LP weight, as compared to control animals. LSESR did not reduce the weight of the lateral lobes. This phenomenon was probably due to the low T level. Thus the ability of LSESR to inhibit 5α-reductase is less clear. Finasteride, however, clearly decreased LP weight in castrated, T-implanted animals. Finasteride acts by inhibiting 5α-reductase. Unlike LSESR, finasteride had a significant effect under these experimental conditions. Both LSESR and finasteride were ineffective in castrated, DHT-implanted rats, because inhibition of 5α-reductase had no effect on the exogenous contribution of the implant to DHT levels. In castrated and T-implanted animals, 30 days of sulpiride injections enhanced the weight of the LP. In such animals, LSESR at 100 and 320 mg/kg/day induced a nonsignificant tendency towards a decrease in lateral lobe weight. Nevertheless, both LSESR at 640 mg/kg/day and finasteride (5 mg/kg/day) significantly reduced LP weight, suggesting that they may inhibit 5α-reductase activity as well as the effects of PRL. However, unlike finasteride, LSESR reduced the weight of the lateral prostate of castrated, DHT-implanted and sulpiride-treated animals. Under these conditions, LSESR had no effect on the DHT delivered by the implant. These results indicate that, in addition to its antiandrogenic activity, LSESR also inhibits the effects of hyperprolactinemia.

A large double-blind comparative study was realized with LSESR and finasteride [4]. This work demonstrated that these two drugs produced similar improvements in BPH symptoms. Nevertheless, finasteride is more efficient than LSESR in inhibiting 5α-reductase activity [47]. This implies that LSESR could also act via other pathways in BPH, as inhibition of inflammation [34] and PRL action, as demonstrated in the present study. According to these results, we characterized two types of LSESR action: inhibition of androgen stimulation and inhibition of the hyperprolactinemia-induced effects. Finasteride only inhibits the effect of androgen on LP growth, which corresponds to its known inhibiting effect on the type-II 5α-reductase isoform [45].

The mechanisms of PRL action on the prostate are not well-known, apart from the fact that PRL potentiates androgen actions [21,22]. Nevertheless, some *in vitro* studies identified a direct effect of PRL in prostate cells [24]. Human and rat prostate cells possess PRL receptors. They also synthesize PRL, which may act via PRL receptors, mainly localized on the apical side of the epithelial cells of acini [19]. The mechanisms by which LSESR affects this process are unknown. LSESR may inhibit PRL transduction or modify the activity of PRL receptors, as shown by Vacher *et al.* in CHO cells transfected with PRL receptors [48]. In these cells, LSESR interferes with PRL receptors and signal transduction. Estrogens are implicated in the enhancement of PRL secretion [49,50] and in rat prostate growth, probably via PRL action [17,18,33]. LSESR has antiestrogenic activity [34,51], which may explain its antiprolactinic action on rat prostate enlargement. Furthermore, Lane *et al.* [17] and Tangbanluekal and Robinette [18] demonstrated that bromocriptine (a type-2 dopamine receptor agonist, which inhibits PRL secretion from the pituitary gland) antagonizes the dorsolateral rat prostate dysplasia and inflammation induced by T and estradiol

implants. LSESR also inhibits the rat prostate enlargement caused by the same cotreatment [34]. As shown in Figure 8, LSESR also appears to display an antiinflammatory action which is consistent with an antiprolactinic effect. LSESR may decrease the PRL secretion mediated by estrogens and/or inhibit the direct effect of hyperprolactinemia (induced by sulpiride) on LP enlargement and inflammation. However, the exact mechanisms by which LSESR inhibits PRL action require further investigations.

As shown by Yatani *et al.* [52], elevated PRL levels are associated with prostate cancer in humans. Some clinical studies demonstrated the beneficial effects of bromocriptine (an agonist of the type-2 dopamine receptor which inhibits pituitary PRL secretion) in prostate cancer [53–55] and in BPH [56,57]. Thus, using antiprolactinic molecules or extracts, in addition to antiandrogen therapies, could be beneficial in BPH and especially in the androgeno-independent forms of prostate cancer in humans.

CONCLUSIONS

This study demonstrates that LSESR inhibits the lateral rat prostate hyperplasia induced by hyperprolactinemia. Finasteride, a specific 5α-reductase inhibitor, is ineffective in antagonizing PRL action. Further experiments are required to identify the actions of different subfractions of LSESR in this *in vivo* model of prostate hyperplasia in order to determine which active component inhibits this PRL-induced hyperplasia.

The pleiotropic effects of LSESR partly explain the effectiveness of this drug in treating human benign prostate hyperplasia.

ACKNOWLEDGMENTS

We thank Ariane Bouteillier, Claudine Carbon, and Christelle Milluy for carrying out the histological technical procedures.

REFERENCES

1. Berry SJ, Coffey DS, Walsh PC, Ewing LL. The development of human benign prostatic hyperplasia with age. J Urol 1984;132: 474–479.
2. Walsh PC. Benign prostatic hyperplasia: etiological considerations. Proc Clin Biol Res 1984;145:1–25.
3. Horton R. Benign prostatic hyperplasia: new insights. J Clin Endocrinol Metab 1992;74:504.
4. Carraro JC, Raynaud JP, Koch G, Chisholm GD, Di Silverio F, Teillac P, Da Silva FC, Cauquil J, Chopin DK, Hamdy FC, Hanus M, Hauri D, Kalinteris A, Marencak J, Perier A, Perrin P. Comparison of phytotherapy (Permixon) with finasteride in the treatment of benign prostate hyperplasia: a randomized international study of 1,098 patients. Prostate 1996;29:231–240.
5. Di Silverio F, Monti S, Sciarra A, Varasano PA, Martini C, Lanzara S, D'Eramo G, Di Nicola S, Toscano V. Effects of long-term treatment with *Serenoa repens* (Permixon) on the concentrations and regional distribution of androgens and epidermal growth factor in benign prostatic hyperplasia. Prostate 1998;37:77–83.
6. Gormley GJ, Stoner E, Bruskewitz RC, Imperato-McGinley J, Walsh PC, McConnell JD, Andriole GL, Geller J, Bracken BR, Tenover JS, Vaughan D, Pappas F, Taylor A, Binkowitz B. The effect of finasteride in men with benign prostatic hyperplasia. N Engl J Med 1992;327:1185–1191.
7. George FW, Wilson JD. Sex determination and differentiation. In: Knobil E, Neill JD, editors. The physiology of reproduction. New York: Raven Press; 1994. p 3–28.
8. Boccon-Gibot L, Fournier G, Bottet P, Marechal JM, Guiter J, Rischman P, Hubert J, Soret JY, Mangin P, Mallo C, Fraysse CE. Flutamide versus orchidectomy in the treatment of metastatic prostate carcinoma. Eur Urol 1997;32:391–395.
9. Limonta P, Morett RM, Dondi D, Montagnani Marelli M, Motta M. Androgen-dependent prostatic tumors: biosynthesis and possible actions of LHRH. J Steroid Biochem Mol Biol 1994;49: 347–350.
10. Vacher P. Gn-RH agonist in the treatment of prostatic carcinoma. Biomed Pharmacother 1995;49:325–331.
11. Davidson JM, Chen JJ, Crapo L, Gray GD, Greenleaf WJ, Catania JA. Hormonal changes and sexual function in aging men. J Clin Endocrinol Metab 1983;57:71–77.
12. Nankin HR, Calkins JH. Decreased bioavailable testosterone in aging normal and impotent men. J Clin Endocrinol Metab 1986; 63:1418–1420.
13. Hammond GL, Kontturi M, Maattala P, Puukka M, Vihko R. Serum FSH, LH and prolactin in normal males and patients with prostatic diseases. Clin Endocrinol 1977;7:129–135.
14. Vekemans M, Robyn C. Influence of age in serum prolactin levels in women and men. Br Med J 1975;4:738–739.
15. Costello LC, Franklin RB. Effect of prolactin on the prostate. Prostate 1994;24:162–166.
16. Wennbo H, Kindblom J, Isaksson OGP, Tornell J. Transgenic mice overexpressing the prolactin gene develop dramatic enlargement of the prostate gland. Endocrinology 1997;138:4410–4415.
17. Lane KE, Leav I, Ziar J, Bridges RS, Rand WM, Ho SM. Suppression of testosterone and estradiol-17β-induced dysplasia in the dorsolateral prostate of Noble rats by bromocriptine. Carcinogenesis 1997;18:1505–1510.
18. Tangbanluekal L, Robinette CL. Prolactin mediates estradiol-induced inflammation in the lateral prostate of Wistar rats. 1993; 132:2407–2416.
19. Nevalainen MT, Valve EM, Ingleton PM, Nurmi M, Martikainen PM, Harkonen PL. Prolactin and prolactin receptors are expressed and functioning in human prostate. J Clin Invest 1997; 99:618–627.
20. Nevalainen MT, Valve EM, Ahonen T, Yagi A, Paranko J, Harkonen PL. Androgen-dependent expression of prolactin in rat prostate epithelium in vivo and in organ culture. FASEB J 1997;11:297–307.
21. Farnsworth WE. Prolactin effect on the permeability of human benign hyperplastic prostate to testosterone. Prostate 1988;12: 221–229.
22. Prins GS. Prolactin influence of cytosol and nuclear androgen receptors in the ventral, dorsal and lateral lobes of the rat prostate. Endocrinology 1987;120:1457–1464.
23. Smith C, Assimos D, Lee C, Grayhack JT. Metabolic action of

prolactin in regressing prostate: independent of androgen action. Prostate 1985;6:49–59.
24. Reiter E, Lardinois S, Klug M, Sente B, Hennuy B, Bruyninx M, Closset J, Hennen G. Androgen-independent effects of prolactin on the different lobes of the immature rat prostate. Mol Cell Endocrinol 1995;112:113–122.
25. Kledzik GS, Marshall S, Campbell GA, Gelato M, Meites J. Effects of castration, testosterone, estradiol, and prolactin on specific prolactin-binding activity in ventral prostate of male rats. Endocrinology 1976;98:373–379.
26. Aragona C, Bohnet HG, Friesen HG. Localization of prolactin binding in prostate and testis: the role of serum prolactin concentration on the testicular LH receptor. Acta Endocrinol (Copenh) 1977;84:402–409.
27. Fekete A. Receptors for luteinizing hormone-realizing hormone, somatostatine, prolactin and epidermal growth factor in rat and human prostate cancers and in benign prostate hyperplasia. Prostate 1979;14:191–208.
28. Robaire B, Ewing LL, Irby DC, Desjardins C. Interactions of testosterone and estradiol-17β on the reproductive tract of the male rate. Biol Reprod 1979;21:455–463.
29. Isaacs JT. Antagonistic effect of androgen on prostatic cell death. Prostate 1984;5:545–557.
30. Jahn GA, Deis RP. Stress-induced prolactin release in female, male and androgenized rats: influence of progesterone treatment. Endocrinology 1986;110:423–428.
31. Donnerer J, Lembeck F. Different control of the adrenocorticotropin-corticosterone response and of prolactin secretion during cold stress, anesthesia, surgery, and nicotine injection in the rat: involvement of capsaicin-sensitive sensory neurons. Endocrinology 1990;126:921–926.
32. Fujikawa T, Soya H, Yoshizato H, Sakaguchi K, Doh-Ura K, Tanaka M, Nakashima K. Restraint stress enhances the gene expression of prolactin receptor long form at the choroid plexus. Endocrinology 1995;136:5608–5613.
33. Robinette C. Sex-hormone-induced inflammation and fibromuscular proliferation in the rat lateral prostate. Prostate 1988;12: 271–286.
34. Paubert-Braquet M, Richardson FO, Servent-Saez N, Gordon WC, Monge MC, Bazan NG, Authie D, Braquet P. Effect of *Serenoa repens* extract (Permixon) on estradiol/testosterone-induced experimental prostate enlargment in the rat. Pharmacol Res 1996;34:171–179.
35. Paubert-Braquet M, Cousse H, Raynaud JP, Mencia-Huerta JM, Braquet P. Effect of *Serenoa repens* (Permixon) and its major components on basic fibroblast growth factor-induced proliferation of cultures of human prostatic biopsies. Europ Urol 1998;3:340–347.
36. Bayne CW, Grant ES, Chapman K, Habib FK. Characterisation of a new co-culture model for BPH which expresses 5α-reductase type 1 and 2: the effects of Permixon on DHT formation [abstract]. J Urol 1997;157:194.
37. Plosker GL, Brogden RN. *Serenoa repens* (Permixon). A review of its pharmacology and therapeutic efficacy in benign prostatic hyperplasia. Drugs Aging 1996;9:379–395.
38. Carilla E, Briley M, Fauran F, Sultan C, Duvilliers C. Binding of Permixon, a new treatment for prostatic benign hyperplasia, to the cytosolic androgen receptor in the rat prostate. J Steroid Biochem 1984;20:521–523.
39. Paubert-Braquet M, Mencia Huerta JM, Cousse H, Braquet P. Effect of the lipidosterolic extract of *Serenoa repens* (Permixon) on the ionophore A23187-stimulated proliferation of leukotriene B4 (LTB4) from human polymorphonuclear neutrophils. Prostaglandins Leukotrienes Essent Fatty Acids 1997;57:299–304.
40. Casarosa C, Cosci di Coscio M, Fratta M. Lack of effects of a lipidosterolic extract of Serenoa repens on plasma levels of testosterone, follicle-stimulating hormone, and luteinizing hormone. Clin Ther 1988;10:585–588.
41. Prahalada S, Rhodes L, Grossman SJ, Heggan D, Keenan D, Keenan KP, Cukierski MA, Hoe CM, Berman C, van Zwieten MJ. Morphological and hormonal changes in the ventral and dorsolateral prostatic lobes of rats treated with finasteride, a 5-alpha reductase inhibitor. Prostate 1998;35:157–164.
42. Price D. Comparative aspects of development and structure in the prostate. Natl Cancer Inst Monogr 1963;12:351–369.
43. Debeljuk L, Rozados R, Daskal H, Velez V, Mancini AM. Acute and chronic effects of sulpiride on serum prolactin and gonadotropin levels in castrated male rats (38581). Proc Soc Biol Med 1975;148:550–552.
44. Nakagawa K, Obara T, Matsubara M, Kubo M. Relationship of changes in serum concentrations of prolactin and testosterone during dopaminergic modulation in males. Clin Endocrinol 1982;17:345–352.
45. Span PN, Voller MC, Smals AG, Sweep FG, Schalken JA, Feneley MR, Kirby RS. Selectivity of finasteride as an *in vivo* inhibitor of 5 alpha-reductase isoenzyme activity in the human prostate. J Urol 1999;161:332–337.
46. Rittmaster RS, Manning AP, Stuart Wright A, Thomas LN, Whitefield S, Norman RW, Lazier CB, Rowden G. Evidence for atrophy and apoptosis in the ventral prostate of rats given the 5α-reductase inhibitor finasteride. Endocrinology 1995;136:741–748.
47. Strauch G, Perles P, Vergult G, Gabriel M, Gibelin B, Cummings S, Malbecq W, Malice MP. Comparison of finasteride (Proscar) and Serenoa repens (Permixon) in the inhibition of 5-alpha reductase in healthy male volunteers. Eur Urol 1994;26:247–252.
48. Vacher P, Prevarskaya N, Skryma R, Audy MC, Vacher AM, Odessa MF, Dufy B. The lipido-sterolic extract of *Serenoa repens* interferes with prolactin receptor signal transduction. J Biomed Sci 1995;2:357–365.
49. Neill JD, Reichert LD. Control of the proestrus surge of prolactin and luteinizing hormone secretion by oestrogens in the rat. Endocrinology 1971;89:1448–1453.
50. Shin SH. Estradiol generates pulses of prolactin secretion in castrated male rats. Neuroendocrinology 1979;29:270–275.
51. Di Silverio F, D'Eramo G, Lubrano C, Flammia GP, Sciarra A, Palma E, Caponera M, Sciarra F. Evidence that *Serenoa repens* extract displays an anti-estrogenic activity in prostatic tissue of benign prostatic hypertrophy patients. Eur Urol 1992;21:309–314.
52. Yatani R, Kusano I, Shiraishi T, Miura S, Takanari H, Liu PI. Elevated prolactin level in prostates with latent carcinoma. Ann Clin Lab Sci 1987;17:178–182.
53. Rana A, Habib FK, Halliday P, Ross M, Wild R, Elton RA, Chisholm GD. A case for synchronous reduction of testicular androgen, adrenal androgen and prolactin for the treatment of advanced carcinoma of the prostate. Eur J Cancer 1995;31:871–875.
54. Jeromin L. The serum levels of testosterone and prolactin in patients with prostatic carcinoma treated with various doses of fostrolin and bromocriptine. Int Urol Nephrol 1982;14:51–56.
55. Jacobi GH, Sinterhauf K, Kurth KH, Altwein JE. Testosterone metabolism in patients with advanced carcinoma of the prostate: a comparative in vivo study of the effects of oestrogen and antiprolactin. Urol Res 1978;6:159–165.
56. Van Poppel H, Boeckx G, Westelinck KJ, Vereecken RL, Baert L. The efficacy of bromocriptine in benign prostatic hypertrophy. A double-blind study. Br J Urol 1987;60:150–152.
57. Matos-Ferreira A, Corte-Real J, Palma J, Durao V. The effect of bromocriptine in benign prostatic hypertrophy and vesicosphincteric dynamics. 1987;60:143–149.

4- Conclusion générale de la première partie

Afin de caractériser l'implication de la PRL dans la croissance de la prostate, nous avons mis au point un modèle animal basé sur l'emploi de rats de souche Wistar subissant une augmentation du taux de PRL plasmatique. Cette étude nous a permis de démontrer que la PRL agit à la manière d'un cofacteur avec les androgènes. Par ailleurs, l'hyperprolactinémie déclenche une hyperplasie et une hypertrophie glandulaire localisée spécifiquement sur le lobe latéral de la prostate de rat. Ce fait s'avère fort intéressant dans le sens où ce lobe est homologue à la région de la prostate humaine où se développent les HBP (Price, 1963). Deux mécanismes peuvent expliquer l'effet de la PRL : une augmentation de la prolifération cellulaire et/ou une diminution de l'apoptose. Actuellement, peu de données sont connues concernant les relations unissant la PRL et la prolifération cellulaire. Nous prévoyons de réaliser cette étude au moyen de mesures immunohistochimiques. Nous avons par ailleurs découvert que la PRL induit la surexpression de la protéine antiapoptotique Bcl-2 dans la prostate latérale. Il est donc vraisemblable que la PRL puisse provoquer une diminution du pourcentage de cellules apoptotiques. Ce fait s'avère capital si l'on considère que le cancer de la prostate, à évolution lente, est le résultat d'une baisse du pourcentage de cellules apoptotiques plutôt que d'une augmentation de la prolifération cellulaire.

Le modèle animal, que nous avons créé, nous a permis également de réaliser une évolution cinétique des poids prostatiques d'animaux soumis ou non à une hyperprolactinémie. Des mesures de prolifération cellulaire et d'apoptose réalisées sur des coupes histologiques devraient nous permettre de déterminer la manière dont la PRL agit sur la croissance de la prostate.

Nous avons également mis en évidence que la voie prolactinique constitue une cible pharmacologique privilégiée pour traiter le HBP. En effet, l'E.L.S.S.R., outre son activité anti 5α-reductase, inhibe également l'effet trophique de la PRL et entraîne une réduction du poids prostatique. Nous espérons, grâce à cette étude et à celles qui suivront, que la PRL puisse être prise en compte dans les traitements des HBP et des cancers de la prostate.

DEUXIEME PARTIE

ETUDE DES MECANISMES D'ACTION DE LA PROLACTINE SUR LA PROLIFERATION ET L'APOPTOSE DES CELLULES DE LA PROSTATE.

Deux processus peuvent expliquer l'effet de la PRL sur la prostate. La PRL pourrait (i) stimuler la prolifération cellulaire et/ou (ii) inhiber l'apoptose des cellules prostatiques. Au cours de ce second volet, l'étude de la régulation de la prolifération cellulaire et de l'apoptose par la PRL a été poursuivie au moyen d'études *in vitro* grâce à l'emploi de cellules normales (cultures primaires de cellules de prostate latérale de rat) et de cellules tumorales de prostate humaine (lignée LNCaP).

Il est connu que la transduction du signal prolactinique, dans les cellules CHO transfectées avec l'ADNc codant pour la forme longue du récepteur de la PRL, implique d'une part, la stimulation des canaux potassiques dépendants du voltage et d'autre part, l'augmentation de la concentration intracellulaire en calcium grâce à l'activation de canaux calciques indépendants du voltage (Prevarskaya *et al.*, 1995). Par ailleurs, l'activation des canaux potassiques constitue l'un des premiers phénomènes intervenant dans la prolifération cellulaire (Wonderlin *et al.*, 1996 ; Vaur *et al.*, 1998 ; Skryma *et al.*, 1997). C'est la raison pour laquelle nous nous sommes appliqués à décrypter les liens unissant la PRL, les canaux ioniques et la prolifération cellulaire.

Par ailleurs, les variations de concentration en calcium intracellulaire sont des événements précoces participant au déclenchement de l'apoptose (Dowd, 1995). Cependant, les mécanismes fins qui régissent l'homéostasie calcique et l'apoptose sont peu étudiés. En utilisant les techniques de microspectrofluorimétrie et d'imagerie calcique d'une part et les techniques de détection de l'apoptose d'autre part (Hoescht) , nous nous sommes lancés dans l'étude de la régulation de l'apoptose des cellules prostatiques par le calcium.

1- PREMIERE HYPOTHESE : La prolactine stimule la prolifération cellulaire

Ces travaux ont été réalisés sur deux modèles : (i) sur des cellules normales de prostate de rat et (ii) sur des cellules cancéreuses humaines (lignée LNCaP), sensibles aux androgènes (Horoczewicz *et al.*, 1983), qui expriment la forme longue du récepteur de la PRL.

1.1- Effet de la PRL sur les cellules normales de prostate de rat

Nous avons procédé en deux temps afin d'aborder ce sujet. Tout d'abord, nous avons identifié et caractérisé les canaux potassiques présents sur les cellules provenant des lobes latéraux et dorsaux de prostate de rat. Aucune étude électrophysiologique n'avait été entreprise sur ce sujet. Puis, nous avons analysé la réponse de ces cellules suite à une stimulation par la PRL.

1.1.1- Caractérisation de canaux potassiques dans les cellules de prostate de rat

Cette étude a été entreprise dans le but de caractériser les différents canaux ioniques présents dans les cellules épithéliales normales de prostate de rat en culture primaire. Les

cellules épithéliales sont caractéristiques (de grosses cellules ovales et allongées) des fibroblastes (plus fins). La caractérisation immunocytochimiques des différents types cellulaires indique l'existence de trois populations : épithéliales (positives à la pan-cytokératine) ; myoépithéliales (positives à l'α-actine) et fibroblastes (positifs à la vimentine). Les anticorps utilisés sont spécifiques des ces types cellulaires. Grâce à la technique de patch-clamp en configuration cellule entière, nous avons pu, pour la première fois, mettre en évidence la présence de canaux K^+ dépendants du voltage, de type Kv1.3, dans les cellules épithéliales des prostates latérales et dorsales. Ces canaux sont impliqués dans la régulation du potentiel de membrane puisque leur inhibition provoque une variation de potentiel de repos. De plus, une augmentation de la concentration en calcium intracellulaire se traduit par une diminution du courant macroscopique potassique.

Le manuscrit ci-dessous, relatant ce travail, est publié dans le journal « Febs Letters ».

CONCLUSION

Nous avons caractérisé l'expression de canaux potassiques de type Kv1.3 dans les cellules de la prostate latérale et dorsale. Les canaux Kv1.3 sont impliqués dans de nombreux processus physiologiques : la sécrétion (Price *et al.*, 1989), la prolifération cellulaire (Chandy *et al.*, 1984), la signalisation calcique (Lin *et al.*, 1993) et la cytotoxicité (Schlichter *et al.*, 1986). Nous prévoyons d'étudier la spécificité de ce canal vis-à-vis de la prostate, son implication dans la prolifération cellulaire et dans la réponse aux stimuli hormonaux.

FEBS 22565

FEBS Letters 459 (1999) 15–21

Potassium channels in rat prostate epithelial cells

Halima Ouadid-Ahidouch[a,*], Fabien Van Coppenolle[a], Xuefen Le Bourhis[b], Abdelmajid Belhaj[a], Natalia Prevarskaya[a]

[a] *Laboratoire de Physiologie Cellulaire, Université de Lille I, INSERM EPI 9938, 59655 Villeneuve d'Ascq Cedex, France*
[b] *Laboratoire de Biologie de Développement, Equipe Facteurs de Croissance, Université de Lille I, 59655 Villeneuve d'Ascq Cedex, France*

Received 27 July 1999

Abstract **Voltage-dependent K^+ channels were identified and characterized in primary culture of rat prostate epithelial cells. A voltage-dependent, inactivating K^+ channel was the most commonly observed ion channel in both lateral and dorsal cells. The K^+ current exhibited a voltage threshold at −40 mV. Averaged half-inactivation potential ($V_{1/2}$) and the slope factor (k) values were −26 mV and 6, respectively. It showed a monoexponential decay with an inactivation time constant of about 600 ms at +60 mV. The deactivation time constant at −60 mV was 30 ms and the reversal potential was estimated at −80 mV, suggesting that current was carried by potassium ions. The scorpion venom peptides charybdotoxin (5 nM) and margatoxin (1 nM), inhibited K^+ current at all membrane potentials with a rapid and a slow reversibility respectively. Both tetraethylammonium (10 mM) and 4-aminopyridine (50 μM) reduced K^+ current by ~40%. We conclude that plasma membranes of lateral and dorsal rat prostate epithelial cells contain Kv K^+ channels that have biophysical and pharmacological properties consistent with those of the Kv1.3 family.**

Key words: Kv K^- channel; Whole cell recording; Prostate

1. Introduction

Potassium channels in the plasma membranes of non-excitable cells play crucial roles in cell development, volume regulation, stabilization of membrane potential and cell proliferation [1–4]. A number of studies have suggested that Kv1.3 K^- channels play a functional role in the onset of cellular events associated with both T and B lymphocyte activation. Thus, Kv1.3 K^- channels are implicated in the proliferation and interleukin 2 secretion of human B lymphocytes [5]. Recent studies have demonstrated that K^- channel activity is also a key determinant for cell progression through the G1 phase of mitosis [4]. Kv1.3 K^- channels have been linked to progression through the G1 phase in T lymphocytes. Ca^{2-}-activated K^- channels may also play a role in regulating progression through G1 in MCF-7 human mammary epithelial cells [6]. Several recent studies have reported that the factors which determine cell volume strongly influenced the mechanisms controlling cell proliferation [7–9].

In several cell types, enhanced K^- channel gene expression or increased K^- channel activity has been found to be associated with mitogenesis [10]. Rane [11] and Huang and Rane [12] showed that ras oncogene-transformed 3T3 fibroblasts had Ca^{2-}-activated K^- channels not present in non-transformed cells. In other cell lines, Teulon et al. [13] found that renal tubule epithelial cells transformed by simian virus 40 had three new K^- channel amplitudes in addition to the K^- channels normally present. Skryma et al. [14] found a new non-inactivating voltage-activated K^- channel in the androgen-dependent human cancer prostate cell line LNCaP. This channel was sensitive to tetraethylammonium (TEA) and directly and reversibly inhibited by a rise in intracellular Ca^{2-}. When these K^- channels were blocked, thymidine incorporation and proliferation decreased [14]. Although the K^- channels in the human prostate cancer cell line LNCaP have been studied in great detail, very little is known about ionic conductance in both human or rat normal prostate cells and their role in signal transduction or cell growth regulation. Therefore, we first performed a primary culture of the adult rat prostate and characterized the ionic channels in these cells.

Both lateral and dorsal rat prostate epithelial cells expressed K^- channels with the same properties as those of the Kv1.3 family.

2. Materials and methods

2.1. Dissociation of prostate tissue for primary culture

The lateral and dorsal lobes of 10–14-week-old Wistar rats were removed, freed of connective tissue and cut with scissors into ~1 cm^2 fragments. Tissue pieces were placed in 10 ml of a solution containing 500 units of collagenase (type XI, Sigma France) and 200 units of hyaluronidase (type X, Sigma France) and incubated for 90 min at 37°C. Cells were then washed three times by centrifugation at 1000 rpm for 15 min. Cells were suspended in 5 ml of the solution and incubated at 37°C in a humidified atmosphere of 5% CO_2 and 95% air. The culture medium was changed on days 3 and 5.

The lateral and dorsal cells were cultured in Eagle's minimum essential medium (EMEM) supplemented with 5% horse serum, 16 ng/ml insulin, 2 mM L-glutamine, 500 IU/ml penicillin, 500 IU/ml streptomycin, 10 ng/ml EGF, and 0.06% HEPES buffer, and maintained at 37°C in a humid atmosphere of 5% CO_2 in air.

2.2. Immunophenotyping of stromal and epithelial cells in primary culture

Monoclonal murine antibodies specific for the following proteins were used in this study: α-smooth muscle actin, vimentin, and pan-cytokeratin. Cells were plated in multichamber slides for immunocytochemical analysis. After ethanol fixation at 4°C, they were rinsed twice with PBS, then incubated with PBS containing 3% BSA (blocking solution) for 45 min at room temperature. Cells were incubated with primary antibodies overnight at 4°C, then with bridging goat anti-mouse immunoglobulin G, and lastly with peroxidase-antiperoxidase complex. The reaction product was revealed with diaminobenzidine tetrahydrochloride and hydrogen peroxidase. Cells were counterstained with Harris hematoxylin to facilitate identification of culture elements.

2.3. Whole-cell/patch-clamp technique

For electrophysiological analysis, cells were cultured in 35 mm petri dishes. The petri dishes were substituted every 30–45 min. Currents

*Corresponding author. Fax: (33) 3 20 43 40 66.
E-mail: halima.ouadid@univ-lille1.fr

0014-5793/99/$20.00
PII: S0014-5793(99)01121-7

and membrane potential were recorded under voltage-clamp or current-clamp mode, respectively, with an Axopatch 200 B patch-clamp amplifier (Axon Instruments, Burlingame, CA, USA). pClamp software (ver. 6.03, Axon Instruments) and Labmaster hardware (Digidata 2000) were used to control voltage and to acquire and analyze data. The whole-cell mode of the patch-clamp technique was used with borosilicate fire-polished pipettes (A-M systems, Everette, WA, USA) with 3–5 MΩ resistance. Seal resistance was typically in the 10–20 GΩ range. We carefully compensated the series resistance. The maximum uncompensated series resistance was < 10 MΩ during whole-cell recordings, so the voltage error was < 5 mV for a current amplitude of 500 pA. Recordings where series resistance resulted in errors greater than 5 mV in voltage commands were discarded. Liquid-liquid junction potentials were compensated using the Axopatch internal circuit. Whole-cell currents were allowed to stabilize for 5 min before K^+ currents were measured. Currents were filtered at 2 kHz with the filter of the Axopatch amplifier. The P/4 subpulse correction of cell leakage and capacitance was used to study the outward K^+ currents.

Cells were allowed to settle in petri dishes placed at the opening of a 250 μm i.d. capillary for extracellular perfusions (MSC-200, Manual solution changer, Bio-Logic Instruments, France). The cell under investigation was continuously superfused with control or test solutions.

All electrophysiological experiments were performed at room temperature.

2.4. Analysis

In all experiments, cells were depolarized every 30 s from −60 mV to different test potentials for 200 ms. At each voltage, the conductance (G_K) was calculated as $I_{peak}/(V_m - E_K)$, where E_K calculated was −86 mV. For activation, G_K during each voltage was normalized to maximal value (G_{max} at +40 mV). To obtain the half-maximal voltage ($V_{1/2}$) and the slope factor (k) values for K^+ current activation, we fitted data to a Boltzmann equation: $G = G_{max}/(1 + \exp^{(V_{1/2} - V_m)/k})$.

Experimental values are given as mean ± S.E.M. of n experiments.

2.5. Solutions

External and internal solutions had the following compositions (in mM): External: NaCl 140, KCl 5, $CaCl_2$ 2, $MgCl_2$ 2, HEPES 10, glucose 5, $NaHCO_3$ 4, Na_2HPO_4 0.3, KH_2PO_4 0.4, penicillin 0.16, streptomycin 0.068 at pH 7.4 (NaOH). Internal: KCl 150, $CaCl_2$ 0.05, HEPES 10, EGTA 1.1, $MgCl_2$ 2, at pH 7.2 (KOH). Osmolarities of bath and pipette solutions were 300–310 and 300 mosmol/l, respectively, measured with a freezing point depression osmometer.

Free Ca^{2+} concentrations for the solutions applied from the inner side of the membrane were buffered with 1.1 mM EGTA and calculated using Maxc Software (from Chris Patton, Hopkins Marine Station, Stanford University). For example, to produce 0.5 μM and 1 μM free Ca^{2+} solutions with (in mM): 0.826 $CaCl_2$, 2 $MgCl_2$, 1.1 EGTA and 0.944 $CaCl_2$, 2 $MgCl_2$, 1.1 EGTA were used respectively.

2.6. Chemicals

Margatoxin (MgTX) and charybdotoxin (ChTX) (Latoxan, France) were made up in BSA 1%, HEPES 5 mM (pH 7.2). Final concentrations were obtained by appropriate dilution in external control solution.

3. Results

3.1. Immunophenotyping of primary cell cultures derived from rat prostate lobes

Several studies have shown that prostate tissue is made up

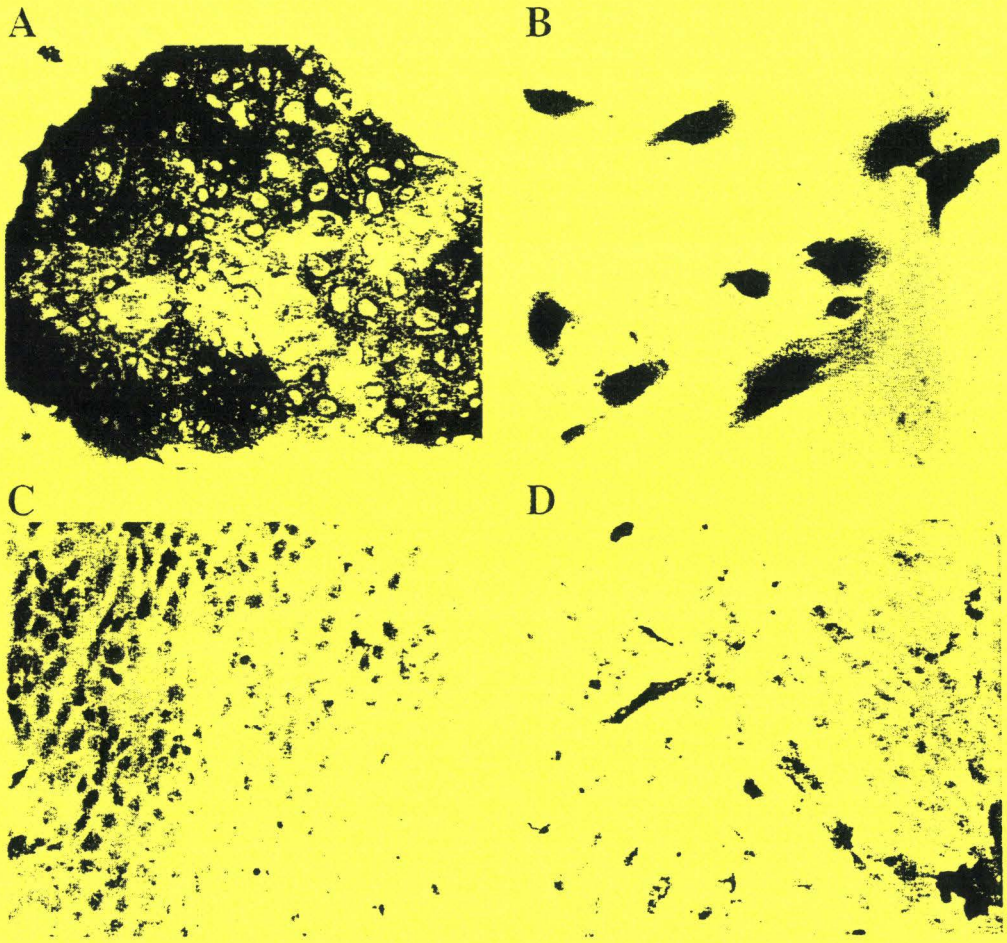

Fig. 1. Immunophenotyping of stromal and epithelial cells derived from the lateral lobe in primary culture. A: Epithelial cells were strongly positive for pan-cytokeratin. B: Isolated epithelial cells positive to pan-cytokeratin. Epithelial cells were negative for both α-actin (C) and vimentin (D).

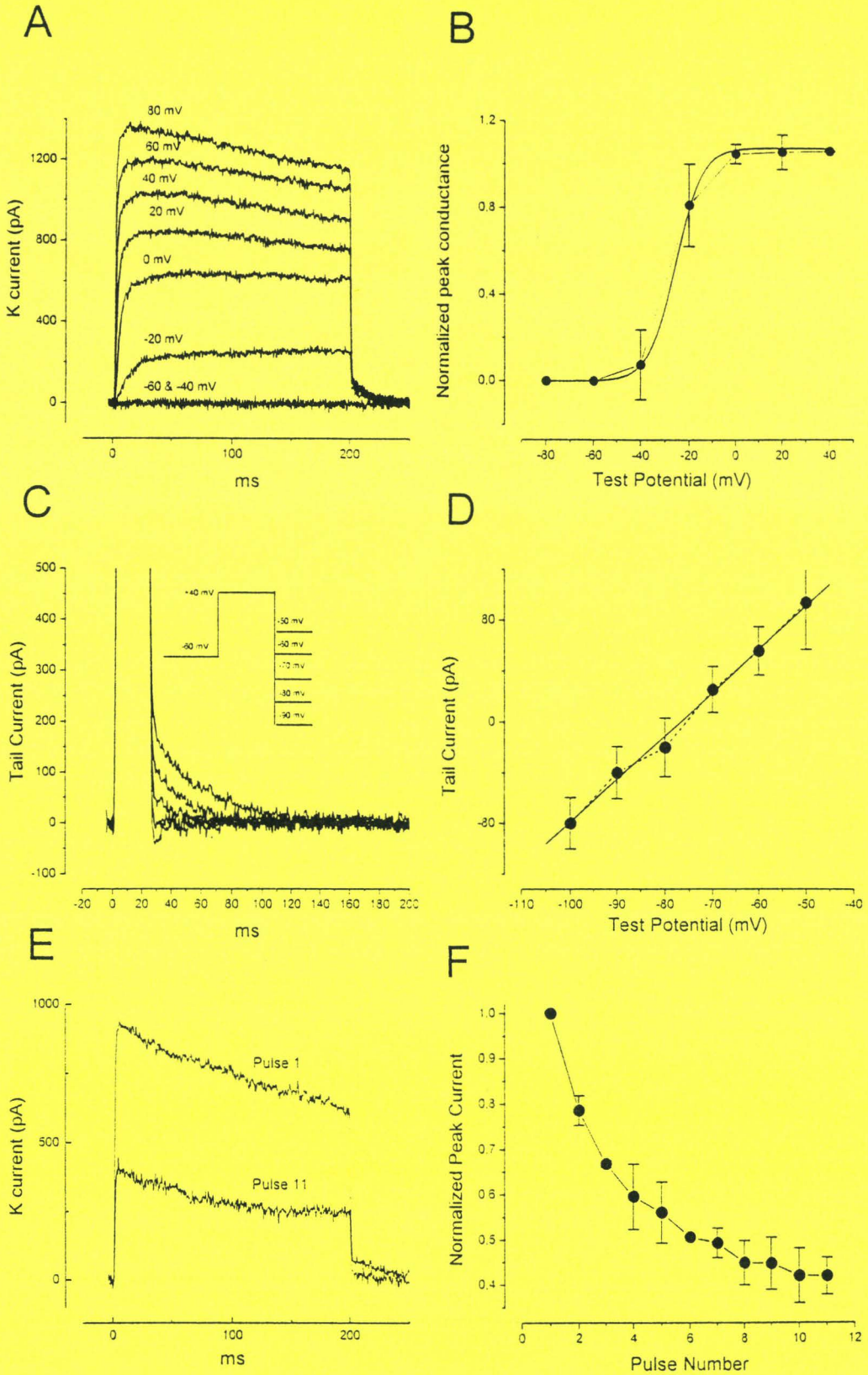

Fig. 2. Characterization of voltage-activated K^+ channel in lateral rat prostate epithelial cells. A: Examples of original K^+ currents obtained by stepping the membrane potential from −60 mV in 20 mV increments for 200 ms. B: Voltage dependence of activation. Activation curve was fitted to the Boltzmann equation (see Section 2.4). Means ± S.D. are shown ($n = 10$). C: Deactivation, tail currents after shifting to potentials of −90 to −50 mV following rapid activation to +40 mV at 30s intervals. D: Tail current-voltage relationship. E: Current was elicited by a series of 11 depolarizing voltage steps to +40 mV once every second from a holding potential of −60 mV. F: Mean normalized peak K^+ current during the series of depolarizing voltage steps (from −60 mV to +40 mV) at 1 s intervals.

of different types of cells: fibroblasts, smooth muscle, and epithelial cells [15–16]. The epithelial phenotype of cells in primary culture derived from lateral and dorsal rat lobes was verified by immunocytochemical assays. Fig. 1 shows the immunochemical staining of cells derived from lateral lobes. The majority of cells expressed pan-cytokeratin (Fig. 1A,B) but not anti-smooth muscle α-actin (Fig. 1C) or vimentin (anti-fibroblasts) (Fig. 1D). The epithelial phenotype of cells derived from dorsal rat lobe was also confirmed by immunocytochemical assays. A similar profile was observed (positive to pan-cytokeratin and negative to both α-actin and vimentin; data not shown).

3.2. *Membrane potential and membrane capacitance of rat epithelial cells*

Membrane potential obtained 5 min after accessing the intracellular compartment was -42 ± 4 mV ($n = 22$) and -40 ± 5 mV ($n = 25$) for lateral and dorsal epithelial cells, respectively. The whole-cell capacitance was 14 ± 3 pF ($n = 10$) for lateral cells and 19 ± 6 pF ($n = 15$) for dorsal cells.

3.3. *Whole-cell currents in prostate lateral cells*

Currents were elicited with 200 ms depolarizing voltage steps from −60 mV to +80 mV in 20 mV increments (Fig. 2A). The outward current reached a peak within 9.6 ± 0.68 ms ($n = 10$) and then slowly inactivated. The activation time constant (measured at +60 mV) was 1.5 ± 0.3 ms ($n = 10$). The outward currents appeared to present a single population of channels that activated at a depolarizing potential between −40 and −30 mV. The voltage dependence of this channel was determined by calculating normalized peak conductance values from the peak current amplitudes at different potentials and fitting them to a Boltzmann function (see Section 2.4). The average $V_{1/2}$ and k were -26 ± 4 mV ($n = 10$) and 5.5 ± 0.6 ($n = 10$), respectively (Fig. 2B). Moreover, the mean outward current density was 76 ± 38 pA/pF at +60 mV ($n = 10$).

To identify the reversal potential and, therefore, the ionic nature of the outward current, we studied tail currents following repolarization to different test potentials. As shown in Fig. 2C, the tail current following a 15 ms conditioning pulse to +40 mV test pulse was clearly inward at −90 mV and outward at −70 mV. From the current-voltage relationship of the tail currents, the reversal potential of the outward current was estimated to be -77 ± 6 mV ($n = 7$, Fig. 2D). The reversal potential was close to the K^+ equilibrium potential calculated under our conditions ($E_K = -86$ mV), suggesting that the outward current was predominantly carried by K^+ ions. Channel deactivation provides another convenient property for distinguishing between different types of K^+ channel. The time constant measured at −60 mV ranged from 21 to 50 ms with a mean of 30 ± 2 ms ($n = 11$). The time constant of inactivation ranged from 500 to 700 ms with a mean of 642 ± 79 ms ($n = 7$).

Inactivation of certain K^+ channels accumulates during repetitive depolarizing pulses delivered at 1 Hz because recovery during the inter-pulse interval is incomplete. This property was visualized as a reduction in current amplitude. The application of repetitive depolarization to K^+ channels induced a reduction in the amplitude of I_K ($63 \pm 14\%$, $n = 12$, Fig. 2E). The normalized peak current rapidly diminished (Fig. 2F). Thus, this channel exhibited a cumulative inactivation like that of Kv1.3.

The pharmacological profile provides a further test for defining Kv1.3 channels. We used two toxins known to inhibit Kv1.3 channels: a selective inhibitor (margatoxin, MgTX) and a less selective one (charybdotoxin, ChTX).

MgTX, a peptide purified from venom of the *Centruroides margaritatus* scorpion, blocks a brain Kv1.3 channel with a K_d of 50 pM in electrophysiological experiments [17,18]. The only other Shaker-like K^+ channel that was sensitive to MgTX is Kv1.6, but it is blocked with a 100-fold lower potency [17,18]. Originally, ChTX was reported to specifically block current through Ca^{2+}-activated K^+ channels in skeletal muscle [19]. In recent years, however, it has become clear that this toxin can also block voltage-gated K^+ channels [17,18] including Kv1.3 [20].

The extracellular perfusion of MgTX (1 nM) completely inhibited the outward current (Fig. 3A). The effect of MgTX reached a maximum at 6 min and was partially reversible after 15 min washing (Fig. 3B). The current-voltage relationships are shown in Fig. 3C. MgTX inhibited I_K at all potentials. The extracellular perfusion of ChTX (5 nM) reduced the amplitude of I_K by 73% (Fig. 3D, $66 \pm 2\%$, $n = 6$). In contrast to the effect of MgTX, the effect of ChTX on K^+ channels was immediate and completely reversible (Fig. 3E). Like MgTX, ChTX reduced I_K at all potentials (Fig. 3F). Moreover, ChTX used at 50 nM almost totally inhibited I_K ($87 \pm 3\%$, $n = 5$, data not shown).

We also tested the effect of other K^+ channel blockers: TEA and 4-aminopyridine (4-AP). These were already known to inhibit several types of K^+ channels, including Kv channels, in various cell types [18]. TEA (10 mM) and 4-AP (50 μM) reduced the K^+ channel amplitude by $43 \pm 7\%$ ($n = 6$) and $42 \pm 6\%$ ($n = 5$), respectively (data not shown).

3.4. *Whole-cell currents in prostate dorsal cells*

In dorsal epithelial cells, voltage steps from a holding po-

Table 1
Comparison of the biophysical properties of Kv1.3

	K^+ current in prostate cells	Kv1.3	Reference
Activation			
$V_{1/2}$	−26 ± 4	−21 mV	[32]
		−26 mV	[31]
		−35 mV	[33]
k	5.5	5.9	[32]
		7	[31]
Deactivation	30 ± 1.9	46 ms	[32]
		39 ms	[31]
Inactivation	600 ms	256.5 ms	[32]
Cumulative inactivation	Yes	Yes	

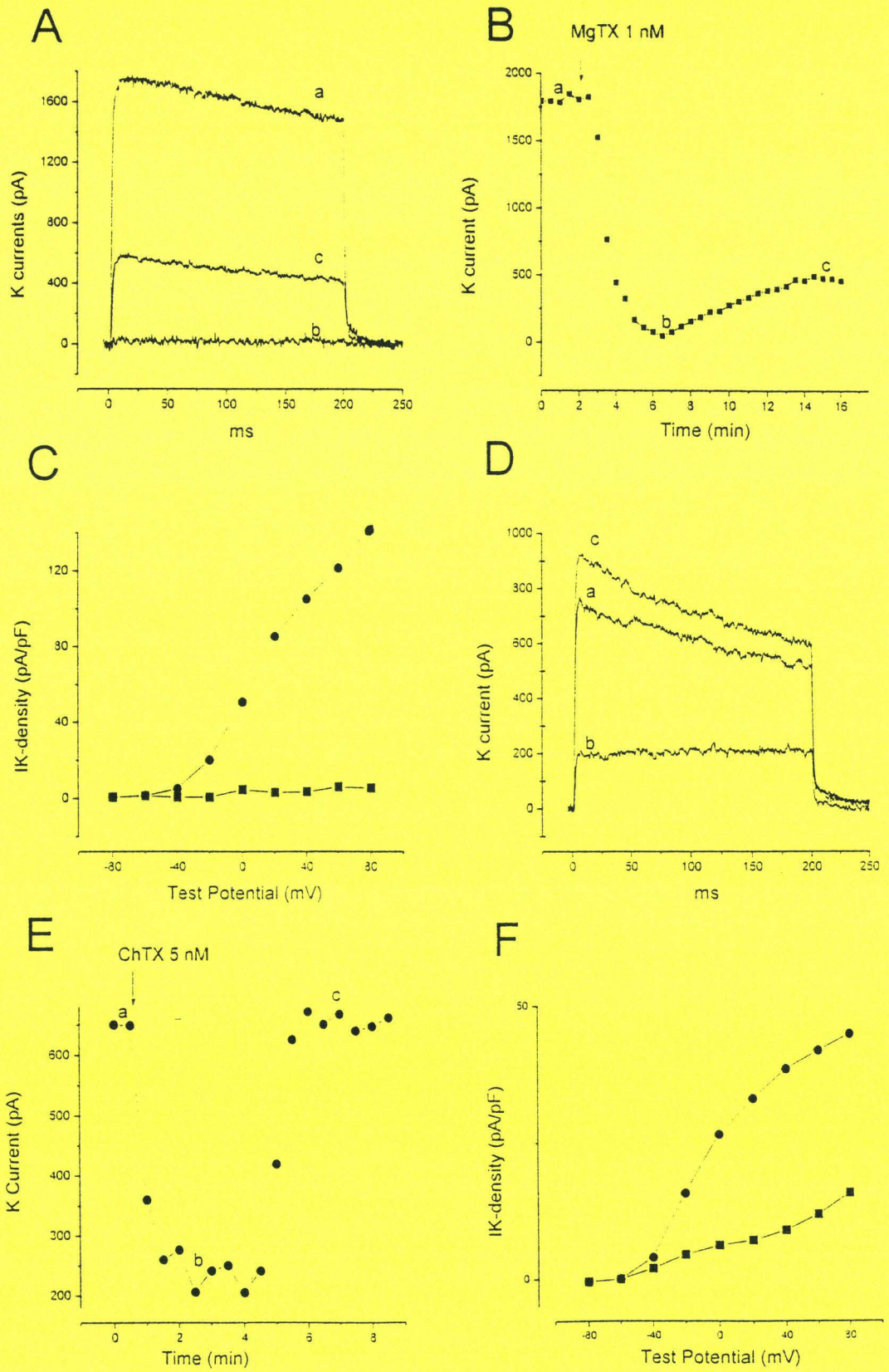

Fig. 3. Pharmacological characteristics of the K^+ current in cells derived from the lateral lobe. A: Individual K^+ current traces evoked by a depolarizing pulse from −60 mV to +60 mV. (a) I_K recorded in the control solution. (b) 6 min after 1 nM MgTX perfusion and (c) 10 min after MgTX wash. B: Time course of the K^+ current recorded in the control and after 1 nM MgTX application. C: Current-voltage relationship in the absence (●) and presence (■) of 1 nM MgTX. D: Individual current traces recorded from −60 mV to +60 mV. (a) I_K control. (b) I_K in the presence of 5 nM ChTX and (c) wash of ChTX. E: Time course of the K^+ current in the control and after 5 nM ChTX application. F: Current-voltage relationship in the absence (●) and presence (■) of 5 nM ChTX.

tential of −60 mV to +80 mV in 20 mV increments lasting 200 ms elicited an outward current that activated between −40 and −30 mV and inactivated. Average $V_{1/2}$ and k values were −26 ± 3 mV and 6 ± 0.8 (n = 9), respectively. Inactivation time constant measured at +60 mV ranged from 400 ms to 680 ms, with a mean of 568 ± 116 ms (n = 15). The mean deactivation time constant (measured at −60 mV) was 28 ± 2 ms (n = 6).

Like their counterparts recorded in lateral epithelial cells, the K^+ currents exhibited cumulative inactivation during the 200 ms depolarizing pulses to +40 mV from a holding potential of −60 mV, repeated once per second (data not shown).

K^+ current was also completely inhibited by 1 nM MgTX (n = 8) and reduced by 5 nM ChTX (65 ± 7%, n = 6, data not shown).

We also tested the effect of the increase of free $[Ca^{2+}]_i$ on K^+ current. In both lateral and dorsal epithelial cells, the increase of internal free Ca^{2+} to 0.5 μM or 1 μM (see Section 2.5 for free Ca^{2+} calculation) has no effect on the peak of K^+ current for periods of up to 15 min (n = 10).

4. Discussion

4.1. Immunophenotyping of primary cell cultures derived from rat prostate lobes

The rat prostate gland is composed of several distinct lobes: ventral, dorsal, lateral, and anterior (also called the coagulating gland) [21]. Each prostatic lobe is different in its morphology, secretions and response to hormones. The dorsolateral lobes (i) give rise to spontaneous and experimental tumors with varied hormone responsiveness [22], (ii) are considered to be the most homologous to the human prostate [21], and (iii) may play an important role in prostate cancer development [23,24]. Furthermore, the lateral lobe is considered to be the most hormone-sensitive part of the prostate [25,26].

In our studies, rat prostate cells derived from lateral or dorsal lobes retain cellular markers characteristic of epithelial cells. They expressed pan-cytokeratin but neither vimentin nor α-actin. Moreover, we report conditions that support the rapid, sustained proliferation of isolated normal prostate epithelial cells derived from the gland.

Different procedures of enzymatic digestion of rat ventral [16] or dorsolateral [15] prostates have been reported. To our knowledge, we were the first to culture the lateral and dorsal prostatic epithelial cells separately.

4.2. K^+ channels expressed in rat prostate epithelial cells

Our experiments demonstrated the existence of one type of K^+ channel in lateral and dorsal rat prostate epithelial cells. Essential properties of K^+ channels are: (i) voltage dependence (activated at −40 mV); (ii) cumulative inactivation; and (iii) high sensitivity to MgTX and ChTX, but moderate sensitivity to TEA.

The properties of the Kv channels expressed in lateral and dorsal prostate cells are consistent with the 'n' (normal) type described by Decoursey et al. [2]. N-type K^+ channels have been characterized in detail in human T lymphocytes, immature thymocytes, natural killer cells, murine thymocytes, and B lymphocytes [2,27–30].

We then compared the biophysical and pharmacological properties of the Kv1.3 channel in rat epithelial cells with those of cloned Kv1.3 expressed in mammalian cells [31,32] and *Xenopus* oocytes [33]. Further comparison was made with the activation, deactivation, and inactivation (see Table 1) of the native channel expressed in mouse or human T cells [3].

Thus, the K^+ currents expressed in both lateral and dorsal rat prostate epithelial cells closely resembled those expressed in *Xenopus* oocytes [33] or mammalian cells [31,32], as well as the native channels in mouse or human T cells.

However, the time constant of the inactivation of K^+ channels expressed in rat prostate cells was about two times slower than that of Kv1.3 (600 ms instead of 256 ms). Several studies have described that inactivation is slower with Cl ($\sim$500 ms) than with others anions, especially fluoride ($\sim$180 ms) [34,35].

The pharmacological profile provides a further test for defining K^+ channels in rat prostate cells. Both lateral and dorsal Kv1.3 channels, like their native Kv1.3 counterparts, are highly sensitive to the peptide toxins MgTX and ChTX, and moderately sensitive to TEA.

An inhibitory effect of $[Ca^{2+}]_i$ on Kv1.3 has been previously reported. Bregestovski et al. [36] observed a 4.5-fold reduction of current amplitude with pipette solutions buffered to 1 μM. However, the data reported by Verheugen [37] and Grissmer and Cahalan [38] show no effect of free $[Ca^{2+}]_i$ on the Kv1.3 current amplitude in physiological concentrations (< 10 μM) and even for concentrations as high as 2 mM. In our study, no inhibition of K^+ current by $[Ca^{2+}]_i$ with pipette solution buffered up to 1 μM of free Ca^{2+} was observed.

Thus, our results indicate that the biophysical and pharmacological properties of rat prostate K^+ channels are very similar to those of native Kv1.3 channels, except for the time constant of inactivation.

The physiological relevance of K^+ channels in normal prostate cells is questionable. Kv1.3 is involved in several physiological process: interleukin 2 secretion [5], cell proliferation [39], Ca^{2+} signaling [40], and cytotoxic killing [28]. Moreover, Kv1.3 channels are also involved in the K^+ efflux during the regulatory volume decrease that follows lymphocyte swelling [7]. There is a correlation with the level of endogenous Kv1.3 expression and the ability of mouse T cell lines to regulate volume [7]. Moreover, Kv1.3 is also implicated in promoting Ca^{2+} entry by maintaining the negative membrane potential [28]. In prostate cells, the Kv 1.3 K^+ channel may be a major determinant of the resting membrane potential that establishes the electrochemical driving force for Ca^{2+} influx. Furthermore, potassium channels are also associated with mitogenesis [10]. In the human prostate cancer cell line LNCaP, Skryma et al. [14] found a new non-inactivating voltage-activated K^+ channel which was sensitive to TEA and directly and reversibly inhibited by a rise in intracellular Ca^{2+}. Thus, we can also suggest that changes in the ion channel profiles may be linked to prostate cancer. However, the physiological role(s) of K^+ channel in prostate cells rest to determine.

The overall properties of the rat prostate epithelial cell K^+ channel suggest that it is a Kv 1.3-like K^+ channel. If this channel is specific to the prostate, as the *Slo3* channel is specific to the testis, pharmacological agents that target this K^+ channel may be useful in the study of prostate development. Further experiments using molecular biology techniques will be required to clone and study the expression of this channel in mammalian prostate cells.

Acknowledgements: This work was supported by la Region Nord-Pas de Calais, le Ministère de l'Education Nationale de l'Enseignement

Superieur et de la Recherche, l'INSERM, l'Association de la Recherche contre le Cancer (ARC, France), and la Ligue contre le Cancer (France).

References

[1] Amigorena, S., Choquet, D., Teillaud, J.L., Korn, H. and Fridman, W.H. (1990) J. Immunol. 144, 2038–2045.
[2] Decoursey, T.E., Chandy, K.G., Gupta, S. and Cahalan, M.D. (1984) Nature 307, 465–468.
[3] Decoursey, T.E., Chandy, K.G., Gupta, S. and Cahalan, M.D. (1987) J. Gen. Physiol. 89, 379–404.
[4] Wonderlin, W.F. and Strobl, J.S. (1996) J. Membr. Biol. 154, 91–107.
[5] Price, M., Lee, S.C. and Deutsch, C. (1989) Proc. Natl. Acad. Sci. USA 86, 10171–10175.
[6] Ouadid-Ahidouch, H., Le Bhouris, X.F., Toiton, R.A. and Prevarskaya, N. (1998) J. Physiol. 513, 136P.
[7] Deutsch, C. and Chen, L.Q. (1993) Proc. Natl. Acad. Sci. USA 90, 10036–10040.
[8] Rouzaire-Dubois, B. and Dubois, J.M. (1998) J. Physiol. 510, 93–102.
[9] Grinstein, S. and Foskett, J.K. (1990) Annu. Rev. Physiol. 52, 399–414.
[10] Dubois, J.M. and Rouzaire-Dubois, B. (1993) Prog. Biophys. Mol. Biol. 59, 1–21.
[11] Rane, S.G. (1991) Am. J. Physiol. 260, C104–112.
[12] Huang, Y. and Rane, S.G. (1993) J. Physiol. 461, 601–618.
[13] Teulon, J., Ronco, P.M., Geniteau-Legendre, M., Baudouin, B., Estrade, S., Cassingena, R. and Vandewalle, A. (1992) J. Cell. Physiol. 151, 113–125.
[14] Skryma, R.N., Prevarskaya, N., Dufy-Barbe, L., Odessa, M.F., Audin, J. and Dufy, B. (1997) Prostate 33, 112–122.
[15] Nishi, N., Matuo, Y., Nakamoto, T. and Wada, F. (1988) In Vitro Cell Dev. Biol. 24, 778–786.
[16] Taketa, S., Nishi, N., Takasuga, H., Okutani, T., Takenaka, I. and Wada, F. (1990) Prostate 17, 207–218.
[17] Garcia, M.L., Knaus, H.G., Munujos, P., Slaughter, R.S. and Kaczorowski, J. (1995) Am. J. Physiol. 269, C1–C10.
[18] Garcia, M.L., Honner, M., Knaus, H.G., Koch, R., Schmalhofer, H., Slaughter, R.S. and Kaczorowski, G.J. (1997) Adv. Pharmacol. 39, 425–471.
[19] Miller, C., Moczydlowski, E., Latorre, R. and Phillips, M. (1985) Nature 313, 316–318.
[20] Sands, S.B., Lewis, R.S. and Cahalan, M.D. (1989) J. Gen. Physiol. 93, 1061–1074.
[21] Price, D. (1963) Natl. Cancer Inst. Monogr. 12, 351–369.
[22] Pollard, M. (1998) Prostate 36, 168–171.
[23] Janssen, T., Kiss, R. and Schulman, C. (1995) Acta Urol. Belg. 14, 7–14.
[24] Nevalainen, M.T., Valve, E.M., Ahonen, T., Yagi, A., Paranko, J. and Harkonen, P.L. (1997) FASEB J. 11, 1297–1307.
[25] Robinette, C. (1988) Prostate 12, 271–286.
[26] Schacht, M.J., Niederberger, C.S., Garnett, J.E., Sensibar, J.A., Lee, C. and Grayhack, J.T. (1992) Prostate 20, 51–58.
[27] Schlichter, L.C., Sidell, N. and Hagiwara, S. (1986) Proc. Natl. Acad. Sci. USA 83, 5625–5629.
[28] Schlichter, L.C., Sidell, N. and Hagiwara, S. (1986) Proc. Natl. Acad. Sci. USA 83, 451–455.
[29] Choquet, D.C. and Korn, H. (1988) Biochem. Pharmacol. 37, 3797–3802.
[30] Lewis, R.S. and Cahalan, M.D. (1990) Annu. Rev. Physiol. 52, 415–430.
[31] Grissmer, S., Nguyen, A.N., Aiyar, J., Hanson, D.C., Mather, R.J., Gutman, G.A., Karmilowicz, M.J., Auperin, D.D. and Chandy, K.G. (1994) Mol. Pharmacol. 45, 1227–1234.
[32] Spencer, R.H., Sokolov, Y., Li, H., Takenaka, B., Milici, A.J., Aiyar, J., Nguyen, A., Park, H., Jap, B.K., Hall, J.E., Gutman, G.A. and Chandy, K.G. (1997) J. Biol. Chem. 272, 2389–2395.
[33] Grissmer, S., Dethlefs, B., Wasmuth, J.J., Goldin, A.L., Gutman, G.A., Cahalan, M.D. and Chandy, K.G. (1990) Proc. Natl. Acad. Sci. USA 87, 9411–9415.
[34] Cahalan, M.D., Chandy, K.G., Decoursey, T.E. and Gupta, S. (1985) J. Physiol. 358, 197–237.
[35] Verheugen, J.A.H., Oortgiesen, M. and Vijverberg, H.P.M. (1994) J. Membr. Biol. 137, 205–214.
[36] Bregestovski, P., Redkozubov, A. and Alexeev, A. (1986) Nature 319, 776–778.
[37] Verheugen, J.A.H. (1998) J. Physiol. 508, 167–177.
[38] Grissmer, S. and Cahalan, M.D. (1989) J. Gen. Physiol. 93, 609–630.
[39] Chandy, K.G., Decoursey, T.E., Cahalan, M.D., McLaughlin, C. and Gupta, S. (1984) J. Exp. Med. 160, 369–385.
[40] Lin, S., Boltz, R.C., Blake, J.T., Nguyen, M., Talento, A., Fisher, P.A., Springer, M.S., Sigal, N.H., Slaughter, R.S., Garcia, M.L., Kaczorowski, G.J. and Koo, G.C. (1993) J. Exp. Med. 177, 637–645.

1.1.2- Effets de la PRL sur les canaux potassiques de la prostate latérale de rat

Nous avons étudié les effets de la PRL sur les cellules épithéliales de prostate de rat en patch-clamp (configuration cellule entière). La PRL a été perfusée dans le milieu extracellulaire à la concentration de 5 nM. La PRL stimule l'amplitude du courant macroscopique de 25 % (figure 24 A). La figure 24 B décrit les variations de l'amplitude du courant (à +60 mV) pendant l'application de PRL. L'effet maximal de la PRL est obtenu au bout de 4 minutes 30 secondes environ.

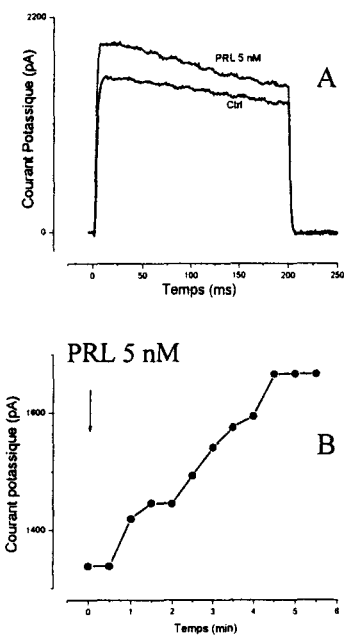

Figure 24: A: Courants potassiques obtenus en configuration whole cell (dépolarisation de -60 mV à + 60 mV pendant 200 ms). B: Cinétique obtenue à partir de l'amplitude maximale du courant potassique en fonction du temps pendant l'application de PRL (5 nM).

CONCLUSION

Les lobes latéraux de prostate de rat possèdent des récepteurs fonctionnels à la PRL (Nevalainen *et al.*, 1997). Nous avons mis en évidence, dans cette étude, que la PRL augmente l'amplitude du courant potassique macroscopique dans les cellules épithéliales de prostate de rat. Nous prévoyons d'étudier le rôle de ces canaux et de celui de la PRL dans le contrôle de la prolifération cellulaire. Ces travaux pourraient expliquer la manière dont l'hyperprolactinémie induit une hyperplasie de la prostate latérale, *in vivo*, chez le rat.

1.2- Effet de la PRL sur les cellules cancéreuses hormono-sensibles de la prostate humaine LNCaP

Cette étude a été menée sur la lignée cancéreuse humaine LNCaP (Horoszewicz *et al.*, 1993) qui a conservé sa dépendance vis-à-vis des androgènes (Furuya *et al.*, 1995). Comme dans le cadre de l'étude des cellules normales de prostate de rat, nous nous sommes d'abord appliqués à caractériser les propriétés électrophysiologiques des canaux potassiques des cellules LNCaP. Par la suite, nous avons analysé la réponse de ces cellules envers la PRL.

1.2.1- Caractérisation des canaux potassiques des cellules cancéreuses humaines

Nous nous sommes intéressés aux mécanismes de régulation de l'activité de ces canaux afin de déterminer leur rôle dans la prolifération cellulaire. Nous avons ainsi démontré que les canaux potassiques des cellules LNCaP sont inhibés par une augmentation du taux de calcium intracellulaire. Ces travaux ont été publiés dans « Receptors and Channels ».

Receptors and Channels, Vol. 6, pp. 241–253
Reprints available directly from the publisher
Photocopying permitted by license only

Characterization of Ca^{2+}-inhibited Potassium Channels in the LNCaP Human Prostate Cancer Cell Line

ROMAN SKRYMA[a], FABIEN VAN COPPENOLLE[a], LUCE DUFY-BARBE[b], BERNARD DUFY[b] and NATALIA PREVARSKAYA[a,*]

[a] *Laboratory of Cell Physiology, University of Lille I, INSERM 4U007D, Lille, France;*
[b] *Laboratory of Neurophysiology, University of Bordeaux II, CNRS URA 5543, Bordeaux, France*

(Received 30 July 1998; Revised 9 November 1998; Accepted 12 November 1998)

Potassium plasma membrane channels have been studied in the LNCaP androgen-sensitive human prostate cancer cell line, derived from a lymph node of a subject with metastatic carcinoma of the prostate. Membrane currents were recorded by the patch-clamp technique, using the cell-attached, cell-free and whole-cell mode. A voltage-dependent, non-inactivating potassium channel (delayed rectifier) was the most commonly observed ion channel in LNCaP cells. The slope conductance of K^- channels in a symmetrical 140 mM K^- gradient was 78 pS. In excised inside-out patches, the channel was inhibited by increasing the cytoplasmic Ca^{2-} concentration (with half-block at 0.5 μM Ca^{2-}) over a wide range of membrane potentials. The K^- channel had a high sensitivity to tetraethylammonium (TEA), that reduced the single channel conductance with Kd of 280 ± 27μM. The K^- channel open probability was inhibited by α-dendrotoxin (DTX) (with a half-blocking concentration of ~5 nM) and mast cell degranulating peptide (MCDP) (with half-blocking concentration of ~70 nM) at all membrane potentials and with very slow reversibility. In view of the biophysical and pharmacological properties of K^- channels in LNCaP cells, it is not possible to classify these channels as one of the previously characterized types of voltage- or ligand-gated K^- channels in other cell lines.

Keywords: Intracellular Ca^{2-}, K^- channels, LNCaP cells, Patch clamp

INTRODUCTION

Lymph Node Carcinoma of the Prostate (LNCaP) is an androgen-sensitive human prostate cancer cell line, derived from a lymph node of a subject with metastatic carcinoma of the prostate (Horoszewicz *et al*, 1983). This cell line is a useful experimental tool, as it maintains some of the characteristics of human prostate carcinoma, including androgen dependence, the presence of androgen receptors, the production of acid phosphatase, etc. (Furuya *et al*, 1995). It has also been shown that LNCaP cells

* Corresponding author. Laboratoire de Physiologie Cellulaire, Centre de Biologie Cellulaire, USTL, Bat. SN3, 59655 Villeneuve d'Ascq Cedex, France. Tel.: 33-3-20-33-60-18. Fax: 33-3-20-43-40-66. E-mail: R. Skryma: roman.skryma@univ-lille1.fr.

express plasma membrane receptors for neuropeptides such as gonadotropin-releasing hormone (GnRH) (Limonta *et al*, 1992) and vasoactive intestinal peptide (VIP) (Solano *et al*, 1996), hormones such as prolactin (PRL) (Janssen *et al*, 1996; Franklin *et al*, 1997) and growth factors such as epidermal growth factor (EGF), fibroblast growth factor (FGF), and transforming growth factor (TGF) (Sherwood *et al*, 1998; Carstens *et al*, 1997). Thus LNCaP cells are widely used for receptor-transduction studies and, particularly, for studies on proliferation and programmed cell death.

Studies of PRL- (Prevarskaya *et al*, 1995) and GnRH-receptor signal transduction (Prevarskaya *et al*, 1994) have shown that the activation of potassium or calcium channels is the primary event in PRL- and GnRH-receptor signal transduction, respectively. Calcium channels, both voltage-dependent and second-messenger-activated, have been shown to be involved in growth factor signal transduction (Peppelenbosch *et al*, 1992; Lovisolo *et al*, 1997). Ion channels also play an important role in the control of cell growth (Dubois and Rouzaire-Dubois, 1993; Wonderlin and Strobl, 1996; Nilius and Droogmans, 1994; Lepple-Wienhues *et al*, 1996; Yu *et al*, 1997). However, very little is known about the membrane ion channels in prostate cells (either normal or malignant) and their role in signal transduction or cell growth regulation.

Our previous studies using the whole cell patch-clamp technique (Skryma *et al*, 1997) showed that LNCaP human prostate cancer cells express only outward voltage-activated K^+ channels, as neither Na^+ nor Ca^{2+} currents were observed. We have also shown that these K^+ channels are involved in controlling LNCaP cell proliferation (Skryma *et al*, 1997).

In this work, we used both whole-cell and single-channel patch-clamp recording techniques to study and characterize K^+ channels in LNCaP cells. We found that voltage-dependent potassium 78 pS conductance was the predominant ion conductance in these cells. For the first time, we show a negative relationship between the intracellular calcium concentration, $[Ca^{2+}]i$, in LNCaP cells and the K^+ channel activity: the open probability of the channel was reversibly inhibited at all relevant membrane potentials by a rise in $[Ca^{2+}]i$.

RESULTS

K^+ Conductance Characterization

An outward K^+ current was revealed by whole-cell patch-clamp recordings in 77 cells out of the 85 tested (91%). Figure 1A presents examples of sustained outward currents, obtained by stepping the membrane potential from −60 to +50 mV in 10 mV increments for 80 ms. On depolarization, channels opened with a sigmoïdal time course. The current had a time to peak of 24 ± 4 ms at +20 mV ($n = 6$), and was not inactivated within the depolarization time. The current–voltage relationship for this K^+ current is shown in Fig. 1B. The voltage dependence of the channel was determined by calculating normalized peak conductance values from the peak current amplitudes at different potentials and fitting a Boltzmann function to the data: the fit gave a value for $V_{1/2} = -20 \pm 2$ mV, the voltage at which half of the channels were activated, and $k = 16 \pm 1$, a value for the gradient of the voltage dependence ($n = 9$). Deactivation rates (channel closing upon repolarization) were determined by first opening the channels with a 50 ms conditioning pulse to +30 mV and then forcing the channels to close by repolarization to different potentials (Skryma *et al*, 1997). The closing rate of K^+ channels was quantified by fitting single-exponential functions to the decay of the K^+ current during repolarization. Tail-current time constant (τ) measured at −60 mV was 15 ± 5 ms, $n = 3$. We did not observe any cumulative or "use-dependent" inactivation (inactivation accumulated during repetitive depolarizing pulses delivered at 1 Hz due to incomplete recovery during the interpulse interval) of K^+ channels ($n = 9$). The relationship between the normalized peak current and the depolarizing pulse number is shown in Fig. 1C.

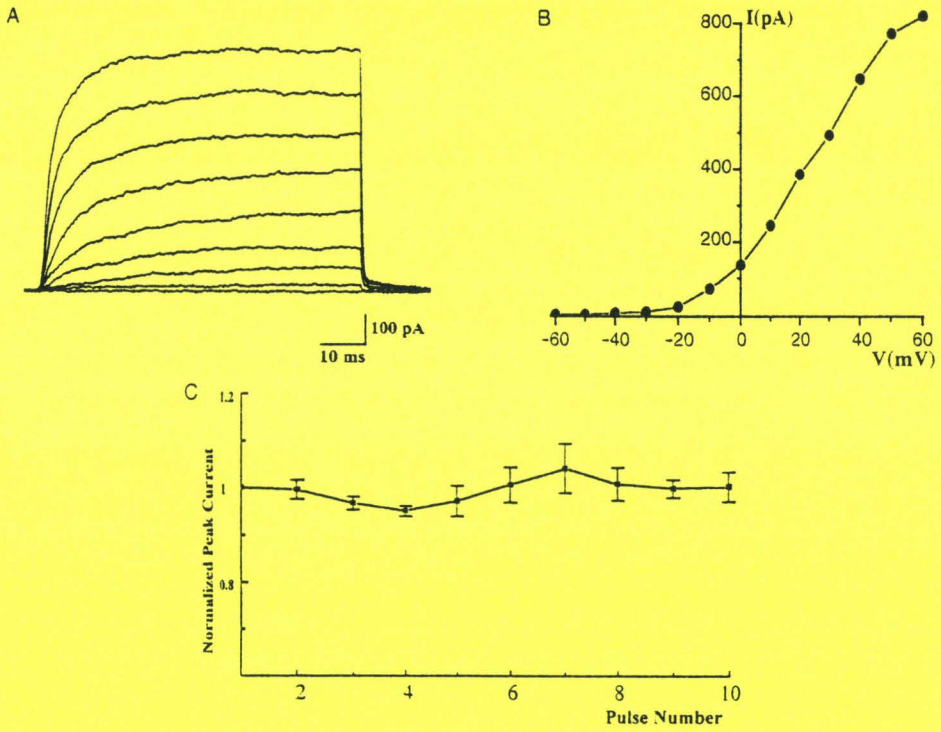

FIGURE 1 Characterization of voltage-activated K^+ conductance in LNCaP cells. A: Examples of original K^+ currents obtained by stepping the membrane potential from −60 mV to −20–+50 mV in 10 mV increments for 80 ms. The first trace corresponds to a membrane potential of −60 mV. B: Current–voltage (I–V) relationship corresponding to A. C: Cumulative (use-dependent) inactivation of K^+ current during repetitive depolarizations. Peak K^+ currents during the series of depolarizing voltage steps are plotted. Means ± SD are depicted ($n = 9$).

K^+ single-channel activity was recorded in LNCaP cells using outside-out, inside-out, and cell-attached patches ($n = 51$). Figure 2A presents examples of the activity and voltage sensitivity of the K^+ channel in a symmetrical 140 mM K^+ gradient. The traces were recorded from a holding potential of −70 mV to various depolarizing voltage steps. The slope conductance of K^+ channels in a symmetrical 140 mM K^+ gradient was 78 pS. This value was obtained from the I–V relationship by linear regression fitted to the combined data from inside-out, cell-attached, and outside-out patches ($n = 9$) (Fig. 2A). An example of an amplitude histogram (for the patch demonstrated in Fig. 2A) for membrane potential +20 mV ($\mu = 1.43$ pA) is presented in Fig. 2B.

As the external K^+ concentration decreased from 140 to 75 and 5 mM, the current–voltage curves for the channel shifted to the left (to −15 ± 2 mV, $n = 5$ and −80 ± 5 mV, $n = 5$, respectively), as would be expected for a channel mainly permeable to K^+ (not shown).

In some cells, channels with smaller unitary amplitudes were also occasionally recorded. However, these appeared much less frequently than large-conductance channels. This type of channel was not systematically analyzed.

Neither sodium nor calcium voltage-dependent conductance was observed in LNCaP cells under our experimental conditions, at a wide range of membrane potentials.

Ca^{2+} Dependence of K^+ Conductance

The standard pipette solution contained approximately 0.01 μM Ca^{2+} (see Materials and Methods). K^+ channel activity was stable under the control conditions of excised-patch experiments. No decrease in channel open probability (or "run-down")

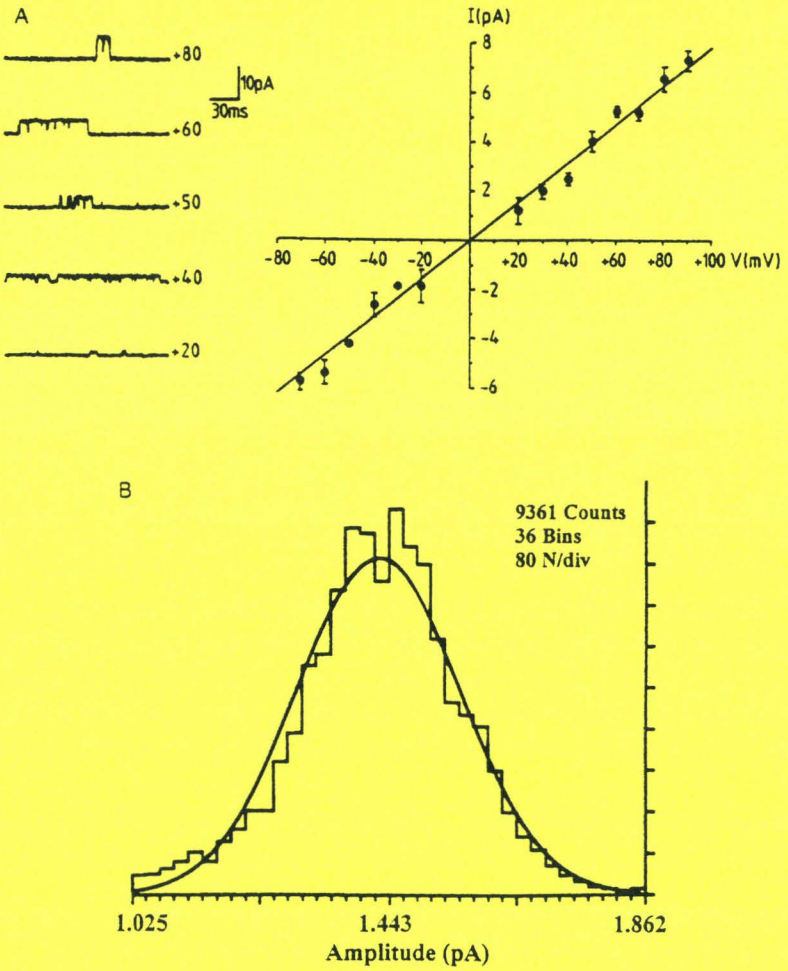

FIGURE 2 Single-channel currents recorded from excised LNCaP membrane patches exposed to symmetrical K^+ gradients. A: single-channel current traces from an outside-out membrane patch in symmetrical 140 mM K^+ gradient are presented on the left panel. Patch potential was held at −70 mV and stepped to different depolarizing potentials. Membrane potentials at which individual traces were obtained are indicated. Upward deflections represent outward current. Right panel: single channel I–V plot for 9 different patches. Data were compiled from inside-out, cell-attached, and outside-out patches. The line was fitted to all data points by linear regression and gave a slope conductance of 78 pS and a reversal potential of 0 mV. B: Example of an amplitude histogram for a membrane potential of −20 mV for the patch presented in A.

was observed during recordings lasting 20 min or more, suggesting that the channel activity did not depend on the intracellular metabolism.

However, the open probability for the K^+ channel decreased as internal free Ca^{2+} was augmented. When the internal solution applied to the cytoplasmic side of the membrane (inside-out configuration) contained increasing concentrations of free Ca^{2+} (0.2–1 μM), the open probability of the channel dramatically decreased in 11/11 patches. The original K^+ channel recordings presented in Fig. 3 were obtained from an inside-out patch during a depolarizing step to a membrane potential of +40 mV before, during, and after the application of 1 μM free Ca^{2+}. The time dependence of the K^+ channel open probability is presented in Fig. 3B. In this patch, as well as several others ($n = 11$), the blocking effect of Ca^{2+} was reversible. Figure 3C shows the $[Ca^{2+}]i$ dependence of K^+ channel open probability at a membrane potential of +30 mV,

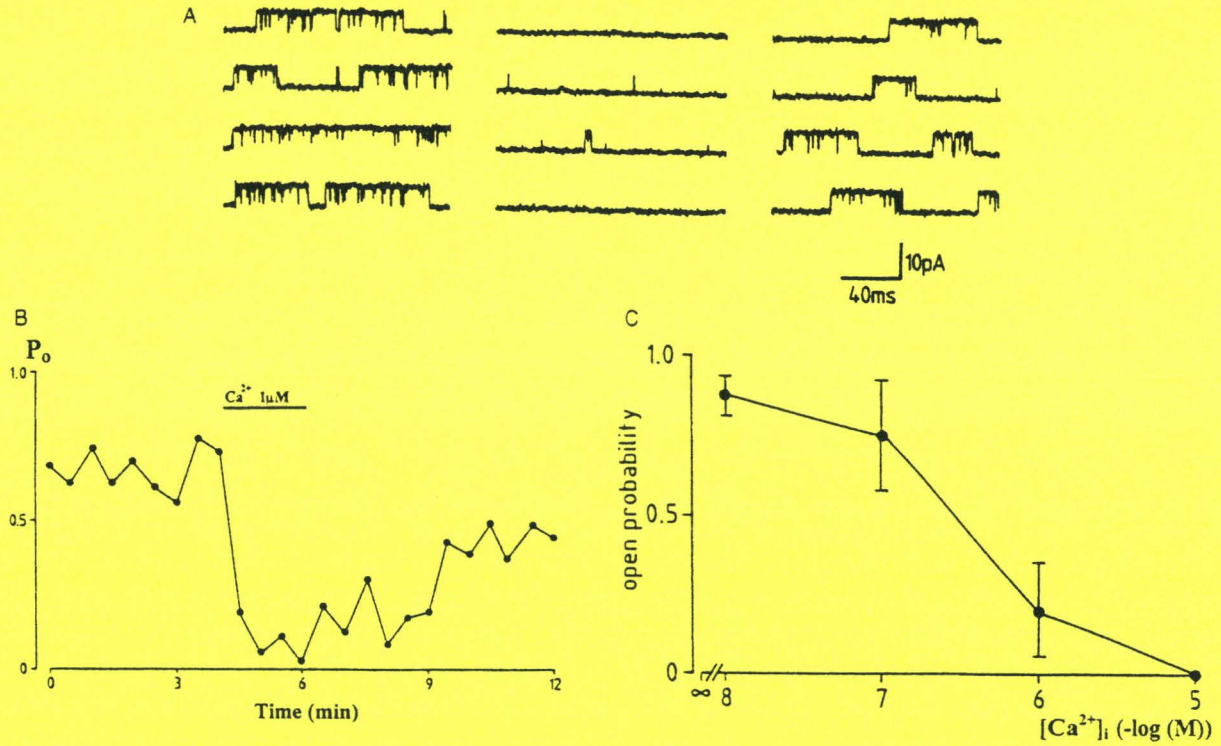

FIGURE 3 $[Ca^{2+}]i$ sensitivity of K^- channel (in 5 mM external and 140 mM internal K^- gradient). A: Effect of the rise of $[Ca^{2+}]i$ to 1 μM on K^+ channel activity. Representative records of single K^+ currents at a membrane potential of +40 mV from an excised (inside-out) membrane patch are shown for control solution (left), 3 min after 1μM Ca^{2-} application (middle), and 7 min after washout. B: The time course of the open probability of the K^+ channels in control and after application of 1 μM Ca^{2-}. The horizontal bar indicates an episode of application. C: Dose–response curves for the inhibition of K^+ channel open probability by intracellular Ca^{2-}.

with half-maximal inhibition occurring at approximately 0.5 μM. This Ca^{2+} inhibition of K^+ channels was voltage-independent.

The $[Ca^{2+}]i$ level did not markedly affect the single-channel conductance, as the slope conductance of the channel was not changed by increasing $[Ca^{2+}]i$ from 0.01 to 1 μM ($n = 5$, data not shown).

Pharmacology of K^+ Channels

We investigated the sensitivity of K^+ channels in LNCaP cells to various pharmacological K^+ channel blockers.

We first studied the effect of a potent K^+ channel blocker, tetraethylammonium (TEA), already known to inhibit various types of K^+ channels in various cell models (for review see Garcia *et al*, 1997; Pongs, 1992). TEA block was expressed as a reversible reduction in single-channel amplitude. Figure 4A presents outside-out patch recordings of the K^+ channels during a depolarizing step to a membrane potential of +50 mV. When a 200 μM TEA solution was applied, the K^+ channel amplitude was strongly depressed (Fig. 4B).

We measured the dose–response characteristics of the block by external TEA. The concentration dependence of TEA inhibition was measured as the percentage reduction of single-channel amplitude (Fig. 4C). The continuous curve represents a theoretical dose–response curve for a one-to-one drug-to-receptor binding scheme:

$$\text{Percentage inhibition} = \frac{100\%}{1 + Kd/Co}$$

where Kd is the dissociation constant and Co is the external TEA concentration. The theoretical

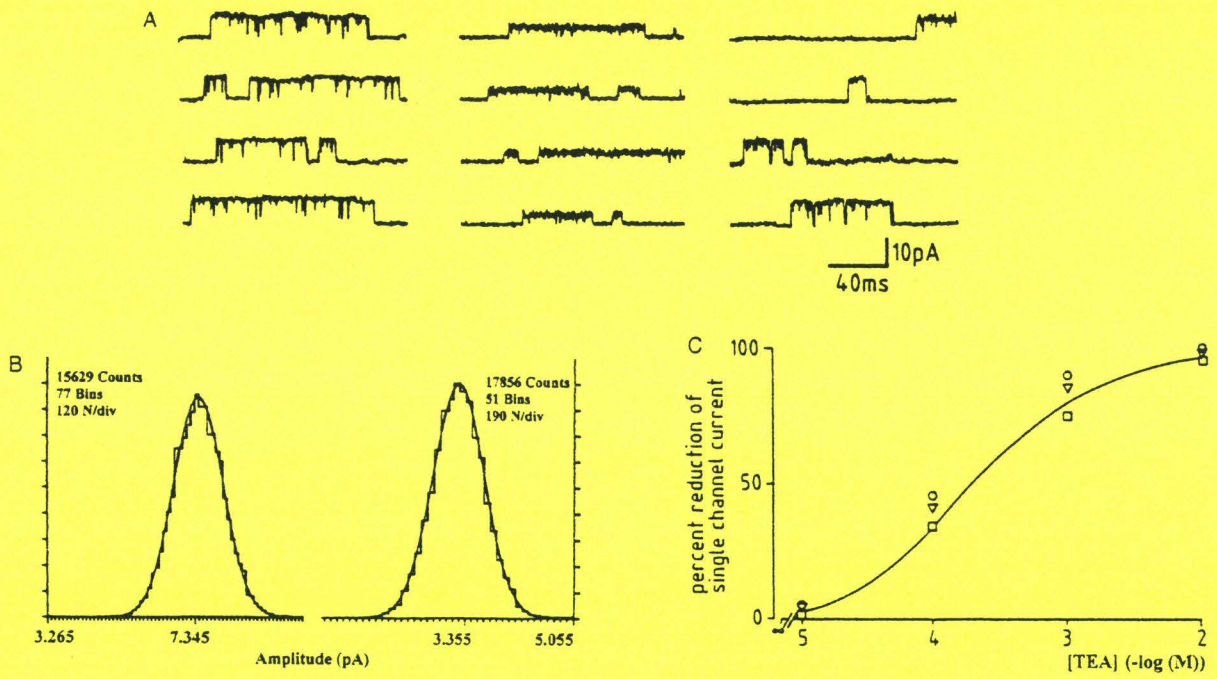

FIGURE 4 The effect of TEA on K^+ channel activity channel (in 5 mM external and 140 mM internal K^+ gradient). A: Representative records of single K^+ currents in excised (outside-out) membrane patch at a membrane potential of +50 mV. Records are shown for the control solution (left panel), 1 min after 200 μM TEA application (middle panel), and after 3 min of recovery (right panel). B: Amplitude histograms for recordings of control (left) and in the presence of 200 μM TEA (right) (for the patch presented in A). C: Dose–response curves for the TEA block of K^+ channels. The percentage reduction in the single-channel current is plotted against the external TEA concentration. The different symbols represent data obtained from five different patches containing K^+ channels. The curve represents the best-fit theoretical dose–response curve for one-to-one drug-to-receptor binding scheme.

dose–response curves were fitted to the data points by a least-squares minimization algorithm. The Kd value obtained from this fit was 280 ± 27 μM (estimate ± standard deviation; CD = 0.95). The blocking of K^+ channels by external TEA was voltage-independent.

We also checked the effect of another "standard" voltage-dependent K^+ channel blocker, 4-amino-pyridine (4-AP), widely used as a selective inhibitor of transient K^+ currents (Garcia *et al*, 1997; Pongs, 1992). 4-AP (1 mM) did not affect K^+ conductance in our studies at all membrane potentials ($n = 5$).

A number of toxins have been used to determine the different kinds of potassium channels expressed in a variety of cells (for review see Garcia *et al*, 1997; Pongs, 1992). We used several toxins known to inhibit voltage- and Ca^{2+}-dependent K^+ channels. Charybdotoxin (CTX) (10–100 nM) and Iberiotoxin (IBTX) (1–100 nM), inhibitors of Ca^{2+}-activated K^+ channels and some types of voltage-gated K^+ channels (for review see Garcia *et al*, 1997), had no effect on K^+ channels in LNCaP cells at all membrane potentials.

Conversely, dendrodotoxin (DTX), a polypeptide isolated from the venom of the Green Mamba snake *Dendroaspis angusticeps*, applied to the outside of the membrane patch (outside-out configuration) (Fig. 5A and B, caused a decrease in the open probability of K^+ channels (with a half-blocking concentration of ~ 5 nM), without affecting single channel amplitude. Figure 5A shows the time course of the open probability of the K^+ channels in the control, in the presence of 5 nM DTX, and after washout. This inhibition of K^+ channels by DTX was observed in all seven patches examined. In contrast to the rapid flicker block by

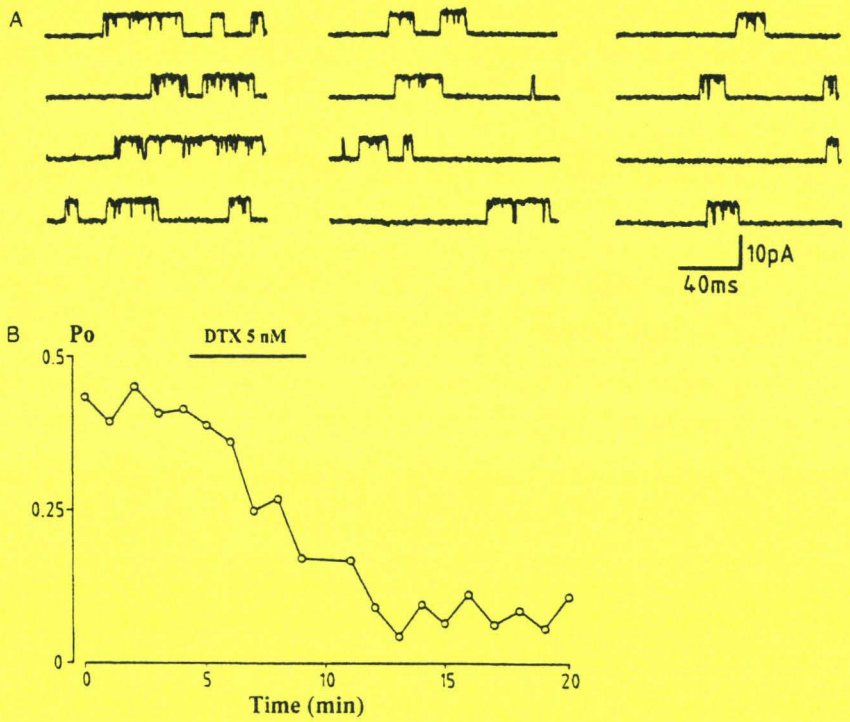

FIGURE 5 The effect of DTX on K^- channel activity channel (in 5 mM external and 140 mM internal K^- gradient). A: Representative recordings of single K^- currents in excised (outside-out) membrane patch at a membrane potential of +40 mV. Records are shown for the control solution (left panel), 5 min (middle panel) and 10 min (right panel) after 5 nM DTX application, respectively. B: The time course of the open probability of the K^- channels in the control and after 5 nM DTX application. The horizontal bar indicates an episode of 5 nM DTX application.

external TEA, the DTX K^+ channel block had very slow kinetics (Fig. 5B). The onset of DTX action depended on the concentration and was slower (about 8 min) for low (0.2–0.5 nM, $n = 4$), than for high DTX concentrations (4 ± 2 min for 2–10 nM, $n = 6$). After DTX wash-out, the K^- channel activity also reversed very slowly: for 5 nM DTX block, the open probability of K^+ channels reversed to maximum of 80% of control values, recovery began approximately 11 min after washout and reached maximal levels by 20 ± 5 min at +40 mV ($n = 3$).

We also used MCDP, mast cell degranulating peptide, extracted from honey bee (*Apis mellifera*) venom, that blocks transient and delayed rectifier voltage-activated K^+ currents in several cell types (Stühmer *et al*, 1989). MCDP inhibited the open probability of K^+ channels in LNCaP cells (with a half-blocking concentration of ~70 nM) with the same slow kinetics as DTX (data not shown). The maximal reduction in the open probability of K^+ channels with MCDP (80 nM) was 60 ± 9% (mean value ± SD, $n = 5$) at a membrane potential of +20 mV (Fig. 6). When the K^+ channel activity was already inhibited by DTX (cells had been incubated for at least 10 min with 5 nM DTX), subsequent application of MCDP was ineffective, indicating that these two peptides affected the same set of K^+ channels.

Quinidine (10 μM), a non-specific K^- channel blocker, inhibiting various types of K^+ channels (Hille, 1992; Stansfeld *et al*, 1996), slightly decreased the open probability of K^+ channels in LNCaP cells (14 ± 12% at membrane potential of +20 mV, $n = 7$) (Fig. 6).

Figure 6 presents summary histograms of the effects of all drugs studied on the ratio of the

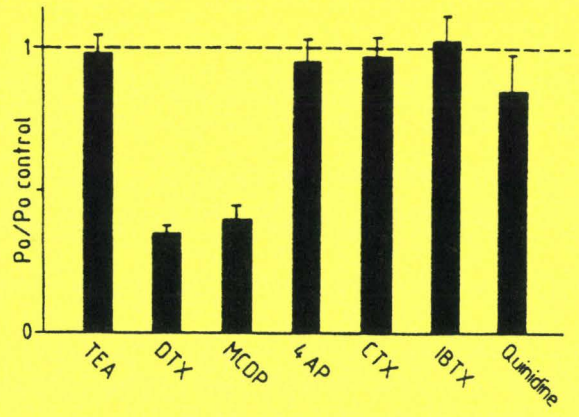

FIGURE 6 Synopsis of Po modulation by K^+ channel inhibitors: TEA 200 μM, DTX 5 nM, MCDP 80 nM, 4-AP 1 mM, CTX 30 nM, IBTX 10 nM, Quinidine 10 μM. The histogram shows the effects of these drugs on the channel open probability ratio (Po).

channel open probabilities (Po), obtained by single-channel recordings.

DISCUSSION

Our experiments demonstrated the existence of at least one type of K^+ channel in LNCaP human prostate cancer cells. In most cells studied, only one non-inactivating type of K^+ current was observed, with kinetic properties of the "delayed rectifier" K^+ current (for review see Garcia *et al*, 1997; Pongs, 1992). However, in view of the biophysical and pharmacological properties of K^+ channels in LNCaP cells, it was not possible to attribute these channels to one of the voltage- or ligand-gated K^+ channels previously identified in other cell models.

The predominant channel type in LNCaP cells is a 78 pS K^+ channel, activated by depolarization. This channel's unitary conductance (78 pS) classifies it as an "intermediate" as opposed to "small" (5–20 pS) and "big" or "maxi" (200–300 pS) (Lang and Ritchie, 1990) K^+ channels. The K^+ channel in LNCaP cells does not correspond to one of the K^+ channels in murine T lymphocytes ("l", large, or "n", normal, with 21 and 12 pS unitary conductance, respectively, according to the classification of Decoursey *et al*, 1987). However, by its sensitivity to TEA (with a half-block of 280 ± 27 μM) the K^+ channel in LNCaP cells is closer to "l" channels (half-block: 50–100 μM) than to "n" channels (half-block: 8–16 mM).

Fast-proliferating small-cell lung cancer (Pancrazio *et al*, 1993) and human melanoma cells (Nilius and Wohlrab, 1992), two non-excitable cancer cell models, have a K^+ channel with kinetic properties similar to those of the non-inactivating channel described here. However, in small-cell lung cancer the K^+ current amplitude is about 50% blocked by 4 mM 4-AP (in LNCaP cells the K^+ current is insensitive to 4-AP) and in human melanoma cells the K^+ channel has a conductance of approximately 10 pS, much smaller than that in LNCaP cells.

We have compared the biophysical properties of the K^+ channel in LNCaP cells with those of several cloned voltage-gated K^+ channels, from *Shaker* (Kv1.1, 1.2, 1.3, 1.5) and *Shaw* (3.1) and K^+-channel families, stable expressed in mammalian cell lines (Grissmer *et al*, 1994). All these channels presented slow inactivation kinetics, similar to those of LNCaP-cell K^+ channels. Kv1.1 channels were reported to be very similar in electrophysiological studies to native channels in C6 glioma cells (Wang *et al*, 1992). Kv1.3 and Kv3.1 channels resembled "n" and "l" channels in T-lymphocytes, respectively (Chung and Schlichter, 1997). Kv1.5 channels were similar to native K^+ channels in the heart (Fedida *et al*, 1993). K^+ channels in LNCaP cells ($V_{1/2}$ about −20 mV, determined by calculating the dependence of normalized peak conductance on membrane potential) activated at more strongly depolarized potentials than Kv1.1, Kv1.3, or Kv1.5 ($V_{1/2}$ about −32, −26 and −14 mV, respectively) but at less depolarized potentials than Kv1.2 ($V_{1/2}$ about +27 mV), but were similar to Kv3.1 ($V_{1/2}$ about +16 mV). The deactivation rate (τ about 15 ms) was similar to Kv1.1 channels ($\tau = 14 \pm 5$ ms). K^+ channels in LNCaP cells exhibited no "use-dependent" inactivation (Kv1.3 channel property) and no stimulation by repetitive pulses (Kv1.2 channel property). The 78 pS unitary

TABLE I Biophysical properties of K^+ currents in different cell lines stably transfected with Kv1.1, Kv1.2, Kv1.3, Kv1.5, Kv3.1 in comparison with those of K^+ channel in LNCaP cells (values are given as mean ± standard error of the number of cells in parentheses)

	mKv1.1 (L929)	rKv1.2 (B82)	mKv1.3 (L929)	hKv1.5 (MEL)	mKv1.3b (L929)	K (LNCaP)
Activation						
$V_{1/2}$ (mV)	−32 ± 2 (2)	27 ± 6 (8)	−26 ± 8 (3)	−14 ± 3 (6)	16 ± 1 (3)	19 ± 2 (9)
k	8.5 ± 0.5 (2)	13 ± 2 (8)	7 ± 1 (3)	12 ± 1 (6)	8.7 ± 0.4 (3)	16 ± 1 (9)
Deactivation, τ_t at −60 mV (ms)	14 ± 5 (2)	23 ± 7 (5)	39 ± 6 (3)	23 ± 4 (6)	1.4 ± 0.2 (3)	15 ± 5 (3)
Cumulative inactivation	No	No	Yes	No	No	No
Single-channel conductance (pS)	10	18	14	8	27	78
Current amplitude (at +40 mV) (pA)	1108 ± 376 (11)	3377 ± 920 (10)	3657 ± 1207 (10)	1211 ± 288 (10)	3836 ± 1116 (10)	580 ± 190 (38)
Cell capacitance (pF)	22 ± 3 (11)	17 ± 3 (10)	15 ± 3 (10)	11 ± 2 (10)	16 ± 2 (10)	16 ± 3 (7)

conductance of the LNCaP-cell K^+ channel is several times larger than that of Kv1.1, Kv1.2, Kv1.3, and Kv1.5, while Kv3.1 varied from 8 to 27 pS. Thus, the LNCaP-cell K^+ channel is not biophysically identical to one of these Kv channels. Table I summarizes the biophysical properties of Kv1.1, Kv1.2, Kv1.3, Kv1.5, and Kv3.1 channels (Grissmer *et al*, 1994) in comparison with those of K^+ channel in LNCaP cells.

The pharmacological data for the K^+ channel in LNCaP cells show that the channel under study has properties similar to those of the Kv1.1 channel inhibited by TEA (Kd = 0.3 mM), DTX (Kd = 20nM), and MCDP (Kd = 0.49 μM). It differs, however, in that, unlike the Kv1.1 channel (Kd = 290 μM), it was not blocked by 4-AP. External TEA interacts with a tyrosine at the carboxyl-terminal end of the P-region (MacKinnon and Yellen, 1990). Kv1.1 and Kv3.1 channels with tyrosines in this position, were half-blocked by ~0.3 mM external TEA. As this K^+ channel has the same sensitivity to TEA, we can suggest that it also has a tyrosine at the carboxyl-terminal end of the P-region. Channels that have a valine (rKv1.2) or arginine (Kv1.5) in place of the tyrosine, are TEA-resistant (Grissmer *et al*, 1994). Channels that have a histidine at the homologous position (Kv1.3) (Douglass *et al*, 1990) are characterized by lesser sensitivity to external TEA (~10 mM half-blocking) and by slow C-type inactivation. DTX and MCDP markedly decreased the K^+ current amplitude and channel open probability in LNCaP cells. Inhibition of the K^+ channel by these toxins displayed very slow kinetics and was almost irreversible, in accordance with their previously demonstrated mode of action on non-inactivating K^+ current in dorsal-root ganglion neurons (Penner *et al*, 1986). Heurteaux and Lazdunski, 1991 suggested that, *in vivo*, DTX and MCDP may act on two distinct classes of channels. We found that the effects of DTX and MCDP were not additive, suggesting a common site of action for the two substances in LNCaP cells. It was also reported (Weller *et al*, 1985) that DTX has an aminopyridine-like action: an increase in the apparent rate of inactivation, suggesting open channel block. In our experiments we never observed any DTX action of this type. However, electrophysiological data obtained from a variety of cell models indicate that DTX and MCDP inhibit a family of K^+ channels that differ greatly in their inactivation kinetics (Garcia *et al*, 1997). CTX, known to inhibit the Kv1.3 channel in T lymphocytes and neuronal tissue (Grissmer *et al*, 1994; Garcia *et al*, 1997), the Kv1.2 channel (Grissmer *et al*, 1994) and high-conductance Ca^{2+}-activated K^+ channels (Skryma *et al*, 1994; Garcia *et al*, 1997), were not able to inhibit the K^+ channels in LNCaP cells. IBTX, known to inhibit maxi-K channels by a reversible bimolecular reaction identical to CTX, was also ineffective. CTX and IBTX are the classical

inhibitors of the *Slo*1 K^+ channel family, characterized by dependence of both depolarization and intracellular calcium increases (Garcia *et al*, 1997). Recently, another member of the *Slo* family was identified in both mouse and human testes by reverse transcription-polymerase chain reaction (RT-PCR), Northern analysis, and *in situ* hybridization: *Slo*3 K^+ channel, a novel pH-sensitive K^+ channel from mammalian spermatocytes (Schreiber *et al*, 1998). This channel is characterized by high testis-specific expression. The *Slo*3 channel is insensitive to intracellular calcium, relatively insensitive to TEA (49 mM half-blocking), and has 90 pS unitary conductance (considerably lower than that of *Slo*1), suggesting that *Slo* channels comprise a multigene family, defined by a combination of sensitivity to voltage and a variety of intracellular factors. Thus, it cannot be ruled out that the LNCaP-cell K^+ channel may be one of the *Slo* channel family as it is also regulated by two factors: voltage and intracellular calcium.

A specific property of LNCaP-cell K^+ channels is that they are directly and reversibly inhibited by a rise in intracellular Ca^{2+}. This property of voltage-dependent K^+ channels has been reported in lymphocytes (Bregestovski *et al*, 1986; Schlichter *et al*, 1993), rat microglial cells (Nörenberg *et al*, 1994), and a human embryonic kidney cell line, stably transfected with rat *ether-à-go-go* (r-*eag*) channel DNA construct (Stansfeld *et al*, 1996). K^+ channels in these cell models were quite different from those in LNCaP cells: the K^+ channel in T-lymphocytes was inhibited by higher $[Ca^{2+}]i$ and had a smaller unitary conductance of 14 pS (Bregestovski *et al*, 1986). In rat microglia, and in cells stably transfected with r-*eag* DNA, the K^+ channels had different pharmacological properties (Nörenberg *et al*, 1994; Stansfeld *et al*, 1996). In inside-out experiments, micromolar levels of cytoplasmic $[Ca^{2+}]i$ were required to block LNCaP-cell K^+ channels (the half-maximal inhibition of open probability occurred at 0.5 μM). However, the $[Ca^{2+}]i$ sensitivity in intact cells may be greater than in excised-patches and whole-cell recordings (Bregestovski *et al*, 1986). K^+ channel inhibition by an increase in $[Ca^{2+}]i$ was observed at all membrane potentials. These excised-patch experiments indicated that Ca^{2+} probably binds directly to the K^+ channel rather than to intermediate cytosolic protein, e.g. calmodulin. However, it remains to be shown whether the channel functions may be modulated by intermediate membrane-bound protein and by certain kinases or phosphatases, that may be Ca^{2+}-dependent. A hypothesis involving the "direct" binding of Ca^{2+} to K^+ channels is in agreement with the model of Grissmer *et al* (1992) proposed for K^+ (Ca^{2+} inhibited) channels in human leukemia T-cells.

The physiological relevance of K^+ channel inhibition by an increase in $[Ca^{2+}]i$ is questionable. The proposed role of the *Slo*1 channel, for example, is to provide negative feedback for the entry of calcium into cells via hyperpolarization-induced closure of voltage-dependent calcium channels. Perhaps because of the versatility of this mechanism, *Slo*1 channels are expressed in many tissues where voltage-gated calcium channels are present, including brain, skeletal and smooth muscle, pancreas, and adrenal gland cells. As voltage-dependent Ca^{2+} channels are not present in LNCaP cells, increases in $[Ca^{2+}]i$ may be caused by Ca^{2+} entry through receptor- and/or second-messenger-operated Ca^{2+} channels, and also by mobilization from intracellular Ca^{2+} pools with subsequent capacitative Ca^{2+} entry. These types of Ca^{2+} entry mechanisms have been shown to be stimulated by numerous growth factors and hormones (for review see Lovisolo *et al*, 1997) influencing cell growth. Such agonist-induced increase in $[Ca^{2+}]i$ would inhibit K^+ channels in LNCaP cells, which, in turn, would induce membrane depolarization with a subsequent reduction in Ca^{2+} influx, representing a negative-feedback of $[Ca^{2+}]i$ regulation in these cells without voltage-operated Ca^{2+} channels.

The overall properties of the LNCaP-cell K^+ channel suggest that it is a new type of channel. If this channel is specific to the prostate, as the *Slo*3 channel is specific to the testis, pharmacological agents that target this K^+ channel may be useful in

the study of prostate cancer development. Further experiments using molecular biology techniques will be required to clone and study the expression of this channel in mammalian prostate cells.

MATERIALS AND METHODS

Cell Culture

LNCaP from the American Type Culture Collection were grown in RPMI 1640 (Biowhittaker, Fontenay sous Bois, France) supplemented with 5 mM L-glutamine (Sigma, L'Isle d'Abeau, France) and 10% fetal bovine serum (Seromed, Poly-Labo, Strasbourg, France). The culture medium also contained 50 000 IU/l penicillin and 50 mg/l streptomycin. Cells were routinely grown in 50 ml flasks (Nunc, Poly-Labo) and kept at 37°C in a humidified incubator in an air/CO_2 (95/5) atmosphere.

For electrophysiological experiments, the cells were subcultured in Petri dishes (Nunc) coated with polyornithine (Sigma, 5 mg/l) and used after 4–6 days.

Electrophysiological Recordings

The whole-cell and single-channel modes of the patch-clamp technique were employed. The technique used was described in detail in previous publications (Skryma *et al.* 1994; Prevarskaya *et al.* 1995).

In short, the cultures were viewed under phase contrast with a Leitz-Diavert (Leitz, Germany) inverted microscope. Electrodes were positioned with Leitz (Germany) micromanipulators. Grounding was achieved through a silver chloride-coated silver wire inserted into an agar bridge.

An Axopatch-1D amplifier (Axon Instruments, USA) was used for voltage clamping. Stimulus control, as well as data acquisition and processing were carried out with a PC (IBM, USA), fitted with a Labmaster TL-1 interface, using Pclamp 5.5.1 software (Axon Instruments, USA – interface and software).

The pipettes had an average resistance of 2–4 MΩ. Electrode offset was balanced before forming a giga-seal. Seal resistance was typically in the 13–30 GΩ range. Leakage and capacitive current subtraction protocols were composed of four hyperpolarizing pulses one-fourth of the test pulse size, applied from the holding potential before the test pulses. During data analysis, leak data were scaled and subtracted from the raw data. Series resistance was compensated. The maximum uncompensated series resistance was 8 MΩ during whole-cell recordings, so voltage error was about 5 mV for a current amplitude of 400 pA. Recordings where series resistance resulted in errors greater than 5 mV in voltage commands were discarded. Liquid–liquid junction potentials were compensated using the Axopatch internal circuit.

Under whole-cell voltage clamp, the capacitive transient current decayed according to an exponential function, indicating a cell capacitance of 16 ± 3 pF ($n = 7$). Currents were low-pass filtered at 2.5 kHz with an 8pole Bessel filter (−3 dB) and digitized at 10 kHz for storage and analysis.

Data Analysis and Statistics

Single channel data (Pclamp 5.5.1 Software) was analyzed after elimination of capacity transients and leak current by subtraction of recorded averages without channel activity from each current record. Channel opening and closing was detected using a criterion of a 50% excursion between fully open and fully closed states to determine the occurrence of the opening or closing event, such as crossings of the line at a half-distance between zero current level and a level corresponding to the average open channel amplitude. The open probability was calculated as the open time integral divided by the number of channels in the patch and the duration of the data segment analyzed. The number of channels was estimated by examining the record for multiple openings under conditions of high open probability ($P > 0.75$). Data segments of 8 s (160 ms for 1 episode, 50–100 episodes) were analyzed for open probability estimates.

Results are expressed as means ± standard deviation where appropriate. Each experiment was repeated several times. Student's *t*-test was used for statistical comparison among means, and differences with $P < 0.05$ were considered significant.

Recording Solutions

The extracellular solution contained (in mM): 140 NaCl, 5 KCl, 2 $CaCl_2$, 2 $MgCl_2$, 0.3 Na_2HPO_4, 0.4 KH_2PO_4, 4 $NaHCO_3$, 5 glucose, 10 HEPES (N-2-hydroxyethylpiperazine-N'-2-ethano-sulfonic acid). The osmolarity of the external salt solution was adjusted to 300–310 mosmol l^{-1} with sucrose, and the pH adjusted to 7.3 ± 0.01 with NaOH. The recording pipette in whole cell and outside-out experiments was filled with an artificial intracellular saline containing (in mM): 140 KGlu, 1 $MgCl_2$, 0.5 $CaCl_2$, 8 EGTA (ethylene glycol bis(β-aminoethyl ether-N,N,N',N'-tetraacetic acid), 5 HEPES (pH 7.2 ± 0.01 with KOH), osmolarity 290 mosmol l^{-1}. The solutions used in inside-out and cell-attached patch experiments were (in mM): 140 KGlu, 1 $MgCl_2$, 0.5 $CaCl_2$, 5 HEPES, 8 EGTA (pH 7.2) for the bath; 140 NaCl, 5 KCl, 2 $CaCl_2$, 2 $MgCl_2$, 0.3 Na_2HPO_4, 0.4 KH_2PO_4, 4 $NaHCO_3$, 5 glucose, 10 HEPES (pH 7.3) for the pipette and 140 KGlu, 1 $MgCl_2$, 0.5 $CaCl_2$, 8 EGTA, 5 HEPES (pH 7.2) for the pipette in the case of symmetrical K^+ gradients.

Free Ca^{2+} concentrations for the solutions applied from the inner side of membrane were buffered with 8–12 M EGTA and calculated using "Maxc Software" (from Chris Patton, Hopkins Marine Station, Stanford University). For example, to produce 0.01, 0.1 and 1 μM free Ca^{2+} solutions with (in mM): 0.5 $CaCl_2$, 1 $MgCl_2$, 8 EGTA ; 4 $CaCl_2$, 1 $MgCl_2$, 10 EGTA ; 9.5 $CaCl_2$, 1 $MgCl_2$, and 11 EGTA were used, respectively.

Test substances were applied to the cells by low-pressure ejection from an additional "pouring" micropipette (tip diameter 5–10 μm). This pipette was filled with the same extracellular saline as that used in the bath and the drug under investigation was added to it in appropriate concentrations. The pipette was brought to a distance of 30–60 μm from the investigated cell. All experiments were performed at room temperature (20–22°C).

Chemicals

Tetraethylammonium (TEA), α-Dendrodotoxin (DTX), and mast cell degranulating peptide (MCDP) were obtained from Sigma (L'Isle d'Abeau, France). Charybdotoxin (CTX) and Iberiotoxin (IBTX) were obtained from "Latoxan" (France).

Acknowledgment

This work was supported by grants from INSERM, the Association pour la Recherche sur les Tumeurs de la Prostate (ARTP), Laboratoires Pierre Fabre, La Ligue Nationale Contre le Cancer, La Fondation pour la Recherche Médicale and l'ARC (France).

References

Bregestovski P Redkozubov A and Alexeev A (1986) *Nature* **319** 776–778.
Carstens RP Eaton JV Krigman HR Walther PJ and Garcia-Blanco MA (1997) *Oncogene* 3059–3065.
Chung I and Schlichter LC (1997) *Am J Physiol* **273** (*Cell Physiol* 42) C622–C633.
Decoursey TE Chandy KG Gupta S and Cahalan MD (1987) *J Gen Physiol* **89** 379–404.
Douglass J Osborne PB Cai YC Wilkinson M Christie MJ and Adelman JP (1990) *J Immunol* **144** 4841–4850.
Dubois JM and Rouzaire-Dubois B (1993) *Prog Biophys Molec Biol* **59** 1–21.
Fedida D Wible B Wang Z Fermini B Faust F Nattel S and Brown AM (1993) *Circ Res* 73 210–216.
Franklin RB Zou J Gorski E Yang YH and Costello LC (1997) *Mol Cell Endocrinol* **127**(1) 19–25.
Furuya Y Lin XS Walsh JC Nelson WG and Isaacs JT (1995) *Endocrinology* **136** 1898–1906.
Garcia ML Honner M Knaus HG Koch R Schmalhofer W Slaughter RS and Kaczorowski GJ (1997) *Adv Pharmacol* **39** 425–471.
Grissmer S Lewis RS and Cahalan D (1992) *J Gen Physiol* **99** 63–84.
Grissmer S Nguyen AN Aiyar JA Hanson DC Mather RJ Gutman GA Karmilowicz MJ Auperin DD and Chandy KG (1994) *Pharmacol* **45** 1227–1234.
Heurteaux C and Lasdunski M (1991) *Brain Res* **554** 22–29.
Hille B (1992) Sinauer Associates Inc., Sunderland, MA, 2nd ed.
Horoszewicz JS Leong SS Kawinski E Karr JP Rosenthal H Chu MT Mirand MT and Murphy GP (1983) *Cancer Res* **43** 1908–19182.

Janssen T Darro F Petein M Raviv G Pasteels JL Kiss R and Schulman CC (1996) *Cancer* **77** 144–149.
Lang DG and Ritchie AL (1990) *J Physiol* (Lond) **45** 117–132.
Lepple-Wienhues A Berweck S Böhmig M Leo CP Meyling B Garbe C and Wiederholt M (1996) *J Membrane Biol* **151** 149–157.
Limonta P Dondi D Moretti RM Maggi R and Motta M (1992) *J Clin Endocrinol Metab* **75** 207–212.
Lovisolo D Distasi C Antoniotti S and Munaron L (1997) *New Physiol Sci* **12** 279–285.
MacKinnon R and Yellen G (1990) *Science* **250** 276–279.
Nilius B and Wohlrab W (1992) *J Physiol* (Lond) **445** 537–548.
Nilius B and Droogmans G (1994) *News Physiol Sci* **9** 105–110.
Nörenberg W Gebicke-Haerter PJ and Illes P (1994) *J Physiol* (Lond) **475** 15–32.
Pancrazio JJ Tabbara JA and Kim YJ (1993) *Anticancer Res* **13** 1231–1234.
Penner R Petersen M Pierau FK and Dreyer F (1986) *Pflügers Arch* **407** 365–369.
Peppelenbosch MP Tertoolen LGJ Den Hertog J and De Laat SW (1992) *Cell* **69** 295–303.
Pongs O (1992) *Physiol Rev* **72**(4) S69–S88.
Prevarskaya N Skryma R Vacher P Bresson-Bepoldin L Odessa MF Rivel J San Galli F Guerin J and Dufy-Barbe L (1994) *Mol and Cell Neurosci* **5** 699–708.
Prevarskaya NB Skryma RN Vacher P Daniel N Djiane J and Dufy B (1995) *The J Biol Chem* **270**(41) 24292–24299.
Sherwood ER Van Dongen JL Wood CG Liao S Kozlowski JM and Lee C (1998) *Brit J Cancer* **77**(6) 855–861.
Schlichter LC Pahapill PA and Schumacher PA (1993) *Receptor Channel* **1** 201–215.
Schreiber M Wei A Yuan A Gaut J Saito M and Salkoff L (1998) *The J Biol Chem* **273**(6) 3509–3516.
Skryma R Prevarskaya N Vacher P and Dufy B (1994) *Am J Physiol* **267** C544–C553.
Skryma R Prevarskaya N Dufy-Barbe L Odessa MF Audin J and Dufy B (1997) *Prostate* **32** N4 112–122.
Solano RM Carmena MJ Carrero I Cavallaro S Roman F Hueso C Travali S Lopez-Fraile N Guijarro G and Prieto JC (1996) *Endocrinology* **137**(7) 2815–2822.
Stansfeld CE Röper J Ludwig J Weseloh RM Marsh SJ Brown DA and Pongs O (1996) *PNAS* **93** 9910–9914.
Stühmer W Ruppersberg JP Schröter KH Sakmann B Stocker M Giese KP Perschke A Baumann A and Pongs O (1989) *Embo J* **8** 3235–3244.
Wang SY Castle NA and Wang GK (1992) *Glia* **5** 146–153.
Weller H Bernhardt U Siemen D Dreyer F Vogel W and Habermann E (1985) *N-S Arch Pharmacol* **330** 77–83.
Wonderlin WF and Strobl JS (1996) *J Membrane Biol* **154** 91–107.
Yu SP Yeh CH Sensi SL Gwag BJ Canzoniero LMT Farhangrazi ZS Ying HS Tian M Dugan LL and Choi DW (1997) *Science* **278** 114–117.

CONCLUSION

La caractérisation biophysique de ces canaux nous permet de conclure qu'ils appartiennent à une nouvelle catégorie de canaux ioniques. Leur spécificité vis-à-vis des tissus prostatiques sera analysée au moyen de la biologie moléculaire. L'étude de ces canaux potassiques nous a permis de démontrer leur sensibilité vis-à-vis de la concentration intracellulaire en calcium. En effet, l'augmentation du taux de calcium cytosolique s'accompagne d'une inhibition de la probabilité d'ouverture de ces canaux. Cependant, dans les cellules LNCaP, l'application de TEA ne change pas le taux de calcium intracellulaire. Il n'est donc pas possible pour ces cellules d'expliquer la diminution de la prolifération par des modifications du taux de calcium.

Un autre facteur pourrait rendre compte du rôle des canaux potassiques dans le contrôle de la prolifération cellulaire : le volume cellulaire (Rouzaire-Dubois et Dubois, 1991 ; 1998). D'après l'hypothèse de ces auteurs, l'activation de la conductance potassique par un agent mitogène provoquerait une diminution du volume cellulaire. Le rétrécissement cellulaire provoque une augmentation de la concentration des solutés cytosoliques et une modification du cytosquelette induisant la synthèse d'ADN et donc la division cellulaire.

1.2.2- Rôle de la prolactine dans l'activation des canaux K^+ des cellules LNCaP

En collaboration avec le Professeur J. Djiane (INRA, Jouy en Josas, France), nous avons montré que les cellules LNCaP expriment la forme longue du récepteur de la PRL (R-PRL). Cette isoforme possède la capacité de pouvoir déclencher un mécanisme de

transduction du signal prolactinique (Sorin *et al.*, 1998). Nous avons démontré que la PRL augmente l'intensité du courant macroscopique potassique et la probabilité d'ouverture de ces canaux potassiques.

L'activation des canaux potassiques constitue un événement précoce dans les phénomènes de transduction du récepteur de la PRL (Prevarskaya *et al.*, 1995 sur des cellules CHO transfectées avec le récepteur à la PRL. Aucune étude similaire n'avait été entreprise sur des cellules prostatiques.

Le manuscrit reportant nos résultats est soumis au journal « B.B.R.C. ».

CONCLUSION

Il est connu que la PRL stimule la prolifération cellulaire de lignées cancéreuses prostatiques humaines (DU-145, PC-3 et LNCaP) (Janssen *et al.*, 1996) ainsi que celle de cellules provenant d'hypertrophies bénignes de la prostate en culture primaire (Syms *et al.*, 1985). Au cours de cette étude, nous avons démontré que la PRL augmente l'intensité du courant macroscopique potassique et la probabilité d'ouverture de ces canaux. Nous avons également mis en évidence que les LNCaP expriment la forme longue du récepteur de la PRL. L'activation de ces canaux potassiques est l'un des événements précoces de la transduction du signal prolactinique dans les cellules LNCaP via une tyrosine kinase. Nous pouvons donc émettre l'hypothèse que l'activation des canaux potassiques représente l'un des mécanismes par lequel la PRL stimule la prolifération.

PROLACTIN STIMULATES K^+ CHANNELS THROUGH A LONG FORM OF PROLACTIN RECEPTOR IN HUMAN PROSTATE CANCER CELLS

Fabien VAN COPPENOLLE*[1], Roman SKRYMA*[1], Halima OUADID-AHIDOUCH[1], Sandrine HUMEZ[1], Isabelle GOURDOU[2], Jean DJIANE[2], and Natacha PREVARSKAYA**[1]

*** These authors equally contribute to this work.**

1. Laboratoire de Physiologie Cellulaire, INSERM EPI 9938, Université des Sciences et Technologies de Lille, Bâtiment SN 3, 59655 Villeneuve d'Ascq CEDEX, France.
2. Laboratoire d'Endocrinologie Moléculaire, INRA, 78352 Jouy en Josas, France.

** To whom all correspondance should be addressed :

Professeur Natacha PREVARSKAYA

Laboratoire de Physiologie Cellulaire, INSERM EPI 9938, Université des Sciences et Technologies de Lille, Bâtiment SN 3, 59655 Villeneuve d'Ascq Cedex, France.

Fax : 0033320434066

E-mail : natacha.prevarskaya@univ-lille1.fr

ABSTRACT

This work was conducted on an androgen-sensitive human prostate cell line (LNCaP) which possess voltage-dependent K^+ channels blocked by TEA, dendrotoxin and involved in the proliferation. Using RT-PCR analysis we show that these cells express a long form of the prolactin receptor. Application of prolactin (5 nM) increased both the whole-cell K^+ current amplitude (by 35 ± 11 %, n = 32) and the single K^+ channel open. The increase of the single channel activity by 5 nM prolactin was reduced by the tyrosine kinase inhibitor genistein (with a half-blocking concentration of ~ 10 μM), whereas the inactive analogue, genistin (up to 100 μM), was without effect.

Thus, as K^+ channels are involved in LNCaP cells proliferation, we suggest that K^+ channel modulation by prolactin, via a tyrosine kinase pathway, is the primary event in the prolactin signal transduction which probably turn on the cells to proliferate.

Key words : prostate cancer, PRL receptor, K^+ channels, tyrosine kinase.

INTRODUCTION

For years, the normal and pathological growth of the prostate has been assumed to be primarily regulated by androgens. However, it is now becoming apparent that polypeptide hormone prolactin (PRL) is essential for the normal growth and development of the prostate (1-3). Morever, PRL is also involved in the development and regulation of benign prostatic hyperplasia and prostate cancer (4-6). It was also shown that normal, hyperplastic, and neoplastic prostate are rich in PRL receptors (PRL-R) (7-10). Nevertheless, the mechanism(s) of PRL signal transduction in prostate cells are still poorly understood.

Most of the data concerning the first events in intracellular PRL signal transduction were obtained in the PRL-dependent rat T lymphona cell line Nb_2 and in chinese hamster ovary (CHO) cells, stably transfected with the PRL-R cDNA (11-13). It has been reported that, following binding of PRL to the PRL-R, dimerization of the receptor occurs prior to phosphorylation of an associated tyrosine kinase (JAK2) (14-15). In CHO cells, stably transfected with the long form of PRL-R cDNA, the activation of tyrosine kinase induced by PRL stimulates two types of ion channel activity : voltage-dependent K^+ channel, regulated through tyrosine phosphorylation (13, 16) and voltage-independent Ca^{2+} channels (16-17).

The LNCaP cell line, the androgen-receptor positive, derived from a lymph mode of subject with metastatic carcinoma of the prostate (18), is currently used as a model for studies of prostate cancer cell growth (19-20). At present, it is clear that LNCaP cells express voltage-activated, Ca^{2+}-inhibited K^+ channels (21-22) and that these K^+ channels are involved in the controlling of cell proliferation (21). However, the studies about the effect of PRL on these K^+ channels and the nature of the receptor localized in LNCaP cells remained to be elucidate.

Using RT-PCR analysis, we show that the long isoform of the human PRL-R is expressed in LNCaP cells. Furthermore, using whole-cell and single-channel configurations of patch-clamp techniques, we demonstrate that PRL stimulates K^+ channel activity by

increasing channel open probability. We also demonstrate that the activation of tyrosine kinase induced by PRL stimulates the K^+ currents.

Thus, the presence, on human epithelial prostate cells of PRL receptors, which stimulate K^+ channel activity may explain one of the mechanisms by wich PRL stimulates prostate cell proliferation.

MATERIALS AND METHODS

Cell culture

LNCaP from the American Type Culture Collection were grown in RPMI 1640 (Biowhittaker, Fontenay sous Bois, France) supplemented with 5 mM L-glutamine (Sigma, L'Isle d'Abeau, France), and 10% fetal bovine serum (Seromed, Poly-Labo, Strasbourg, France). The culture medium also contained 50,000 IU/L Penicillin and 50 mg/L Streptomycin. Cells were routinely grown in 50 ml flasks (Nunc, Poly-labo) and kept at 37° C in a humidified incubator in an air/CO_2 (95/ 5) atmosphere.

For electrophysiological experiments, the cells were subcultured in Petri dishes (Nunc) coated with 5 mg/L polyornithine (Sigma) and used after 4 to 6 days.

Electrophysiology

The whole-cell and single-channel modes of the patch-clamp technique were employed. The technique used was described in detail in previous publications (13, 21 ; 22).

In short, the cultures were viewed under phase contrast with a Leitz-Diavert (Leitz, Germany) inverted microscope. Electrodes were positioned with Leitz (Germany) micromanipulators. Grounding was achieved through a silver chloride-coated silver wire inserted into an agar bridge.

An Axopatch-1D amplifier (Axon Instruments, USA) was used for voltage clamping. Stimulus control, as well as data acquisition and processing were carried out with a PC computer (IBM, USA), fitted with a Labmaster TL-1 interface, using Pclamp 5.5.1 software (Axon Instruments, USA - interface and software).

The pipettes had an average resistance of 2-4 MΩ. Electrode offset was balanced before forming a giga-seal. Seal resistance was typically in the 13-30 GΩ range. Leakage and capacitive current subtraction protocols were composed of four hyperpolarizing pulses one-fourth of the test pulse size, applied from the holding potential before the test pulses. During data analysis, leak data were scaled and subtracted from the raw data. Series resistance was compensated. The maximum uncompensated series resistance was 8 MΩ during whole-cell recordings, so voltage error was about 5 mV for a current amplitude of 400 pA. Recordings where series resistance resulted in errors greater than 5 mV in voltage commands were discarded. Liquid-liquid junction potentials were compensated using the Axopatch internal circuit.

Under whole-cell voltage clamp, the capacitive transient current decayed according to an exponential function, indicating a cell capacitance of 16 ± 3 pF (n = 7). Currents were low-pass filtered at 2.5 kHz with an 8pole Bessel filter (-3dB) and digitized at 10 kHz for storage and analysis.

Cells were allowed to settle in Petri dishes placed at the opening of a 250 μm-inner diameter capillary for extracellular perfusions. The cell under investigation was continuously perfused with control or test solutions.

Data analysis and statistics

Single channel data (Pclamp 5.5.1 Software) was analyzed after elimination of capacity transients and leak current by subtraction of recorded averages without channel activity from each current record. Channel opening and closing was detected using a criterion of a 50% excursion between fully open and fully closed states to determine the occurrence of the opening or closing event, such as crossings of the

line at a half-distance between zero current level and a level corresponding to the average open channel amplitude. The open probability was calculated as the open time integral divided by the number of channels in the patch and the duration of the data segment analyzed. The number of channels was estimated by examining the record for multiple openings under conditions of high open probability ($P > 0.75$). Data segments of 8 s (160 ms for 1 episode, 50-100 episodes) were analyzed for open probability estimates.

Results are expressed as means ± standard deviation where appropriate. Each experiment was repeated several times. Student's t-test was used for statistical comparison among means, and differences with $P < 0.05$ were considered significant.

Recording solutions

The extracellular solution contained (in mM): 140 NaCl, 5 KCl, $2CaCl_2$, 2 $MgCl_2$, 0.3 Na_2HPO_4, 0.4 KH_2PO_4, 4 $NaHCO_3$, 5 glucose, 10 HEPES (N-2hydroxyethylpiperazine-N'-2-ethano-sulfonic acid). The osmolarity of the external salt solution was adjusted to 300-310 mosmol l^{-1} with sucrose, and the pH adjusted to 7.3 ± 0.01 with NaOH. The recording pipette in whole cell and outside-out experiments was filled with an artificial intracellular saline containing (in mM): 140 KGlu, 1 $MgCl_2$, 4 $CaCl_2$, 10 EGTA (ethylene glycol bis (β-aminoethyl ether-N,N,N',N'-tetraacetic acid), 5 HEPES (pH 7.2 ± 0.01 with KOH), osmolarity 290 mosmol l^{-1}. Free Ca^{2+} concentration of this solution was 0.1 μM (calculated using "Maxc Software" from Chris Patton, Hopkins Marine Station, Stanford University).

Chemicals

PRL (o-PRL-19) was kindly provided by the NIDDK (National Hormone and Pituitary Program, University of Maryland School of Medicine, Baltimore, MD). Tetraethylammonium (TEA) was obtained from Sigma, France, Dentrotoxin (DTX) was obtained from Latoxan, France.

RNA extraction and RT-PCR analysis

Total RNA from LNCaP human prostate tumor cell line and human placental tissue was isolated using the guanidinium isotiocyanate-phenol method (23). The isolated RNA was used for reverse transcription-polymerase chain reaction (RT-PCR) analysis.

Prior RT reaction, in order to eliminate DNA contamination, a DNase treatment was carried out on each RNA sample, under the following conditions : 20 µf of total RNA, 40 U ribonuclease inhibitor (Promega, Lyon, france), 4U RNase-free DNase I (promega), 5 mM $MgCl_2$ and 50mM Tris-HC1 (pH 7.5), in a final volume of 100 µl. the DNase reaction is performed at 37° C for 60 min, followed by a phenol/chloroform extraction and a precipitation with 3 M sodium acetate and ethanol.

Complementary DNA (cDNA) was synthesized under the following conditions : 3 µg of total RNA was incubated with 200 U Monoley murine leukemia virus reverse transcriptase (life Technologies SARL, cergy Pontoise, france), in buffer (50 mM TRIS-HC1 (pH 8.3), 40 mM KC1 and 6 mM $MgC1_2$), with 1 mM each deoxynucleotide triphosphate, 20 U RNase inhibitor, 10 mM dithiothreitol and 650 ng random hexamer oligonucleotides, in a total volume of 20 µl. The reaction was performed at 42° C for 50 min and stopped by heating at 95° C for 10 min.

A negative control experiment was performed : RNA was incubated in buffer containing the RT reagents except the reverse transcriptase. The cDNAs obtained by RT reaction were

then amplified by PCR. Each cDNA (1 µl RT product) was incubated with 0.2 mM each deoxynucleotide triphosphate, 50 pM each of both oligonucleotide primers (Gensetn Paris, France), 2.5 U of Taq DNA polymerase (Oncor-Appligene, Illkirch, France), in buffer (25 mM TAPS (pH 9.3), 50 mM KC1, 2 mM $MgC1_2$, 1 mM 2-mercaptoethanol), in a final volume of 50 µl. Amplifications were carried out in a Perkin-Elmer/Cetus Thermal Cycler (Perkin Elmer cetus, St Quentin en Yvelines, France) for 30 cycles. Samples were denatured at 94° C for 45 sec, annealed at 66° C for 45 sec and extended at 72° C for 45 sec. A final extension period at 72° C for 10 min completed the amplification. After amplification, 6 µl of each PCR products were electrophoresed through a 1,6 % agarose gel stained with ethidium bromide (5 µg/ml) and th RT-PCR products visualized under UV light. The oligonucleotide primers used in this study were designed from the human PRL-R cDNA sequence (24). Sense primer was a 24 mer (5'- GACTATGAGGACTTGCTGGTGGAG-3') encoding nucleotides 916-939 of the cytoplasmic domain of the hPRL-R. Antisense primer (5'-CACTTGCTTGATGTTGCAGTGAAG-3') was a 24 mer encoding a downstream portion (nucleotides 1782-1805) of the hPRL-R cytoplasmic domain. The predicted size of the PCR-amplified product was 890 bp.

Southern blot analysis

Specificity of the amplified PCR was confirmed by Southern blot analysis using an HindIII fragment (3.4 kb) of the rabbit PRL-R cDNA as probe (25). The probe was radiolabelled using a random primer DNA labelling kit (Roche Diagnostics, Meylan, France) and [α-^{32p}] dCTP 3000 Ci/mmol (Amersham, Saclay, France). After amplification by PCR, 10 µl of each sample was loaded on a 1.6% agarose gel stained with 5 µg/ml ethidium bromide. The gel was denatured (0.2 N NaOH, 0.5 NaCl), neutralized (0.5 M Tris-HC1 (pH 8.0), 0.5 M NaCl). DNA was then transferred overnight to a Hybond N nylon membrane (Amersham) in

10 XSSC buffer (150 mM Tri-sodium citrate and 1.5 M NaCl, pH 7.0). Following fixation of DNA to membrane (UV exposure), the membrane was prehybridized at 65° C in a buffer containing 5 g of fat-free milk, 0.5 M EDTA, 3.6 M NaCl, 0.2 M $NaP0_4$, 1% SDS and 6% PEG 6000. Hybridization was performed overnight at 65° C in the same buffer containing 3.10^6 cpm of the labelled PRL-R cDNA probe-ml and 1.10^6 cpm of the ϕX-HaeIII probe. The blot was washed once a room temperature for 10 min in 4XSSC, 0.1% SDS, and four times for 15 min at 55° C in the same solution. The blot was then exposed to a Kodak film (X-OMAT, kodak AR film (Amersham), at -70° C for 4 min.

RESULTS

LNCaP human prostate tumor cell line express a long form of PRL-R

We examined the expression of the PRL-R messenger RNA (mRNA) in LNCaP cells using RT-PCR analysis. We used human placenta tissue as a positive control of this experiment. As described in Materials and Methods, each cDNA was subjected to PCR using oligonucleotides primers selected to encode a part of the cytoplasmic domain of the long human PRL-R isoform (Fig. 1A). A single amplified product corresponding in lenght to the predicted size (890 bp) between PRL-R primers was detected in agarose gel electrophoresis of samples used in the present study (Fig. 1B). To clarify the identity of this PRL-R mRNA, we performed Southern blot analysis after agarose gel electrophoresis. As shown in Fig. 1C, each PCR product hybridized with rabbit probe containing the entire nucleotic sequene of the PRL-R cDNA.

Effect of PRL on K^+ current

To investigate the action of PRL on K^+ conductance, LNCaP cells were voltage clamped at - 60 mV, which is close to the mean value of the resting membrane potential (21). Sustained K^+ outward currents were obtained by stepping up the membrane potential from the holding potential to +60 mV during 200 ms. The extracellular perfusion of PRL (5 nM) induced an increase of the K^+ current amplitude in 32 of 40 cells (Fig. 2A). The amplitude of the steady state K^+ current was increased by 35 ± 11% of the control (n = 32). Figure 2B shows the time course for the increase of the K^+ current by PRL (5 nM). The peak effect was reached, in this instance, in 11 min (average 8.9 ± 1.1, n = 6) with an incomplete return to control levels after 10 min of wash. The current-voltage curve obtained under control conditions (circles) and after PRL application (squares) shows that the PRL induced

potentiation at all potentials (Fig. 3C). The increase of K^+ current by PRL was completly inhibited by 4 mM TEA (n = 7) or by 5 nM dendrotoxin (n = 3) (data not shown).

PRL activates K^+ channels by increasing their open probability

A serie of outside-out patch-clamp experiments was carried to investigate the effect of PRL on K^+ channels in LNCaP cells. PRL (5 nM) stimulated K^+ channel activity in 73% (11 of 15) patches examined (Fig. 3A). PRL (5 nM) caused an increase in the open probability of the channels (Fig. 3C), displaying the half-maximum increase in the open probability within 4.2 ± 1.4 min. The open probability of the channel after the addition of PRL was not constant, but oscilated between lower and higher open probability values (Fig. 3C).

The amplitude histograms (Fig. 3B) for K^+ channels in control (mean = 7.1 pA) and in the presence of PRL (mean = 7.1 pA) demonstrate that PRL does not activate additional conductances. Moreover, in the presence of TEA (4 mM) or dendrotoxin (5 nM), PRL (5 nM) did not stimulate K^+ channel activity, indicating that PRL activated the DTX-sensitive voltage-dependent K^+ channels and no other type of outward channels.

To resolve a possible participation of the tyrosine kinase activation in PRL-induced K^+ channel stimulation, we used genistein, a tyrosine kinase inhibitor (26). Subsequent to PRL bath application of genistein (50 μM) caused a progressive and complete inhibition of K^+ channel open probability (Fig. 3 A,C, n = 7/9 patches). The inhibition of K^+ channel open probability by genistein in this concentration was always complete within 14 ± 3 min (Fig. 3C). After genistein was washed out, K^+ channel activity stimulated by PRL gradually recovered, indicating that the depression was reversible. The onset of genistein action depended on the concentration and was slower (about 8 min) for low (5-10 μM), than for high genistein concentrations (3 ± 1 min for 50 μM, n = 6). Genistin (100 μM), an inactive

analog of genistein that lacks protein tyrosine kinase inhibitory activity (26), had no effect neither on K^+ channel open probability in control nor in PRL-stimulated LNCaP cells (n = 3).

Furthermore, the amplitude histogram (Fig. 3B) for K^+ channels in the presence of genistein confirms (mean = 7.3 pA), that genistein inhibits the K^+ channels stimulated by PRL.

We also tested two structurally distinct protein tyrosine kinase inhibitors, herbimycin A (14) and Lavendustin A (26). As genistein, herbimycin A (1.5 μM) (n = 4/5 patches) and lavendustin A (10 μM) (n = 3/3) did not depressed K^+ channel activity in control conditions. However, they inhibited K^+ channel open probability increased by PRL, without affecting single-channel conductance.

As protein thyrosine kinase inhibitors at high concentrations are known to be able to inhibit not only thyrosine kinase but also protein kinase A and protein kinase C in some cell types (26), we checked the putative involvement of these kinases in the effect of PRL on K^+ channel activity. We tested both activators and inhibitors of protein kinases A and C pathways (1 mM 8-bromo-cAMP, 2 μM forskolin, 10 nM PMA and 250 μM phloretin) on K^+ channel activity and on the stimulated effect of PRL. All of these drug were without effect (data not shown).

As in our experiments in CHO cells transfected with long form of PRL-R cDNA, PRL induced not only stimulation of K^+ channel activity but also increase in $[Ca^{2+}]_i$, we have studied if PRL modify the cytosolic Ca^{2+}-concentration in LNCaP cells. However PRL (0.5-50 nM) did not affect the intracellular Ca^{2+} neither by Ca^{2+} mobilization from intracellular stores, nor by inducing extracellular Ca^{2+} entry (n = 21, data not shown).

DISCUSSION

Our results clearly demontrated that *(i)* androgen-dependent human cancer prostate cells LNCaP express a long form of PRL-R and *(ii)* PRL stimulated the K^+ channels by increasing the open probability via the activation of a tyrosine kinase pathway. Thus, the activation of K^+ channels by PRL is the primary ionic event in PRL-R signal transduction.

The expression of PRL-R have been previously shown in rat prostate (7) and in organ culture of human prostate tissue (8). Our study is the first demonstration of PRL-R in human cancer prostate LNCaP cells, currently used as an androgen-sensitive experimental model in numerous studies of prostate cell proliferation, differentiation and apoptosis (19-20). However, the cascade of ionic events induced by PRL and the nature of ion channels involved has not yet been studied in LNCaP cells. Our previous studies showed that human prostate cancer cells LNCaP express a new type of outward voltage-activated Ca^{2+} dependent K^+ channels (21). Neither Na^+ nor Ca^{2+} voltage-activated channels were observed. Now, we demonstrate that PRL stimulates these K^+ channels by increasing their open probability. The effect of PRL on K^+ channels was dependent from tyrosine kinase activation as it was inhibited by three distinct tyrosine kinase inhibitors. Experiments using protein kinase C and protein kinase A activators and inhibitors showed that these kinases are not involved in PRL effect.

In CHO cells stably transfected with long form cDNA of PRL-R, we have shown that K^+ channels are constitutively associated with tyrosine kinase because tyrosine kinase inhibitors not only inhibited the effect of PRL on K^+ channels, but also almost completely inhibited the constitutive channel activity (13). In LNCaP cells, the K^+ channel activity in the control conditions was not inhibited by tyrosine kinase inhibitors, however the stimulation effect of PRL was inhibited in the presence of these drugs. This difference between CHO and LNCaP cells could be explained by the K^+ channel types and/or channel sensitivity to

phosphorylation. In effect, the CHO cells express a voltage-dependent maxi- K^+ channels (≈ 210 pS), activated by the increase in $[Ca^{2+}]_i$ and inhibited by charybdotoxin (13) in contrast, the intermediate K^+ channels (78 pS) in LNCaP cells are inhibited by the increase in $[Ca^{2+}]_i$ and also by dendrotoxin (21). Furthermore, PRL did not increase cytosolic Ca^{2+} concentration in LNCaP cells as it did in CHO cells stably transfected with long form cDNA PRL-R. Using CHO cells transfected with mutated PRL-R cDNA, Sorin et al., (27) have shown that exposure of cells deleted from box 1 or the 141 amino acids of the COOH-terminal region did not modify $[Ca^{2+}]_i$, suggesting that box 1 and COOH-terminal regions are both needed for PRL-induced Ca^{2+} changes. However, our findings show that in LNCaP cells expressing classically described long form of PRL-R, the intracellular Ca^{2+} also is not involved in PRL signal transduction. Thus, the mechanisms of PRL signal in prostate cells are different from those in CHO cells.

As in LNCaP cells, we have never observed second-messenger-opening Ca^{2+} channels, K^+ channels seem to play the most important role in PRL signal transduction and cell proliferation.

ACKNOWLEDGEMENTS

This work was supported by the Région Nord-Pas de Calais, the Ministère de l'Education Nationale de l'Enseignement Supérieur et de la Recherche (EA1030), by INSERM (EPI 9938), Association de la Recherche contre le Cancer (ARC, France), the Ligue du Nord contre le Cancer and the Association pour la Recherche sur les Tumeurs de la Prostate (ARTP).

REFERENCES

1. Castello, L.C., and Franklin, R.B. (1994) *The Prostate* **24**, 126-166.

2. Negro-Vilar, A., Saad, W.A., and McCann, S.M. (1977) *Endocrinol.* **100**, 729-737.

3. Prins, G.S. (1987). *Endocrinology* **120**, 1457-1464.

4. Kadar, T., Ben-David, M., Pontes, J.E., Fekete, M., and Schally, A.V. (1988). *The prostate* **12**, 299-307.

5. Janssen, T., Kiss, R., and Schulman, C. (1995) *Acta Urol. Belg.* **14**, 7-14.

6. Syms, A.J., Harper, M.E., and Griffiths, K. (1985) *The Prostate* **6**, 145-153.

7. Nevalainen, M.T., Valve, E.M., Ahonen, T., Yagi, A., Paranko, J., and Harkonen, P.L. (1997a) *FASEB J.* **11**, 1297-1307.

8. Nevalainen, M.T., Valve, E.M., Ingleton, P.M., Nurmi, M., Martikainen, P.M., and Harkonen, P.L. (1997b) *J. Clin. Invest.* **99**, 618-627.

9. Witorsch, R. (1989) In Nagasawa H (ed) : « Prolactin and lesions in Breast, Uterus, and Prostate », Boca Raton : CRC Press, 199-221.

10. Dave, J.R., Vick, R.S., Wong, V.L.Y., and Witorsch, R.J. (1990) In Famsworth W.E, Ablin R.J (eds) : « The prostate as an Endocrine Gland », Boca Raton : CRC Press 97-117.

11. Bole-Feysot, C., Goffin, V., Edery, M., Binart, N., Kelly, P.A. (1998) *Endocrine Reviews* **19**, 225-268.

12. Clevenger, C.V., Medaglia, M.V. (1994) *Mol. Endocrin.* 674-681.

13. Prevarskaya, N.B., Skryma, R.N., Vacher, P., Daniel, N., Djiane, J., and Dufy, B. (1995) *J. Biol. Chem.* **270**, 24292-24299.

14. Rui, M., Kirken, R.A., and Farrar, W.L. (1994) *J. Biol. Chem.* **269**, 5364-5368.

15. Lebrun, J.J., Ali, S., Sofer, L., Ulrich, A., and Kelly, P. (1994) *J. Biol. Chem.* **269**, 14021-14026.

16. Prevarskaya, N., Skryma, R., Vacher, P., Daniel, N., Bignon, C., Djiane, J., and Dufy, B. (1994) *Am. Physiol. Soc.* 554-562.

17. Ratovondrahona, D., Fahmi, M., Fournier, B., Odessa, M.F., Skryma, R., Prevarskaya, N., Djiane, J., and Dufy, B. (1998) *J. Mol. Endocrin.* **21**, 85-95.

18. Horoszewicz, J.S., Leong, S.S., Kawinski, E., Karr, J., Rosenthal, H., Chu, M.T., Mirand, E.A., Murphy, G.P. (1983) *Cancer Res.* **43**, 1908-1918.

19. Castagnetta, L.A., Miceli, M.D., Sorci, C.M.G., Pfeiffer, U., Farrugio, R., Oliveri, G., Calabra, M., and Carruba, G. (1995) *Endocrinology* **136**, 2309-2319.

20. Limponta, P., Dondi, D., Moretti, R.M., Maggi, R., and Motta, M. (1995) *Endocrinology* **75**, 207-212.

21. Skryma, R.N., Prevarskaya, N.B., Dufy-Barbe, L., Odessa, M.F., Audin, J., and Dufy, B. (1997) *The Prostate* **33**, 112-122.

22. Skryma, R., Van Coppenolle, F., Dufy-Barbe, L., Dufy, B., and Prevarskaya, N. (1999) *Receptors and Channels* **6**, 241-253.

23. Puissant, C., and Houdebine, L.M. (1990) *BioTechniques* **8**, 148-149.

24. Boutin, J.M., Edery, M., Shirota, M., Jolicoeur, C., Lesueur, L., Ali, S., Gould, D., Djiane, J., and Kelly, P.A. (1989) *Mol. Endocrinol.* **3**, 1455-1461.

25. Gourdou, I., Gabou, L., Paly, J., Kermabon, A.Y., Belair, L., and Djiane, J. (1996) *Mol. Endocrinol.* **10**, 45-56.

26. O'dell, T.J., Kandel, E.R., and Grant, S.G. (1991) *Nature* **353**, 558-560.

27. Sorin, B., Goupille, B., Vacher, A.M., Paly, J., Djiane, J., and Vacher, P. (1998) *J. Biol. Chem.* **273**, 28461-28469.

A.

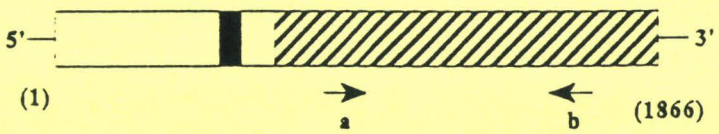

B.

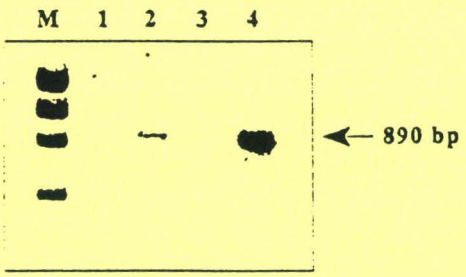

C.

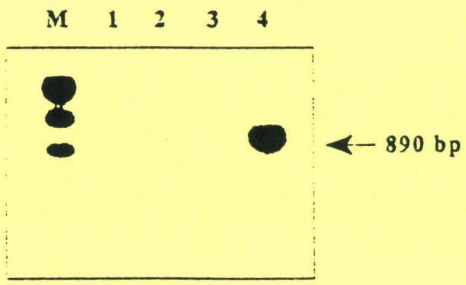

FIG.1. RT-PCR analysis of the PRL-R cDNA

A) Schematic representation of cDNA encoding the long form of human PRL-R mRNA. The positions of oligonucleotide primers complementary to sequences encoding the cytoplasmic domain specific to the long form (probes a and b) were shown. The transmembrane domain was indicated in black. The cytoplamic domain specific to the long form was crosshatched. Oligonucleotides used as primers were represented as horizontal arrows. the lenght of the cDNA was indicated in nucleotides.

B) Agarose gel electrophoretic pattern of RT-PCR products.

Total RNA of each sample was isolated, reverse transcribed and amplified with oligonucleotide primers a and b (Fig. 1A), as described in Materials and Methods.

The predicted size of the amplified product was 890 bp. RT-PCR reactions were separated on a 1,6% agarose gel.

The lanes contain PCR products obtained from LNCaP cell line (1-2) and placenta tissue (3-4). lanes (1, 3) negative control (RNA incubated without reverse transcriptase) ; lane (M) a size standard DNA marker. The size of the PCR product was indicated.

C) Southern blot analysis with a rabbit cDNA probe.

The PCR products were analyzed by the method of Southern, by hybridation with a cDNA probe encoding the entire rabbit PRL-R nucleotidic sequence.

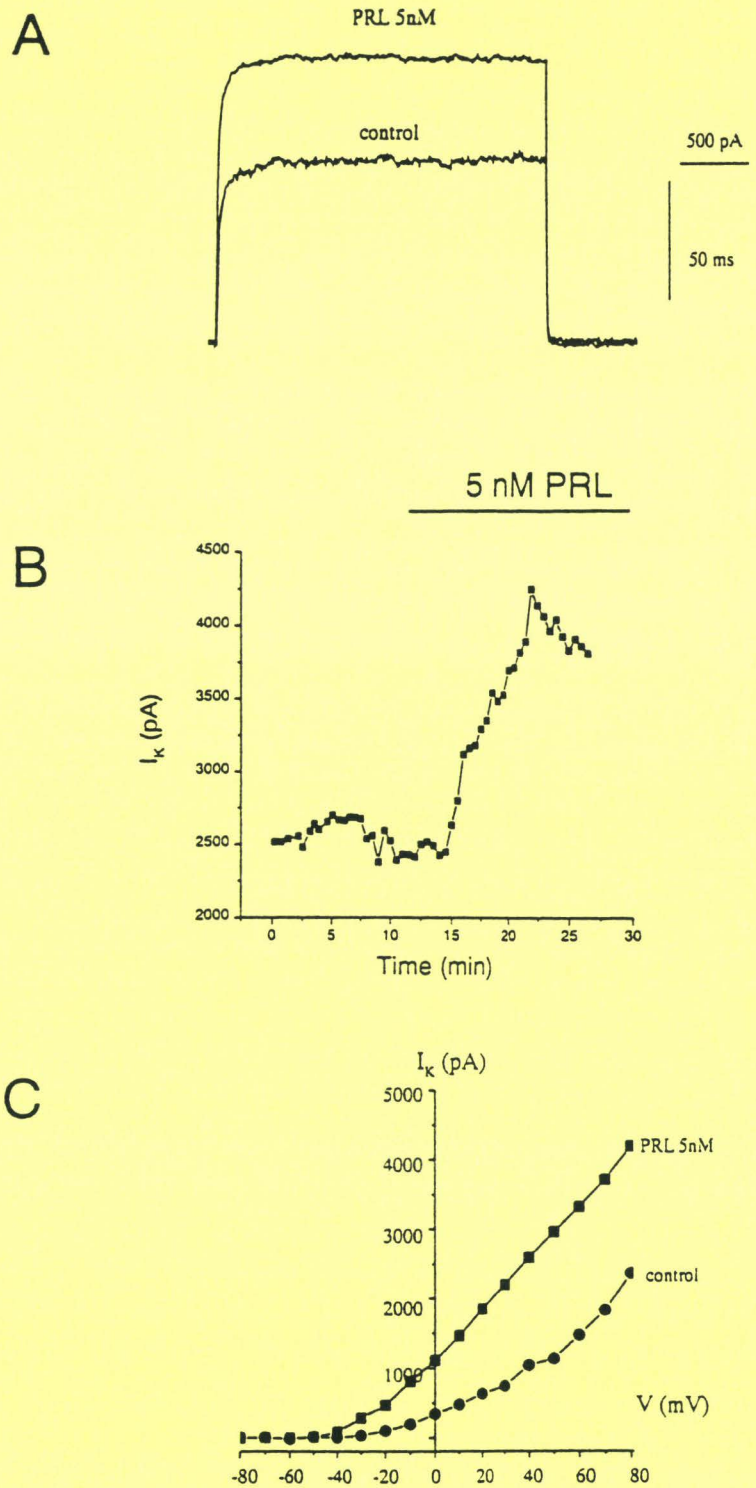

FIG. 2. Effects of PRL on whole K^+ current

A) Example of effect of PRL on K^+ current recorded before and after 11 min of PRL application. Cell was depolarized from a holding potential -60 mV to +60 mV for 200 ms the duration.

B) Time course of the effect of PRL (5 nM) on the K^+ current.

C) The potentiation effect of PRL (5 nM) on the current-voltage relationships of K^+ current, (circles) in the control conditions and (squares) after application of PRL (5 nM).

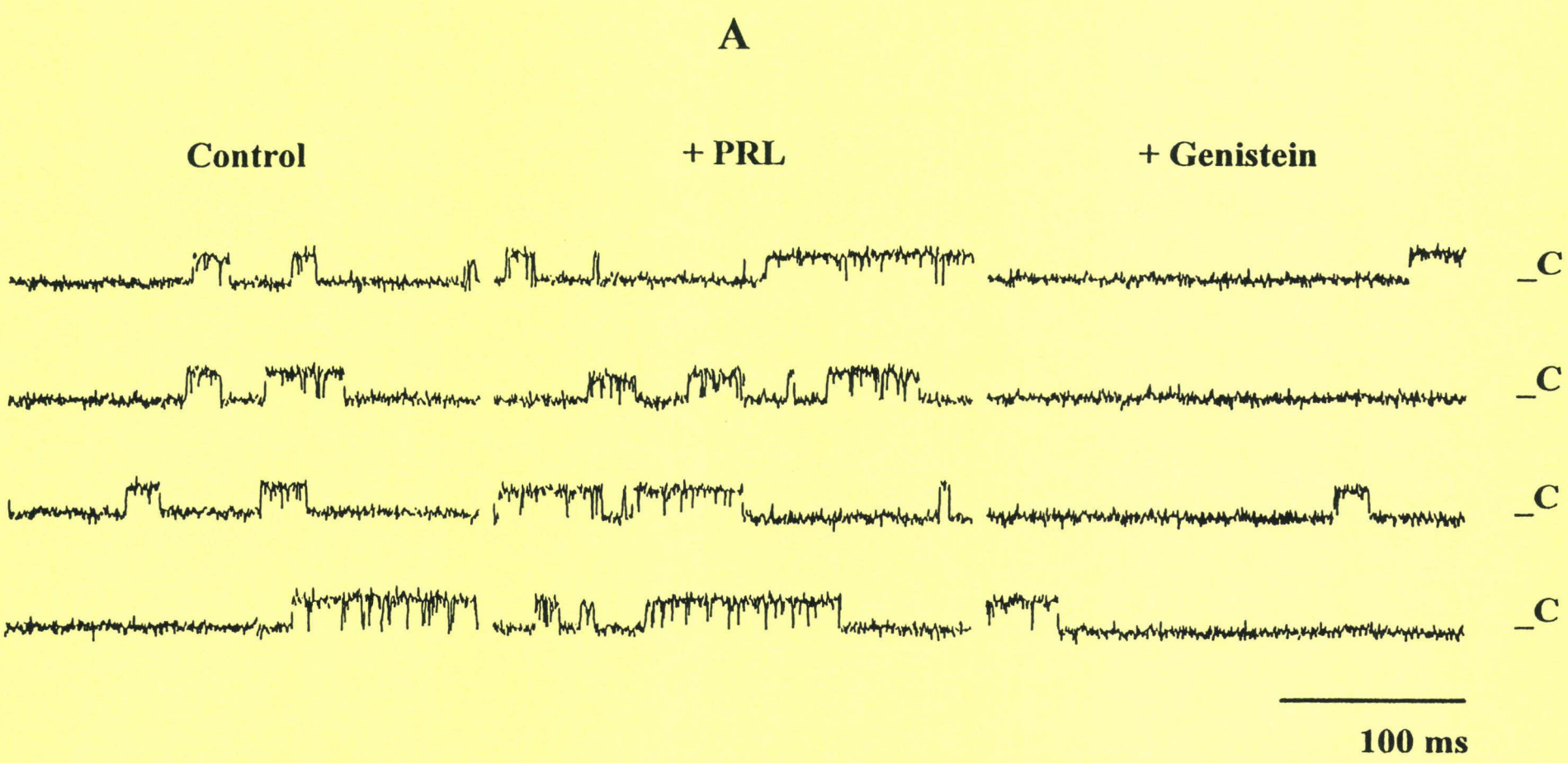

Fig. 3. F. VAN COPPENOLLE et all.

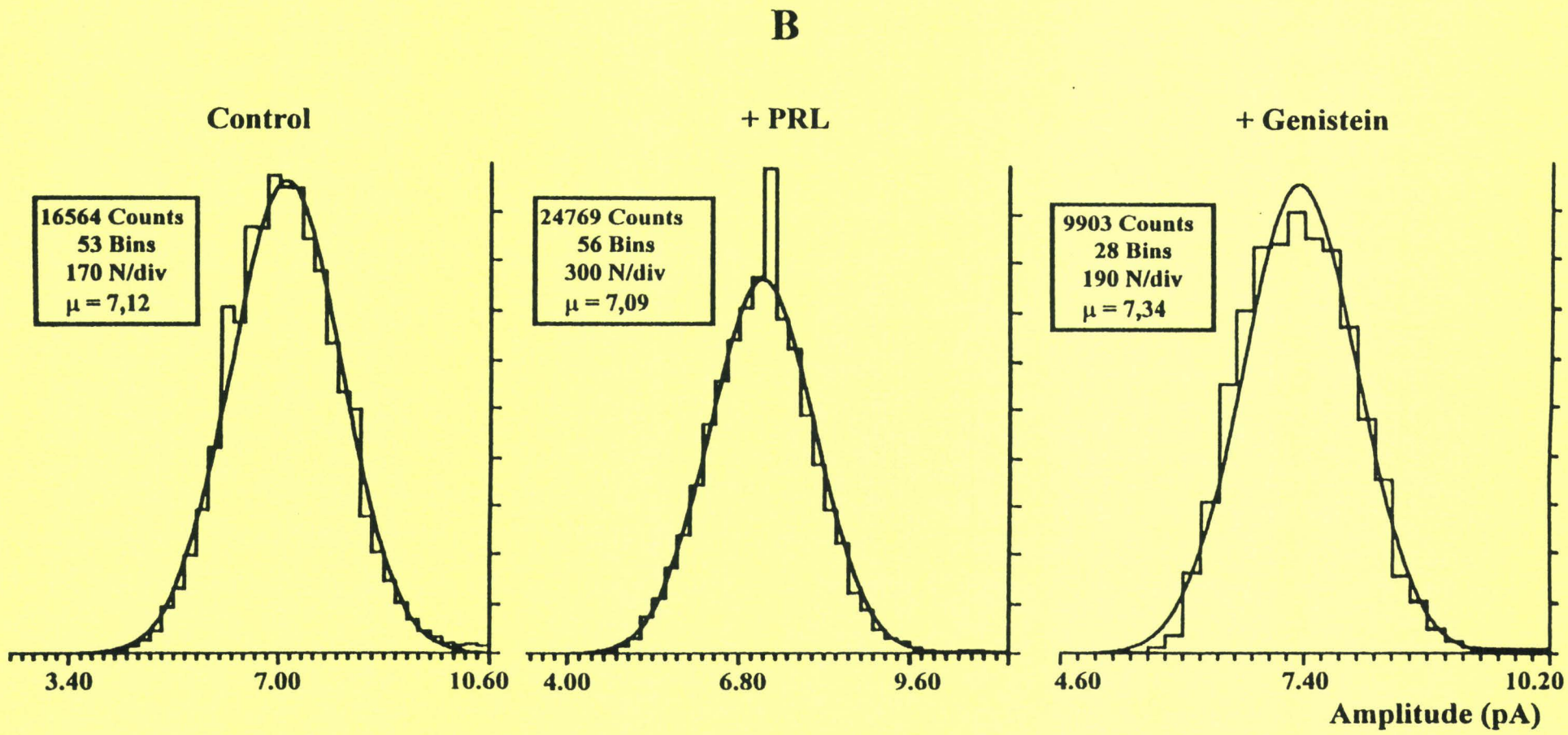

Fig. 3. F. VAN COPPENOLLE et all.

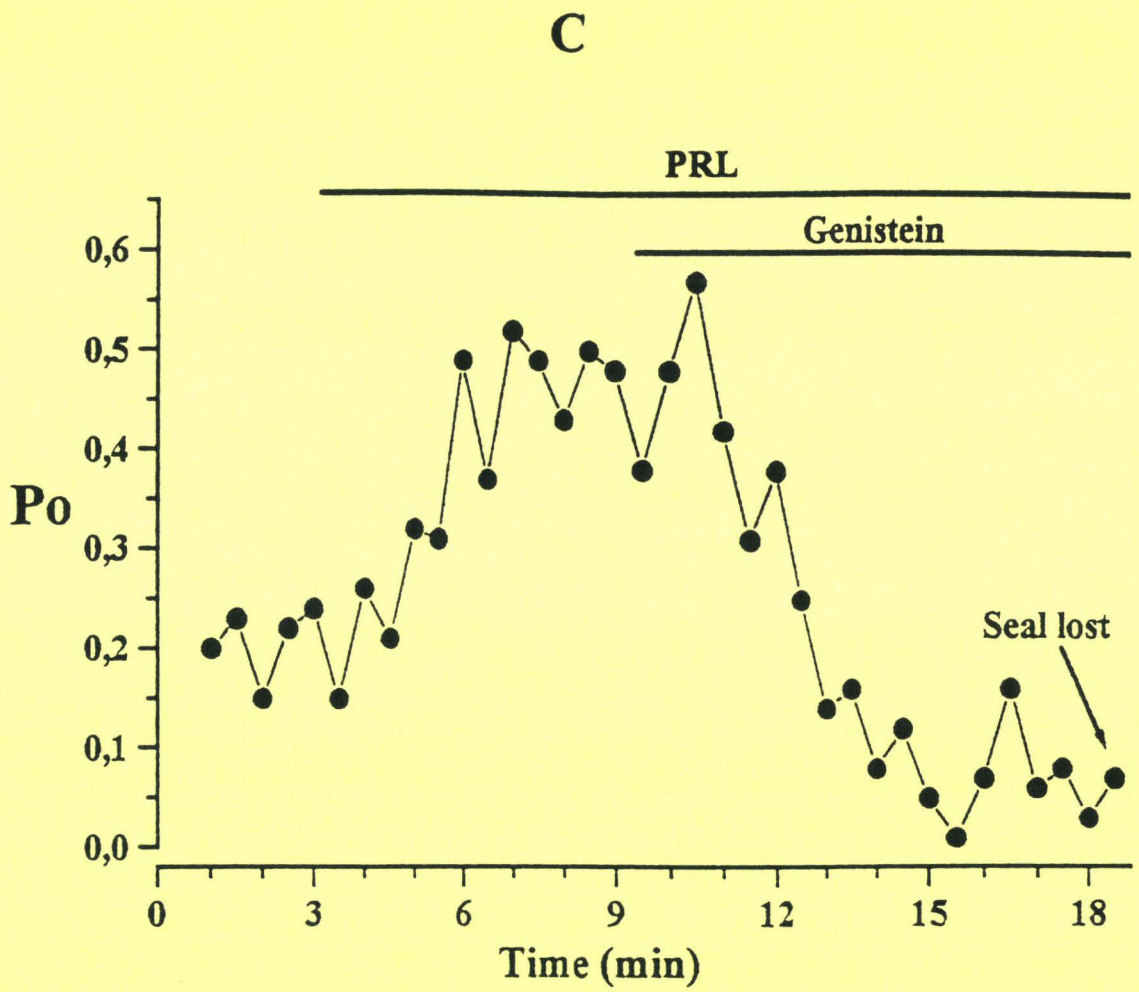

Fig. 3 . VAN COPPENOLLE et all.

FIG. 3. Modulation of K^+ single channel activity by PRL and its inhibition by genistein. (A) illustrates representative recordings of single K^+ currents in a cell-free patch in the outside-out configuration. Recordings are show for the control solution, 6 min after application of 5 nM PRL, and 8 min after the subsequent application of 50 μM of genistein, respectively. (B) illustrates the amplitude histograms for single K^+ channel conductance for control, in the presence of 5 nM PRL and in the presence of 50 μM genistein (C). Time course of the open probability of the K^+ channels in the control and in the presence of 5 nM PRL and 50 μM genistein.

1.3- Conclusion de la première hypothèse

Au cours de notre étude, nous avons voulu tout d'abord caractériser et comparer les types de canaux potassiques présents dans les cellules saines et tumorales de la prostate. Les cellules normales de prostate de rat expriment un canal de type Kv1.3 (Article sous presse dans « Febs Letters »). Dans la lignée tumorale humaine LNCaP, au contraire, nous avons mis en évidence la présence d'un canal potassique d'un nouveau type directement impliqué dans la prolifération cellulaire (Skryma *et al.*, 1997 ; 1999). Le courant véhiculé par les canaux potassiques de type Kv1.3 s'inactive (diminution de l'amplitude du courant macroscopique au cours de la stimulation), comme dans le cas des cellules normales de prostate de rat. Au contraire, celui des cellules LNCaP ne s'inactive pas. Par ailleurs, ces deux types de canaux sont inhibés par les hausses de concentration intracellulaire en calcium. Au vu de ces résultats, nous émettons l'hypothèse d'une mutation ou d'une néoexpression d'un canal potassique dans les cellules cancéreuses. Nous prévoyons de vérifier cette voie chez le rat et chez l'homme. Nous caractériserons les propriétés des canaux potassiques de cellules de prostate de rat en culture primaires provenant de tissus sains, hypertrophiés et cancéreux. Nous réaliserons le même type de comparaison sur des cellules humaines issues de biopsies de prostates « saines », hypertrophiées et cancéreuses.

Nous avons mis en évidence, grâce aux travaux sur l'animal, l'effet trophique de la PRL sur la prostate de rat. Nous postulons que la PRL pourrait agir selon deux processus : (i) en stimulant la prolifération cellulaire et/ou (ii) en réduisant les processus apoptotiques. Concernant la prolifération cellulaire, nous avons analysé les modifications engendrées par la PRL sur l'activité des canaux potassiques de cellules de prostate de rat et de cellules LNCaP. Les cellules épithéliales de prostate de rat expriment le récepteur de la PRL (Nevalainen *et al.*, 1997). De même, les cellules LNCaP

expriment la forme longue du récepteur de la PRL et répondent à la PRL par une augmentation de la probabilité d'ouverture des canaux potassiques qui se traduit par un courant macroscopique plus important. Cette stimulation, par la PRL, est réalisée via une tyrosine kinase.

L'activation, par la PRL, des canaux potassiques est donc un événement précoce de la transduction du signal prolactinique. L'augmentation de l'activité de ces canaux pourrait expliquer l'effet prolifératif de la PRL. L'étude des mécanismes de transduction de la PRL sur les cellules saines et cancéreuses de la prostate nous permettra de répondre à cette question.

2- DEUXIEME HYPOTHESE : La prolactine inhibe l'apoptose des cellules de la prostate

Les phénomènes apoptotiques sont régulés, soit positivement, soit négativement par un grand nombre de protéines. Les balances ioniques d'une cellule jouent un rôle important dans les processus apoptotiques. Le calcium est un second messager ubiquitaire qui possède une action pleiotrope dans la physiologie cellulaire, allant de la prolifération, de la différenciation à l'apoptose. Le calcium agit de façon multiple dans la cascade de transduction menant à l'apoptose. Connaître les mécanismes de modulation de l'homéostasie calcique est primordial pour caractériser la manière dont l'apoptose est régulée. Par ailleurs, la mort cellulaire programmée, dans le cadre de notre étude, revêt une importance particulière puisque l'on considère que le cancer de la prostate, à évolution lente, serait dû à une inhibition de l'apoptose plutôt qu'à un accroissement de la prolifération cellulaire.

Si le rôle du calcium dans les processus apoptotiques est indéniable, les mécanismes fins de l'homéostasie calcique induisant l'apoptose sont très peu étudiés. Le réticulum endoplasmique constitue, avec les mitochondries et le noyau, le lieu de stockage principal du calcium (Berridge, 1992). La vidange de ces stocks déclenche une entrée de calcium, via la membrane plasmique, appelée « entrée capacitative » (Putney *et al.*, 1986 ; Putney, 1990). Ce flux de calcium est utilisé par la cellule pour remplir les stocks calciques précédemment vidés. L'entrée de calcium ne peut se faire via des canaux calciques dépendants du voltage, car les cellules LNCaP en sont dépourvues, mais se réalise via des canaux CRAC (calcium release activated current). La caractérisation de ces canaux peut être d'un grand intérêt dans l'étude du cancer de la prostate. En effet, des inhibiteurs spécifiques des canaux de type CRAC, utilisés lors de tests cliniques, ont permis de juguler la prolifération de cellules cancéreuses. Par ailleurs, les stocks calciques et les canaux de type CRAC peuvent intervenir dans la régulation de l'apoptose

Au cours de cette étude, nous nous sommes appliqués à caractériser les mécanismes de régulation de la concentration intracellulaire en calcium dans les cellules tumorales humaines LNCaP et leur implication dans les processus apoptotiques. Puis, nous nous sommes penchés sur le rôle de la PRL dans la modulation des phénomènes régulant l'homéostasie calcique de ces cellules.

2.1- Importance des stocks intracellulaires de calcium dans l'induction de l'apoptose des cellules LNCaP

Comme cité précédemment, le calcium est un élément clé dans la régulation de l'apoptose. En effet, dans plusieurs modèles cellulaires, une augmentation en calcium intracellulaire déclenche l'apoptose (Martikainen *et al.*, 1991 ; Juin *et al.*, 1998). Par ailleurs, de nombreuses molécules induisant l'apoptose provoquent une augmentation de la

concentration en calcium intracellulaire. En revanche, le rôle des stocks calciques intracellulaires dans l'induction de l'apoptose reste encore obscur.

Nous nous sommes donc lancés dans cette étude afin de comprendre la manière dont la thapsigargine induit l'apoptose dans les cellules LNCaP. Grâce aux techniques de patch-clamp et de microspectrofluorimétrie, nous avons mis en évidence que la vidange des stocks provoque l'apoptose sans que l'entrée capacitative ou toute autre élévation de la concentration en calcium intracellulaire ne soit nécessaire.

Ces travaux sont actuellement soumis dans « Cancer Research ».

CONCLUSION

Au cours de cette étude, nous avons démontré que la vidange des stocks calciques, induite par la thapsigargine, provoque une entrée capacitative dans les cellules cancéreuses prostatiques humaines LNCaP. Néanmoins, nous avons mis en évidence que ce flux calcique n'intervient pas dans l'induction de l'apoptose. Nous avons également mis en évidence que la vidange des stocks, seule, c'est à dire la diminution de la concentration calcique dans le réticulum endoplasmique, provoque l'apoptose des cellules LNCaP. Ces cellules sont dépendantes des androgènes pour proliférer. Au contraire, les cellules prostatiques hormono-indépendantes (DU-145) nécessitent l'activation de l'entrée capacitative et l'augmentation de la concentration cytosolique en calcium pour que l'apoptose se produise (Kyprianou *et al.*, 1994).

Store-Depletion and Store-Operated Ca^{2+} Current in Human Prostate Cancer Cells LNCaP: Involvement in Apoptosis

Roman Skryma[1]*, Pascal Mariot[1]*, Fabien Van Coppenolle*, Yaroslav Schuba*, Guillaume Legrand*, Sandrine Humez*, Xuefen Le Bourhis, Benoni Boilly** and Natalia Prevarskaya[2]***

* *Laboratoire de Physiologie Cellulaire, INSERM EPI-9938, USTL, Villeneuve d'Ascq;*

** *Laboratoire de Biologie du Développment, USTL, Villeneuve d'Ascq, France*

Running title: Sustained Ca entry is not required for apoptosis of human prostate cancer LNCaP cells

Key words: Prostate cancer, apoptosis, store-operated Ca^{2+} current, thapsigargin.

This work was supported by grants from INSERM, Ministère de l'Education Nationale, ARC (Association pour la Recherche Contre le Cancer), Ligue Nationale Contre le Cancer, ARTP (Association pour le Recherche sur les Tumeurs de la Prostate), France.

[1]R. S. and P. M. contributed equally to this work.

[2] to whom all correspondence should be addressed: Laboratoire de Physiologie Cellulaire, INSERM EPI-9938, USTL, Bat. SN3, 59655 Villeneuve d'Ascq Cedex, France.

Fax. 33 3 20 43 40 66. E-mail: phycel@pop.univ-lille1.fr

ABSTRACT

Ca^{2+} ions are major players in the complex intracellular pathway leading to apoptosis. However the exact mechanism(s) by which Ca^{2+} trigger apoptosis remain poorly understood. In the present study, we investigated the Ca^{2+} mechanisms involved in apoptosis induction by the Ca^{2+}-ATPase inhibitor, thapsigargin, in androgen-dependent human cancer prostate cells, LNCaP. Thapsigargin depleted intracellular Ca^{2+} stores and induced a consecutive extracellular Ca^{2+} entry through a plasma membrane, store-operated Ca^{2+} current (I_{STORE}). For the first time we have identified and characterized the I_{STORE} current in prostate cells using whole-cell, cell-attached, and perforated patch-clamp techniques, combined with fura-2 microspectrofluorimetric and Ca-imaging measurements. I_{STORE} current in LNCaP cells displays an inwardly rectifying current-voltage relation, lacks voltage-depending gating, and has significant unitary current noise. The unitary conductance of I_{STORE} channels is 3.2 ± 0.45 pS. Current has a high selectivity for Ca^{2+} over monovalent cations and is inhibited by Ni^{2+} (1-3 mM) and La^{3+} (1 μM).

Treatment of LNCaP cells with TG (0.1 μM) induced apoptosis as judged by morphological changes. Removal of extracellular Ca^{2+} or adding of Ni^{2+} augmented apoptosis due to thapsigargin. These results indicate that in androgen-dependent prostate cancer cells the depletion of intracellular Ca^{2+} stores may trigger apoptosis but that there is no requirement for the activation of store-activated Ca^{2+} current and sustained Ca^{2+} entry in induction and development of programmed cell death. Our results provide not only further information on the link between Ca2+ pools and apoptosis of cancer cells but also evidence for a potentially important signaling pathway involved in transition from hormono - dependent to hormono - independent prostate cancer.

INTRODUCTION

Prostate cancer is the second cause of cancer death in men (1,2). Androgen withdrawal therapy is commonly used to delay the progression of disease (3). However, prostate cancer under hormonal ablation therapy will in most cases exhibit androgen-independent characteristics and the tumors will continue to progress. The androgen-independent prostate cancer cells are characterized by a very low proliferation rate that renders the typical chemotherapy agents ineffective. For this reason, targeting programmed cell death, or apoptosis, may be particularly relevant for prostate cancer therapy.

It has now been established that Ca^{2+} ions are major players in an intracellular signaling system that translates extracellular stimuli into the regulation and control of cellular events leading to programmed cell death (for the review see ref. 4-6). Increases in intracellular Ca^{2+} concentration ($[Ca^{2+}]i$) have been shown to trigger apoptosis (7,8) and numerous apoptosis inducers increase $[Ca^{2+}]i$ (9,10). However, the precise mechanism(s) by which Ca^{2+} ions trigger apoptosis remain poorly understood. Ca^{2+} stores are intracellular compartments characterized by their high intraluminal Ca^{2+} content and their participation in the regulation of $[Ca^{2+}]i$ through rapid Ca^{2+} accumulation and release (12,13). The depletion of Ca^{2+} stores induces a "Ca^{2+}-refilling mechanism", a plasma membrane Ca^{2+} entry initially called capacitative Ca^{2+} influx by Putney at al (14,15) or store-operated Ca^{2+} current (I_{STORE}). This mechanism has been demonstrated in a variety of nonexcitable cells (for review see ref.16). Store-operated Ca^{2+} channels (SOCs) have been shown to be involved in controlling many important physiological and physiopathological functions: secretion, gene transcription, cell cycle, proliferation, and also apoptosis (4, 17-20). While the implication of Ca^{2+} ions in the induction of apoptosis is now generally accepted, the data concerning the role of store-

operated current in this process are rather contradictory and confusing. Two hypotheses have been proposed. The first assumes that apoptosis may be triggered by endoplasmic reticulum (ER) calcium pool depletion without any requirement for the cytosolic Ca^{2+} elevation due to store-operated Ca^{2+} entry (21,22). Moreover, according to this hypothesis the Ca^{2+} capacitative current may be important for optimal ER pool filling and apoptosis inhibition. The second hypothesis on the contrary assumes that a sustained elevation in cytosolic Ca^{2+} to a critical level is the initiator of apoptosis (23,24).

This last hypothesis was deduced from experiments where apoptosis was induced by the sarco-endoplasmic reticulum Ca^{2+}-ATPase (SERCA pump) inhibitor, thapsigargin (TG), in androgen-independent human prostate cancer cells from the TSU-Pr1, DU-145, and PC-3 cell lines (23). However, nothing is known about apoptosis-inducing Ca^{2+} signals in androgen-dependent prostate cancer cells, where the androgen receptor (AR) plays a critical role in regulating growth and differentiation. The study of Ca^{2+}-regulating mechanisms involved in apoptosis in androgen-dependent human prostate cancer cells could be of great importance as it was shown by Gong et al. that, in such cells, intracellular calcium is a potent regulator of androgen receptor gene expression (25). It has been found in this work that the calcium ionophore A23187 and thapsigargin down-regulate steady state AR mRNA levels. On the other hand, androgen depletion is known to induce apoptosis in androgen-dependent cancer cells and this mechanism involves Ca^{2+} signals (26). The transition of prostate cancer cells from androgen-dependence to androgen-independence may also involve modifications in Ca^{2+} homeostasis and, probably, in store-operated current functions. This current, assumed to play an essential role in cancer cell apoptosis, has never been characterized using patch-clamp techniques in both androgen-dependent and -independent prostate cells. In view of the fact that abnormalities in this current may give rise to human disorders, it is important to understand how this current is regulated and how it affects prostate cell behavior.

In this work we identify the mechanism by which thapsigargin induces apoptosis in androgen-dependent human prostate cancer cells LNCaP. We characterize for the first time the store-operated Ca^{2+} current in prostate cancer cells, using patch-clamp and fluorimetric (fura-2) single-cell techniques. We also show that the depletion of intracellular Ca^{2+} stores in androgen-dependent prostate cancer cells may trigger apoptosis without the activation of a store-activated Ca^{2+} current or sustained Ca^{2+} entry. Our results provide not only further information on the link between Ca2+ pools and apoptosis of cancer cells but also evidence for a potentially important signaling pathway involved in transition from hormono - dependent to hormono - independent prostate cancer.

MATERIALS AND METHODS

Cell Lines. LNCaP from the American Type Culture Collection were grown in RPMI 1640 (Biowhittaker, Fontenay sous Bois, France) supplemented with 5mM L-glutamine (Sigma, L'Isle d'Abeau, France) and 10% fetal bovine serum (Seromed, Poly-Labo, Strasbourg, France). The culture medium also contained 50,000 IU/L Penicillin and 50 mg/L Streptomycin. Cells were routinely grown in 50 ml flasks (Nunc, Poly-labo) and kept at 37°C in a humidified incubator in an air/CO_2 (95/ 5) atmosphere.

For electrophysiological experiments, the cells were subcultured in Petri dishes (Nunc) coated with polyornithine (Sigma, 5 mg/L) and used after 4 to 6 days.

Recording Solutions. Bath Ringer's solution contained (in mM): 140 NaCl, 5 KCl, 2$CaCl_2$, 2 $MgCl_2$, 0.3 Na_2HPO4, 0.4 KH_2PO4, 4 NaHCO3, 5 glucose, 10 HEPES (pH 7.3 ± 0.01 with NaOH).

In perforated-patch experiments, the recording pipette was filled with an artificial intracellular saline containing (in mM): 55 KCl, 70 K_2SO_4, 7 $MgCl_2$, 1 $CaCl_2$, 5 D-glucose, 10 HEPES (pH 7.2 with KOH) with nystatin at 200 μg/ ml. To obtain Ca^{2+} currents in the absence of K^+ current, Cs^+ salts were substituted for K^+ salts.

In whole-cell experiments, the recording pipette was filled with an artificial intracellular saline containing (in mM): 140CsCl, 2 $MgCl_2$, 1 $CaCl_2$, 10 EGTA, 5 HEPES (pH 7.3 ± 0.01 with CsOH), osmolarity 290 mosmol/kg.

In cell-attached experiments, the pipette solution contained 80 mM $CaCl_2$ as a charge carrier plus (in mM): TEA-Cl-30, glucose-5, HEPES-10, 4,4'-diisothiocyanostilbene-2,2'-disulphonic acid (DIDS)-0.1, pH 7.3 (adjusted with TEA-(OH)). The presence in the pipette of K^+ channel blocker, TEA, and Cl^- channel blocker, DIDS, ensured maximal suppression of potentially contaminating K^+ and Cl^- single-channel activities. All experiments were performed at room temperature (20-22°C).

Electrophysiological Recording. The electrodes were pulled on a PIP 5 (HEKA, Germany) puller in two stages from borosilicate glass capillaries (BBL,WPI, USA) (1.5 mm in diameter) to a tip diameter of 1.5 - 2.0 μm.

The cultures were viewed under phase contrast with a Axiovert 135 (Zeiss, Germany) inverted microscope. Electrodes were positioned with List-Medical (Germany) micromanipulators. Grounding was achieved through a silver chloride-coated silver wire inserted into an agar bridge.

Perforated-patch recordings were performed with 200 μg/ml nystatin in the pipette, which was first back-filled with normal Ringer's to allow reliable seal formation. Access to the cell generally began within 10 min, and reached a steady value of 20 - 100 MΩ.

Perforated-patch and whole-cell recordings were carried out using an Axopatch-200B amplifier (Axon Instruments, USA). Stimulus control, as well as data acquisition and

processing were carried out with a PC computer (IBM, USA), fitted with a DigiData 1200 series interface, using Pclamp 6 software (Axon Instruments, USA - interface and software).

The activity of single store-dependent plasma membrane Ca^{2+} channels was recorded in cell attached configuration, following depletion of intracellular Ca^{2+} stores by 0.1 μM thapsigargin, and using Ca^{2+}-free HBSS as a bath solution. Single-channel recordings were carried out using EPC9 patch clamp amplifier (HEKA, Germany). The currents in response to voltage-clamp pulses were low-pass filtered at 1.5 kHz and digitized at 10 kHz. Under such filtering conditions the rms noise was 0.09 pA. The single channel data were analyzed using PulseFit (HEKA, Germany) and Origin-5 software, USA. The techniques have previously been described in detail (27,28).

Data and Statistical Analysis. Results were expressed as mean ± standard deviation where appropriate. Each experiment was repeated several times. Student's t-test was used for statistical comparison among means and differences, with $P< 0.05$ considered significant.

Fluorescence Measurements of $[Ca^{2+}]i$ with Fura-2. For fura-2 measurements, cells were excited alternately at 340 and 380 nm. Fluorescence emitted at 510 nm was captured and analyzed by a photomultiplier-based system (Photon Technologies International Ltd, Princeton, NJ, USA). $[Ca^{2+}]i$ was calculated from the ratio of the emitted fluorescence, acquired at 340 and 380 nm in turn, using the Grynkiewicz, Poenie & Tsien equation (29).

For microfluorimetric measurements, cells were grown on glass coverslips for at least three days before the experiment, loaded for 30 minutes with the acetoxymethyl ester derivative of the dye (5 μM fura2-AM), and subsequently washed three times with a dye-free solution.

Determination of Apoptosis. Cells were seeded in 8-chamber culture slides (Lab-Tek) in RPMI medium containing 10% fetal calf serum. After 24 h, cells were treated with Ni^{2+} or thapsigargin for varying periods of time. At the end of the treatment, cells were fixed

with ice-cold methanol for 10 min and washed twice with phosphate buffer saline (PBS). Cells were then stained with 5 μg/ml Hoescht 33258 for 10 min at room temperature and mounted in glycergel (DAKO). Nuclear morphology was displayed on an Olympus BH-2 fluorescence microscope (405-435 nm). The percentage of apoptotic cells was determined by counting at least 500 cells in random fields.

Chemicals. All chemicals were bought from Sigma except for Fura 2/AM, SK&F 96365 and thapsigargin, which were purchased from Calbiochem.

RESULTS

SERCA pump inhibitors induce a biphasic Ca^{2+} rise in LNCaP cells. The $[Ca^{2+}]i$ resting level of LNCaP cells in a solution containing 2 mM $CaCl_2$ was about 81 ± 7 nM (n=103) and remained stable during the recording up to 60 min.

A common means used for discharging the Ca^{2+} stores is to inhibit SERCA pump activity (30, 31). Potent, selective Ca^{2+} pump inhibitors such as thapsigargin (32) or cyclopiazonic acid (CPA) (33) deplete intracellular Ca^{2+} pools and concomitantly promote a sustained capacitative Ca^{2+} entry (34). This makes Ca^{2+} pump inhibitors useful tools for studying controlled intracellular calcium changes and their consequences in cell physiology.

Exposure of Fura-2 loaded LNCaP cells to 0.1 μM thapsigargin in the presence of extracellular calcium produced a large initial increase in intracellular Ca^{2+} as a result of the depletion of intracellular stores (Fig.1A). This was followed by a sustained plateau, corresponding to a Ca^{2+} influx. This depletion-activated Ca^{2+} entry was confirmed by the fact that Ni^{2+} (0.5 - 3mM), La 3+ (1 μM) and Ca^{2+}- free medium blocked the sustained Ca^{2+} rise (Fig.1B, C). When Ca^{2+} was added to the extracellular medium again, the Ca^{2+} influx was restored (Fig.1C).

To ensure that the effects of thapsigargin resulted from its action on intracellular Ca^{2+}-ATPase, we also examined the effects of CPA, a structurally unrelated agent that similarly inhibits the SERCA pump. CPA (10 μM) produced similar effects on $[Ca^{2+}]i$ to those of thapsigargin, also inducing an initial Ca^{2+} mobilization followed by Ca^{2+} entry (not shown, n = 11).

Depletion of intracellular Ca^{2+} stores activates a Ca^{2+} current through store-operated channels. We used the perforated patch recording technique combined with $[Ca^{2+}]i$ measurement to compare the kinetics of the $[Ca^{2+}]i$ increase induced by TG, and the development of the I_{STORE} Ca^{2+} current. As illustrated in Fig. 2, within 15 ± 6 sec, TG stimulated an initial $[Ca^{2+}]i$ increase due to the mobilization of Ca^{2+} from intracellular stores. An inward current appeared within 25 ± 5 sec after TG application (n=11). The application of Ca^{2+}-free solution inhibited the second phase of $[Ca^{2+}]i$ increase induced by TG and the corresponding inward current (Fig. 2A, n=7). When Ca^{2+} was added again the sustained plateau was restored and the Ca^{2+} current was induced. I_{STORE} was inhibited in LNCaP cells by Ni^{2+} (mM). Moreover, when Ni^{2+} was present in the extracellular solution, TG only induced an initial Ca^{2+} rise due to Ca^{2+} mobilization, but I_{STORE} was not stimulated (n=9, Fig. 2B). Likewise, TG induced a monophasic increase in $[Ca^{2+}]i$ under Ca^{2+}-free extracellular conditions (not shown, n=7).

We used the whole-cell patch-clamp technique to study the voltage dependence of I_{STORE} in LNCaP cells. Ca^{2+} stores were emptied by incubating cells in a Ca^{2+}-free solution supplemented with 0.1 μM TG for 15 min while dialyzing the cell's interior with a strongly buffered Ca^{2+} solution (see Materials and Methods section). I_{STORE} calcium current was elicited by adding 22 mM CaCl2 to the bath at different holding membrane potentials. An example of such an experiment and its current-voltage (I/V) relationship are shown in Fig. 2C. The store-operated calcium channels in LNCaP cells were non-conducting at very depolarized

potentials. On the contrary, the current amplitude increased following membrane hyperpolarization and the I/V relationship displayed an inward rectification (Fig. 2C).

The activity of single store-dependent Ca^{2+} channels. Cell-attached patch-clamp configuration was used to study the unitary activity of SOC in LNCaP cells and to identify its unitary conductance. The activity of single store-dependent plasma membrane Ca^{2+} channels following depletion of intracellular Ca^{2+} stores with 0.1μM thapsigargin was studied using Ca^{2+}-free HBSS as a bath solution and 80 mM CaCl2 in the pipette. Under these conditions, we recorded a unitary activity that had inward direction and due to the activation of single store-dependent Ca^{2+} channels. This unitary activity only occurred in response to hyperpolarizing voltage clamp pulses (with respect to the cell's resting potential) and was characterized by low amplitude (0.3-0.4 pA) and high frequency flickering between open and closed states. In order to examine this type of activity over a broad range of membrane potentials and, at the same time, to measure its I-V relationship, we used a complex pulse protocol consisting of two steady levels of hyper- and depolarizing potentials linked with a voltage ramp (Fig. 3A, top row). Fig. 3A shows recordings of single channel activity in response to this protocol. Single channel activity was only elicited by hyperpolarization, and only in the inward direction. Averaging, and subsequent smoothing of the amplitudes of the unitary events during the ramp portion of the pulse protocol gave the I-V relationship of observed single channel activity (Fig.3B). The resulting I-V curve showed a strong rectification in the inward direction: no current could be detected at potentials more positive than the resting potential. The slope conductance, determined by the linear fit of the I-V relationship at negative potentials, was found to be 3.2 pS (Fig. 3B).

The following findings support our notion that the unitary activity described thus far is associated with the activation of single store-operated plasma membrane Ca^{2+} channels: i.) The activity can only be observed in TG-treated cells. ii.) The activity shows a strong inward

rectification which is typical of Ca^{2+} selective channels. iii.) Neither K^+ (35,36) nor Cl^- (Shuba et al., unpublished observation) channels known to be present in LNCaP cells were capable of producing a similar type of activity under these experimental conditions. iv.) No other Ca^{2+}-selective conductance has been described so far in LNCaP cells.

Changing external Na+ (replaced by choline) had no significant effect on I_{STORE} in all patch-clamp configurations used: whole-cell, perforated patch, and cell-attached. I_{STORE} was also insensitive to SK&F 96365 (100 μM), one of the suggested capacitative Ca^{2+} current inhibitors.

Thapsigargin induces apoptosis in LNCaP cells. Hoescht staining was used to determine apoptosis induced by TG treatment. Typical apoptotic features induced by treatment with 0.1 μM TG for 24 h are shown in Fig.5C. TG induced apoptosis in a time-dependent manner (Fig.4A) ; 70% of cells attained apoptosis at 48h.

Sustained elevation of cytosolic Ca^{2+} due to SOC activation is not required for induction of apoptosis by thapsigargin. As it has previously been reported that, in androgen-independent prostate cancer cells (23), I_{STORE} activation is required for TG-induced apoptosis, we tested this hypothesis in androgen-dependent prostate cancer LNCaP cells.

To determine whether the I_{STORE} in LNCaP cells is important in apoptosis induction by TG, we examined the ability of TG to induce apoptosis under different experimental conditions. In patch-clamp experiments, I_{STORE} was completely abolished by Ni^{2+}. According to the hypothesis stated above, TG-induced apoptosis should decrease in cells treated with Ni^{2+}. Unexpectedly, TG-induced apoptosis increased significantly in cells treated with 0.5 mM Ni^{2+} (Fig.4 A). Fig 5 D shows the apoptotic features of LNCaP cells after combined treatment with TG and Ni^{2+} for 24 h . Cell treatment with Ni^{2+} alone did not induce apoptosis in LNCaP cells (Fig.5 B). To further explore the role of I_{STORE} in TG-induced apoptosis we examined the ability of TG to induce apoptosis in a Ca^{2+}-depleted medium. This medium contained no

added Ca^{2+} and dialyzed serum was used to remove Ca^{2+} contaminants (as well as other low-molecular-weight species). TG-induced apoptosis also increased significantly in this Ca^{2+}-depleted medium (Fig.4B). The increase in TG-induced cell apoptosis by Ni^{2+} and Ca^{2+}-depleting medium was really due to apoptosis and not necrosis. This was confirmed by an increase in the morphological indicators of apoptosis, i.e. the extent of internucleosomal degradation and DNA ladder formation (data not shown). Furthermore, the percentage of cells excluding trypan blue was not affected by incubation with Ni^{2+} or Ca^{2+}-depleting medium.

To assess how calcium is affected by these apoptosis-inducing conditions, we compared cytoplasmic Ca^{2+} levels in LNCaP cells after 24h, 30h, and 48 h treatment with TG, Ni^{2+}, and TG combined with Ni^{2+}. $[Ca^{2+}]i$ remained at high levels throughout the 48 h, and even longer when cells were treated with TG alone, while the $[Ca^{2+}]i$ level in cells treated with Ni^{2+} or TG combined with Ni^{2+} was almost the same as those of the control (Fig .4 C). This indicates that a sustained high level of $[Ca^{2+}]i$ is not required for induction of apoptosis by TG and its subsequent development.

Transient $[Ca^{2+}]i$ increase due to depletion of Ca^{2+} stores is not responsible for apoptosis induction by thapsigargin. As thapsigargin is still capable of inducing a rise in $[Ca^{2+}]i$ in the absence of extracellular Ca^{2+}, due to a passive leak of Ca^{2+} through the ER membrane, we checked whether this initial transient increase in $[Ca^{2+}]i$ was involved in apoptosis induction. To eliminate the transient rise in $[Ca^{2+}]i$, LNCaP cells were incubated for 20 min in the presence of 50 μM BAPTA-AM, an intracellular Ca^{2+} chelator. This procedure resulted in sufficient intracellular Ca^{2+} buffering to completely eliminate the transient rise in$[Ca^{2+}]i$ that occurred when thapsigargin was added to a Ca^{2+}-free medium (not shown). BAPTA-AM treatment for 20min without TG did not induce apoptosis in LNCaP cells (< 0.1% of apoptotic cells in control after 48h and < 0.1% of apoptotic cells after 48h following 20 min incubation with BAPTA-AM). The cells were then treated with 0.1 μM TG for 48h

and the percentage of apoptotic cells was compared with that of cells not loaded with BAPTA. The ability of TG to induce apoptosis in LNCaP cells was not reduced by BAPTA loading (90 ± 5% apoptotic cells in BAPTA-loaded, TG-treated cells, as compared with 91 ± 4 % in TG-treated cells in a Ca^{2+}-deficient medium).

DISCUSSION

The present study demonstrates that emptying intracellular Ca^{2+} stores by SERCA pump inhibitors stimulates a Ca^{2+} current, I_{STORE}, through specific store-operated channels, SOCs, in androgen-dependent human prostate cancer LNCaP cells. These channels are activated by intracellular store depletion, and had not previously been identified and characterized in prostate cells.

The presence of store-operated Ca^{2+} entry has been documented in a large variety of cells, mainly on the basis of measurements of intracellular Ca^{2+} levels after store depletion by thapsigargin (16). However, Ca^{2+} current in response to store depletion can only be measured directly using the patch-clamp technique. The first electrophysiological demonstration of a store-operated Ca^{2+} current was carried out in mast cells by Hoth and Penner (37), who called it Ca^{2+} Release-Activated Current (I_{CRAC}). I_{CRAC} is now the best-characterized store-operated Ca^{2+} current. It is known to be activated by depleting intracellular Ca^{2+} stores and has the highest selectivity for Ca^{2+} over other cations (37-39). Although I_{CRAC} was the first store-operated Ca^{2+} current to be described, recent studies using patch-clamp techniques have now clearly established the existence of a number of store-operated Ca^{2+} currents in several nonexcitable cell types, differentiated by their unitary conductance, selectivity, and pharmacology (for review see ref. 16). Regardless of some differences in channel properties, store-operated channels form a family of channels characterized by several specific, common features. The first of these consists of current activation by emptying the intracellular stores,

using a variety of procedures. In our experiments, I_{STORE} was identified by emptying intracellular stores using TG. As in basophilic leukemia (RBL) cells, or Jurkat T cells, I_{STORE} in LNCaP cells appears to be the critical Ca^{2+} influx pathway as LNCaP cells do not have voltage-activated Ca^{2+} channels (35,36). The second important property of I_{STORE} is its characteristic voltage-dependence. I_{STORE} could be considered a voltage-independent Ca^{2+} current, as it is not gated by membrane voltage changes (39,40). However, once it has been activated by store depletion, I_{STORE} increases when the membrane potential shifts toward negative values. The current-voltage relation also shows a pronounced inward rectification at negative voltages (39,40). In LNCaP cells, I_{STORE} is relatively large (50 pA at -80 mV) and decreases to 5 pA at +10 mV. Current-voltage relationships for both macroscopic or unitary I_{STORE} currents show prominent inward rectification, typical of I_{CRAC} in other cell models. The I_{STORE} reversal potential was above +50 mV, as expected for selective Ca^{2+} currents. Changing external Na+ has no significant effect on I_{STORE} in LNCaP cells, demonstrating that Na+ does not permeate the channel in the presence of external Ca^{2+}. I_{STORE} was inhibited by Ni^{2+} and La3+, thus corresponding to the typical pharmacological profile of store-operated currents in other cells (40-42). SK&F- 96365, one of the proposed inhibitors of capacitative Ca^{2+} current, did not inhibit I_{STORE} in LNCaP cells. However, blocking the Ca^{2+} current by this inhibitor is not an evidence for capacitative current as it can also block other channels in similar concentrations (43).

We also studied I_{STORE} at the single-channel level. The unitary conductance of the I_{STORE} channel was identified as 3.2 pS, which is rather large in comparison with classical I_{CRAC} single-channel conductance, which is usually under 1 pS (16,39). Large single-channel conductances of 2 pS and 11 pS were also observed for store-operated currents in A 431 epidermal cells (44) and endothelial cells (45), respectively. Thus, some properties of I_{STORE} in

human cancer prostate LNCaP cells suggest that it belongs to the "store-operated" channel family, but that it is not the same as I_{CRAC} .

Our study provides the first direct demonstration and characterization of a store-operated current in prostate cells. SOCs characterization could be of great interest in prostate cancer studies as these channels were suggested to be the target of a Ca^{2+} - influx inhibitor, which has been found, in clinical trials, to slow down the growth of certain aggressive cancer cells (46).We studied the role of SOCs in TG-induced apoptosis in androgen-dependent prostate cancer LNCaP cells. TG induces apoptosis in many cell types (13, 21-23). Based on the changes in Ca^{2+} homeostasis induced by TG, three hypotheses can be proposed to explain the apoptosis induction mechanism. Apoptosis is induced by: (i) a transient increase in $[Ca^{2+}]i$ due to a passive leak of Ca^{2+} through the ER membrane, (ii) Ca^{2+} pool depletion, or (iii) a sustained rise in cytosolic Ca^{2+} secondary to Ca^{2+} entry through I_{STORE} channels. In this report we show that neither the transient nor the sustained increase in $[Ca^{2+}]i$ are required for induction of apoptosis by TG. The transient increase in $[Ca^{2+}]$ was observed in LNCaP cells by TG application in the absence of extracellular Ca^{2+}. We strongly buffered $[Ca^{2+}]i$ by preincubating with the Ca^{2+} chelator, BAPTA-AM to eliminate this transient rise in $[Ca^{2+}]i$. Preincubation did not inhibit apoptosis induced by TG, suggesting that the transient increase in $[Ca^{2+}]i$ is not responsible for apoptosis induction. On the basis of these results, we can exclude another possible consequence of ER depletion that might induce apoptosis: mitochondrial overloading (6). The build-up of mitochondrial Ca^{2+} that could initiate a program of events leading to cell death (6,47) was prevented by cytosolic Ca^{2+} chelation using BAPTA-AM. These data are consistent with the findings of others on lymphoid cells (21,22) and murine hypothalamic cell lines (48). However, surprisingly, they are in contrast with those described in androgen-independent prostate cancer cells (23). In these cells, as in thymocytes (49), TG-induced apoptosis was inhibited by preincubating cells with BAPTA-

AM, or by overexpressing the cytosolic Ca^{2+} binding protein, calbindin. On the basis of these results, the increase in cytosolic Ca^{2+} was considered to play a role in apoptosis induction by TG. Moreover, the authors suggested that TG-induced apoptosis was critically dependent upon an adequate, sustained elevation of Ca^{2+} (i.e.,>1h) due to store-operated Ca^{2+} current activation (23). Our results show that I_{STORE} activation is not required for apoptosis induction by TG in LNCaP cells. In contrast, I_{STORE} inhibition by a Ca^{2+}-free medium or Ni^{2+} enhanced TG-induced apoptosis. The cytosolic Ca^{2+} concentration measured after 24h and 48h of cell treatment by TG remained at high levels. Indeed, in cells treated with TG in Ni^{2+}-containing medium, it was almost the same as in control cells. Thus, it appears that Ca^{2+} pool depletion, and not the increase in cytosolic Ca^{2+}, induces apoptotic cell death in androgen-dependent human prostate cancer cells. Our data also show that the inhibition of I_{STORE} (by Ca^{2+}-free or Ni^{2+}-containing medium) enhances apoptosis induced by TG, suggesting that an increase in cytosolic Ca^{2+} due to capacitative Ca^{2+} entry through I_{STORE} channels may be required for optimal ER pool filling and apoptosis inhibition. Our results are in agreement with those of Distelhorst group (21) on WEH17.2 lymphoma cells. The authors suggested that ER calcium pool depletion by TG could trigger apoptosis and that overexpression of Bcl-2 anti-apoptotic protein, that anchors to intracellular membranes, maintains Ca^{2+} homeostasis within the ER, thereby inhibiting apoptosis induction by TG.

The exact mechanism by which calcium pool depletion induces apoptosis is not known. The high levels of Ca^{2+} within the lumen of ER are essential not only for Ca^{2+} signal transduction, but also for protein synthesis and processing, and cell division (13, 50-52). Three potential mechanisms by which ER depletion might contribute to apoptosis have been proposed (21): (i) depletion of the ER Ca^{2+} pool might destabilize the Ca^{2+}-protein gel and its associated membrane, leading to vesiculation and the formation of apoptotic blebs ; (ii) disruption of protein processing and transport within the ER may contribute to TG- induced

apoptosis ; (iii) TG-induced ER Ca^{2+} pool depletion releases an endonuclease into the nucleus responsible for DNA fragmentation. Thus, the decline in ER calcium levels leads to the activation of stress signals that switch on the genes associated with death. Although the importance of intraluminal ER Ca^{2+} storage in apoptosis appears to be evident, other mechanisms depending on extracellular, cytosolic, mitochondrial, or nuclear- Ca^{2+} have been shown to contribute to apoptosis in a variety of cell models (for review see ref. 4,5, 53). Therefore, the general applicability of the store-depletion hypothesis is doubtful and the relationship between intracellular Ca^{2+} stores, Bcl-2, and apoptosis may be cell specific.

The reasons why the progression from androgen-dependence to androgen-independence in prostate cancer cells is associated with changes in Ca^{2+} store-dependent mechanisms involved in apoptosis remain intriguing. It is known that such progression is also associated with expression of the intracellular membrane protein, bcl-2 (54,55). Bcl-2 expression modulates intracellular signaling and preserves the integrity of the ER Ca^{2+} pool in cells exposed to various apoptosis-inducing stimuli, including cytotoxic Ca^{2+} ionophores, TG, and reactive oxygen species (21,56). Moreover, it has been shown that Bcl-2 preserves the ER Ca^{2+} store via an upregulation of calcium pump SERCA gene expression. Bcl-2 may possibly interact with this pump as well (57). Another Ca^{2+}-regulating protein, calreticulin (58), has been identified in prostate cells. The expression of this highly conserved intracellular Ca^{2+}-binding protein in the lumen of the endoplasmic reticulum is regulated by androgen (59).The down-regulation of calreticulin by androgen ablation correlates with apoptosis and the up-regulation of calreticulin by androgen replacement in castrated rats correlates with proliferation and differentiation of epithelial cells in the prostate (59,60). The induction of calreticulin by androgen in prostate organ culture partially resists protein synthesis inhibition, suggesting that calreticulin is a direct androgen-response gene (59). Furthermore, Mery et al . have shown in a mouse L fibroblast cell line that overexpression of calreticulin increases

intracellular Ca^{2+} storage and decreases store-operated Ca^{2+} current suggesting an active involvement of calreticulin in intracellular Ca^{2+} pools refilling regulation (61). Thus, as calreticulin is a major intracellular Ca^{2+} binding protein involved in Ca^{2+} homeostasis and is regulated by androgens, it could be a promising candidate for mediating androgen regulation of intracellular calcium levels in prostate cells.

In summary, we have characterized the Ca^{2+}-regulated mechanisms involved in thapsigargin-induced apoptosis in androgen-dependent human prostate cancer cells, LNCaP. We have shown that a decrease in ER calcium is the major factor in apoptosis induction in these cells. In contrast to the situation in androgen-independent prostate cancer cells, the activation of I_{STORE}, responsible for ER refilling, and increasing cytosolic Ca^{2+} are not required for TG-induced apoptosis. Further studies are needed to identify the precise Ca^{2+}-regulated mechanisms involved in the progression of prostate cancer cells from androgen-dependence to androgen-independence.

ACKNOWLEDGMENTS

The authors gratefully acknowledge the technical assistance of Isabelle Servant.

REFERENCES

1. Woolf, S. H. Screening for prostate cancer with prostate specific antigen. An examination of the evidence. Engl. J. Med., *333*: 1401-1405, 1995.

2. Parker, S. L., Jone, J., Balden, S., Wingo, P. A. Cancer statistics. CA Cancer J. Clin., *47*: 5-27, 1997.

3. Montironi, R., Magi-Galluzzi, C., Muzzunigro, G., Prete, E., Polito, M., Fabris, G. Effects of combinaison endocrine treatment on normal prostate, prostatic intraepithelial neoplasia, and prostatic adenocarcinoma. J. Clin. Pathol., *47*: 906-913, 1997.

4. McConkey, D. J., Orrenius, S. The role of calcium in the regulation of apoptosis. Biochemical and Biophysical Research Communications, *239*: 357-366, 1997.

5. Down, D. R.. Calcium Regulation of Apoptosis. Advances in Second Messenger and Phosphoprotein Research, *30*: 255-279, 1995.

6. Berridge, M. J., Bootman, M. D., Lipp, P. Calcium-a life and death signal. Nature, *935*: 645-648, 1998.

7. Martikainen, P., Kyprianou, N., Tucker, R. W., Isaacs, J. T. Programmed death of nonproliferating and ragen independent prostatic cancer cells. Cancer Res., *51*: 4693-4700, 1991.

8. Juin, P., Pelletier, M., Oliver, L., Tremblais, K., Grégoire, M., Meflah, K., Vallette, F. M. Induction of a caspase-3-like activity by calcium in normal cytosolic extracts triggers nuclear apoptosis in a cell-free system. The Journal of Biological Chemistry, *273(28)*: 17559-17564, 1998.

9. McConkey, D. J., Nicotera, P., Hartzell, P., Belloms, G., Wyllie, A. M ., Orremius S. Glucocorticoids activate a suicide process in thymocytes through an elevation of cytosolic Ca^{2+} concentration. Arch Biochem Biophys., *269*: 365-370, 1989.

10. Spielberg, H., June, C. H., Blair, O. C., Nystron-Rosander, C., Cereb, N., Deeg, H. J. UV irradiation of lymphocites triggers an increase in intracellular Ca^{2+} and prevents lectin-stimulated Ca^{2+} mobilization : evidence for UV-and nifedipine-sensitive Ca^{2+}channels. Exp Hematol., *19*: 4742-4748, 1991.

11. Schieven, G. L., Kirihara, J., M., Gililand L. K., Uckun, F. M., Ledbetter, J. A. Ultraviolet radiation rapidly induces tyrosine phosphorylation and calcium signaling in lymphocytes. Mol. Biol. Cell., *4*: 523-530, 1993.

12. Berridge, M. J. Elementary and global aspects of calcium signalling. Journal of Physiology., *499(2)*: 291-306, 1997.

13. Gill, D. L., Waldron, R. T., Rys-Sikora, K. E., Ufret-Vincenty, C. A., Graber, M. N., Favre, C.J., Alfonso, A. Calcium pools, calcium entry, and cell growth. Bioscience Reports., *16(2)*: 139-157, 1996.

14. Putney, J. W. Jr. A model for receptor-regulated calcium entry. Cell Calcium, 7: 1-12, 1986.

15. Putney, J. W. Jr. Capacitative calcium entry revisited. Cell Calcium, *11*: 611-624, 1990.

16. Parekh, A. B., Penner, R. Store depletion and calcium influx. Physiological Reviews, *77(4)*: 901-929, 1997.

17. Parekh, A. B., Penner, R. Activation of store-operated calcium influx at resting $InsP_3$ levels by sensitization of the $InsP_3$ receptor in rat basophilic leukaemia cells. J. Physiol., *489*: 377-382, 1995.

18. Fanger, C. M., Hoth, M., Crabtree G. R., Lewis, R. S. Characterization of T cell mutants with defects in capacitative calcium entry : genetic evidence for the physiological roles of CRAC channels. J. Cell Biol., *131*: 655-667, 1995.

19. Santella, L. The role of calcium in the cell cycle : facts and hypotheses. Biochemical and Biophysical Research Communications, *244*: 317-324, 1998.

20. Berridge, M. J. Calcium signalling and cell proliferation. Bioessays, *17(6)*: 491-500, 1995.

21. He, H., Lam, M., McCormick, T. S., Distelhorst, C. W. Maintenance of calcium homeostasis in the endoplasmic reticulum by bcl-2. J. of Cell Biology, *138(6)*: 1219-1228, 1997.

22. Bian, X., Hughes, F. M. Jr., Huang, Y., Cidlowski, J. A., Putney, J. W. Jr. Roles of cytoplasmic Ca^{2+} and intracellular Ca^{2+} stores in induction and suppression of apoptosis in S49 cells. Am. J. Physiol., *272 (Cell Physiol. 41)*: C1241-C1249, 1997.

23. Furuya, Y., Lundmo, P., Short, A. D., Gill, D. L., Isaacs, J. T. The role of calcium, pH, and cell proliferation in the programmed (apoptotic). Death of androgen-independent prostatic cancer cells induced by thapsigargin. Cancer Res., *54*: 6167-6175, 1994.

24. Dowd, D. R., McDonald, P. N., Komm, B. S., Haussler, M. R., Miesfeld, R. Stable expression of the calbindin-D28K complementary DNA interferes with the apoptotic pathway in lymphocytes. Mol. Endocrinol., *6*: 1843-1848, 1992.

25. Gong, Y., Blok, L. J., Perry, J. E., Lindzeys, J. K., Tindall, D. J. Calcium regulation of androgen receptor expression in the human prostate cancer cell line LNCaP. Endocrinology., *136*: 2172-2178, 1995.

26. Isaacs, J. T., Lundmo, P. I., Berges, R., Martikainen, P., Kyprianou, N., English, H. F. Androgen regulation of programmed death of normal and malignant prostatic cells. Journal of Andrology., *13(6)*: 457-464, 1992.

27. Skryma, R., Prevarskaya, N., Vacher, P., Dufy, B. Voltage-dependent ionic conductances in Chinese hamster ovary cells. Am. J. Physiol., *267* : 544-553, 1994.

28. Prevarskaya, N., Skryma, R., Vacher, P., Daniel, N., Djiane, J., Dufy, B. Rôle of tyrosine phosphorylation in potassium channel activation. J. Biol. Chem., *270* : 24292-24299, 1995.

29. Grynkiewicz, G., Poenie, M., Tsien, R.Y. A new generation of Ca^{2+} indicators with greatly improved fluorescence properties. J. Biol. Chem., 260 : 3440-3450, 1985.

30. Parekh, A. B., Penner, R. Regulation of store-operated calcium currents in mast cells. Organellar Ion Channels and Transporters, 231-239, 1996.

32. Thastrup, O., Cullen, P. J., Drobak, B. K., Hanley, M. R., Dawson, A. P. Thapsigargin a tumor promoter discharges intracellular Ca^{2+} stores by specific inhibition of the endoplasmic reticulum Ca^{2+}-ATPase. Proc. Natl. Acad. Sci., *87*: 2466-2470, 1990.

33. Mason, M. J., Garcia, R. C., Grinstein, S. Coupling between intracellular calcium stores and the calcium permeability of the plasma membrane comparison of the effects of thapsigargin 2,5-di-tert-butyl 14-hydroquinone and cyclopiazonic acid in rat thymic lymphocytes. J. Biol. Chem., *266*: 20856-20862, 1991.

31. Huang, Y., Putney, J. W. Relationship between intracellular calcium store depletion and calcium release-activated calcium current in a mast cell line (RBL-1). J. of Biol. Chem., *273* : 19554-19559, 1998.

32. Skryma, R. N., Prevarskaya, N. B., Dufy-Barbe, L., Odessa, M. F., Audin, J., Dufy, B. Potassium conductance in the androgen-sensitive prostate cancer cell line, LNCaP : Involvement in cell proliferation. The Prostate, *33*: 112-122, 1997.

33. Skryma, R. N., Van Coppenolle, F., Dufy-Barbe, L., Dufy, B., Prevarskaya, N. Characterization of Ca^{2+}-inhibited potassium channels in the LNCaP human prostate cancer cell line. Receptors and Channels, 1999 (in press).

34. Hoth, M., Penner, R. Depletion of intracellular calcium stores activates a calcium current in mast cells. Nature, *355*: 353-356, 1992.

35. Berridge, M. J. Capacitative calcium entry. Biochemical Journal, *312*: 1-11, 1995.

36. Zweifach, A., Lewis, R. S. Mitogen-regulated Ca^{2+} current of T lymphocytes is activated by depletion of intracellular Ca^{2+} stores. Proc. Natl. acad. Sci., USA, *90*: 6295-6299, 1993.

37. Hoth, M., and Penner, R. Calcium release-activated calcium current in rat mast cells. J. Physiol., *465*: 359-386, 1993.

38. Schlegel, W., Mollard, P., Demaurex, N., Theler, J. M., Chiavaroli, C., Guérineau, N., Vacher, P., Mayr, G., Krause, K. H., Wollheim, C. B., Lew P. D. Calcium signalling : comparison of the role of Ca^{2+} influx in excitable endocrine and non-excitable myeloid cells. Advances in Second Messenger and Phosphoprotein Research, *28*: 142-152, 1993.

39. Grudt, T. J., Usowicz, M. M., Henderson, G. Ca^{2+} entry following store depletion in SH-SY5Y neuroblastoma cells. Molecular Brain Research, *36*: 93-100, 1996.

40. Franzius, D., Hoth, M., Penner, R. Non-specific effects of calcium entry antagonists in mast cells. Pflüggers Arch., *428*: 433-438, 1994.

41. Lückhoff, A., Clapham, D. E. Calcium channels activated by depletion of internal calcium stores in A431 cells. Biophysical Journal, *67*:177-182, 1994.

42. Vaca, L., Kunze, D. L. Depletion of intracellular Ca^{2+} stores activates a Ca^{2+}-selective channel in vascular endothelium. Am. J. Physiol., *269 (Cell Physiol. 38)*: C733-C738, 1995.

43. Kohn, E. C., et al. Clinical investigation of a cyanotic calcium influx inhibitor in patients with refractory cancers. Cancer Research, *56(3)*: 569-573, 1996.

44. Green, D. R., Reed, J. C. Mitochondria and apoptosis. Apoptosis, *281* : 1309-1316, 1998.

45. Wei, H., Wei, W., Bredesen, D. E., Perry, D. C. Bcl-2 protects against apoptosis in neuronal cell line caused by thapsigargin-induced depletion of intracellular calcium stores. Journal of Neurochemistry, *70(6)*: 2305-2314, 1998.

46. Jiang, S., Chow, S. C., Nicotera, P., Orremius, S. Intracellular Ca^{2+} signals activate apoptosis in thymocytes : studies using the Ca^{2+}-ATPase inhibitor thapsigargin. Exp. Cell. Res., *212*: 84-92, 1998.

47. Sambrook, J. F. The involvement of calcium in transport of secretary proteins from the endoplasmic reticulum. Cell, *61*: 197-199, 1990.

48. Koch, G. L. E. The endoplasmic reticulum and calcium storage. Bioessays, *12*: 527-531, 1990.

49. Kuznetsov, G., Brostrom, M. A., Brostrom, C. O. Role of endoplasmic reticular calcium in oligosaccharide processing of alpha 1-antitrypsin. J. Biol. Chem., *268*: 2001-2008, 1992.

50. Marin, M. C., Fernandez, A., Bick, R. J., Brisbay, S., Buja, L. M., Snuggs, M., McConkey, D. J., Von Eschenbach, A. C., Keating, M. J., McDonnell, T. J. Apoptosis suppression by bcl-2 is correlated with the regulation of nuclear and cytosolic Ca^{2+}. Oncogene, *12*: 2259-2266, 1996.

51. Raffo, A. J., Perlman, H., Chen, M. W., Day, M. L., Streitman, J. S., Buttyan, R. Overexpression of bcl-2 protects prostate cancer cells from apoptosis *in Vitro* and confers resistance to androgen depletion *in Vivo*. Cancer Res., *55*: 4438-4445, 1995.

52. Chaudhary K. S., Abel, P. D., Lalani, E. N. Role pf the bcl-2 gene family in prostate cancer progression and its implications for therapeutic intervention. Environmental Health Perspectives, *107*: 49-57, 1999.

53. Disthelhorst, C. W., Lam, M., McCormick, T. S. Bcl-2 inhibits hydrogen peroxyde-induced ER Ca^{2+} pool depletion. Oncogene, *12*: 2051-2055, 1996.

54. Kuo, T. H., Kim, H. R. C., Zhu, L., Yu, Y., Lin, H. M., Tsang, W. Modulation of endoplasmic reticulum calcium pump by bcl-2. Oncogene, *17*: 1903-1910, 1998.

55. Krause, K. H., Michalak, M. Calreticulin. Cell, *88*: 439-443, 1997.

56. Zhu, N., Pewitt, E. B., Cai, X., Cohn, E. B., Lang, S., Chen, R., Wangs, Z. Calreticulin : an intracellular Ca^{2+}-binding protein abundantly expressed and regulated by androgen in prostatic epithelial cells. Endocrinology, *139(10)*: 4337-4344, 1998.

57. Zhu, N., Wang, Z. Calreticulin expression is associated with androgen regulation of the sensitivity to calcium ionophore-induced apoptosis in LNCaP prostate cancer cells (in process citation). Cancer Res., *59(8)*: 1896-1902, 1999.

58. Mery, L., Mesaeli, N., Michalak, M., Opas, M., Lew, D. P., Krause, K. H. Overexpression of calreticulin increases intracellular Ca^{2+} storage and decreases store-operated Ca^{2+} influx. J. of Biol. Chem., *271(16)* : 9332-9339, 1996.

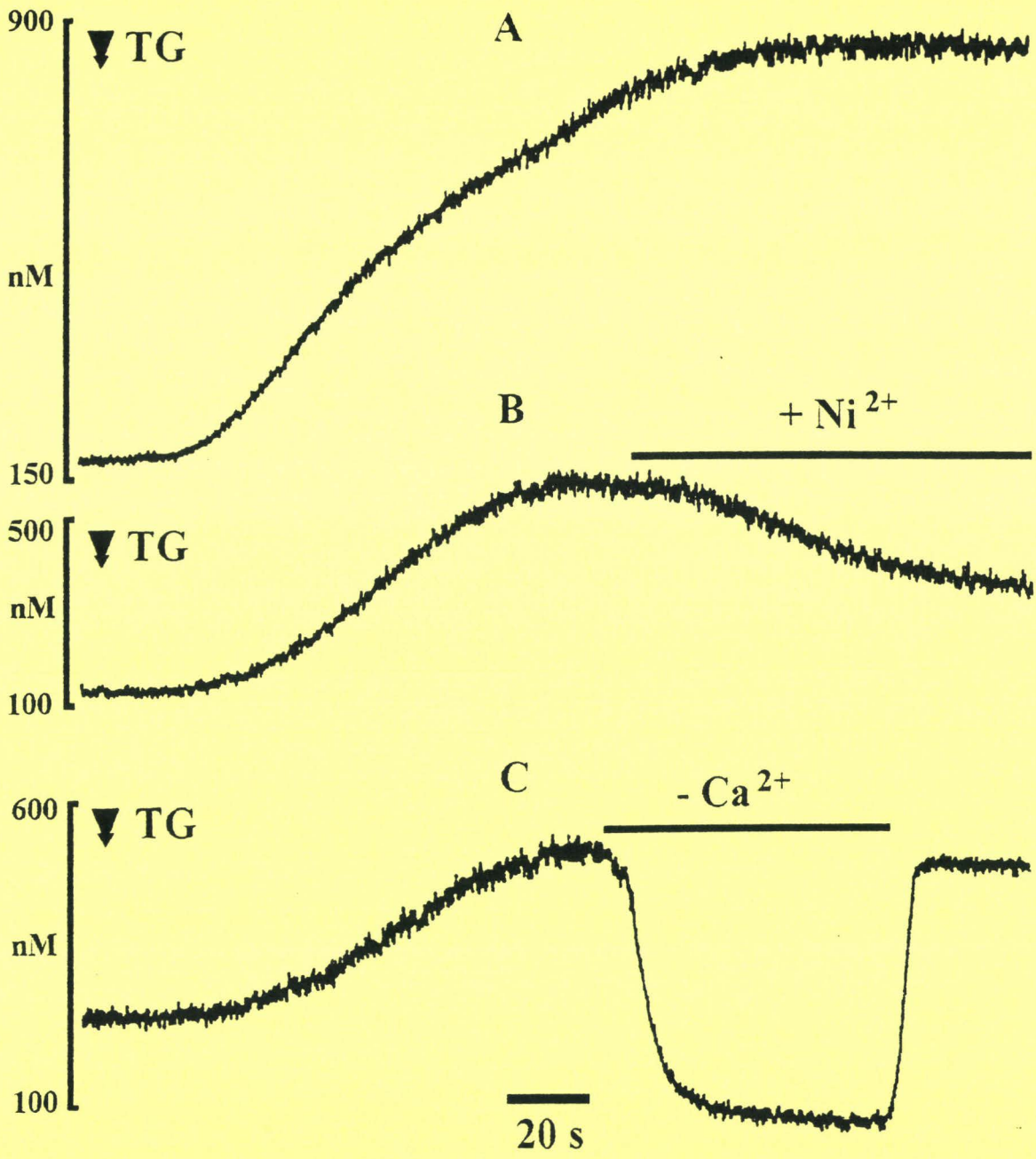

Fig. 1. Stimulation of Ca^{2+} influx by thapsigargin in LNCaP cells. A . Thapsigargin (0.1 μM) - induces a biphasic increase in Ca^{2+} in LNCaP cells and stimulates Ca^{2+} release with consecutive Ca^{2+} entry. B. The effect of thapsigargin (0.1 μM) in Ca^{2+} containing medium in the presence of Ni^{2+} (3 mM). C. Dependence of thapsigargin-induced Ca^{2+} influx on extracellular Ca^{2+}. Removing Ca^{2+} from external medium blocks the thapsigargin-stimulated Ca^{2+} entry. 0.1 μM thapsigargin was added at the time indicated by arrows. Ca^{2+} - free and Ni^{2+} - contained Ringer's solutions were applied from puffing pipette during the periods indicated by bars.

A

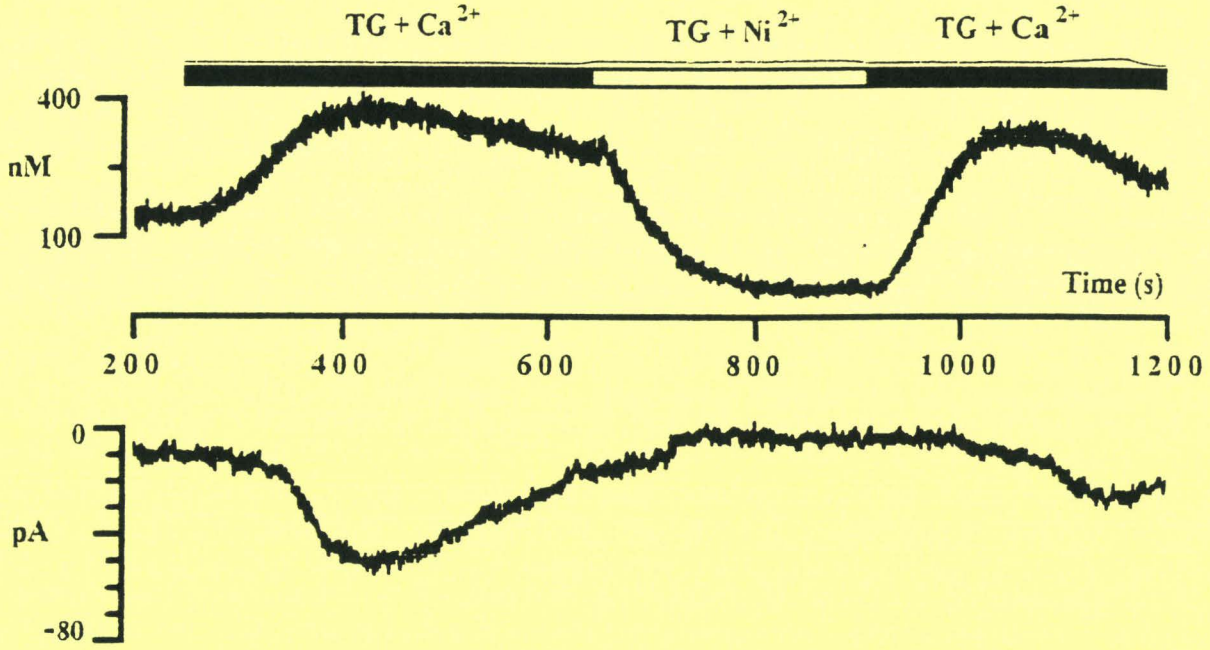
TG + Ca 2+
TG + Ni 2+
TG + Ca 2+
400
nM
100
Time (s)
200
400
600
800
1000
1200
0
pA
-80

B

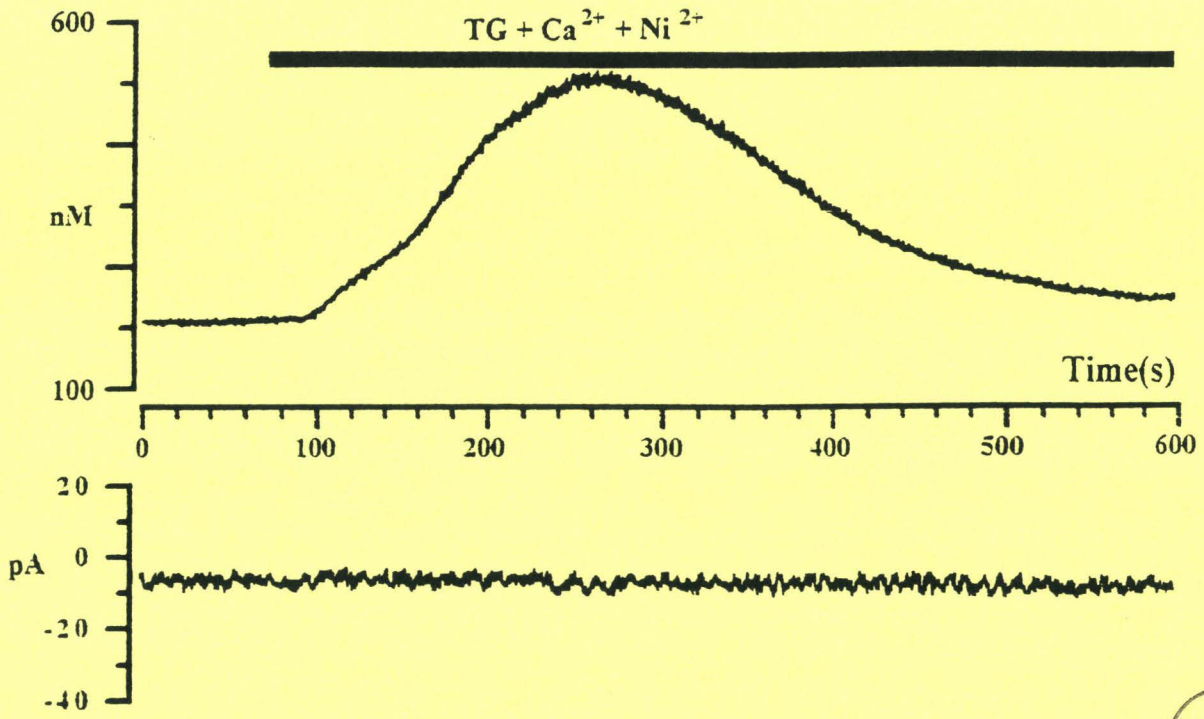
TG + Ca 2+ + Ni 2+
600
nM
100
Time(s)
0
100
200
300
400
500
600
20
pA 0
-20
-40

C

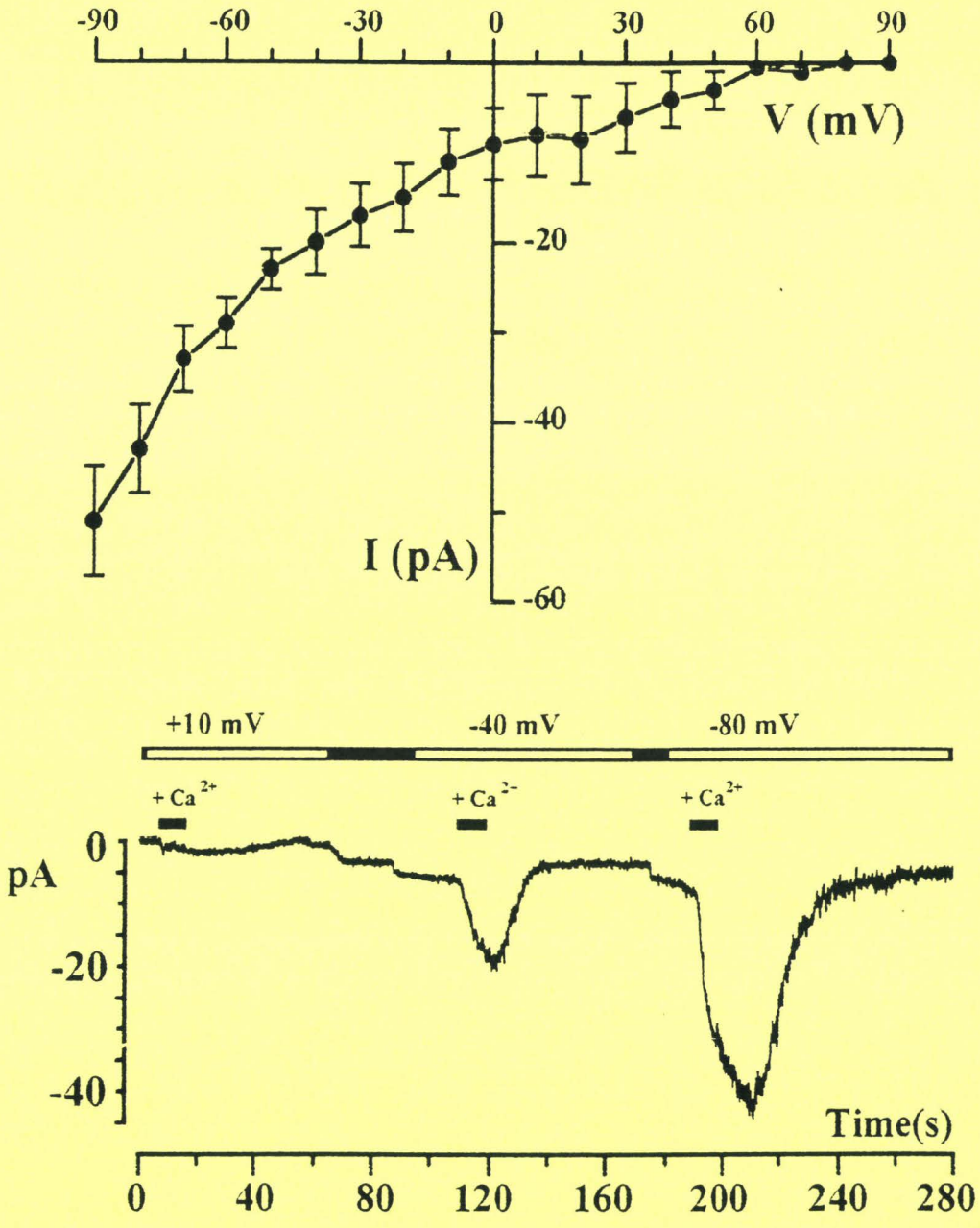
-90
-60
-30
0
30
60
90
V (mV)
-20
-40
-60
I (pA)
+10 mV
-40 mV
-80 mV
+ Ca 2+
+ Ca 2-
+ Ca 2+
pA
0
-20
-40
Time(s)
0
40
80
120
160
200
240
280

Fig 2 C

Fig. 2. Patch-clamp recordings of store-operated Ca^{2+} current in LNCaP cells. A, B. Combined perforated-patch and microspectrofluorimetric single-cell recordings of the thapsigargin-activated store-operated Ca^{2+} current at holding potential of - 80 mV. A. Reversible blockade of Ca^{2+} current by Ni^{2+} (3mM). B. Thapsigargin induces Ca^{2+} mobilization but does not induce store-operated Ca^{2+} current in the presence of Ni^{2+}. C. Whole-cell patch - clamp recordings of store-operated Ca^{2+} current at different holding membrane potentials. Current-voltage relationship shows that the store-operated Ca^{2+} current is inwardly rectifying and not activated by depolarization .

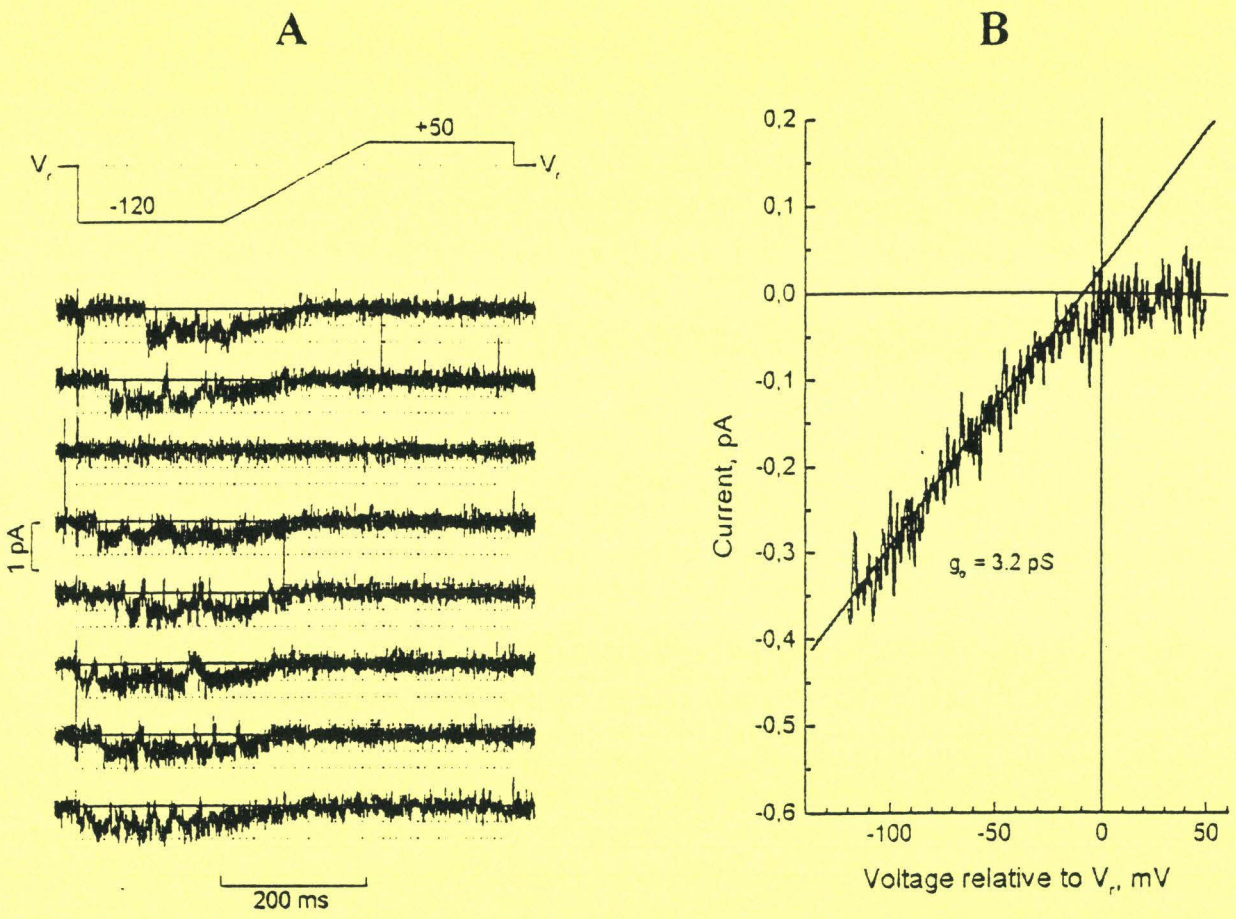

Fig. 3. The activity of single store-dependent Ca^{2+} channels. A. Single channel recordings obtained in response to the consecutive application of voltage-clamp pulses (shown on the upper row, 10 s inter-pulse interval) to the cell-attached patch in TG-treated LNCaP cells; superimposed solid lines indicate zero current levels; downward deflection corresponds to the inward current. The recordings presented probably reflect the activity of two store-dependent Ca^{2+} channels. Dotted lines indicated two levels of single-channel amplitudes of -0.35 pA and -0.7 pA. B. The I-V relation of single store-dependent Ca^{2+} channel; the I-V was constructed from the ramp portions of single channel recordings by selecting the parts corresponding to the opening of one channel with subsequent averaging and digital smoothing of the resulting curve to reduce noise; superimposed linear fit provides the value of the slope conductance of 3.2 pS.

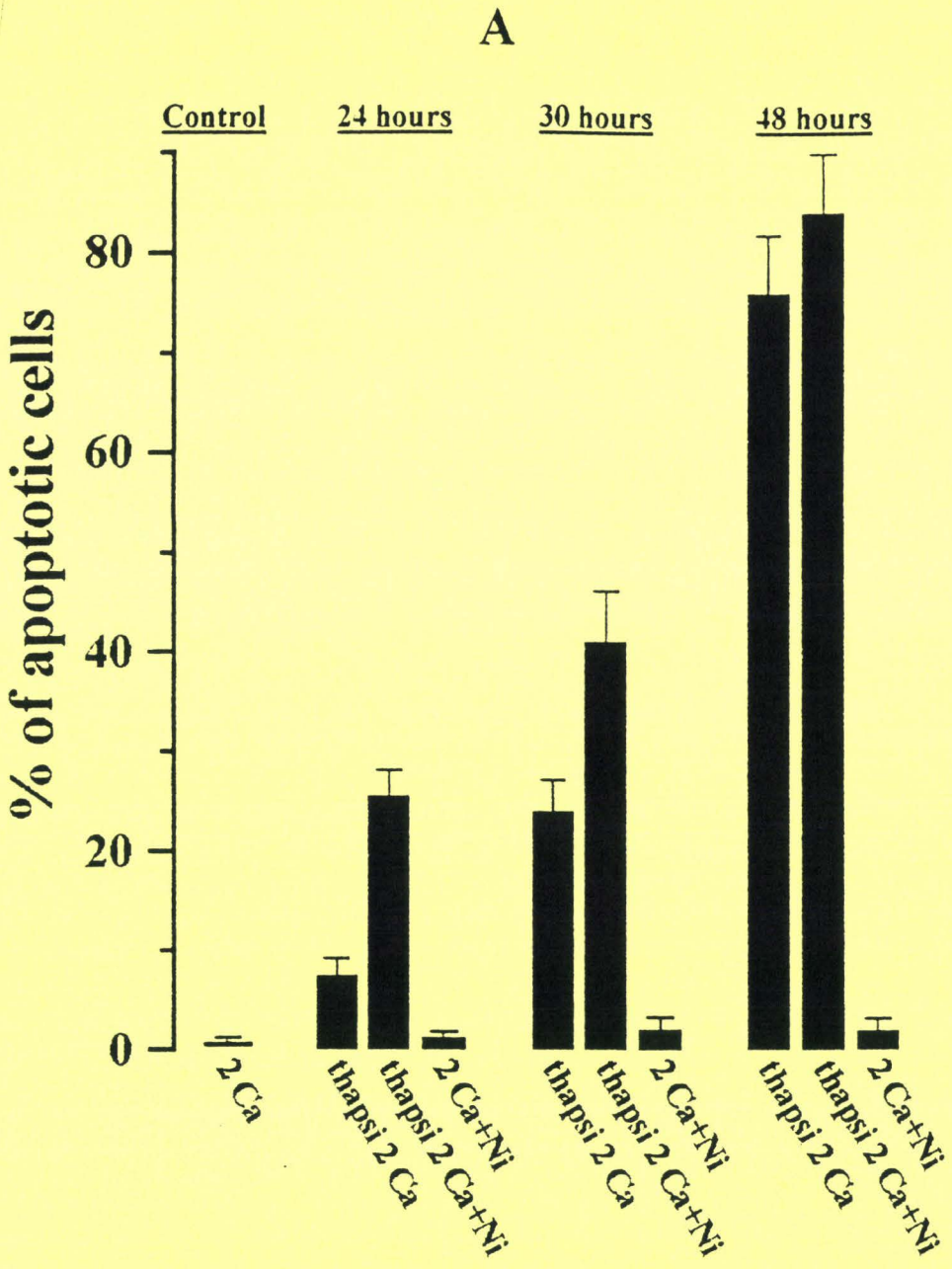
A
Control
24 hours
30 hours
48 hours
% of apoptotic cells
0
20
40
60
80
2 Ca
thapsi 2 Ca
thapsi 2 Ca+Ni
2 Ca+Ni
thapsi 2 Ca
thapsi 2 Ca+Ni
2 Ca+Ni
thapsi 2 Ca
thapsi 2 Ca+Ni
2 Ca+Ni

Fig. 4

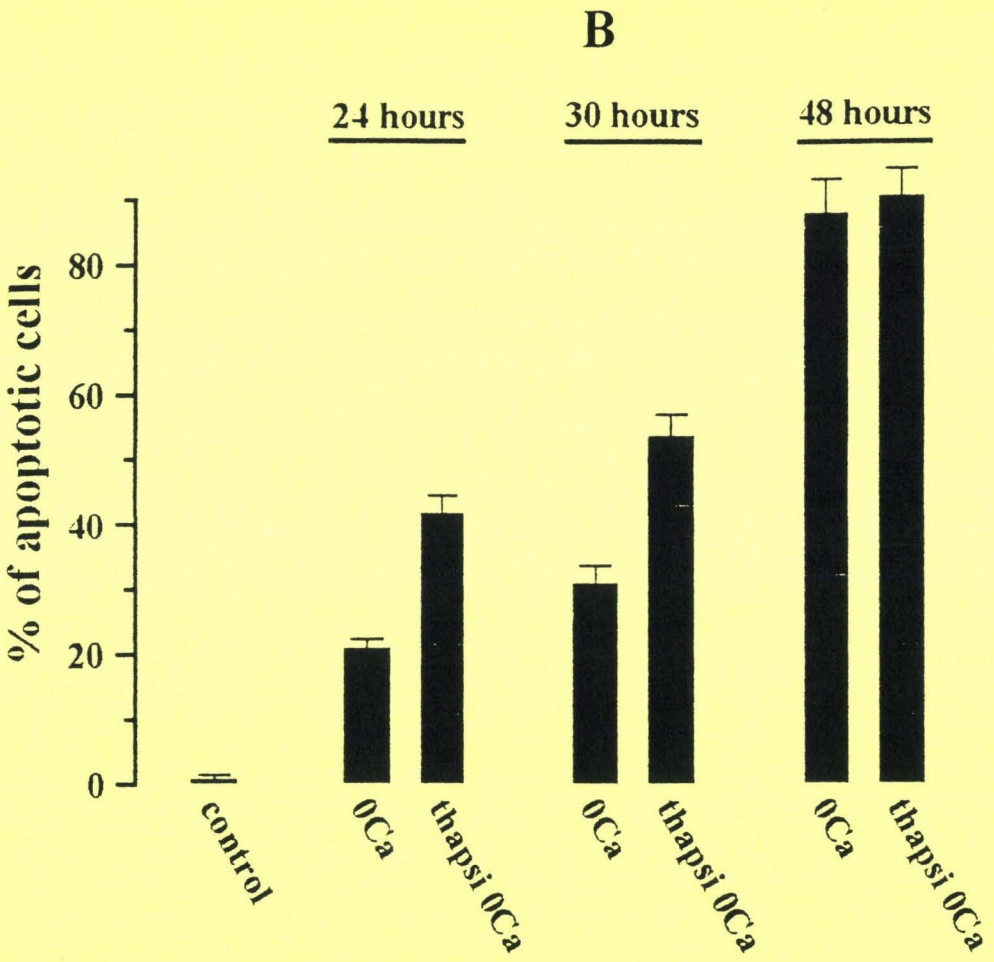
B
24 hours
30 hours
48 hours
% of apoptotic cells
0
20
40
60
80
control
0Ca
thapsi 0Ca
0Ca
thapsi 0Ca
0Ca
thapsi 0Ca

Fig. 4

C

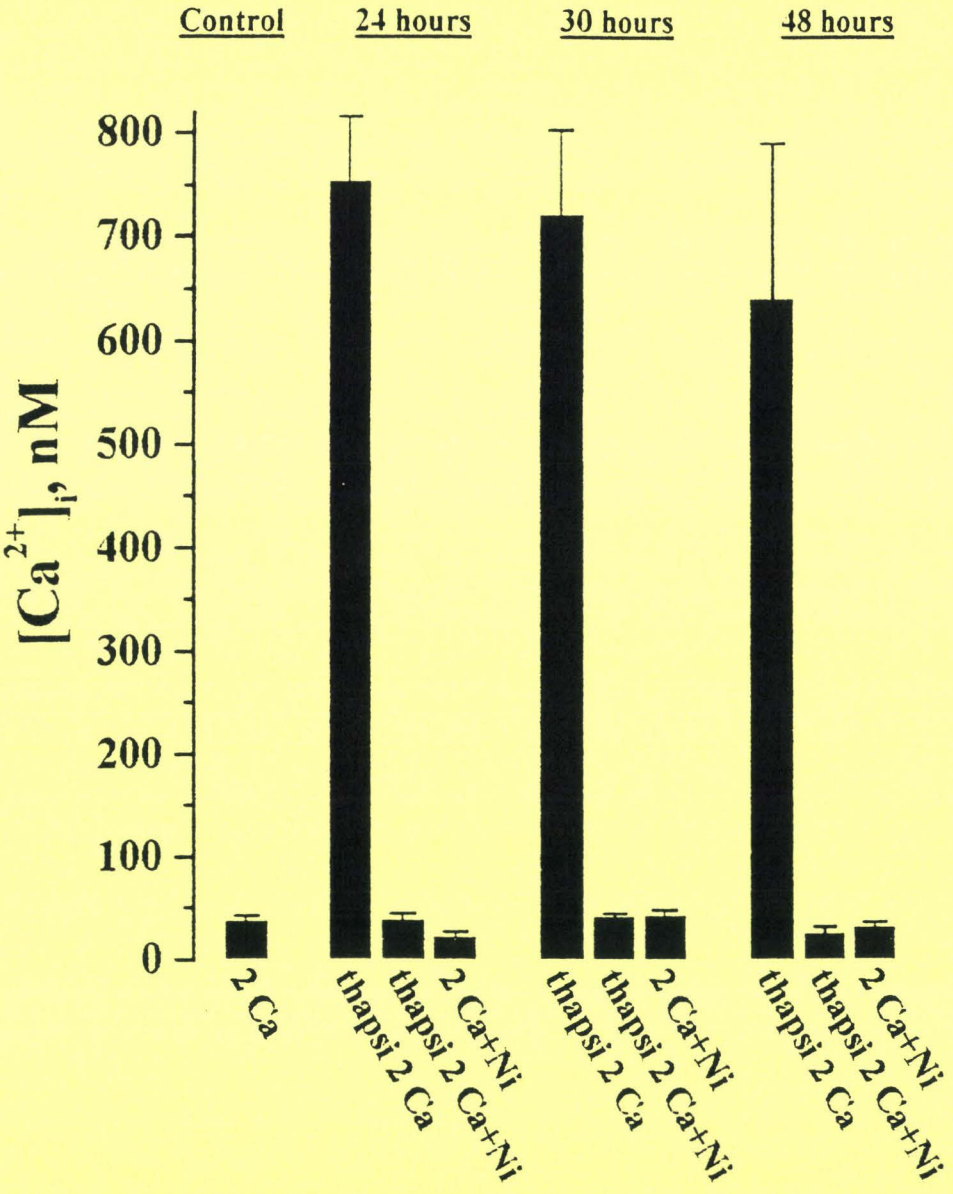
Control
24 hours
30 hours
48 hours
800
700
600
500
400
300
200
100
0
[Ca2+]i, nM
2 Ca
thapsi 2 Ca
thapsi 2 Ca+Ni
2 Ca+Ni
thapsi 2 Ca
thapsi 2 Ca+Ni
2 Ca+Ni
thapsi 2 Ca
thapsi 2 Ca+Ni
2 Ca+Ni

Fig. 4

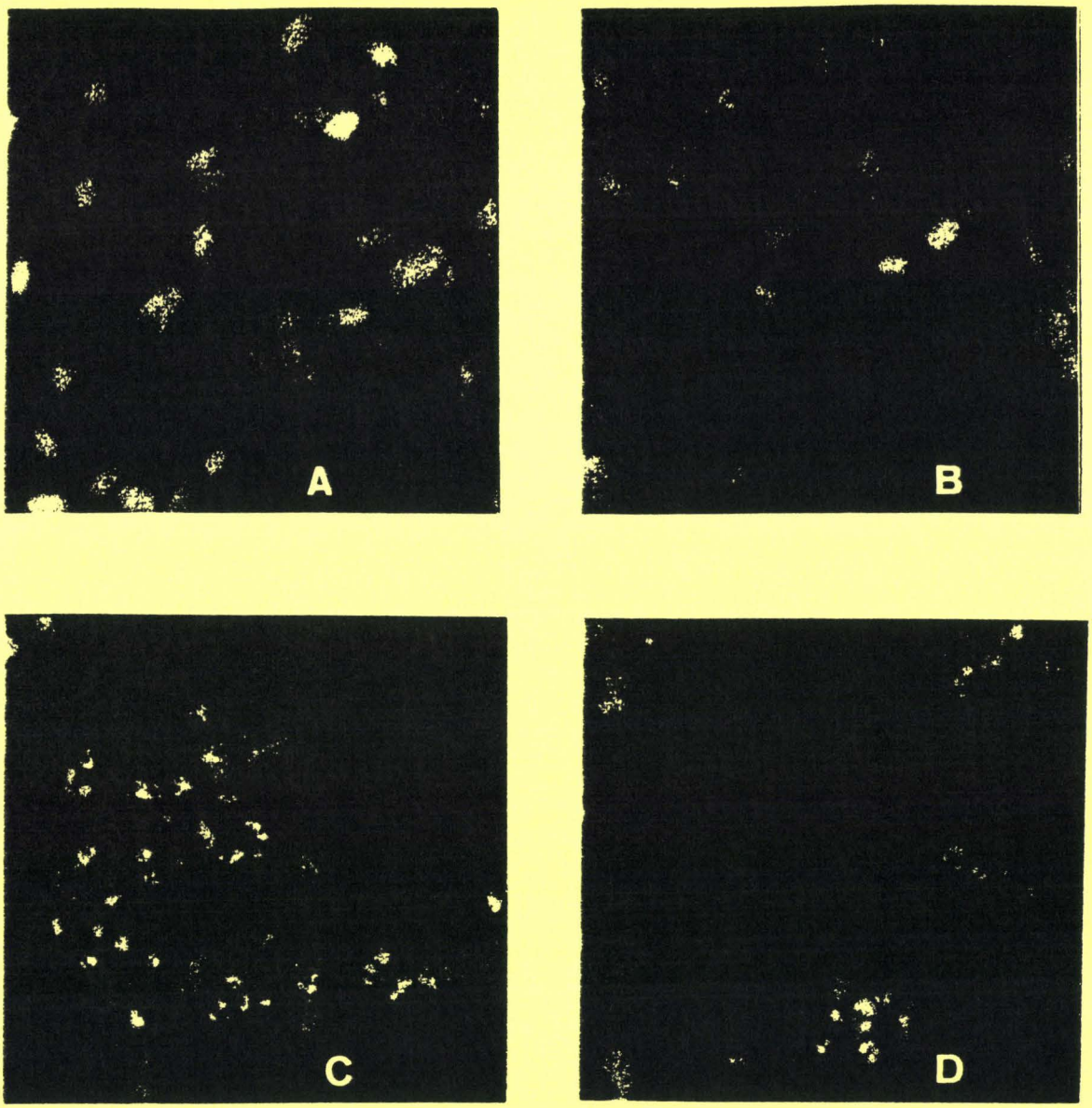

Fig. 5. LNCaP prostate cells (staining with 5 μg/ml Hoescht) undergoing apoptosis due to treatment with thapsigargin. A - control cells ; B - cells treated with 0.5 mM Ni^{2+} (72) h; C - cells treated with 0.1 μM TG (72h) ; D - cells treated with 0.1 TG μM + 0.5 mM Ni^{2+} (72 h).

Fig. 4. Temporal changes in apoptosis and in cytosolic Ca^{2+} concentration of the LNCaP cells. A. Temporal changes in apoptosis of the LNCaP cells (estimated by the number of apoptotic cells) treated with 0.1 μM TG , 0.5 mM Ni^{2+} or 0.1 μM TG combined with 0.5 mM Ni^{2+}. B. Temporal changes in the apoptosis of LNCaP cells in free-Ca^{2+} medium (estimated by the number of apoptotic cells). C. Temporal changes in cytosolic Ca^{2+} concentration of the LNCaP cells treated with 0.1 μM TG , 0.5 mM Ni^{2+} or 0.1 μM TG combined with 0.5 mM Ni^{2+}.

Les mécanismes de régulation de l'homéostasie calcique pourraient expliquer la manière dont des cellules hormono-dépendantes initialement donnent naissance, dans la majeur partie des cas, à des cancers androgeno-indépendants aujourd'hui incurables.

Nous allons poursuivre cette étude au moyen de cellules LNCaP qui surexpriment la protéine antiapoptotique Bcl-2. Ces cellules nous ont été envoyées par le Professeur R. Buttyan (New-York, USA). Ces cellules initialement androgeno-dépendantes deviennent hormono-indépendantes lorsqu'elles sont transfectées avec Bcl-2 (Raffo *et al.*, 1995). L'une des clés gouvernant l'évolution d'un cancer hormono-dépendant vers un cancer de la prostate androgeno-indépendant incurable pourrait être le fait de modifications de l'homéostasie calcique. Nous espérons ainsi découvrir les implications de l'homéostasie calcique dans le phénomène d'échappement en vue de l'élaboration de nouvelles voies thérapeutiques.

2.2- Rôle des récepteurs à la ryanodine dans l'apoptose des cellules LNCaP

Les récepteurs à la ryanodine participent à l'homéostasie calcique. Ces canaux calciques intracellulaires ont été décrits dans un premier temps dans le muscle squelettique, dans le muscle cardiaque et dans le cerveau (Imagawa *et al.*, 1987 ; Lai *et al.*, 1988 ; Leeb *et al.*, 1998).

2.2.1- Identification des récepteurs à la ryanodine dans les cellules LNCaP : implication dans l'apoptose

L'étude précédente a confirmé le rôle capital du calcium et des stocks calciques dans le déclenchement de l'apoptose des cellules LNCaP. Grâce aux techniques de microspectrofluorimétrie, d'imagerie calcique et de dosage des ARNm, nous avons mis en évidence la présence de récepteurs à la ryanodine fonctionnels de type RyR1 et RyR2 dans les

cellules LNCaP. Nous avons également démontré que l'activation de ces récepteurs induit l'apoptose (par la vidange des stocks calciques) et que leur inhibition, au contraire, protège les cellules LNCaP de la mort cellulaire programmée.

Cette étude a permis l'élaboration du manuscrit suivant, actuellement sous presse dans le journal « The Prostate ».

CONCLUSION

Nous avons caractérisé la présence de récepteurs à la ryanodine fonctionnels de type RyR1 et RyR2 dans les cellules cancéreuses prostatiques humaines LNCaP. Ces récepteurs sont impliqués dans le contrôle de l'homéostasie calcique. Nous avons démontré que l'activation de ces récepteurs, libère du calcium des stocks. Cette mobilisation du calcium induit l'entrée capacitative. Cette augmentation soutenue de calcium permet par la suite de remplir les stocks intracellulaires.

En conclusion, les récepteurs à la ryanodine jouent un rôle fondamental dans la régulation de l'apoptose des cellules cancéreuses de la prostate humaine. Les récepteurs de la ryanodine sont activés par les augmentations de la concentration intracellulaire en calcium (Sitsapesan *et al.*, 1997). Nous pensons qu'une hausse du calcium cytosolique provoquée par la stimulation de la cellule par un facteur de croissance ou une hormone, due à une réponse de type IP3, provoquerait une mobilisation de calcium par les récepteurs à la ryanodine, puis l'entrée capacitative (figure 25). La modulation de la vidange des stocks, par ces récepteurs pourrait conduire ou non la cellule vers l'apoptose. Ces résultats sont capitaux, car il serait possible de ralentir la prolifération

The Prostate 43:000–000 (2000)

Evidence of Functional Ryanodine Receptor Involved in Apoptosis of Prostate Cancer (LNCaP) Cells

Pascal Mariot,[1] Natalia Prevarskaya,[1] Morad M. Roudbaraki,[1] Xuefen Le Bourhis,[2] Fabien Van Coppenolle,[1] Karine Van Overberghe,[1] and Roman Skryma[1]*

[1]*Laboratoire de Physiologie Cellulaire, INSERM EPI 9938, Bâtiment SN3, USTL, Villeneuve d'Ascq, France*

[2]*Laboratoire de Biologie du Développement, USTL, Villeneuve d'Ascq, France*

BACKGROUND. Very little is known about the functional expression and the physiological role of ryanodine receptors in nonexcitable cells, and in prostate cancer cells in particular. Nonetheless, different studies have demonstrated that calcium is a major factor involved in apoptosis. Therefore, the calcium-regulatory mechanisms, such as ryanodine-mediated calcium release, may play a substantial role in the regulation of apoptosis.

METHODS. We assessed the presence of such functional receptors in LNCaP prostate cancer cells, using fluorimetric measurements of intracellular calcium and expression assays of mRNA encoding ryanodine receptors.

RESULTS. We show here that LNCaP cells responded to caffeine, a ryanodine receptor agonist, by mobilizing calcium. Another ryanodine receptor agonist, 4-chloro-*m*-cresol, had a similar effect and promoted calcium release. These effects were inhibited by pretreatment with ryanodine or thapsigargin. In addition to a calcium release, caffeine was able to produce a calcium entry blocked by nickel. We used a reverse transcription-polymerase chain reaction assay to investigate the expression of ryanodine receptors in LNCaP cells. Two types of ryanodine receptor mRNAs were expressed in LNCaP cells: RyR1 and RyR2 mRNAs. Finally, we show that ryanodine receptor activation by caffeine slightly stimulates apoptosis of prostate cancer cells, and that the inhibition of these receptors by ryanodine protects the cells against apoptosis.

CONCLUSIONS. The combination of results showed that LNCaP cells, derived from a human prostate cancer, had functional RyRs able to mobilize Ca^{2+} from intracellular stores and which might control apoptosis. *Prostate 43:000–000, 2000.*

KEY WORDS: **intracellular calcium; ryanodine receptor; apoptosis; prostate**

INTRODUCTION

Ryanodine receptors are a family of intracellular Ca^{2+} channels playing important roles in cellular Ca^{2+} homeostasis. The ryanodine receptor (RyR) and the functional ryanodine-sensitive calcium pool were first described in skeletal and cardiac muscles [1,2], and for some time the expression of these Ca^{2+} channels was believed to be strictly muscle-specific, controlling the excitation-contraction coupling: RyR1 in skeletal and RyR2 in cardiac muscles [3,4]. Ryanodine receptors were then shown to be expressed in other types of excitable cells, including neurons [5,6], neuroendo-

Grant sponsor: INSERM; Grant sponsor: Association pour la Recherche Contre le Cancer, France; Grant sponsor: Ligue Nationale Contre le Cancer; Grant sponsor: Association pour la Recherche sur les Tumeurs de la Prostate; Grant sponsor: Fondation de la Recherche Medicale, France.

M.M.R. is presently at the Laboratory of Cell Pharmacology, Department of Molecular Cell Biology, KUL, Herestraat 49, B-3000 Leuven, Belgium.

P.M and N.P. contributed equally to this work

*Correspondence to: Roman Skryma, Laboratoire de Physiologie Cellulaire, INSERM EPI 9807, Bâtiment SN3, Université des Sciences et Technologies de Lille, 59655 Villeneuve d'Ascq, France.

E-mail: phycel@pop.univ-lille1.fr

Received 12 July 1999; Accepted 31 December 1999

crine cells [7,8], and smooth muscle [5,6]. To date, three members of this ryanodine receptor family have been identified (RyR1, RyR2 and RyR3), initially described in the skeletal muscle, the cardiac muscle, and the brain, respectively.

Ryanodine receptors were thought to be rather specific to excitable cells, where they represented the counterpart of IP3 receptors [9]. However, recent studies showed that some types of nonexcitable cells, where voltage-dependent Ca^{2+} channels are lacking, may also express ryanodine receptors [10]. The results concerning the expression and functional evidence of RyRs in nonexcitable cells are rather contradictory. In hepatocytes, for example, the effects of ryanodine on agonist-induced calcium signals have been demonstrated [11], but RyR mRNA expression has not been detected [5,12]. Larini et al. [13] suggested a ryanodine-like Ca^{2+} channel expression in nonexcitable cells; however, their Western blot analysis of total cell extracts failed to demonstrate the presence of an RYR-band in many cell types except for fibroblasts. A recent study [10] also showed that, while RyR mRNA was very occasionally present in a few nonexcitable cell types, the function of these receptors was not clear, as the agonists of RyRs, such as caffeine and ryanodine, were unable to release Ca^{2+}.

Furthermore, and more importantly, if some role has been ascribed to ryanodine receptors in excitable cells, e.g., its involvement in calcium-induced calcium release and excitation-contraction coupling [14], none has been demonstrated in nonexcitable cells and prostate cancer cells in particular. Nonetheless, different studies have shown that calcium is a major factor involved in apoptosis [15–17]. Therefore, the calcium regulatory mechanisms, such as IP3- or ryanodine-mediated calcium release, may play a substantial part in the regulation of apoptosis. Apoptosis is of prime importance for cancer cells and mostly for prostate cancer cells that proliferate very slowly. Calcium-stores depletion with thapsigargin induces apoptosis in many cell types, and among them, prostate cancer cells [18]. However, which of the intracellular calcium channels is implicated in apoptosis is still not known. Then, the identification of the existence of functional ryanodine receptors in prostate cancer cells would be of great consequence in an understanding of how apoptosis can be regulated.

In this work, using RT-PCR and Fura 2 fluorimetry and imaging, we show evidence of functional RyR in LNCaP prostate cancer cells. mRNAs of RyR1 and RyR2, but not RyR3, were identified in LNCaP cells. These cells do not possess the properties of excitable cells, as they do not express voltage-dependent inward currents, i.e., calcium and/or sodium currents [19]. However, in our experiments, LNCaP cells responded to several ryanodine receptor agonists: caffeine, 4 chloro-*m*-cresol, and ryanodine itself. Moreover, caffeine was able not only to mobilize calcium from a ryanodine-sensitive pool but also to promote calcium entry. We then show that apoptosis is enhanced by the activation of ryanodine receptors in prostate cancer cells and that inhibition of these receptors could protect the cancer cells against apoptosis.

MATERIALS AND METHODS

Chemicals

All chemicals were bought from Sigma Chemical Co. (St. Louis, MO) except for Fura 2/AM, ryanodine, and thapsigargin, which were purchased from Calbiochem France Biochem (Meudon, France).

Cell Culture

LNCaP prostate cancer cells were maintained in culture in RPMI-1640 medium supplemented with 10% fetal calf serum, penicillin (50 IU/ml), and streptomycin (50 μg/ml). Cells were grown in a humidified atmosphere containing 5% CO_2. Prior to fluorescence measurements, they were trypsinized and transferred to glass coverslips. They were used 1–4 days after trypsinization.

Calcium Measurements

The culture medium was replaced by an HBSS solution containing 142 mM NaCl, 5.6 mM KCl, 1 mM $MgCl_2$, 2 mM $CaCl_2$, 0.34 mM Na_2HPO_4, 0.44 mM KH_2PO_4, 10 mM HEPES, and 5.6 mM glucose. The osmolarity and pH of this solution were adjusted to 310 mOsm and 7.4, respectively. When a calcium-free medium was required, $CaCl_2$ was omitted and replaced by equimolar $MgCl_2$, and 0.1 mM EGTA was used to chelate calcium. Dye loading was achieved by transferring the cells into a standard HBSS solution containing 1 μM Fura 2/AM for 40 min at 37°C, and then rinsing them three times with the same dye-free solution. Intracellular calcium was measured by a photometric system (Photon Technology International, Monmouth Junction, NJ) or an imaging system (Quanticell 900, Applied Imaging, Sunderland, UK). In both cases, the glass coverslip was mounted in a chamber on a Nikon microscope equipped for fluorescence. Fura 2 fluorescence was excited at 340 nm and 380 nm, and the emitted fluorescence was measured above 510 nm using a long-pass filter. The $[Ca^{2+}]i$ was derived from the ratio of the fluorescence intensities for each of the excitation wavelengths (F340/F380), and from the equation of Grienkewicz et al. [20]. All

recordings were carried out at room temperature. The cells were continuously perfused with the HBSS solution, and chemicals were added via the perfusion system. Two different perfusion systems were used in these experiments: first, a local application system using a glass pipette placed nearby the recorded cell (about 100–200 μm); and second, a whole-chamber perfusion. Kinetics of the calcium changes could be affected by these differences, since a whole-chamber perfusion only gradually modifies the solution surrounding the recorded cells. The flow rate of the whole-chamber perfusion was set to 1 ml/min and the chamber volume was 500 μl. However, even with differences in kinetics, caffeine raised intracellular calcium to the same level using both procedures. Unless specified in the figure legends, traces shown in this article were recorded using whole-chamber perfusion.

As previously shown by Islam et al. [21], we observed that application of caffeine led to small parallel increases of fluorescence at both excitation wavelengths, 340 and 380 nm, giving sometimes a slight decrease of the fluorescence ratio F340/F380. This has been demonstrated to be due to interference of caffeine with Fura 2 [21]. However, these variations at both wavelengths were negligible and did not impede calcium measurements.

RNA Isolation and RT-PCR Analysis

Total RNA from LNCaP cells was isolated by the guanidium thiocyanate-phenol-chloroform extraction procedure [22]. Five micrograms of total RNA were reverse-transcribed into complementary DNA (cDNA) at 42°C, using random hexamer primers (Perkin Elmer, Foster City, CA) and MuLV reverse transcriptase (Perkin Elmer) in a final volume of 20 μl. Then, a 1-μl aliquot was used for the PCR reaction, with RyR primers based on the sequences of the human RyRs. For RyR mRNA detection by RT-PCR, three oligonucleotide primers were synthesized by aligning the previously published RyR1, RyR2, and RyR3 sequences [23–25]. To detect each isoform of RyR mRNA, a reverse primer (RyR1-, RyR2-, and RyR3-specific) (hRyRB) complementary to the common transmembrane domain coding region (5′-TACATCTTCCAGACATAAGA-3′) was combined with either an RyR2-RyR3-specific sense primer (hRyRF1) (5′-GTAACTCACAATGGCAAACAG-3′) or an RyR1-RyR3-specific primer (hRyRF2) (5′-TCAACTTCTTCCGCAAGTTCTACAA-3′) corresponding to the same transmembrane domains. The predicted sizes of the PCR-amplified products were 554 base pairs (bp) and 476 bp, using hRyRF1/hRyRB and hRyRF2/hRyRB, respectively. RNA samples were assayed for DNA contamination by PCR prior reverse transcription. Each sample was amplified by AmpliTaq Gold DNA Polymerase (Perkin Elmer) in an automated thermal cycler (Perkin Elmer GeneAmp PCR System 2400). DNA amplification conditions were the same for both pairs of primers and included an initial denaturation step of 10 min at 95°C (which, at the same time, activated the gold variant of the Taq Polymerase) and 40 cycles of 30 sec at 95°C, 30 sec at 56°C, and 30 sec at 72°C. The RT-PCR samples were electrophoresed on a 2% agarose gel and stained with ethidium bromide (0.5 μg/ml). One microgram of 1 kb Plus DNA ladder (Life Technologies, Merelbeke, Belgium) was also run on agarose gel as a DNA size marker.

Restriction Enzyme Analysis of RT-PCR Products

In order to study the isoform expression of RyRs in LNCaP cells, the RT-PCR products were subjected to restriction enzyme analysis. PCR products precipitated by ethanol, suspended in water, and aliquots were digested by *Hae*III, *Bgl*II, or *Sac*I (Boehringer Mannheim, Brussels, Belgium). For hRyRF1/hRyRB-amplified PCR product, *Hae*III was expected to cut RyR1 (if amplified) into 225-, 168-, 85-, and 38-bp fragments, RyR2 into 301- and 253-bp fragments, and RyR3 into 255-, 253-, and 46-bp fragments. *Sac*I was expected to cut RyR1 only (if amplified), to produce fragments of approximately 295, 213, and 96 bp. *Bgl*II was expected to cut RyR2 only, producing 312- and 242-bp fragments. For RT-PCR products obtained using hRyRF2/hRyRB primers, *Sac*I was expected to cut RyR1 only, producing fragments of 167, 213 and 96 bp. *Bgl*II was expected to cut RyR2 only, into 312- and 164-bp fragments. Digested products were analyzed by electrophoresis on ethidium bromide-stained 2% agarose gel, and 1 kb Plus DNA ladder (Life Technologies, Merelbeke, Belgium) was used as the DNA size marker.

Apoptosis Assay

Cells were fixed in cold methanol (−20°C) for 10 min and washed twice with PBS before staining with 4 μg/ml Hoechst 33258 for 30 min at room temperature in the dark. Cells were then washed with PBS and mounted with coverslips, using glycergel. Apoptotic cells exhibiting condensed and fragmented nuclei were counted under an Olympus-BH2 fluorescent microscope. A minimum of 500–1,000 adherent cells was examined for each case, and the results were expressed as the number of apoptotic cells over the total number of cells counted.

Data Analysis

Results were expressed as mean ± SEM. Plots were produced using Origin 5.0 (Microcal Software, Inc., Northampton, MA).

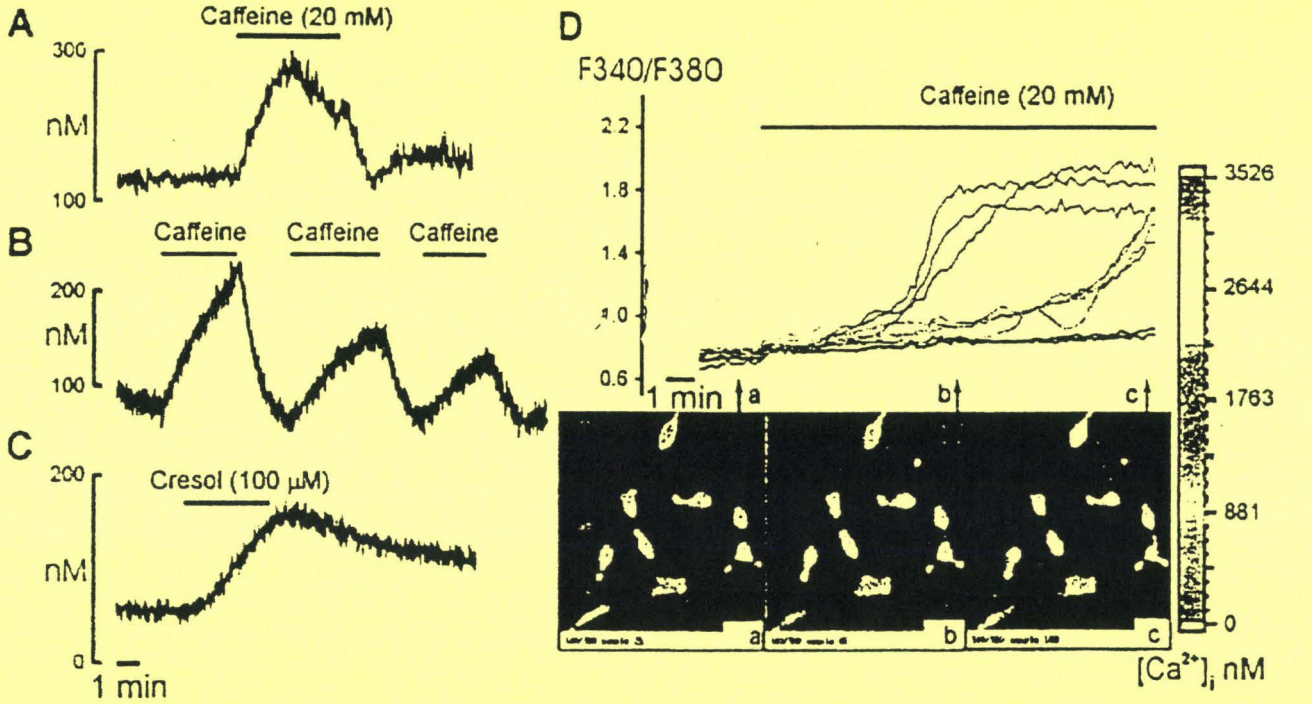

Fig. 1. Fluorescence measurements indicate that ryanodine receptor agonists increase $[Ca^{2+}]i$ in LNCaP cells. Microfluorimetric measurements of calcium $Ca^{2+}i$ (**A–C**) and calcium imaging (**D**) show that the activation of ryanodine receptor pools using 20 mM caffeine (**A, B, D**) or 100 µM 4-chloro-*m*-cresol (cresol, in **C**) induces a calcium increase.

RESULTS

When LNCaP cells were bathed in a solution containing 2 mM $CaCl_2$, their intracellular calcium was about 76 ± 6 nM (n = 91) and remained stable during the recording (15–60 min). In order to investigate the existence of a ryanodine-sensitive store in LNCaP cells, we first studied how caffeine affected the cytosolic calcium concentration. Figure 1A shows that caffeine induced a rise in $[Ca^{2+}]i$ when applied at 20 mM. Most cells tested (87%, n = 54) responded in a similar pattern. The calcium increased from 87 ± 6 nM to 406 ± 79 nM. This increase could be reproduced several times on the same cell, with a slight decrease in the calcium peak in most cases (Fig. 1B). A similar calcium rise could be mimicked by 100 µM 4-chloro-*m*-cresol (n = 7, Fig. 1C), a potent ryanodine receptor activator [26]. Fura 2 imaging confirmed the increase in intracellular calcium after application of caffeine (Fig. 1D). Calcium imaging showed that the calcium increase kinetics differed from one cell to another, with some cells responding earlier than the others (e.g., the three cells left of b, in Fig. 1D).

We assessed the target of caffeine by pretreating LNCaP cells with ryanodine, which blocks calcium release from ryanodine-sensitive stores when used at high concentrations [27,28]. When ryanodine (10 µM)

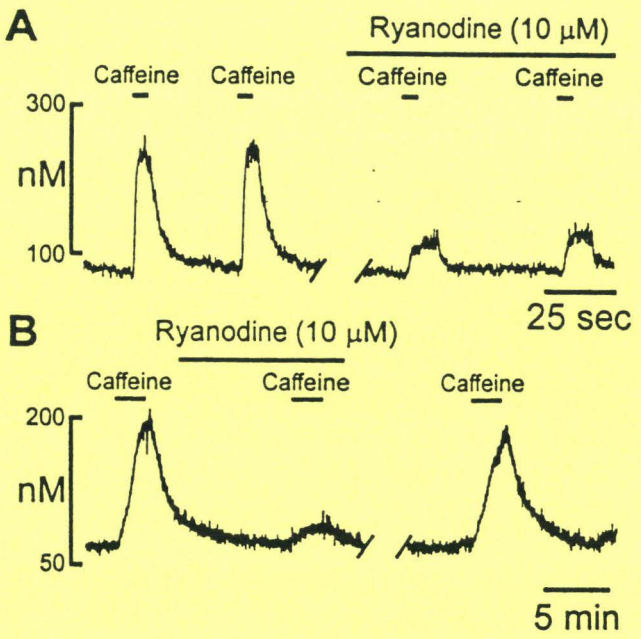

Fig. 2. Caffeine-induced $[Ca^{2+}]i$ increase is inhibited by ryanodine. **A:** Inhibition of caffeine-induced calcium increase by ryanodine (10 µM). Solutions are applied in this experiment usung a local application pipette. **B:** Effect of caffeine recovered following the removal of ryanodine. Recordings were interrupted for 3 min in both A and B.

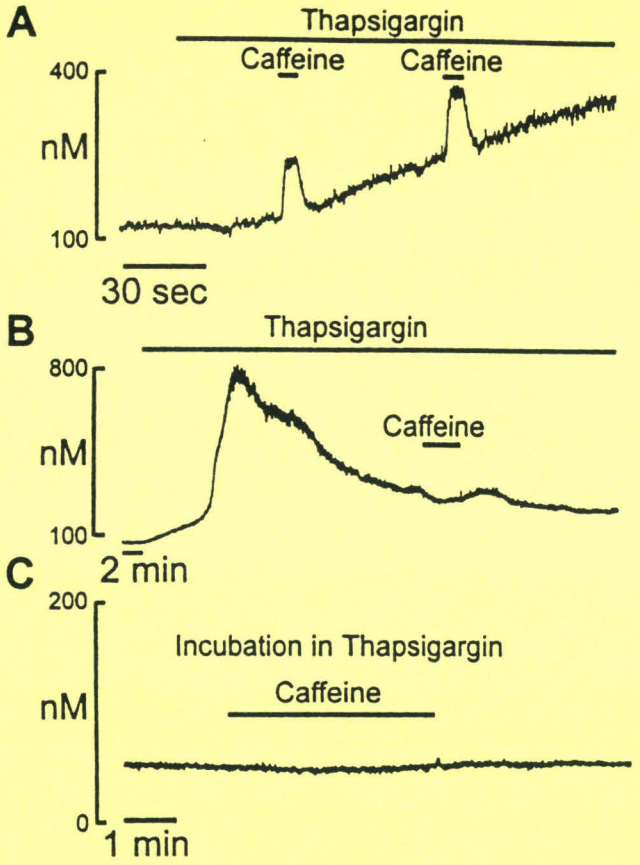

Fig. 3. Caffeine-induced $[Ca^{2+}]i$ increase is gradually abolished by thapsigargin, an inhybitor of endoplasmic reticulum ATPases. Thapsigargin (0.1 μM) induced an increase in $[Ca^{2+}]i$, followed by a gradual return to initial values. Thapsigargin was perfused for different lengths of time before caffeine was applied. Caffeine was applied (**A**) during the calcium increase induced by thapsigargin, (**B**) during the recovery phase, or (**C**) after a complete return to the basal calcium level. In A, solutions were applied with a local application pipette.

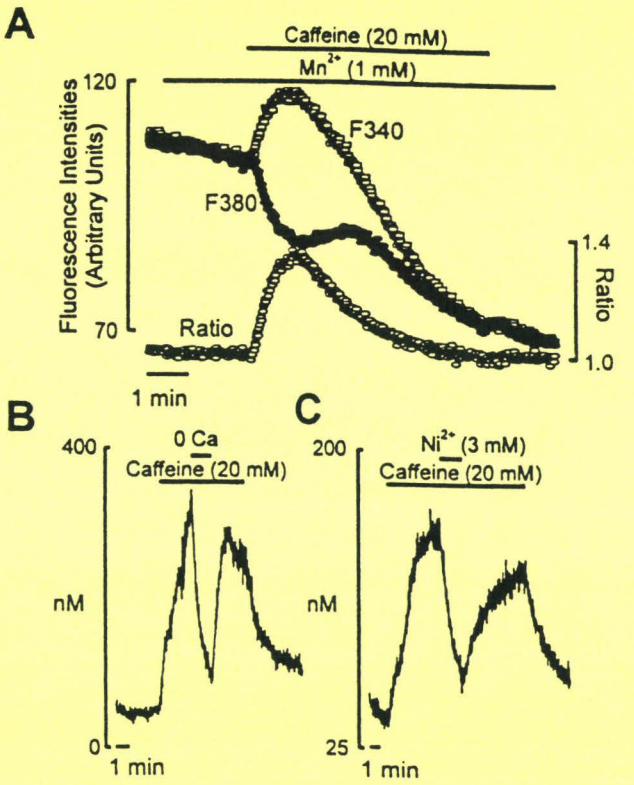

Fig. 4. Caffeine-induced $[Ca^{2+}]i$ increase occurs via a calcium mobilization and a calcium entry. **A:** Manganese quenching experiments under calcium-free conditions showed that caffeine first induced an increase in Fura 2 fluorescence at 340 nm and a decrease at 380 nm, thus indicating a calcium mobilization from internal stores. A rapid decrease in Fura 2 fluorescence was then observed at both wavelengths, showing a quenching of the Fura 2 fluorescence by manganese and indicating manganese entry into the cell. **B:** The calcium rise induced by caffeine was counteracted by an application of calcium-free medium, or (**C**) by 3 mM $NiCl_2$.

was applied before caffeine, the response to caffeine was almost completely abolished (n = 15, Fig. 2A,B). The inhibitory effect of ryanodine was reversible and the response to caffeine recovered (n = 3, Fig. 2B) after 5-min washing in a ryanodine-free medium, indicating that caffeine response was mediated by ryanodine-sensitive receptors.

We used thapsigargin (0.1 μM), a Ca^{2+} ATPase blocker [29], to check whether caffeine mobilized Ca^{2+} ions from intracellular stores. Emptying intracellular calcium stores led to a gradual inhibition of the response to caffeine, indicating a calcium mobilization from internal stores (n = 45). The application of thapsigargin induced a calcium increase up to 800 ± 20 nM, followed by a slow recovery (Fig. 3). Caffeine was still able to induce a rise in $[Ca^{2+}]i$ when applied during the increase in intracellular calcium due to thapsigargin (Fig. 3A). This effect no longer occurred when caffeine was perfused after the calcium peak (Fig. 3B). If thapsigargin was allowed to perfuse the cells long enough, i.e., more than 15 min, the cytosolic calcium concentration eventually returned to resting values, but caffeine was still unable to produce a calcium rise (Fig. 3C).

A calcium-free medium containing 1 mM $MnCl_2$ was used to further determine the origin of the calcium. Under these conditions, a calcium mobilization from internal stores should induce opposite variations on the two wavelengths: an increase in fluorescence intensity at 340 nm and a decrease at 380 nm. On the contrary, if caffeine led to calcium entry, these experimental conditions should produce a manganese entry and the quenching of Fura 2 fluorescence [30]. We observed that caffeine first induced a calcium increase, with opposite variations on the two wavelengths (Fig. 4A). This shows that in the absence of extracellular calcium, caffeine is able to produce a calcium mobilization from internal stores. After this initial phase, a rapid decrease in fluorescence intensity was observed

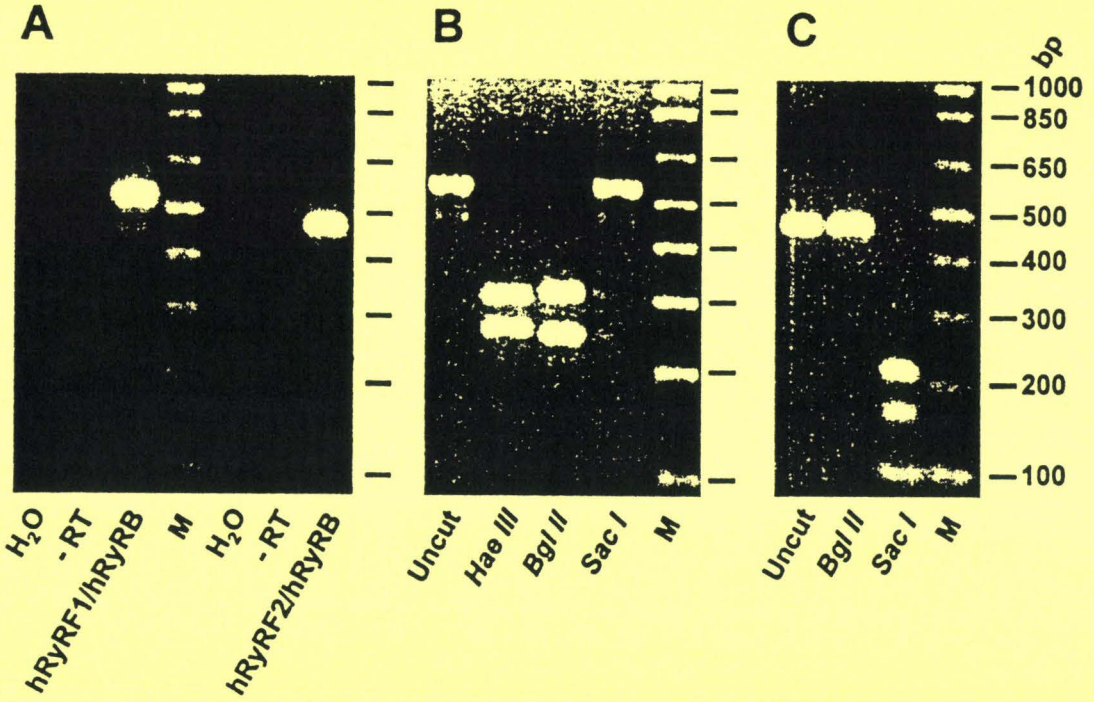

Fig. 5. Expression of RyRs in LNCaP cells. **A:** RT-PCR detection of RyRs in LNCaP cells. RT-PCR was performed with either of the following pairs of primers: hRyRF1/hRyRB or hRyRF2/hRyRB. PCR products of either 554 bp or 476 bp were detected in LNCaP cDNA but not in control reactions containing H_2O (**lane H_2O**) or LNCaP RNA without reverse transcription (**lane −RT**). **B:** Restriction enzyme digest of RyR RT-PCR products obtained using hRyRF1/hRyRB. **C:** Restriction enzyme digest of RyR RT-PCR products obtained using hRyRF2/hRyRB. **Lane M**, size markers.

at both wavelengths, indicating a quenching of Fura 2 fluorescence by manganese entering through plasma membrane channels. This indicated that caffeine was capable of increasing intracellular calcium concentrations via two pathways: calcium mobilization from internal stores, followed by calcium entry. This calcium entry was confirmed by applying a calcium-free medium during the response to caffeine (Fig. 4B). This led to a decrease in $[Ca^{2+}]i$ down to resting levels. Perfusion of $NiCl_2$ (3 mM), shown to inhibit capacitive calcium entry [31], produced a similar effect (Fig. 4C).

We used an RT-PCR assay to study RyR mRNA expression in LNCaP cells. By aligning the previously published RyR sequences, we designed primers to amplify either RyR2 and RyR3 (hRyRF1/hRyRB) or RyR1 and RyR3 (hRyRF2/hRyRB). The pairs of primers generated fragments of the expected sizes of 554 and 476 bp, respectively (Fig. 5A). To determine the isoforms expressed, we performed restriction digests on these PCR products, using specific enzymes for each isoform. The hRyRF1/hRyRB PCR product was completely cut by *Bgl*II (RyR2-specific), giving fragments of 312 and 242 bp, and also by *Hae*III, generating fragments of 301 and 253 bp, corresponding to the restriction profile of RyR2 (Fig. 5B). These observations show the expression of RyR2 but not RyR3 mRNA in LNCaP cells. In order to study the expression of RyR1 mRNA in these cells, we studied the enzyme restriction of the hRyRF2/hRyRB PCR product (amplifying RyR1 and RyR3). The PCR product was completely cut by *Sac*I (RyR1-specific) into 167-, 213-, and 96-bp products (Fig. 5C), showing that RyR1 mRNA was also expressed in these cells. Taken together, these results showed the expression of mRNAs of RyR1 and RyR2, but not RyR3, isoforms in LNCaP cells.

To study the physiological role of RyRs in LNCaP cells, we next assessed the effects of ryanodine receptor activation on apoptosis. Cells were treated with 5 mM caffeine for 48 hr in the presence or absence of 15 μM ryanodine. Figure 6 demonstrates that both untreated and ryanodine-treated cells exhibited a very low apoptotic index (less than 0.1%). By contrast, when the cells were treated with caffeine, about 3.5% of adherent cells were induced into apoptosis. Ryanodine partially inhibited the caffeine-induced apoptosis. These observations suggest that ryanodine-sensitive calcium stores mediate the induction of apoptosis by caffeine.

DISCUSSION

We conclude from these findings that LNCaP prostate cells express functional ryanodine receptors. We showed that caffeine was able to release calcium from

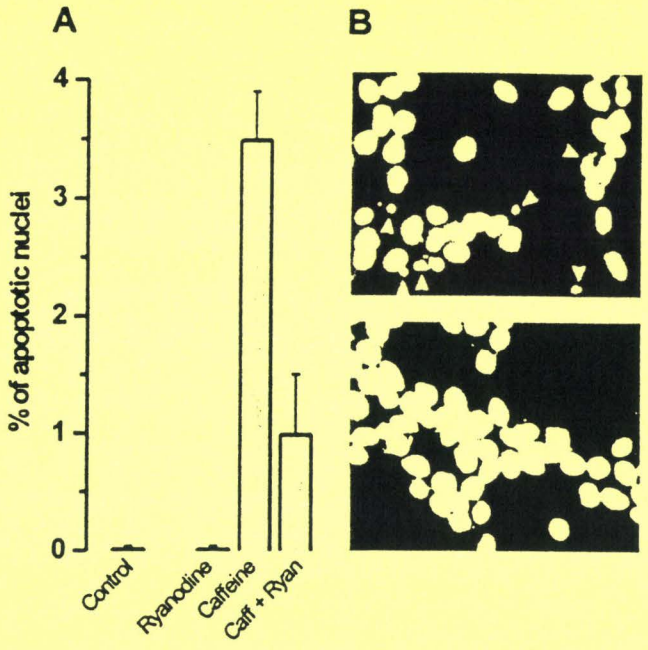

Fig. 6. Effect of ryanodine on induction of apoptosis by caffeine. Cells were seeded in RPMI-1640 medium containing 10% fetal calf serum. Two days later, cells were treated with 5 mM caffeine in the presence or absence of 15 μM ryanodine for 48 hr. Apoptosis was determined as described in Materials and Methods. Shown here are results of a triplicate assay in one experiment, which is representative of two independent experiments. **A:** Histogram showing percent of apoptotic cells in the presence or absence of caffeine and ryanodine. **B:** Fluorescence photographs of cells in the presence of caffeine (**top**), and in the presence of caffeine and ryanodine (**bottom**). Arrowheads indicate apoptotic nuclei.

ryanodine-sensitive intracellular stores in LNCaP cells. Caffeine has also been shown to elevate intracellular calcium in many cell types by other means such as inhibition of K_{ATP} channels, leading to a depolarization and then a calcium influx, or by increasing cAMP through its action on phosphodiesterase or by stimulating a ryanodine receptor-independent calcium influx [21,32]. We show here that the action of caffeine occurs through ryanodine receptors, since a similar calcium rise was reproduced using 4 chloro-*m*-cresol, another ryanodine receptor agonist [26]. Furthermore, this effect was inhibited by ryanodine, an inhibitor of calcium-induced calcium release. In addition, unlike in systems where caffeine produces a calcium entry [21], thapsigargin, a calcium ATPase inhibitor which depletes intracellular calcium stores [29], completely inhibited the calcium rise induced by caffeine in our experiments. Also, in the absence of external calcium (quench experiment, Fig. 4A), caffeine still produced antiparallel variations of the Fura 2 fluorescence, indicating that there is not a strict requirement for extracellular calcium for the initial cytosolic calcium increase. We thus conclude that LNCaP cells, which are nonexcitable, possess intracellular ryanodine-sensitive calcium stores, and that caffeine is able to mobilize these calcium stores.

A recent study showed that ryanodine receptor mRNA could be detected in only 2 of 12 different nonexcitable cell types [10]. However, the function of RyRs in these cells could not be determined, as they did not respond to caffeine. The fact that the response to an IP3 agonist was attenuated by ryanodine led the authors to suggest that stimulation of ryanodine receptors would promote an amplification of the 1,4,5-IP3-induced calcium release. As nonexcitable cells where ryanodine receptors are expressed are usually nonresponsive to caffeine, LNCaP cells appear to be an original cell model. Using an RT-PCR assay, we showed that RyR1 and RyR2 mRNAs were expressed in LNCaP cells. This is rather surprising as, in the few nonexcitable models where RyRs have been detected by RT-PCR, only RyR3 and RyR2 have been identified in epithelial gut cells [33], T lymphocytes [34], HeLa cervix carcinoma [10], and epithelial kidney cells [35]. To our knowledge, the only nonexcitable cells where RyR1 has been shown to be expressed are parotid cells [36].

In excitable cells, besides the well-known role of RyRs in excitation-contraction coupling in muscles [37–39], other functions have been suggested for these receptors, including an involvement in synaptic plasticity [40], as well as regulation of cell proliferation [34]. When present in nonexcitable cells, the function of ryanodine receptors is not clear, as opposed to excitable cells, where they are closely linked to dihydropyridine receptors and respond to plasma membrane depolarization [37] or calcium entry during depolarization [38] by releasing intraluminal calcium into the cytosol. It is nonetheless possible that ryanodine receptors are also implicated in calcium-induced calcium release in nonexcitable cells through a coupling to voltage-independent or ligand-gated Ca^{2+} channels.

In order to define the role of ryanodine receptors in calcium homeostasis in prostate cancer cells, we investigated the relationship between ryanodine receptor activation and another source of calcium, calcium entry through plasma membrane channels. We show here that ryanodine receptor activation by caffeine is closely associated with calcium influx. As there are no voltage-dependent calcium channels in these cells [19], this may be due to a capacitive calcium entry, a "calcium-refilling mechanism" induced by the depletion of calcium stores [41]. This type of calcium entry was first described in mast cells [42] and then in various cell models. It is now considered a typical response of nonexcitable cells to the agents that stimulate the phospholipase C/IP3 pathway, mobilizing Ca^{2+} from internal stores [41]. Capacitive calcium en-

try has also been described in excitable cells [43,44] and has been reported to be activated following ryanodine receptor activation in PC12 cells [45] and muscle cells [46,47]. In our experiments, the calcium influx was able to permeate manganese and was inhibited by nickel (one of the most potent capacitive calcium entry inhibitors) [31]. Our results show that calcium entry, and thus refilling of internal calcium stores, was promoted by the activation of ryanodine-sensitive calcium stores in nonexcitable prostate cancer cells.

We then investigated the role of ryanodine receptors in apoptosis. Calcium has been shown to be involved in apoptosis [15–17], but it is not clear which of the calcium levels in the cytosol and the filling state of the intracellular stores is the important factor implicated. In hormone-independent prostate cancer cells, thapsigargin stimulates apoptosis by a Ca^{2+} mobilization from intracellular pools and a following sustained Ca^{2+} entry [18]. We have also observed in hormone-dependent prostate cancer cells that apoptosis can be triggered by thapsigargin but independently of the capacitative calcium entry (R. Skryma, unpublished findings). We have shown in our experiments that activation of RyRs with caffeine slightly stimulated apoptosis and that this effect was inhibited by ryanodine. By this way, RyRs could modulate apoptosis in prostate cancer cells by regulating the calcium levels in the cytosol or in intracellular stores. In nonexcitable cells, and in cancer cells in particular, growth factors and hormones trigger Ca^{2+} entry through voltage-independent Ca^{2+} channels stimulated by tyrosine or serine/threonine kinase phosphorylation, or stimulate calcium release from IP3-sensitive stores [9,48,49]. This calcium entry or release could in turn activate RyRs by a CICR mechanism and by this way induce apoptosis. The connection between ryanodine-sensitive stores and apoptosis has not yet been demonstrated. If some reports show that caffeine can enhance the cytotoxicity of other drugs, its action was not shown to be dependent on ryanodine receptors [50,51]. On the contrary, the role of IP3 receptors in apoptosis has been better documented [52], and it has been demonstrated that T cells devoid of type 1 IP3 receptors are resistant to the apoptosis induced by various treatments [53]. We show in our experiments that the stimulation of apoptosis by caffeine is relatively low (3.5% of apoptotic cells with caffeine vs. 0.1% in the absence of caffeine). However, one might expect this effect to be large enough to lead to a reduction in cell growth rate. In addition, it must be pointed out that the amount of apoptosis due to caffeine treatment is similar to the percentage of cell death observed in some studies, where cell death was induced by androgen depletion in human prostate cancer cells [54]. We therefore suggest that activation of the other major intracellular calcium receptor, the ryanodine receptor, can also regulate apoptosis in prostate cancer cells.

These results could be of fundamental importance, since the development of prostate tumors can be slowed by inducing apoptosis. Apoptosis may be induced in prostate cells by androgen depletion [55], which is a commonly used therapy. It remains to be determined at that stage if androgen depletion-induced apoptosis involves changes in calcium homeostasis. Furthermore, since the development of prostate cancer is always accompanied in the later stages by the loss of androgen ablation sensitivity due to the presence of androgen-independent cells in the prostate tumor [56], an important issue would be to characterize regulatory mechanisms of ryanodine receptors, and their role in the activation of apoptosis in such androgen-independent cells.

ACKNOWLEDGMENTS

We are grateful to Prof. Carl Denef for allowing us to perform part of the experiments in his Laboratory of Cell Pharmacology, Department of Molecular Cell Biology (Leuven, Belgium). We are grateful to I. Servant for excellent technical assistance.

REFERENCES

1. Imagawa T, Nakai J, Takeshima H, Nakasaki Y, Shigekawa M. Purified ryanodine receptor from muscle sarcoplasmic reticulum is the Ca^{2+}-permeable pore of the calcium release channel. J Biol Chem 1987;262:16636–16643.
2. Lai F, Anderson K, Rousseau E, Liu Q, Meissner G. Purification and reconstitution of the calcium release channel from skeletal muscle. Nature 1988;331:315–319.
3. Otsu K, Willard HF, Khanna VK, Zorzat F, Green NM, MacLennan DH. Molecular cloning of cDNA encoding the Ca^{2+} release channel (ryanodine receptor) of rabbit cardiac muscle sarcoplasmic reticulum. J Biol Chem 1990;265:13472–13483.
4. Marks AR, Tempst P, Hwang KS, Taubman MB, Inui M, Chadwick C, Fleischer S, Nadal-Ginard B. Molecular cloning and characterization of the ryanodine receptor junctional channel complex cDNA from skeletal muscle sarcoplasmic reticulum. Proc Natl Acad Sci USA 1989;86:8683–8687.
5. Giannini G, Conti A, Mammarella S, Scrobogna M, Sorrentino V. The ryanodine receptor/calcium channel genes are widely and differentially expressed in murine brain and peripheral tissues. J Cell Biol 1995;128:893–904.
6. Hakamata Y, Nakai J, Takeshima H, Imoto K. Primary structure and distribution of a novel ryanodine receptor/calcium release channel from rabbit brain. FEBS Lett 1992;312:229–235.
7. Islam MS, Rorsman P, Berggren PO. Ca^{2+}-induced Ca^{2+} release in insulin-secreting cells. FEBS Lett 1992;296:287–291.
8. Clementi E, Riccio M, Sciorati C, Nistico G, Meldolesi J. The type 2 ryanodine receptor of neurosecretory PC 12 cells is activated by cyclic ADP-ribose. Role of the nitric oxide/cGMP pathway. J Biol Chem 1996;271:17739–17745.

9. Clapham DE. Calcium signalling. Cell 1995;80:259–268.
10. Bennett DL, Cheek TR, Berridge MJ, De Smedt H, Parys JB, Missiaen L, Bootman MD. Expression and function of ryanodine receptors in nonexcitable cells. J Biol Chem 1996;271:6356–6362.
11. Sanchez-Bueno A, Cobbold PH. Agonist-specifity in the role of Ca^{2+}-induced Ca^{2+} release in hepatocyte Ca^{2+} oscillations. Biochem J 1993;291:169–172.
12. Shoshan-Barmatz V, Pressley TA, Higham S, Kraus-Friedmann N. Characterization of high-affinity ryanodine-binding sites of rat liver endoplasmic reticulum. Differences between liver and skeletal muscle. Biochem J 1991;15:41–46.
13. Larini F, Menegazzi P, Baricordi O, Zorzato F, Treves S. A ryanodine receptor-like Ca^{2+} channel is expressed in nonexcitable cells. Mol Pharmacol 1995;47:21–28.
14. Coronado R, Morrissette J, Sukhareva M, Vaughan DM. Structure and function of ryanodine receptors. Am J Physiol 1994; 266:1485–1504.
15. Berridge MJ. Calcium signalling and cell proliferation. Bioessays 1995;17:491–500.
16. McConkey DJ, Orrenius S. The role of calcium in the regulation of apoptosis. Biochem Biophys Res Commun 1997;239:357–366.
17. Berridge MJ, Bootman MD, Lipp P. Calcium—a life and death signal. Nature 1998;395:645–648.
18. Furuya Y, Lundmo P, Short AD, Gill DL, Isaacs JT. The role of calcium, pH, and cell proliferation in the programmed (apoptotic) death of androgen-independent prostatic cance cells induced by thapsigargin. Cancer Res 1994;54:6167–6175.
19. Skryma R, Prevarskaya N, Dufy-Barbe L, Odessa MF, Audin J, Dufy B. Potassium conductance in the androgen-sensitive prostate cancer cell line, LNCaP: involvement in cell proliferation. Prostate 1997;33:112–122.
20. Grynkiewicz G, Poenie M, Tsien RY. A new generation of Ca^{2+} indicators with greatly improved fluorescence properties. J Biol Chem 1985;260:3440–3450.
21. Islam MS, Larsson O, Nilsson T, Berggren PO. Effects of caffeine in cytoplasmic free Ca^{2+} concentration in pancreatic beta-cells are mediated by interaction with ATP-sensitive K^+ channels and L-type voltage-gated Ca^{2+} channels but not the ryanodine receptor. Biochem J 1995;306:679–686.
22. Chomczynski P, Sacchi N. Single-step methode of RNA isolation by acid guanidium thiocyanate-phenol-chloroform extraction. Anal Biochem 1987;162:156–159.
23. Zorzato F, Fujii J, Otsu K, Phillips M, Green NM, Lai FA, Meissner G, MacLennan DH. Molecular cloning of cDNA encoding human and rabbit forms of the Ca^{2+} release channel (ryanodine receptor) of skeletal muscle sarcoplasmic reticulum. J Biol Chem 1990;265:2244–2256.
24. Tunwell RE, Wickenden C, Bertrand BM, Shevchenko VI, Walsh MB, Allen PD, Lai FA. The human cardiac muscle ryanodine receptor-calcium release channel : identification, primary structure and topological analysis. Biochem J 1996;318:477–487.
25. Leeb T, Brenig B. cDNA cloning and sequencing of the human ryanodine receptor type 3 (RyR3) reveals a novel alternative splice site in the RyR3 gene. FEBS Lett 1998;423:367–370.
26. Hermann-Franck A, Richter R, Sarkozi S, Mohr U, Lehmann-Horn F. 4-chloro-m-cresol, a potent and specific activator of the skeletal muscle ryanodine receptor. Biochim Biophys Acta 1996; 1289:31–40.
27. McPherson PS, Campbell KP: The ryanodine receptor/Ca^{2+} release channel. J Biol Chem 1993;268:13765–13768.
28. Fleischer S, Inui M. Biochemistry and biophysics of excitation-contraction coupling. Annu Rev Biophys Chem 1989;18:333–364.
29. Lytton J, Westlin M, Hanley MR. Thapsigargin inhibits the sarcoplasmic or endoplasmic reticulum Ca-ATPase family of calcium pumps. J Biol Chem 1991;266:17067–17071.
30. Merritt JE, Jacob R, Hallam TJ. Use of manganese to discriminate between calcium influx and mobilization from internal stores in stimulated human neutrophils. J Biol Chem 1989;264: 1522–1527.
31. Schlegel W, Mollard P, Demaurex N, Theler JM, Chiavaroli C, Guerineau N, Vacher P, Mayr G, Krause KH, Wollheim CB. Calcium signalling: comparison of the role of Ca2+ influx in excitable endocrine and non-excitable myeloid cells. Adv Second Messenger Phosphoprotein Res 1993;28:143–152.
32. Ufret-Vincenty CA, Short AD, Alfonso A, Gill DL. A novel Ca^{2+} entry mechanism is turned on during growth arrest induced by Ca^{2+} pool depletion. J Biol Chem 1995;270:26790–26793.
33. Verma V, Carter C, Keable S, Bennett D, Thorn P. Identification and function of type-2 and type-3 ryanodine receptors in gut epithelial cells. Biochem J 1996;319:449–454.
34. Hakamata Y, Nishimura S, Nakai J, Nakashima Y, Kita T, Imoto K. Involvement of the brain type of ryanodine receptor in T-cell proliferation. FEBS Lett 1994;352:206–210.
35. Tunwell REA, Lai FA. Ryanodine receptor expression in the kidney and a non-excitable kidney epithelial cell. J Biol Chem 1996;271:29583–29588.
36. Zhang X, Wen J, Bidasce KR, Besch R Jr, Rubin RP. Ryanodine receptor expression is associated with intracellular Ca^{2+} release in rat parotid acinar cells. Am J Physiol 1997;273:1306–1314.
37. Numa S, Tanabe T, Takeshima H, Mikami A, Niidome T, Nishimura S, Adams BA, Beam KG. Molecular insights into excitation-contraction coupling. Cold Spring Harbor Symp Quant Biol 1990;5:1–7.
38. Stern MD. Theory of excitation-contraction coupling in cardiac muscle. Biophys J 1992;63:497–517.
39. Cheng H, Lederer MR, Xiao RP, Gomez AM, Zhou YY, Ziman B, Spurgeon H, Lakatta EG, Lederer WJ. Excitation-contraction coupling in heart: new insights from Ca^{2+} sparks. Cell Calcium 1996;20:129–140.
40. Chavis P, Fagni L, Lansman JB, Bockaert J. Functional coupling between ryanodine receptors and L-type calcium channels in neurons. Nature 1996;382:719–722.
41. Berridge MJ. Capacitative calcium entry. Biochem J 1995;312:1–11.
42. Hoth M, Penner R. Depletion of intracellular calcium stores activates a calcium current in mast cells. Nature 1992;355:353–356.
43. Miura Y, Henquin JC, Gilon P. Emptying of intracellular Ca^{2+} stores stimulates Ca^{2+} entry in mouse pancreatic beta-cells by both direct and indirect mechanisms. J Physiol 1997;503:387–398.
44. Villalobos C, Garcia-Sancho J. Capacitative Ca^{2+} entry contributes to the Ca^{2+} influx induced by thyrotropin-releasing hormone (TRH) in GH3 pituitary cells. Pflugers Arch 1995;430:923–935.
45. Bennett DL, Bootman MD, Berridge MJ, Cheek TR. Ca^{2+} entry into PC 12 cells initiated by ryanodine receptors or inositol 1,4,5-trisphosphate receptors. Biochem J 1998;329:349–357.
46. Wayman CP, Gibson A, McFadzean I. Depletion of either ryanodine- or IP3-sensitive calcium stores activates capacitative calcium entry in mouse anococcygeus smooth muscle cells. Pflugers Arch 1998;435:231–239.
47. Noguera MA, Madrero Y, Ivorra MD, D'Ocon. Characterization of two different Ca^{2+} entry pathways dependent on depletion of internal Ca^{2+} pools in rat aorta. Naunyn Schmiedebergs Arch Pharmacol 1998;357:92–99.
48. Peppelenbosch MP, Tertoolen LJ, den Hertog J, de Laat SW. Epidermal growth factor activates calcium channels by phospholipase A2/5-lipoxygenase-mediated leukotriene C4 production. Cell 1992;69:295–303.

49. Lovisolo D, Distasi C, Antoniotti S, Munaron L. Mitogens and calcium channels. News Physiol Sci 1997;12:279–285.
50. Takahashi M, Yamamoto Y, Hatori S, Shiozawa M, Suzuki M, Rino Y, Amano T, Imada T. Enhancement of CDDP cytotoxicity by caffeine is characterized by apoptotic cell death. Oncogene Rep 1998;5:53–56.
51. Janss AJ, Levow C, Bernhard EJ, Muschel RJ, McKenna WG, Sutton L, Phillips PC. Caffeine and staurosporine enhance the cytotoxicity of cisplatin and camptothecin in human brain tumor cell lines. Exp Cell Res 1998;25:29–38.
52. Marks AR. Intracellular calcium-release channels: regulators of cell life and death. Am J Physiol 1997;272:597–605.
53. Jayaraman T, Marks AR. T cells deficient in inositol 1,4,5-trisphosphate receptor are resistant to apoptosis. Mol Cell Biol 1997;17:3005–3012.
54. Kyprianou N, English HF, Isaacs JT. Programmed cell death during regression of PC-82 human prostate cancer following androgen ablation. Cancer Res 1990;50:3748–3753.
55. Kyprianou N, Isaacs JT. Activation of programmed cell death in the rat ventral prostate after castration. Endocrinology 1988;122: 552–562.
56. Crawford ED, Eisenberg MA, McLeod DC, Spaulding J, Benson R, Dorr FA, Blumenstein BA, Davis MA, Goodman PJ. A controlled trial of leuprolide with and without flutamide in protastic carcinoma. N Engl J Med 1989;321:419–424.

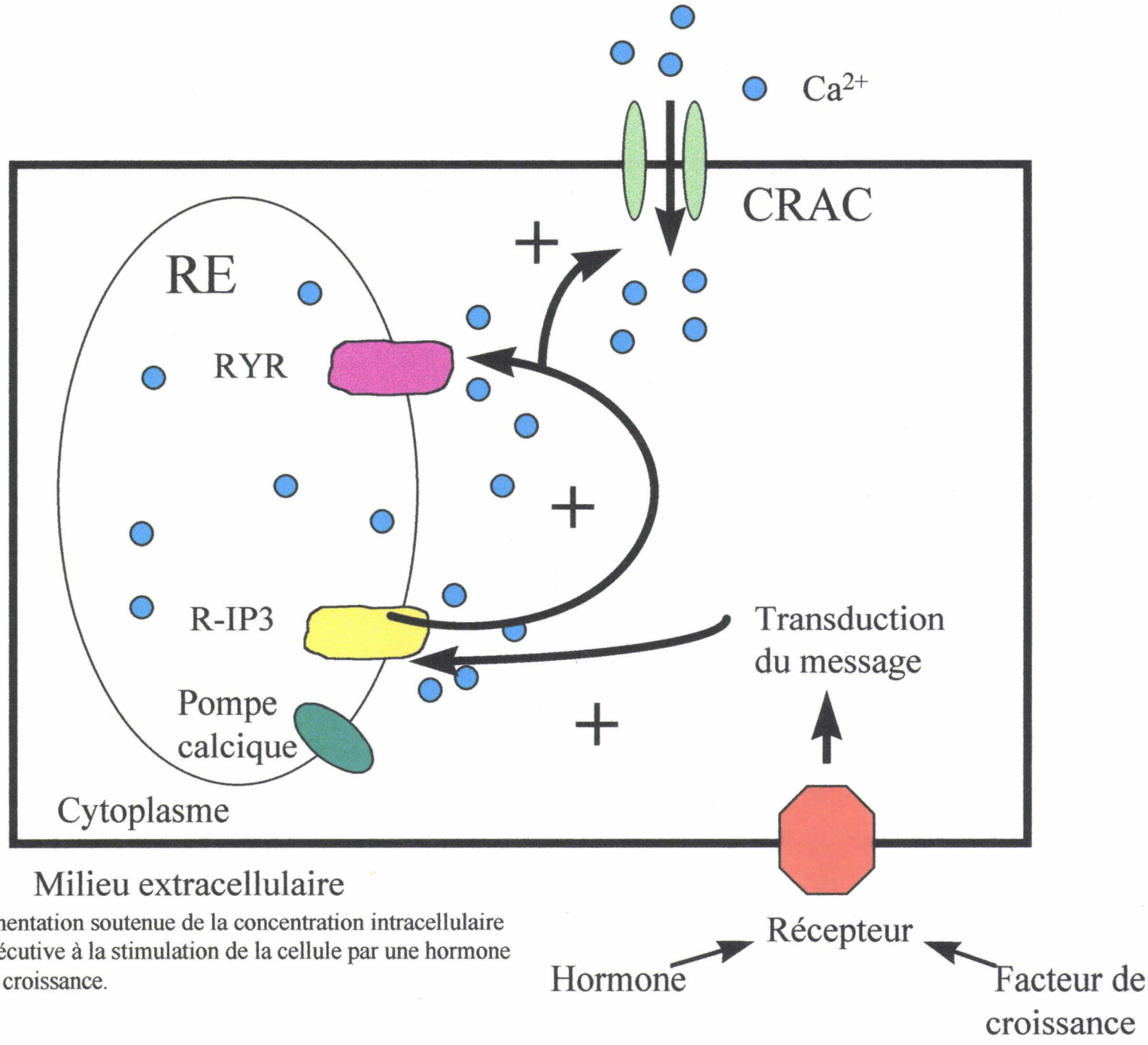

Figure 25: Augmentation soutenue de la concentration intracellulaire en calcium consécutive à la stimulation de la cellule par une hormone ou un facteur de croissance.

des cellules tumorales en induisant l'apoptose via les récepteurs à la ryanodine comme nous l'avons réalisé sur les cellules LNCaP.

2.2.2- Implication des récepteurs à la ryanodine dans la déplétion des stocks calciques induite par la ryanodine

Lors des études précédentes, nous avons démontré que la thapsigargine est capable d'induire l'apoptose des cellules LNCaP. De même, nous avons démontré que les récepteurs à la ryanodine sont impliqués dans l'apoptose.

Au cours de cette étude, nous avons étudié les relations existant entre l'action de la thapsigargine et les récepteurs à la ryanodine afin de mieux appréhender les mécanismes calciques fins qui régissent l'apoptose des cellules cancéreuses prostatiques. Ces travaux sont actuellement soumis au journal "Febs Letters".

CONCLUSION

Cette étude indique, pour la première fois, que les récepteurs à la ryanodine sont activés par la fuite de calcium induite par la thapsigargine. Cette molécule provoque une fuite passive de calcium. Ce flux va, par la suite stimuler les récepteurs à la ryanodine, provoquer la vidange des stocks et ainsi déclencher l'apoptose. Dans les conditions physiologiques, les récepteurs à la ryanodine libèrent du calcium dans le cytoplasme et active l'entrée capacitative. L'entrée de calcium qui en résulte sera utilisée par la cellule pour remplir le réticulum endoplasmique via les pompes Ca^{2+}-ATPases (en absence de thapsigargine).

Influence of Ca^{2+} induced Ca^{2+} release mediated by ryanodine receptors on Ca^{2+} elevation induced by thapsigargin in LNCaP cells

Guillaume LEGRAND[1]*, Sandrine HUMEZ[1]*, Bruno BASTIDE**, Pascal MARIOT*, Fabien VAN COPPENOLLE*, Yvonne MOUNIER **, Roman SKRYMA* and Nathalia PREVARSKAYA[2]*

* Laboratoire de Physiologie Cellulaire, INSERM EPI-9938, USTL, Villeneuve d'Ascq.

** Laboratoire de plasticité neuromusculaire USTL, Villeneuve d'Ascq.

key words

thapsigargin, ryanodine receptor, calcium, LNCaP, prostate

[1] G.L. and S.H. contributed equally to this work

[2] To whom all correspondence should be addressed: Laboratoire de Physiologie Cellulaire, INSERM EPI-9938, USTL, Bat. SN3, 59655 Villeneuve d'Ascq Cedex, FRANCE

Fax: 33 3 20 43 40 66

E-mail: phycel@pop.univ-lille1.fr

ABSTRACT:

This work was conducted on non-excitable LNCaP cells: an androgen-sensitive human prostate cancer cells line. A specific [^{3}H] ryanodine binding is detected in microsomal membranes isolated from LNCaP cells indicating that these non-excitable cells express ryanodine receptors. Furthermore, caffeine (20 mM) is able to promote a measurable increase in the intracellular calcium concentration which is almost completely abolished by ryanodine (10 µM). Thus LNCaP cells possess functional ryanodine receptors. Thapsigargin (1µM), when applied in a Ca^{2+} free medium, induces a transient increase in intracellular calcium concentration whereas it is unable to induce the same response when cells are incubated with ryanodine (10 µM) during 15 min. These data demonstrate for the first time that ryanodine channels can be activated by a Ca^{2+} leak induced by thapsigargin in a non-excitable cell line and can participate to the emptying of intracellular Ca^{2+} stores.

1. Introduction:

Thapsigargin (TG), a sesquiterpene lactone derived from the plant *Thapsia garganica*, is currently used for its ability to deplete Ca^{2+} stores and prevent their refilling. Indeed, TG has been proven to be very useful for intact cell experiments because of its high membrane permeability and its ability to specifically inhibit (Ca^{2+}-Mg^{2+})-ATPases of the endoplasmic reticulum (SERCAs) without interfering with plasma membrane (Ca^{2+}-Mg^{2+})-ATPases (PMCAs) [1, 2]. The ability of TG to deplete Ca^{2+} stores is now currently used to induce and to study the capacitative Ca^{2+} entry, which is present in the plasma membrane of almost all non-excitable cells and in some excitable cells [1,3-5]. Under resting conditions, the steady state Ca^{2+} content of Ca^{2+} stores reflects the balance between an active uptake (virtually mediated by a TG-sensitive ATPase of the SERCA family) and a passive Ca^{2+} efflux. By inhibiting the SERCAs TG displaces the balance and induces the emptying of Ca^{2+} stores. This action of TG on the Ca^{2+} content of Ca^{2+} stores is independent of any production of calcium-releasing signals such as inositol 1,4,5-trisphosphate [6,7].

To date, the role of ryanodine receptors (RYRs), which are the calcium channels of the sarcoplasmic reticulum involved in Ca^{2+} induced Ca^{2+} release (CICR) in the TG induced Ca^{2+} emptying of Ca^{2+} stores has never been studied and has been only recently postulated by Barritt [8]. Indeed, as TG induces a Ca^{2+} leak from Ca^{2+} stores, one may hypothesize that this Ca^{2+} could interact with the ryanodine channels, if those channels are present. This question has never been investigated in non-excitable cells because ryanodine channels were believed to be more specific to excitable cells such as muscle, neuron and neuroendocrine cells [9-12].

In this study we demonstrate that the androgen sensitive human cancer cell line, LNCaP, express functional ryanodine channels and we show that ryanodine channels are activated and participate to the transient Ca^{2+} elevation induced by TG.

2. Materials and Methods:

2.1. Cell Culture

The androgen-sensitive human prostate cancer cell line, LNCaP, obtained from the American Type Culture Collection were maintained in culture in RPMI 1640 medium (Biowhittaker, Fontenay sous Bois, FRANCE) supplemented with 10 % fetal calf serum (Seromed, Poly-Labo, Strasbourg, FRANCE), 5 mM L-glutamine , 50 IU/ml penicillin and 50 µg/ml streptomycin (Sigma, L'Isle d'Abeau, FRANCE). Cells were grown at 37 °C in a humidified atmosphere containing 5% CO2. Prior to fluorescence measurements, the cells were trypsinized and transferred to glass slips. Cells were used 1-4 days after trypsinization.

2.2. Calcium Measurements

The culture medium was replaced by an HBSS solution containing 142 mM NaCl, 5.6 mM KCl, 1 mM $MgCl_2$, 2 mM $CaCl_2$, 0.34 mM Na_2HPO_4, 0.44 mM KH_2PO_4, 10 mM HEPES, and 5.6 mM Glucose. The osmolarity and pH of this solution were adjusted to 310 mOsm and 7.4, respectively. When a calcium-free medium was required, $CaCl_2$ was omitted and replaced by equimolar $MgCl_2$. Dye loading was achieved by transferring the cells into a standard HBSS solution containing 1 µM Fura 2/AM (Calbiochem, Meudon, FRANCE) for 40 minutes at 37°C, then rinsing them three times with the same dye-free solution. Intracellular calcium was measured by a an imaging system (Quanticell 900, Applied Imaging, UK). The glass cover slip was mounted in a chamber on a Nikon microscope equipped for fluorescence. Fura 2 fluorescence was excited at 340 nm and 380 nm and the emitted fluorescence was measured at 510 nm. The $[Ca^{2+}]i$ was derived from the ratio of the fluorescence intensities for each of the excitation wavelengths (F340/F380), and from the Grynkiewicz equation [13]. All

recordings were carried out at room temperature. The cells were continuously perfused with the HBSS solution and chemicals were added via a whole chamber perfusion system. The flowing rate of the whole chamber perfusion was set to 1 ml/min and the chamber volume was 500 µl.

2.3.Preparation of microsomal membrane vesicles from LNCaP cells and skeletal muscles

LNCaP cells were harvested with a versene solution (137 mM NaCl, 3 mM KCl, 8 mM Na2PO4, 1.5 mM KH2PO4 and 0.5 mM EDTA) followed by two washes with ice cold phosphate buffered saline. The cell pellet (600×g, 5 min) was resuspended in ice cold lysis buffer (1 mM EDTA, 10 µg/ml pepstatin A, 10 µg/ml aprotinin, 10 µg/ml leupeptin, 10 mg/ml benzamide, 5µg/ml PMSF, 10 mM HEPES, pH 7.4) before lysis first by 10 strokes in a tight-fitting Dounce homogenizer, second by 15 strokes after the addition of an equal volume of sucrose buffer (500mM sucrose, 10 mM HEPES, pH 7.2). The microsomes were collected by centrifugation of postnuclear supernatant (9.000×g, 15 min) at 100.000×g for 2 hours. The pellet was resuspended in a buffer containing 250 mM sucrose, 10 mM HEPES/TRIS, pH 7.2. The membrane vesicles were stored at -80°C until use. Crude microsomal membranes from rat adult skeletal muscle were prepared by differential centrifugation as previously described [14].

2.4. [^{3}H] Ryanodine binding assays

To measure [^{3}H] ryanodine binding, 100 µg of protein were incubated in 200 µl of 1M KCl, 10 mM HEPES, 25 µM $CaCl_2$, pH7.4 (buffer A) for 90 min at 37 °C, in the presence of various protease inhibitors described above for microsome preparations, at a concentration of 10 nM of [^{3}H] ryanodine. Non specific binding was determined using a 1000-fold excess of unlabeled ryanodine. After 2 hrs, bound [^{3}H] ryanodine was determined by filtration of the

sample volume through a Millipore vacuum filtration apparatus on Whatman GF/B filters. The filters were then washed with 3× 5 mL ice cold buffer A without protease inhibitors. The radioactivity remaining on the filter was determined by liquid scintillation counting. All experiments were performed in duplicate.

2.5. Chemicals:

Ryanodine and thapsigargin were purchased from Calbiochem (Meudon, FRANCE). EDTA, pepstatin A, aprotinin, leupeptin, benzamide and PMSF were purchased from Sigma (L'Isle d'Abeau, FRANCE). [^{3}H] ryanodine was obtained from NEN Life Science Products (Boston, M A, USA).

2.6. Data analysis

Results were expressed as mean ± SEM. Plots were produced using origin 5.0 (Microcal Software, Inc). Each experiment was repeated several times. Student's t-test was used for statistical comparison among means and differences, with $P < 0.05$ considered significant.

3. Results and discussion :

3.1 Evidence for ryanodine receptors in LNCaP Cells:

A microsomal membrane fraction was isolated from cultured LNCaP cells and from rat skeletal muscle, specific [^{3}H] ryanodine binding was 21,66±1,20 fmol/mg protein (n=3) and 2373±200 fmol/mg protein (n=3) respectively. These results indicate the presence of ryanodine receptors in LNCaP cells. The [^{3}H] ryanodine binding is 109 fold lower in LNCaP cells than in rat skeletal muscle microsomes suggesting a very low level of ryanodine receptors in the endoplasmic reticulum of LNCaP cells. However, the level of [^{3}H] ryanodine binding might not exactly reflect the levels of RyRs in the skeletal muscle and LNCaP cells because only a single concentration of this radioligand was employed and a high level of non-specific binding could not be avoided with LNCaP microsomes as previously described in ryanodine binding experiments performed on other cell lines [15].The very low amount of microsomes isolated from cultured LNCaP cells prevented the improvement of the assay parameter of ryanodine binding. To corroborate the functionality of ryanodine channels in intact cells, we have investigated the ability of caffeine to promote calcium release from intracellular stores in LNCaP cells. The basal level of cytoplasmic calcium, [Ca^{2+}]i, measured in HBSS medium was 93±5 nM (n=36). Figure 1 shows that 20 mM caffeine induced an increase in [Ca^{2+}]i typical to caffeine-induced Ca^{2+} mobilization through RyRs as previously shown in excitable cells [16,17]. This Ca^{2+} mobilization was almost completely abolished by 10 µM ryanodine (n=15), a concentration known to block calcium release by RYRs [18-22]. Taken together, these results allow us to conclude that the non-excitable prostate cancer cell line, LNCaP, expresses functional ryanodine receptors. This finding is in agreement with the idea that ryanodine receptors could also play a functional role in non-excitable cells where it

was demonstrated to be expressed as in lung epithelial cells [23] and in various non excitable cells and tissues [24-27].

3.2 Effect of ryanodine on Ca^{2+} release induced by thaspigargin:

TG is currently used to study Ca^{2+} mobilization and capacitative calcium influx because of its ability to deplete intracellular calcium stores. The currently accepted mechanism of action of TG on the Ca^{2+} depletion is an acute and highly specific arrest of the endoplasmic reticulum SERCAs followed by a rapid leak of Ca^{2+} from the stores. This will induce a transient elevation of intracellular calcium before it is pumped across the plasma membrane PMCAs. In many cell types [7, 28-34] it is possible to assess a part of the calcium released from the intracellular stores by monitoring $[Ca^{2+}]i$ when cells are bathed in a calcium free medium. In these conditions, TG induces a transient increase of $[Ca^{2+}]i$. When LNCaP cells were bathed in a calcium free solution, application of thapsigargin (1 μM) induced the classical transient increase of the intracellular calcium concentration from 107 ± 8.3 nM to a maximal value of 266 ± 15 nM (n=30) (Fig. 2A). $[Ca^{2+}]i$ in Ca^{2+} free conditions was not significantly different from cells bathed in a Ca^{2+} containing medium, HBSS medium ($[Ca^{2+}]i$ was 107 ± 8 nM, n=30 versus versus 97± 5 nM, n=36 in Ca^{2+} free and Ca^{2+} containing HBSS medium respectively). As we demonstrated that ryanodine channels are expressed in LNCaP cells, one may postulate that Ca^{2+} ions leaking from TG sensitive stores could activate ryanodine channels by CICR mechanism. LNCaP cells were incubated with ryanodine (10 μM) during 15 min in HBSS medium and then placed in a Ca^{2+} free medium containing the same amount of ryanodine just before TG application (see figure 2B). At this concentration ryanodine was shown to inhibit RYRs in a variety of cells [19-22] and in LNCaP cells (figure 1). In this condition, the basal $[Ca^{2+}]i$ was not statistically different from the control condition. $[Ca^{2+}]i$ was 122±8 nM (n=25) in calcium free medium containing

ryanodine (10 μM) versus 107±8 nM (n=30) in calcium free medium. Figure 2B shows that in the presence of ryanodine (10μM), TG (1μM) was unable to induce the classical transient increase in $[Ca^{2+}]i$ (n=25). Usually, this transient increase in $[Ca^{2+}]i$ induced by TG in a Ca^{2+} free medium is explained by a passive leak of Ca^{2+} from the endoplasmic reticulum through "leak channels" or SERCA itself [2, 35, 36]. However, our results indicate that ryanodine channels are involved in the transient elevation of $[Ca^{2+}]i$ by TG in prostate cancer LNCaP cells and are probably activated by a passive Ca^{2+} leak.

At the stage of this study it is important to assess the ability of TG to induce the sustained Ca^{2+} influx, named capacitative Ca^{2+} entry. As shown above, TG when applied on cells bathed in a Ca^{2+} free solution containing ryanodine (10 μM) was unable to induce a transient $[Ca^{2+}]i$ elevation, but when Ca^{2+} was readmitted into the external solution, a marked increase in $[Ca^{2+}]i$ was observed corresponding to a Ca^{2+} influx into the cells (Fig.3). In these conditions, $[Ca^{2+}]i$ was increased to a value of 827± 63 nM (n=11). This implies that TG is able to induce a capacitative Ca^{2+} entry without measurable transient increase in cytosolic Ca^{2+} in a Ca^{2+} free medium. Thus, in these conditions the Ca^{2+} leak, which was not measurable possibly because PCMAs act quickly enough to remove Ca^{2+} from cytosolic compartment, was sufficient to activate capacitative Ca^{2+} entry.

In addition, as the transient Ca^{2+} increase in a Ca^{2+} free medium is observed in a large variety of cell types [6, 28-34], ryanodine channels could participate to the emptying of the stores in these cells if they are expressed as in LNCaP cells. Indeed, ryanodine channels have been reported in some of the cells where TG produces a transient increase in $[Ca^{2+}]i$ in calcium free medium like basophilic leukemia cells [37], parotid acinar cells [38, 39] tracheal smooth muscle [40], hepatocytes [41], pancreatic cells [42,43] and in neuronal cells [16].

Thus, our results could explain the common mechanism by which TG empties the TG-sensitive Ca^{2+} stores. To our knowledge, this work provides the first direct demonstration of a

possible involvement of ryanodine receptors in a mechanism by which TG empties the intracellular calcium stores.

Acknowledgments

This work was supported by grants from INSERM, ARC (Association pour la Recherche Contre le Cancer, France) and Ligue Nationale contre le cancer (France). Financial support to G. LEGRAND came from ARTP (Association pour la Recherche sur les Tumeurs de la Prostate, France).

References

[1] Putney, J. W.Jr and Bird G.St;J. (1993) Endocr. Rev.14: 610-631.

[2] Thastrup, O., Cullen, P.J., Drobak, B.K., Hanley, M.R., and Dawson, A. P. (1990) Proc. Natl. Acad. Sci. USA.87:2466-2470.

[3] Berridge, M.J. (1995) Biochem J. 312: 1-11.

[4] Birnbaumer, L., Zhu, X., Jiang, M. Boulay, G., Peyton, M., Vannier, B., Brown, D., Platano, D., Sadeghi, H., Stefani, E. and Birnbaumer, M. (1996) Proc Natl Acad Sci USA. 93: 15195-15202.

[5] Putney, J.W.Jr. (1986) Cell Calcium. 7: 1-12.

[6] Takemura, H., Hugues, A. R., Thastrup, O. and Putney, J.W.Jr. (1989) J. Biol. Chem., 264: 12266-12271.

[7] Jackson, T. R., Patterson , S. I., Thastrup, O. and Hanley, M.R. (1988). Biochem. J. 253: 81-86.

[8] Barritt G.J. (1998). Cell Calcium 23(1): 65-75.

[9] Otsu, K., Willard, H.F., Khanna, V.K., Zorzat, F., Green, N.M. and MacLennan, D.H. (1990) J. Biol. Chem. 265: 13472-13483.

[10] Marks, A.R., Tempst, P., Hwang, K.S., Taubman, M.B., Inui, M., Chadwick, C ., Fleischer, S. and Nadal-Ginard, B. (1989) Proc. Natl. Acad. Sci. USA 86: 8683-8687.

[11] Giannini, G., Conti, A., Mammarella, S., Scrobogna, M. and Sorrentino, V. (1995) J. Cell Biol. 128: 893-904.

[12] Hakamata, Y., Nakai, J., Takeshima, H. and Imoto, K. (1992) FEBS Lett. **312**: 229-235.

[13] Grynkiewicz, G., Poenie, M. and Tsien, R. Y. (1985) J. Biol. Chem. 260: 3440-3450.

[14] Catinot, M. P., Bastide, B., Montel, V., Suarez-Kurtz, G. and Mounier, Y. (1997) Acta Physiol. Scand. 160 :199-205.

[15] Mackrill, J.J., Challiss, R. A. J., O'Connell, D. A., Lai, A. and Mahorski, S. (1997) Biochem J. 327 : 251-258.

[16] Pessah, I. N., Stambuk, R.A. and Casida, J. E. (1987) Mol Pharmacol. 31: 232-238.

[17] Verkhratsky, A. and Petersen O. H. (1998) Cell Calcium. 24:333-343.

[18] Meissner, G. (1986) J. Biol. Chem. 260: 6300-6306.

[19] Lattanzio, F.A. Jr. Schlatterer, R. J., Nicar, M., Campbell, K. P. and Sutko, J.L. (1987) J. Biol. Chem. 262: 2711-2718.

[20] Alderson, B. H. and Feher, J.J. (1987) Biochem. Biophys. Acta. 900: 221-229.

[21] McPherson, P. S. and Campbell, K. P. (1993) J. Biol. Chem. 268: 13765-13768.

[22] Fleischer, S. and Inui, M.(1989) Annu. Rev. Biophys. Chem. 18: 333-364.

[23] Giannini, G., Clementi, E., Ceci, R., Marziali, G. and Sorrentino, V. (1992) Science. 257 : 91-94.

[24] Lesh, R. E., Marks, A.R., Somlyo, A.V., Fleischer, S. and Somlyo, A.P. (1993) Circ.Res. 72 : 481-488.

[25] Larini, F, Menegazzi, P., Baricordi, O., Zorzato, F. and Treves, S. (1995) Molecular Pharmacology. 47 : 21-28.

[26] Bennett, D. L. Cheek, T. R.; Berridge M. J., DeSmedt, H., Parys, J.B, Missiaen, L. and Bootman, M. D. (1996) J. Biol. Chem. 271:6356-6362.

[27] Sei ,Y., Gallager ,K .L. and Basile, A. S. (1999) J. Biol. Chem. 274: 5995-6002.

[28] Zhu, X., Jiang, M., Peyton, M., Boulay, G., Hurst, R., Stefani, E. and Birnbaumer, L. (1996) Cell. 85: 661-671.

[29] Louzao, M.C., Riberio , C. M. P., Bird G.St.J. and Putney J.W.Jr. (1996) J. Biol. Chem. 271: 14807-14813.

[30] Yang, C.M. (1998) Cell. Signal. 10: 735-742.

[31] Huang, Y. and Putney, J. W. Jr. (1998) J. Biol. Chem. 273: 19554-19559.

[32] Takemura, H., Sakano, S., Kaneko, M.and Ohshika, H. (1998) Pharmacological letters. 62: 271-276.

[33] Ikari, A., Sakai H. and Takeguchi, N. (1997) Japanese Journal of Physiology. 47: 235-239.

[34] Klishin, A., Sedova, M. and Blatter, L.A. (1998) Am. J. Physiol. 274: C1117-C1128.

[35] Meyer, T. and Stryer, L. (1990) Proc. Natl. Acad. Sci. U.S.A. 87: 3841-3845.

[36] DeMeis, L. and Inesi G. (1992) FEBS Lett. 299: 33-35.

[37] Mohr, F.C, Alojipan, S.V., Dunston, S.K. and Pessah, I.N. (1995) Mol. Pharmacol. 48:512-522.

[38] Zhang, X., Wen, J., Bidasee, K.R., Besch, H.R. and Rubin, R.P. (1997) Am. J. Physiol. 273: c1306-1314.

[39] Zhang X., Wen J., Bidasee, K. R., Besch, H. R. Jr., Wojcikiewicz, R.J., Lee, B. and Rubin R.P. (1999) Biochem. J.340:519-527.

[40] Kannan M.S., Prakash, Y.S., Brenner, T., Mickelson, J.R. and Sieck G.C. (1997) Am. J. Physiol. 272: L659-L664.

[41] Lilly, L.B. and Gollan, J.L. (1995) Am. J. Physiol. 268: G1017-G1024.

[42] Holz, G.G., Leech, C.A., Heller, R.S., Castonguay, M. and Habener J.F. (1999) J. Biol. Chem. 274: 14147-14156.

[43] Leite, M.F., Dranoff, J. A., Gao, L. and Nathanson, M.H. (1999) Biochem. J. 337: 305-309.

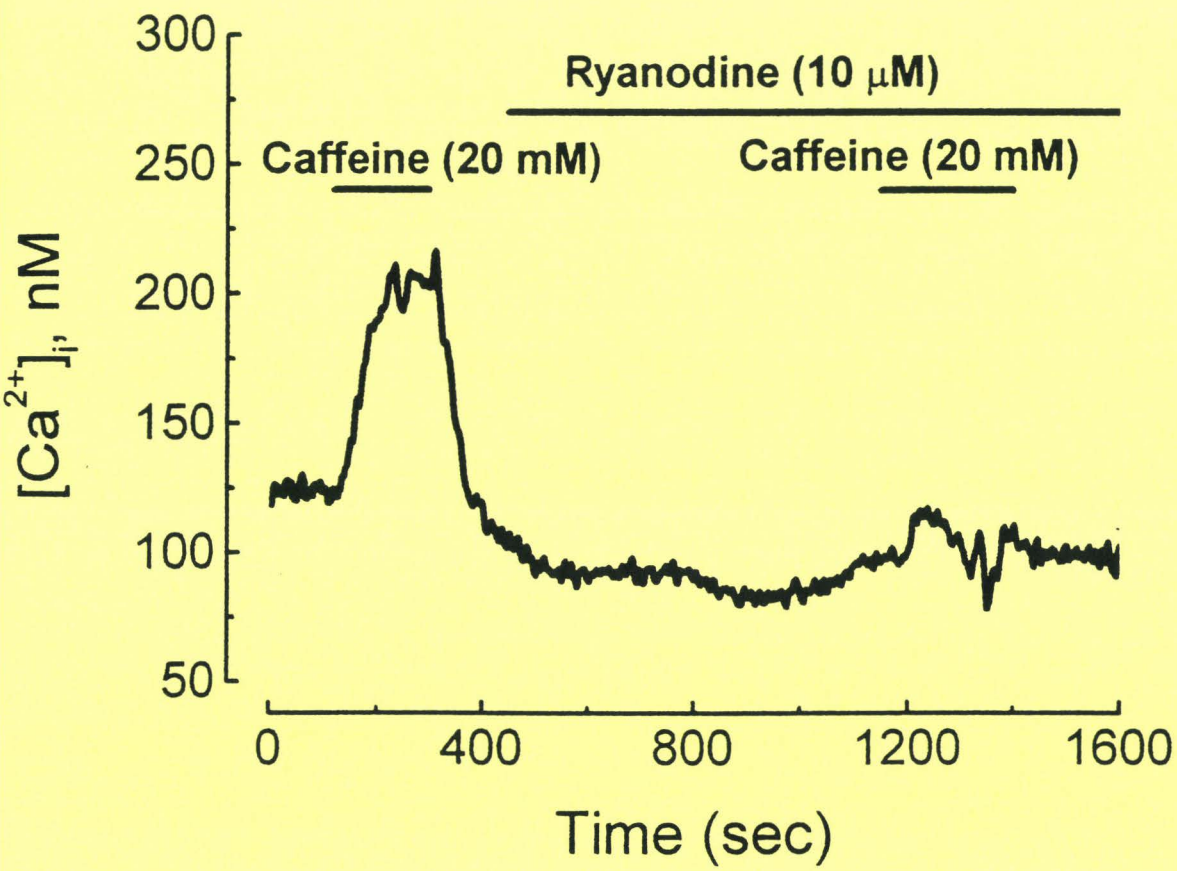

Figure 1: **Cytosolic calcium increase mediated by ryanodine receptors.**

Caffeine (20 mM) application, as indicated by horizontal *bars*, induces an increase in the intracellular concentration which is prevented when ryanodine (10μM) is applied before caffeine. Experiments were conducted in HBSS medium.

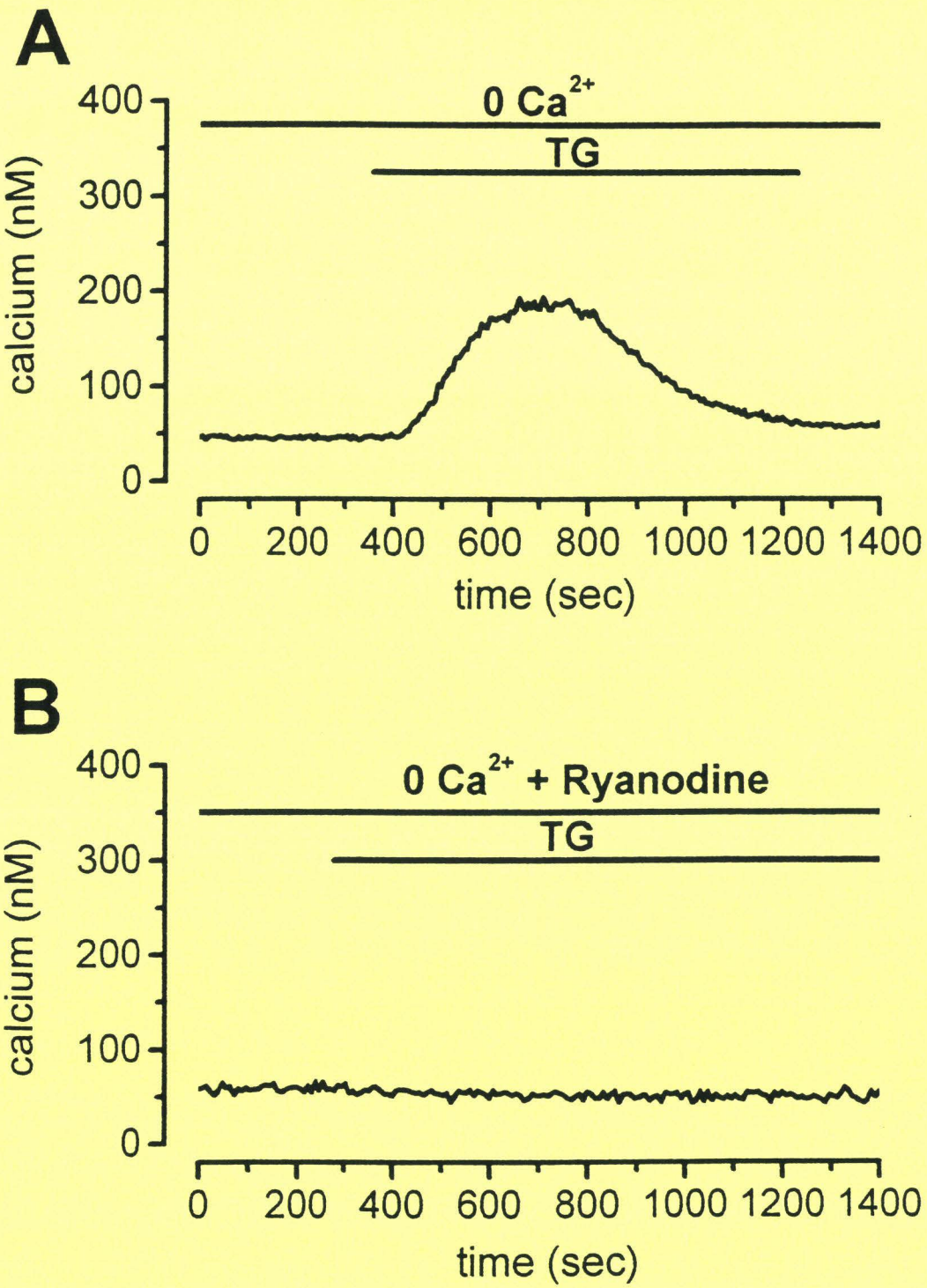

Figure 2: **Ryanodine block the calcium release induced by thapsigargin.**

A- Typical trace showing a transient intracellular calcium elevation induced by thapsigargin (1μM). Cells were bathed in a calcium free medium.

B- Similar experiment after 15 min incubation of the cells with ryanodine (10 μM).

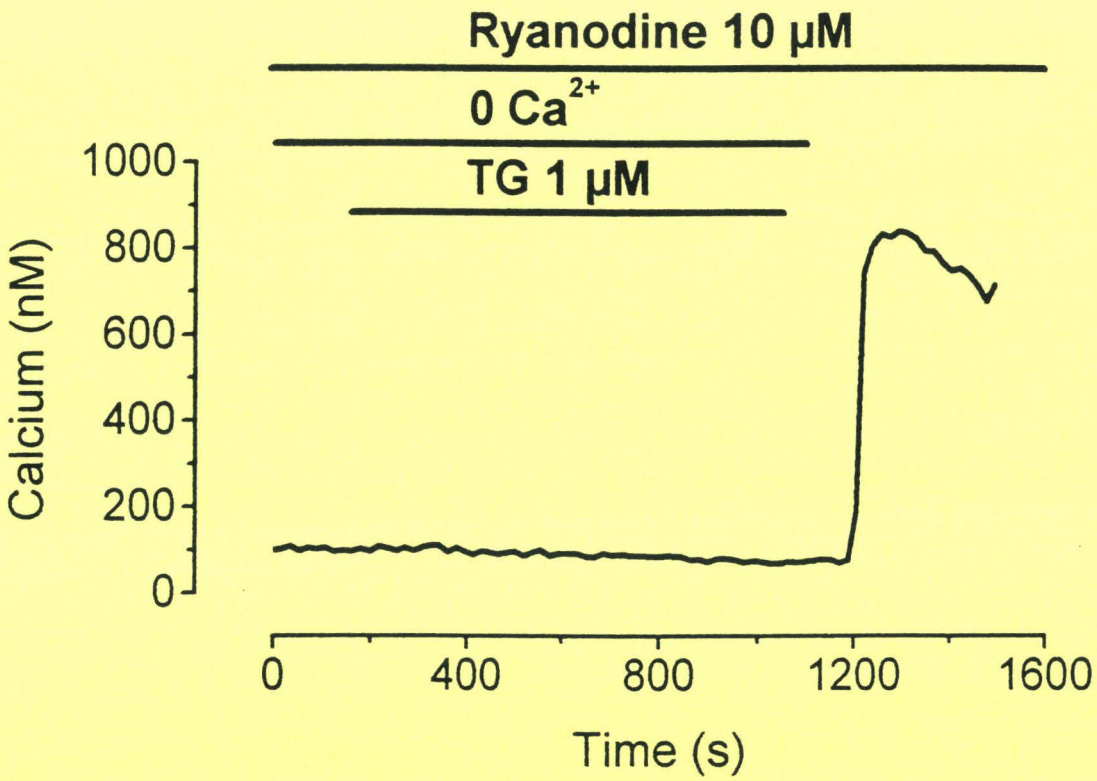

Figure 3: **Utilization of ryanodine does not prevent the capacitative calcium influx induced by thapsigargin.**

Cells were treated 15 min in HBSS medium containing ryanodine (10 µM). After this treatment, as indicated by horizontal *bars*, thapsigargin (1µM) was applied in a calcium free medium. 1100 s after thapsigargin application a calcium containing medium (2 mM $CaCl_2$) was perfused.

2.2.3- Influence de la prolactine sur l'état des réserves calciques des cellules LNCaP

Nous avons démontré que la PRL provoque une surexpression de Bcl-2 dans les cellules épithéliales de la prostate de rat. Cette oncoprotéine est impliquée dans la régulation de l'état des stocks calciques. Nous avons également mis en évidence le rôle de ces réserves de calcium dans l'apoptose. Le but de cette étude est de définir si la PRL agit sur le contenu des stocks calciques et par extension sur l'apoptose.

- Protocole expérimental

Nous avons incubé les cellules LNCaP, pendant 18 heures, dans un milieu contrôle (dépourvu de rouge de phénol et contenant du sérum de veau déstéroïdé), en présence de PRL (5 nM), de DHT (10^{-8}M) ou des deux hormones à la fois, dans un milieu contenant 2 mM de calcium. A l'issu du traitement, nous avons mesuré le taux basal de calcium intracellulaire. Nous avons également estimé le contenu des réserves calciques, en imagerie calcique, en utilisant la thapsigargine (0.1 μM) dans un milieu dépourvu de calcium. En effet, la réponse à la thapsigargine se traduit par une augmentation transitoire de calcium intracellulaire proportionnelle au contenu initial du réticulum endoplasmique en calcium.

	Taux de base	Réponse à la thapsigargine (0.1 μM)
Contrôle (n=15)	105±20 nM	300±32 nM
PRL (5 nM) (n=18)	110±12 nM	875±132 nM
DHT (10^{-8}M) (n=13)	100±14 nM	490±150 nM
PRL (5nM) +DHT (10^{-8}M) (n=21)	125±17 nM	575±123 nM

Tableau 2: Mesures moyennes de calcium intracellulaire (± S.E.M.) obtenues en imagerie calcique sur des cellules LNCaP en conditions contrôle et en présence de PRL (5 nM) dans le milieu extracellulaire.

La PRL ne modifie pas le taux de base de calcium dans les cellules LNCaP. Par contre, en présence de PRL, la réponse à la thapsigargine est pratiquement 3 fois plus importante. Cela signifie que la PRL induit un remplissage accru des réserve intracellulaire en calcium et pourrait ainsi ralentir les processus apoptotiques dans les cellules LNCaP. Nous obtenons des résultats identiques en présence de DHT, avec ou sans PRL. Nous ne savons pas pour le moment par quels moyens ce phénomène se produit. Il est connu que la PRL inhibe l'apoptose et induit la surexpression de Bcl-2 dans les cellules Nb2 (Krumenacker *et al.*, 1998). Il est possible, à l'instar de nos travaux sur les prostates de rat, que la PRL induise la synthèse de Bcl-2 dans les LNCaP et provoque de ce fait, une augmentation quantitative du contenu des stocks calciques.

Cette étude sera poursuivie, en parallèle, sur la lignée de cellules LNCaP transfectées avec le gène codant pour Bcl-2.

2.3- Conclusion de la deuxième hypothèse

Le second volet, *in vitro*, de notre étude a permis de caractériser des processus capitaux dans la régulation de la prolifération cellulaire et de l'apoptose des cellules cancéreuses prostatiques humaines.

Nous avons ainsi mis en évidence le rôle clé des canaux potassiques dans le contrôle de la prolifération cellulaire par la PRL. Les cellules normales et les cellules tumorales expriment des canaux potassiques différents. Dans les deux types cellulaires, ces canaux sont impliqués dans le contrôle de la prolifération cellulaire. Nous pensons qu'il est possible que la cancérogenèse des cellules de la prostate s'accompagne d'un changement de type de canal potassique ou ait pour conséquence une mutation de ce dernier. Nous postulons que l'activation des canaux potassiques pourrait être l'un des mécanismes par lequel la PRL stimule la prolifération des cellules prostatiques.

Nous nous sommes également appliqués à étudier les mécanismes de régulation de l'homéostasie calcique au sein des cellules cancéreuses humaines LNCaP et leurs relations avec la modulation des processus apoptotiques. Nous avons démontré que seule la vidange des stocks calciques, et non l'augmentation de la concentration en calcium intracellulaire, déclenche l'entrée des cellules LNCaP en apoptose. Par contre, dans le cas des cellules hormono-indépendantes, l'augmentation de la concentration intracellulaire en calcium , via la vidange des stocks ou une entrée de calcium, est nécessaire pour provoquer l'apoptose (Furuya *et al.*, 1994). La sensibilité des cellules de la prostate aux variations calciques pourrait expliquer les phénomènes d'échappement survenant quasi-inévitablement lors des traitements des cancers de la prostate en hormonothérapie. Nous avons également mis en évidence la présence de récepteurs à la

ryanodine de type 1 et de type 2 dans les cellules de la prostate. Ces récepteurs, présents sur la membrane des stocks calciques intracellulaires, participent à la régulation de la concentration en calcium dans la cellule (Marks, 1997). L'importance physiologique de ces récepteurs est grande, puisque leur activation provoque l'apoptose des cellules LNCaP. L'inhibition de ces récepteurs, au contraire, les protège de ce processus.

La PRL module également l'homéostasie calcique des cellules LNCaP. En effet, cette hormone induit une augmentation de calcium dans les stocks calciques intracellulaires. Il est possible que la PRL agisse sur le remplissage des stocks calciques en stimulant l'expression de la protéine antiapoptotique Bcl-2, comme elle le réalise sur les cellules Nb2 (Krumenacker *et al.*, 1998). Nous pensons que la PRL pourrait inhiber l'apoptose des cellules de la prostate par ce biais. Nous poursuivrons cette étude sur des cellules LNCaP qui surexpriment la protéine antiapoptotique Bcl-2, connue pour participer activement au remplissage des réserves calciques intracellulaires.

Les travaux portant sur l'apoptose des cellules tumorales revêtent une importance capitale dans le traitement des cancers de la prostate. En effet, ces pathologies graves seraient dues à un dérèglement de la balance prolifération/apoptose en faveur d'une diminution des processus apoptotiques (Bruyninx *et al.*, 1998). Nous pensons que l'une des causes du phénomène d'échappement, qui rendent les cancers de la prostate insensibles aux thérapies hormonales, réside dans un changement profond des mécanismes de régulation du calcium intracellulaire. Connaître les mécanismes fins de régulation de l'homéostasie calcique permettra, nous l'espérons, d'induire les cellules tumorales de la prostate à entrer en apoptose.

Nos travaux ouvrent de nouvelles voies thérapeutiques visant d'une part à inhiber la prolifération cellulaire via les canaux potassiques spécifiques de la prostate et

d'autre part à provoquer l'apoptose des cellules cancéreuses prostatiques en modulant l'homéostasie calcique avec des outils pharmacologiques spécifiques.

CONCLUSION GENERALE ET PERSPECTIVES

Au commencement de ce travail, quelques données laissaient supposer que la PRL pouvait jouer un rôle majeur dans la physiologie de la prostate. Les cellules de la prostate humaine, ainsi que celles de la prostate de rat, possèdent des récepteurs à la PRL (Nevalainen *et al.*, 1997). Par ailleurs, Nevalainen *et al.* (1996) avaient mis en évidence l'action trophique de la PRL sur des cultures organotypiques de prostate de rat. De plus, des taux élevés de PRL plasmatiques sont associés à de mauvais pronostics de survie aux cancers de la prostate.

Il est connu que les androgènes régulent le fonctionnement de la prostate (Cunha *et al.*, 1987). Les troubles prostatiques apparaissent avec l'âge. Chez l'homme âgé, le taux d'androgènes diminue (Davidson *et al.*, 1983), contrairement à celui de la PRL (Vekemans et Robyn, 1975). L'ensemble de ces données suggèrent donc que la PRL participe activement au contrôle hormonal de la physiologie de la prostate. Cependant, la totalité des traitements hormonaux des pathologies de la prostate se basent sur la diminution du taux d'androgènes circulants. Malheureusement, malgré des concentrations basses en hormones masculines, les tumeurs persistent souvent et continuent à se développer. Ce phénomène d'échappement aux traitements hormonaux actuels laisse entendre la présence d'autres facteurs dans la régulation prostatique. Il nous semblait donc primordial d'étudier le rôle de la PRL dans la physiologie et la physiopathologie de la prostate.

Afin de cerner les effets de la PRL, nous avons développé deux volets de recherches complémentaires :

- **une étude *in vivo*, sur plus de 450 rats;**
- **un aspect *in vitro* par l'emploi de cultures primaires de cellules normales et de lignées tumorales prostatiques.**

Cette approche multiple nous a permis de comprendre le rôle de la PRL à l'échelle de l'organe, mais également à l'échelle cellulaire. En effet, dans ce type d'étude, la physiologie intégrée et la physiologie cellulaire sont nécessaires afin d'avoir une vision d'ensemble de la thématique sur laquelle nous nous sommes lancés.

CONCLUSION DE L'ETUDE *IN VIVO*

Nous avons mis au point un modèle animal d'hyperplasie prostatique induite par une hyperprolactinémie, chez le rat. Grâce à cette étude, nous avons démontré que la PRL agit en tant que cofacteur des androgènes et induit le développement d'une hyperplasie et d'une hypertrophie glandulaire uniquement sur le lobe latéral de la prostate de rat. Cette région est homologue à celle de la prostate humaine où se développent les hyperplasies bénignes de la prostate (Price, 1963). Cela renforce l'utilité de ce modèle animal dans le cadre de nos études sur les pathologies de la prostate. Par ailleurs, nous avons détecté une surexpression de la protéine antiapoptotique Bcl-2 au niveau des cellules épithéliales des prostates latérales des animaux ayant subi une hyperprolactinémie. Cette découverte suggère que la PRL pourrait inhiber l'apoptose des cellules de la prostate, à l'instar des androgènes (considérés comme des facteurs de survie (Martikainen et Isaacs, 1990)). Ce résultat est capital, si l'on considère que le cancer de la prostate, à évolution lente, est probablement dû à une inhibition de l'apoptose plutôt qu'à une stimulation de la prolifération cellulaire.

Au cours de la seconde étude *in vivo*, nous avons entamé l'étude des effets de la PRL et des androgènes, dans le temps, sur la croissance de la prostate latérale. La PRL

induit une augmentation du poids de la prostate dés 9 jours de traitement. Nous prévoyons de mesurer le pourcentage de cellules apoptotiques et de cellules en prolifération afin de connaître la manière dont la PRL agit, dans le temps et avec les androgènes, sur la croissance de la prostate.

Notre troisième étude, sur l'animal, a porté sur l'analyse comparée de l'efficacité des deux médicaments utilisés en clinique contre les HBP (l'E.L.S.S.R et le finastéride) sur notre modèle d'hyperplasie induite par l'hyperprolactinémie. L'E.L.S.S.R. est un extrait obtenu à partir du palmier scie (*Serenoa repens*). Ce mélange d'acides gras est connu pour inhiber les deux isoformes de la 5α-reductase (Bayne *et al.*, 1997) et provoque une chute de la concentration en DHT dans l'organisme. Le Finastéride, une molécule synthétique, inhibe spécifiquement la 5α-reductase. Nous avons traité des rats à l'E.L.S.S.R. et au finastéride durant 30 jours. Nous avons, pour la première fois, démontré que l'E.L.S.S.R. abolit les effets trophiques de l'hyperprolactinémie, *i.e.* l'hypertrophie et l'hyperplasie glandulaire. Le finastéride, au contraire, est inefficace dans le traitement des effets de la PRL.

PERSPECTIVES APPORTEES PAR LES ETUDES *IN VIVO*

Ces études offrent de nombreuses voies de recherches ultérieures. La première, entamée au sein du laboratoire, consiste à localiser et à quantifier les récepteurs de la PRL sur des coupes histologiques de prostates de rat et humaines. Cette approche sera réalisée notamment grâce aux techniques d'immunohistochimie et de microscopie électronique.

Il sera alors possible de visualiser la position des récepteurs de la PRL, les zones de la prostate qui en sont riches, ou à l'inverse, qui en sont dépourvues. Nous pourrons également mettre en évidence les cellules sécrétrices de PRL prostatiques et ainsi caractériser la manière cette hormone pourrait agir dans la physiologie et la physiopathologie de la prostate, notamment sur la prolifération cellulaire et l'apoptose.

Nous nous pencherons également sur la modulation du nombre de récepteurs à la PRL induite par les différents traitements hormonaux ou médicamenteux imposés aux animaux. En effet, il est possible que l'hyperprolactinémie provoquée par le sulpiride influe sur le nombre et/ou la localisation des récepteurs de la prolactine (hypophysaire et plasmatique). De même, les androgènes pourraient également modifier la localisation et l'expression des récepteurs de la PRL dans la prostate.

Nous analyserons également les effets fins de l'E.L.S.S.R. sur la sécrétion de PRL hypophysaire et prostatique ainsi que sur l'expression et la localisation des récepteurs de la PRL dans la prostate. Nous pouvons envisager que l'E.L.S.S.R. puisse diminuer la sécrétion de PRL (hypophysaire et/ou prostatiques) et/ou réduire l'expression des réceptuers de la PRL. Il s'agit de deux voies possibles qui conduiraient à une abolition de l'effet trophique de la PRL sur la prostate.

De plus, des études sur des animaux portant des pompes osmotiques (Alzet, USA) libérant de la PRL est en cours de réalisation. Cette étude est complémentaire de celles réalisées precedemment avec le sulpiride. Nous pourrons, grâce à cette étude, visualiser les effets l'application exogène de PRL. L'utilisation des pompes osmotiques permet de libérer de manière constante et continue de la PRL en quantité voulue et est, à notre

sens, la meilleure solution pour induire une hyperprolactinémie. En effet, la demi-vie de la PRL chez le rat étant de 7 minutes, il ne nous est pas possible de l'injecter classiquement au moyen d'une seringue. Une autre méthode pourrait être employée pour apporter de la PRL exogène chez le rat. Cette dernière consiste en l'emploi de pompes péristaltiques. Néanmoins cette technique s'avère excessivement stressante pour l'animale et très lourde à réaliser.

CONCLUSION DE L'ETUDE *IN VITRO*

Le second volet de nos travaux a été réalisé sur une lignée tumorale prostatique humaine (LNCaP), ainsi que sur des cellules normales issues du lobe latéral de prostate de rat. L'effet trophique de la PRL peut s'expliquer de plusieurs manières : par une augmentation de la prolifération cellulaire et/ou par une diminution de l'apoptose.

Au sein des cellules normales de prostate de rat, nous avons caractérisé des canaux potassiques de type Kv1.3 impliqués dans la régulation du potentiel membranaire (Ouadid *et al.*, 1999). Ces canaux sont activés par la PRL suggérant que la stimulation de ces canaux, par la PRL, pourrait constituer l'un des mécanismes intervenant dans la prolifération cellulaire.

Nous avons également étudié les canaux potassiques des cellules cancéreuses humaines LNCaP (Skryma *et al.*, 1997). Ces canaux sont d'une part, impliqués dans la prolifération cellulaire, et d'autre part, sont inhibés par la hausse de la concentration intracellulaire en calcium (Skryma *et al.*, 1999). Les canaux potassiques des cellules LNCaP appartiennent à un nouveau type de canaux ioniques. Par ailleurs, nous avons mis en évidence la forme longue du récepteur de la PRL sur ces cellules. Nous avons

également démontré que la PRL stimule l'activité de ces canaux potassiques. Nous pensons, qu'à l'instar des cellules normales de prostate de rat, ces canaux sont impliqués dans les événements précoces de la cascade de transduction du signal prolactinique menant à la prolifération cellulaire.

L'apoptose est, avec la prolifération cellulaire, un processus important dans le contrôle de l'homéostasie cellulaire. Aussi, nous nous sommes penchés sur les mécanismes de régulation de l'apoptose dans les cellules de la prostate. Les cancers de la prostate se développent lentement. Cette évolution serait la conséquence d'un déséquilibre de l'homéostasie cellulaire de l'organe en faveur d'un déficit en apoptose (Bruyninx *et al.*, 1998). Le calcium est l'un des facteurs majeurs de régulation de la mort cellulaire programmée (Mc Conkey et Orrenius, 1996). Nous nous sommes donc appliqués à caractériser les mécanismes de régulation de l'homéostasie calcique, ainsi que leur implication dans le déclenchement des processus apoptotiques. Enfin, nous avons analysé l'impact de la PRL sur la régulation du calcium dans les cellules de la prostate.

Nous avons tout d'abord démontré que l'apoptose des cellules LNCaP se produit après la vidange des stocks calciques intracellulaires. Une augmentation soutenue du calcium cytosolique n'est pas nécessaire à la survenue de l'apoptose dans les cellules LNCaP, à l'inverse, de ce qui a été démontré dans des cellules prostatiques hormono-indépendantes (Kyprianou *et al.*, 1994). La sensibilité des cellules prostatiques aux variations calciques pourrait être l'une des causes du mécanisme d'échappement, les rendant résistantes au retrait des androgènes.

Nous avons également identifié deux types de récepteurs à la ryanodine fonctionnels dans les cellules LNCaP : Ryr 1 et Ryr 2. Ces récepteurs, présents sur la membrane des stocks calciques, participent à la régulation de la concentration intracellulaire en calcium. En effet, leur activation provoque l'entrée capacitative et donc une hausse de la concentration en calcium dans le cytoplasme. Ce flux calcique est utilisé par la cellule pour remplir les stocks et a pour conséquence de prévenir les processus apoptotiques.

Enfin, nous avons étudié l'état des stocks calciques de manière quantitative en utilisant la thapsigargine (un inhibiteur des pompes calciques présentes sur la membrane du réticulum endoplasmique). Il s'avère que la PRL ne modifie pas la concentration de calcium libre dans les cellules LNCaP. En revanche, la PRL augmente l'état de remplissage des stocks en calcium et pourrait ainsi inhiber l'apoptose.

PERSPECTIVES APPORTEES PAR L'ETUDE *IN VITRO*

Les cellules normales et les cellules cancéreuses de la prostate expriment des formes différentes de canaux potassiques. Ce changement pourrait être l'une des causes précoces du changement de la physiologie des cellules de la prostate. Nous prévoyons d'étudier les canaux potassiques des cellules de prostates humaines (issues de biopsies) et de rat hypertrophiées et cancéreuses (modèle de cancer de la prostate de rat en cours d'élaboration). Il sera alors possible d'étudier les variations de types de canaux

calciques entre des cellules normales et cancéreuses chez le rat. Une étude parallèle nous permettra également de comparer les types de canaux potassiques exprimés sur des cellules hyperplasiques et sur des cellules cancéreuses de prostates humaines issues de plusieurs donneurs. Nous pourrons ainsi vérifier si le développement de l'hyperplasie bénigne et du cancer de la prostate s'accompagne par une modifications des canaux potassiques.

Nous poursuivrons nos recherches dans cette optique grâce à l'emploi de cellules LNCaP rendues androgeno-indépendantes après transfection stable du gène codant pour Bcl-2 (Raffo *et al.*, 1995). Cette lignée surexprime l'oncoprotéine Bcl-2. Cela a pour conséquence que le réticulum endoplasmique de ces cellules est davantage rempli en calcium que les cellules LNCaP non transfectées. Or l'état de remplissage des stocks caliciques est un élément clé dans le déclenchement de l'apoptose. Nous réaliserons des expériences similaires à celles effectuées sur les cellules LNCaP contrôles, à savoir des incubations en présence de thapsigargine et de nickel. Nous mesurerons le taux de calcium intracellulaire ainsi que le pourcentage de cellules apoptotiques dans de telles conditions. Par comparaison avec les résultats que nous avons déjà obtenus sur les cellules non transfectées, nous pourrons en déduire l'effet de la surexpression de Bcl-2 et donc celui de l'état de remplissage des stocks calciques dans les processus apoptotiques.

Nous ne connaissons pas encore par quels mécanismes la PRL module les réserves calciques. Sur la prostate de rat, la PRL induit la surexpression de Bcl-2. Cette protéine participe au maintien de l'homéostasie calcique. Nous prévoyons de quantifier la protéine Bcl-2 sur des cellules traitées à la PRL. En effet, il est possible que la PRL puisse moduler l'expresion de Bcl-2 positivement. Ce processus pourrait expliquer, peu

ou prou, les variations des concentrations calciques du réticulum endoplasmique. Par ailleurs, nous étudierons les effets de la PRL sur la lignée de cellules LNCaP surexprimant Bcl-2. Nous pourrons ainsi vérifier si la PRL possède la capacité d'augmenter l'état de remplissage des stocks calciques dans ces cellules. Si la PRL ne modifie pas le contenu des stocks calciques de ces cellules, cela signifie que son action se réalise par la voie de Bcl-2.

Durant ces trois années, nous avons étudié les effets de la PRL sous deux angles, à la fois *in vivo* et *in vitro*. Il est indéniable que la PRL agit sur la physiologie et la physiopathologie de la prostate. Nous espérons que grâce à nos recherches, la PRL puisse être prise en compte dans le traitement hormonothérapeutique des hyperplasies bénignes et des cancers de la prostate.

PUBLICATIONS :

1- Skryma R., Van Coppenolle F., Dufy-Barbe L., Dufy B., Prevarskaya N.
Characterisation of Ca2+-inhibited potassium channels excised patches of cells from human prostate cancer cell line LNCaP. 1999. Receptors and Channels. **6** : 241-253

2- Ouadid-Ahidouch H., Van Coppenolle F., Le Bourhis X., Belhaj A., Prevarskaya N. Potassium channels in rat prostate epithelial cells. 1999. Febs Letters. **459** : 15-21

3- Ouadid-Ahidouch H., Van Coppenolle F.
Seasonal influence of the functional expression of the endogenous L-type Ca^{2+} channels in Pleurodeles oocytes : role of cAMP ? 1998. Zygote **6** : 97-101

4- Van Coppenolle F., Skryma R., Ouadid H., Ahidouch A., Fournier S. et Prevarskaya N. Etude des mécanismes d'action de la prolactine dans le développement de la prostate. Bulletin de l'Association pour la Recherche sur les tumeurs de la prostate. 1997. **22** : 48-49

5- Van Coppenolle F., Guilbault P., Ouadid H.
Regulation of endogenous calcium channels by cyclic AMP and cyclic GMP-dependent protein kinases in *Pleurodeles* oocytes. Molecular and Cellular Biochemistry. 1997. **168**: 155-161

6- Van Coppenolle F., Le Bourhis X., Carpentier F., Delaby G., Cousse H., Raynaud J-P., Dupouy Jean-Paul, Prevarskaya N.
Pharmacological effect of the lipido-stérolic extract of *Serenoa repens* (Permixon®) on rat prostate hyperplasia. Comparison with Finasteride. Sous presse dans The Prostate.

7- Mariot P., Prevarskaya N., Roudbaraki M., Le Bourhis X., Van Coppenolle F., Vanoverberghe K., Skryma R.
Evidence of functional ryanodine receptor involved in apoptosis of prostate cancer (LNCaP) cells. Sous Presse dans The Prostate.

8- Van Coppenolle F., Slomianny C., Carpentier F., Le Bourhis X., Ahidouch A., Croix D., Legrand G., Fournier S., Cousse H., Authié D., Raynaud J-P., Beauvillain J-C., Dupouy J-P., Prevarskaya N.
Effect of the hyperprolactinemia on the rat prostate growth. Evidence of androgeno-dependence. Soumis à Endocrinology.

9- Skryma R., Mariot P., Van Coppenolle F., Shuba Y., Legrand G., Humez S., Le Bourhis X., Boilly B., Prevarskaya N.
Store-depletion and store-operated Ca2+ current in human prostate cancer cells LNCaP : Involvement in apoptosis. Soumis à Cancer Research.

10- Van Coppenolle F., Skryma R., Ouadid-Ahidouch H., Humez S., Gourdou I., Djiane J., Prevarskaya N.
Prolactin stimulates K+ channels through a long form of prolactin receptor in human prostate cancer cells. Soumis à B.B.R.C.

11- Legrand G., Humez S., Bastide B., Mariot P., Van Coppenolle F., Mounier Y., Skryma R., Prevarskaya N.
Influence of Ca2+ induced Ca2+ release mediated by ryanodine receptors on Ca2+ elevation induced by thapsigargin in LNCaP cells. Soumis à Febs Letters.

BIBLIOGRAPHIE

1. Abastado J.P. (1996). Apoptosis : function and regulation of cell death. Res. Immunol. **147** : 443-456
2. Ali S., Pellegrini I., Kelly P.A. (1991). J. Biol. Chem. **266(20)** : 110-20,117
3. Aronson W.J., de Kernion J.B. (1996). Prostate. Encyclopedia of gerontology. **2** : 355-364
4. Aubert M.L. (1982). Hormone de croissance et prolactine. In : Bertrand J., Rappaport R., Sizonenko P.C., eds. Endocrinologie Pédiatrique. Paris : Doin, Lausanne : Payot. **2** : 50-59
5. Bayne C.W., Grant E.S., Chapman K., Habib F.K. (1997). Characterization of a new co-culture model for BPH which expresses 5α-reductase type 1 and 2 : the effects of Permixon® on DHT formation (abstract). J. Urol. **157(4)** : 194
6. Bennett D.L., Cheek T.R., Berridge M.J., De Smedt H., Parys J.B., Missiaen L., Bootman M.D. (1996). Expression and function of ryanodine receptors in non esxcitable cells. J. Biol. Chem. **271** : 6356-6362
7. Berridge M.J. (1992). Spatiotemporal aspects of calcium signalling. Jpn. J. Pharmacol. **58(suppl.2)** : 142P-149P
8. Berridge M.J. (1997). Elementary and global aspects of calcium signalling. J. Physiol. **499(2)** : 291-306
9. Boockfor F.R., Hoeffler J.P., Frawley L.S. (1986). Estradiol induces a shift in cultured cells that release prolactin or growth hormone. Am. J. Physiol. **250** : E103-105
10. Borson-Chazot F. (1988). Sécrétion de prolactine et régulation. Ed Sandoz. Cycléos. **1** : 2-8

11.Boucherle A., Cousse H. (1981). Pharmaco - Chimie des anisamides. Les entretiens du Carla. 55-67

12.Boutin J.M., Jolicoeur C., Okamura H., Gagnon J., Edery M., Djiane J., *et al.* (1988). Cell. **53** : 69-77

13.Brue T., Pellegrini I., Gunz G., Jaquet Ph. (1989). Les formes moléculaires de la prolactine humaine. Re. Fr. Endocrinol. Clin. **30** : 73-79

14.Bruyninx M., Cornet A., Hennuy B., Reiter E., Klug M., Closset J., Hennen G. (1998) Médecine/Science **14** : 572-9

15.Carlson H.E., Wasser H.L., Levin S.R., Wilkins J.N. (1983). Prolactin stimulation by meals is related to protein content. J. Clean . Endocrinol. Metab. **57** : 334-338

16.Chandy K.G., DeCoursey T.E., Cahalan M.D., McLaughlin C., Gupta S. (1984). Voltage-gated potassium channels are required for human T lymphocyte activation. J. Exp. Med. **160(2)** : 369-385

17.Chandy K.G., Gutman G.A. (1993). Nomenclature for mammalian potassium channel genes. Trends Pharmacol Sci. **14(12)** : 434

18.Clarke L.J., Cummins J.T., Karsch F.T., *et al.* (1987). GnRH-associated peptide (GAP) is cosecreted with GnRH into the hypophysial portal blood of ovariectomized sheep. Biochem. Biophys. Res. Commun. **143** : 665-669

19.Cone C.D., Cone C. (1976). Induction of mitosis in mature neurons in central nervous system by sustained depolarization. Science. **192** : 155158

20.Connor J., Sawczuk I.S., Benson M.C., Tomashefsky P., O'Toole K.M., Olsson C.A., Buttyan R. (1988). Calcium channel antagonists delay regression of androgen-dependent tissues and suppress gene activity associated with cell death. The Prostate. **13(2)** : 119-130

21.Conti A., Togni E., Travaglini P, *et al.* (1987). Vasoactive intestinal polypeptide and dopamine : effect on prolactin secretion in normal women and in patients with microprolactinomas. Neuroendrocrinology. **46** : 241-245

22.Cunha C.R., Donjacour A.A., Cooke P.S., Mee S., Bigsby R.M., Higgins S.J., Sugimura Y. (1987). The endocrinology and developmental biology of the prostate. Endocr. Rev. **8** : 338-361

23.Das R., Vonderhaar B.K. (1995). Transduction of prolactin's (PRL) growth signal through both long and short forms of the PRL receptor. Mol Endocrinol. **9(12)** : 1750-1759

24.Davidson J.M., Chen J.J., Crapo L., Gray G.D., Greenleaf W.J., Catania J.A. (1983). Hormonal changes and sexual function in aging men. J. Clin. Endocrinol. Metab. **57**: 71-77

25.Debeljuk L., Rozados R., Daskal H., Velez V., Mancini AM. (1975). Acute and chronic effects of sulpiride on serum prolactin and gonadotropin levels in castrated male rats (38581). Proc. Soc. Biol. Med. **148 (2)** : 550-552

26.Deutsch C. (1990). K+ channels and mitogenesis. Prog. Clin. Biol. Res. **57(1)** : 251-271

27.DeVos, A.M., Ultsch M., Kossiakoff A.A. (1992). Science. **255** : 306-312

28.Dowd R.D. (1995). Calcium Regulation of apoptosis. Advances in second messenger and phosphoprotein research. **30** : 255-279

29.Dowd D.R., MacDonald P.N., Komm B.S., Haussler M.R., Miesfeld R. (1991). Evidence for early induction of calmodulin gene expression in lymphocytes undergoing glucocorticoid-mediated apoptosis. J. Biol. Chem. **266** : 18423-18426

30.Dubois J.M. (1993). Role of potassium channels in mitogenesis. Prog. Biophys. Mol. Biol. **59(1)** : 1-21

31.Dubois J.M., Combettes L., Coraboeuf E., Faivre J-F. (1999). Les canaux ioniques cellulaires. Editions Polytechnica

32.Emanuelle N.V., Jurgens J.K., Halloran M.M., Tentler J.J., Lawerence A.M., Kelley M.R. (1992). The rat prolactin gene is expressed in brain tissue : detection of normal and alternatively spliced prolactin messenger RNA. Mol. Endocrinol. **6** : 35-42

33.English H.F., Kyprianou N., Isaacs J.T. (1989). Relationship between DNA fragmentation and apoptosis in the programmed cell death in the rat prostate following castration. The Prostate. **15** : 233-250

34.Farnsworth WE. (1988). Prolactin effect on the permeability of human benign hyperplastic prostate to testosterone. The Prostate. **12 (3)** : 221-229

35.Fekete A. (1989). Receptors for luteinizing hormone realising hormone, somatostatine, prolactine and epidermal growth factor in rat0and human prostate cancers and in benign prostate hyperplasia. Prostate, **14**: 191-208

36.Friesen H., Guyda H., Hardy J. (1970). The biosynthesis of human growth hormone and prolactin. J Clin Endocrinol Metab. **31(6)** : 611-624

37.Furuya Y., Isaacs J.T. (1993). Differential gene regulation during programmed cell death (apoptosis) versus proliferation of prostatic glandular cells induced by androgen manipulation. Endocrinology. **133** : 2660-2666

38.Furuya Y., Lundmo P., Short A.D., Gill D.L., Isaacs J.T. (1994). The role of calcium, pH, and cell proliferation in the programmed (apoptotic) death of androgen-independent prostatic cancer cells induced by thapsigargin. Cancer Res. **54** : 6167-6175

39.Garnick M. (1995). Le cancer de la prostate. Pour la Sciencce. **10** : 64-70

40.Gavrieli Y., Sherman Y., Ben-Sasson S. (1992) Identification of programmed cell death in situ via specific labelling of nuclear DNA fragmentation. J. Cell. Biol. **119** : 493-501

41.Geller J. (1989). Pathogenesis and pathological treatment of benign prostatic hyperplasia. The Prostate suppl. **2**: 95-104

42.Gill D.L., Waldron R.T., Rys-Sikora K.E., Ufret-Vicenty C.A., Graber M.N. Favre C.J., Alfonso A. (1996). Calcium pools, calcium entry and cell growth. Bioscience reports. **16(2)** 139-157

43.Goupille O., Daniel N., Bignon C., Jolivet C., Djiane J. (1997). Mol. Cell. Endocrinol. **127** : 155-169

44.Grimes J.A., Fraser S.P., Stephens G.J., Downing J.E., Laniado M.E., Foster C.S., Abel P.D., Djamgoz M.B. (1995). Differential expression of voltage-activated Na+ currents in two prostatic tumour cell lines : contribution to invasiveness in vitro. Febs Letters. **369(2-3)** : 290-294

45.Grynkiewicz G., Poenie M., Tsien R.Y. (1985). A new generation of Ca^{2+} indicators with greatly improved fluorescence properties. J. Biol. Chem. **260(6)** : 3440-3450

46.Hamill O.P., Marty A., Neher E., Sakmann B., Sigworth F.J. (1981). Improved patch-clamp techniques for high-resolution current recording from cells and cell-free membrane patches. Pflugers Arch. **391(2)** : 85-100

47.Handwerger S, Richards R.G., Markoff E. (1990). The physiology of decidual prolactin and other decidual protein hormones. Trends Endocrinol. Metab. **3** : 91-95

48.Haverstick D.M., Gray L.S. (1993). Increased intracellular Ca^{2+} induces Ca^{2+} influx in human T lymphocytes. J. Biol. Cell. **4** : 173-184

49.He H., Lam M., McCormick T.S., Distelhorst C.W. (1997). Maintenance of calcium homeostasis in the endoplasmic reticulum by Bcl-2. J. Cell. Biol. **138(6)** 1219-1228

50.Horoszewicz J.S., Leong S.S. Kawinski E., Karr J., Rosenthal H., Chu M.T., Mirand E.A., Murphy G.P. (1983). LNCaP model of human prostate carcinoma. Cancer Res. **43** : 1908-18

51.Horton R. (1992). Benign prostatic hyperplasia/ New Insights. J. Clin. Endocrinol. Metab. **74**: 504A-504C

52.Hyde J.F., Ben-Jonathan N. (1989). The posterior pituitary contains a potent prolactin-releasing factor : in vivo studies. Endocrinology. **125** : 736-741

53.Imagawa T., Nakai J., Takeshima H., Nakasaki Y., Shigekawa M. (1987). Purified ryanodine receptor from muscle sarcoplasmic reticulum is the Ca^{2+}-permeable pore of the calcium release channel. J. Biol. Chem. **262** : 16636-16643

54.Isaacs J.T. (1990). Importance of the natural history of benign prostatic hyperplasia in the evaluation of pharmacologic intervention. The Prostate. **3** : 1-7

55.Isaacs J.T. (1993). Role of programmed death in carcinogenesis. Environ. Health Perspect. **101** : 27-33

56.Jacobi G.H., Sinterhauf K., Kurth K.H., Altwein J.E. (1978). Testosterone metabolism in patients with advanced carcinoma of the prostate: a comparative in vivo study of the effects of oestrogen and antiprolactin. Urol Res **6**:159-165

57.Jahn G.A., Deis R.P. (1986). Stress-induced prolactin release in female, male and androgenized rats : influence of progesterone treatment. Endocrinology. **110(3)** : 423-428

58.Janssen T., Darro F., Petein M., Raviv G., Pasteels J.L., Kiss R., Schulman C.C. (1996). In vitro characterization of prolactin-induced effects on proliferation in the

neoplastic LNCaP, DU145, and PC3 models of human prostate. Cancer **77(1)** : 144-149

59.Jeromin L. (1982). The serum levels of testosterone and prolactin in patients with prostatic carcinoma treated with various doses of fostrolin and bromocriptine. Int Urol Nephrol **14**:51-56

60.Juin P., Pelletier M., Oliver L., Tremblais K., Grégoire M., Meflah K., Valette F.M. (1998). Induction of caspase-3-like activity by calcium in normal cytosolic extracts triggers nuclear apoptosis in a cell-free system. J. Biol. Chem. **273(28)** : 17559-17564

61.Kaighn M.E., Narayan K.S., Ohnuki Y., Lechner J.F., Jones I.W. (1979). Establishment and characterization of a human prostatic carcinoma cell line (PC-3). Invest. Urol. **17** : 16-23

62.Kaiser N., Edelman I.S. (1977). Calcium dependence of glucocorticoid-induced lymphocytolysis. Proc. Natl. Acad. Sc. USA. **1974** : 638-642

63.Kaplan S.E., De Nicola A.F. (1976). Protein and RNA synthesis in pituitary tumors from F344 rats given implants of estrogens. J. Natl. Cancer Inst. **56** : 37-41

64.Kato Y., Iwasaki Y., Abe H ., Yanaihara N., Imura H. (1978). Prolactine release by vasoactive intestinal polypeptide in rats. Endocrinology. **103** : 554-560

65.Kelly P.A., Ali S., Rozakis M., Goujon L., Nogano M., Pellegrini I., Gould D., Djiane J., Edery M., Finidori J., Postel-Vinay M.C. (1993). Rec. Prog. Horm. Res. **48** : 123-159

66.Kerr J.R., Wyllie A.H., Currie A.R. (1972). Apoptosis : a basic biological phenomenon with wide ranging implications in tissue kinetics. Br. J. Cancer. **26** : 239-257

67.Kiino D.R., Dannies P.S. (1981). Insulin and 17 beta-estradiol increase the intracellular prolactin content of GH4C1 cells. Endocrinology **109** : 1264-1269

68.Kiselyov K., Xu X., Mozhayeva G., Kuo T., Pessah I., Mignery G., Zhu X., Birnbaumer L., Muallem S. (1998). Functional interaction between InsP3 receptors and store-operated Hrtp3 channels. Nature. **396** : 478-482

69.Kledzik G.S., Marshall S., Campbell G.A., Gelato M., Meites J. (1976). Effects of castration, testosterone, estradiol, and prolactin on specific prolactin-binding activity in ventral prostate of male rats. Endocrinology. **98(2)** : 373-379

70.Klee C.B., Vanaman T.C. (1982). Calmodulin. Adv. Protein. Chem. **35** : 213-321

71.Kozlowski J.M., Ellis W.J., Grayhack J.T. (1991). Advanced prostatic carcinoma. Early versus late endocrine therapy. Urol. Clin. North Am. **18** :15-24

72.Krumenacker J.S., Buckley D.J., Leff M.A., McCormack J.T., de Jong G., Goût P.W., Reed J.C., Miyashita T., Magnuson N.S., Buckley A.R. (1998). Prolactin-regulated apoptosis of Nb2 lymphoma cells : pim-1, bcl-2, and bax expression. Endocrine. **9(2)** : 163-170

73.Kuo C.B., Coss D., Walker A.M. (1998). Prolactin Receptor Antagonist. Endocrine. **9** : 121-131

74.Kyprianou N., Isaacs J.T. (1987). Biological significance of androgen levels in the rat ventral prostate following castration. The Prostate. **10(4)** : 313-324

75.Kyprianou N., Isaacs J.T. (1988). Identification of a cellular receptor for transforming growth factor-beta in rat ventral prostate in its negative regulation by androgens. Endocrinology. **123** : 2124-2131

76.Kyprianou N., English H.F., Isaacs J.T. (1988). Activation of a Ca^{2+}-Mg^{2+}-dependent endonuclease as an early event in castration-induced prostatic cell death. The Prostate. **13(2)** : 103-118

77.Kyprianou N., Bains A.K., Jacobs S.C. (1994). Induction of apoptosis in androgen-indépendant human prostate cancer cells undergoing thymineless death. The Prostate. **25(2)** : 66-75

78.Lai F., Anderson K., Rousseau E., Liu Q., Meissner G. (1988). Purification and reconstitution of the calcium release channel from skeletal muscle. Nature. **311** : 315-319

79.Lalani E.N., Laniado M.E., Abel P.D. (1997). Molecular and cellular biology of prostate cancer. Cancer and Metastasis Reviews. **16** : 29-66

80.Lam M., Dubyak G., Distelhorst C.W. (1993). Effect of glucocorticosteroid treatment on intracellular calcium homeostatsis in mouse lymphoma cells. Mol. Endocrinol. **7** : 686-693

81.Lam M., Dubyak G., Chen L., Nunez G., Miesfeld R.D., Distelhorst C.W. (1994). Evidence that Bcl-2 represses apoptosis by regulating endoplasmic reticulum-associated Ca^{2+} fluxes. Proc. Natl. Acad. Sci. USA. **91** : 6569-6573

82.Lane K.E., Leav I., Ziar J., Bridges R.S., Rand W.M., Ho S.M. (1997). Suppression of testosterone and estradiol-17-β-induced dysplasia in the dorsolateral prostate of noble rats by bromocriptine. Carcinogenesis. **18(8)** : 1505-1510

83.Laniado M.E., Lalani E.N., Fraser S.P., Grimes J.A., Bhangal G., Djamgoz M.B., Abel P.D. (1997). Expression and functional analysis of voltage-activated Na+ channels in human prostate cancer cell lines and their contibution to invasion in vitro. Am. J. Phathol. **150(4)** : 1213-1221

84.Lebrun J.J., Ali S., Ulrich A., Kelly P.A. (1995). J. Biol. Chem. **270** : 10,664-10,670

85.Lee C., Hopkins D. Holland J. (1985). Reduction in prostatic concentration of endogenous dihydrotestosterone in rats by hyperprolactinemia. Prostate. **6** : 361-367

86.Lee Y.S., Sayeed M.M., Wurster R.D. (1994). In vitro activity of cromakalin in human brain tumor cells. Pharmacology. **49(2)** : 69-74

87.Leeb T., Brenig B. (1998). cDNA cloning and sequencing of the human ryanodine receptor type 3 (RYR3) reveals a novel alternative splice site in the RYR3 gene. FEBS Lett. **423(3)** 367-370

88.Lin C.S., Boltz R.C., Blake J.T., N'Guyen M., Talento A., Fisher P.A., Springer M.S., Sigal N.H., Slaughter R.S., Garcia M.L. (1993). Voltage-gated potassium channels regulate calcium-dependent pathways involved in human T lymphocyte activation. J. Exp. Med. **177(3)** : 637-645

89.Liu Y.J., Masson D.Y., Johnson G.D., et al. (1991). Germinal center cells express bcl-2 after activation by signals wich prevent their entry into apoptosis. Eur. j. Immunol. **21** : 1905-1910

90.Lobaccaro J.M., Boudon C., Lumbroso S., Lechevallier E., Mottet N., Rebillard X., Sultan C. (1997). 5α-reductase et prostate. Annales d'Endocrinologie (Paris). **58** : 381-392

91.MacConkey D.J., Nicotera P., Hartzell P., Bellomo G., Wylie A.H., Orrenius S. (1989). Glucocorticoids activate a suicide process in thymocytes through an elevation of cytosolic Ca^{2+} concentration. Arch. Biochem. Biophys. **269** : 365-370

92.Marks A.R. (1997). Intracellular calcium-release channels : regulators of cell life and death. Am. J. Physiol. **272** : 597-605

93.Marshall L.A., Martin M.C., Leong S., Jaffe R.B. (1988). Influence of preovulatory estradiol concentration on diurnal pulsatile prolactin secretion patterns. Am. J. Obstet. Gynecol. **159** : 1558-1563

94.Martikainen P., Isaacs J.T. (1990). An organ culture system for the study of programmed cell death in the rat ventral prostate. Endocrinology. **127** :1268-1277

95.Martikainen P., Kyprianou N., Tucker R.W., Isaacs J.T. (1991). Programmed death of nonproliferating and androgen independent prostatic cancer cells. Cancer Res. **51** : 4693-4700

96.Masler I.A., Riddick D.H. (1979). Prolactin production by human endometrium during the normal menstrual circle. Am. J. Obstet. Gynecol. **135** : 751-754

97.Matos-Ferreira A., Corte-Real J., Palma J., Durao V. (1987). The effect of bromocriptine in benign prostatic hypertrophy and vesicosphincteric dynamics. **60**:143-149

98.Maurer R.A. (1982). Estradiol regulates the transcription of the prolactin gene. J. Biol. Chem. **257** : 2133-2136

99.Maurer R.A., Gorski J. (1977). Effects of estradiol-17 beta and pimozide on prolactin synthesis in male and female rats. Endocrinology. **101** : 76-84

100.McConkey D.J., Orrenius S. (1996). Signal transduction pathways in apoptosis. Stem Cells. **14(6)** : 619-631

101.McNeal J.E. (1981). Normal and pathologic anatomy of prostate. Urology. **17** : 11-16

102.Means A.R. (1988). Molecular mechanisms of action of calmodulin. Recent Prog. Hormone Res. **44** : 223-259

103.Montgomery D.W., Shen G.K., Ulrich E.D., Steiner L.L., Parrish P.R., Zukoski C.F. (1992). Human thymocytes express a prolactin-like messenger ribonucleic acid and synthesize bioactive prolactin-like proteins. Endocrinology. **131** : 3019-3026

104.Montpetit M.L., Lawless K.R., Tenniswood M. (1986). Androgen-repressed messages in the rat ventral prostate. The Prostate. **8** : 25-36

105.Moore E.D.W., Becker P.L., Fogarty K.E., Williams D.A., Fay F.S. (1990). Ca^{2+} imanging in single living cells : theoretical and practical issues. Cell Calcium. **11** : 157-179

106.Munaron L., Antoniotti S., Distasi C., Lovisolo D. (1997). Arachidonic acid mediates calcium influx induced by basic fibroblast growth factor in Balb-c 3T3 fibroblasts. Cell Calcium. **22(3)** : 179-188

107.Nakagawa K., Obara T., Matsubara M., Kubo M. (1982). Relationship of changes in serum concentrations of prolactin and testosterone during dopaminergic modulation in males. Clin. Endocrinol. **17(4)** : 345-352

108.Neher E., Sakmann B. (1976). Single-channel currents recorded from membrane of denervated frog muscle fibres. Nature. **260(5554)** : 799-802

109.Neill J.D., Reichert L.E. (1971). Control of the proestrus surge of prolactin and luteinizing hormone secretion by estrogens in the rat. Endocrinology. **89** : 1448-53

110.Nevalainen MT, Valve EM, Ingleton PM, and Harkonen PL. (1996). Expression and hormone regulation of prolactine receptors in rat dorsal and lateral prostate. Endocrinology. **137(7)** : 3078-3088

111.Nevalainen M.T., Valve E.M., Ahonen T., Yagi A., Paranko J., Harkonen P.L. (1997). Androgen-dependent expression of prolactin in rat prostate epithelium in vivo and in organ culture. FASEB J. **11** : 1297-1307

112.Nevalainen M.T., Valve E.M., Ingleton P.M., Nurmi M., Martikainen P.M., Harkonen P.L. (1997). Prolactin and prolactin receptors are expressed and functioning in human prostate. J. Clin. Invest. **99** : 618-627

113.Nilius B., Wholrab W. (1992). Potassium channels and regulation of proliferation of human melanoma cells. J. Physiol. (Lond). **445** : 537-548

114.Ouadid-Ahidouch H., Van Coppenolle F., Le Bourhis X., Belhaj A., Prevarskaya N. (1999). Potassium channels in rat prostate epithelial cells. Febs Letters. **459(1)** : 15-21

115.O'Neal K.D., Yu-Lee L.Y. (1993). Lymphokine Cytokine Res. **12** : 309-312

116.Pappas C.A., Ullrich N., Sontheimer H. (1994). Reduction of glial proliferation by K+ channel blockers is mediated by changes in pHi. Neuroreport. **6(1)** : 193-196

117.Parker D.C. , Rossman L.G., Vanderlaan E.F. (1974). Relation of sleep-entrained human prolactin release to REMnonREM cycles. J. Clin. Endocrinol. Metab. **38** : 646-651

118.Paubert-Braquet M. (1996). Effect of *Serenoa repens* extract (Permixon) on estradiol/testosterone-induced experimental prostate enlargment in the rat. Pharmacol. Res. **34(3-4)** : 171-9

119.Pellegrini I., Lebrun J.J., Ali S., Kelly P.A. (1992). Expression of prolactin and its receptor in human lymphoid cells. Mol. Endocrinol. **6** : 1023-1031

120.Poenie M. (1990). Alteration of intracellular fura-2 fluorescence by viscosity : a simple correction. Cell Calcium. **11** : 85-91

121.Prevarskaya N., Skryma R., Vacher P., Daniel N., Djiane J., Dufy B. (1995). Role of tyrosine phosphorylation in potassium channel activation. J. Biol. Chem. **270**: 24292-24299

122.Price D. (1963). Comparative aspects of development and structure in the prostate. Natl. Cancer Inst. Monogr. **12** : 351-369

123.Price M., Lee S.C., Deutsch C. (1989). Charybdotoxin inhibits proliferation and interleukin 2 production in human peripheral blood lymphocytes. Proc. Natl. Acad. Sci USA. **86(24)** : 10171-5

124.Prins G.S. (1987). prolactin influence of cytosol and nuclear androgen receptors in the ventral, dorsal and lateral lobes of the rat prostate. Endocrinology. **120**: 1457-1464

125.Putney J.W. Jr. (1986). A model for receptor-regulated calcium entry. Cell Calcium. **7** : 1-12

126.Putney J.W. Jr. (1990). Capacitative calcium entry revisited. Cell Calcium. **11** : 611-624

127.Putney J.W. Jr., Bird G.S.J. (1993). The signal for capacitative calcium entry. Cell. **75** : 199-201

128.Quarmby V.E., Beckman W.C., Wilson E.M. (1987). Androgen regulation of c-myc messenger ribonucleic acid levels in rat ventral prostate. Mol. Endocrinol. **1** : 865-874

129.Rackoff J.S., Siler T.M., Sinha Y.N., Yen S.S.C. (1973). Prolactin and growth hormone release in response to sequential stimulation by arginine and synthetic TRH. J. Clin. Endocrinol. Metab. **37** : 641-644

130.Raffo A.J., Perlman H., Chen M.W., Day M.L., Streitman J.S., Buttyan R. (1995). Overexpression of bcl-2 protects prostate cancer from apoptosis in vitro and confers resistance to androgen depletion in vivo. Cancer Res. **55(19)** : 4438-45

131.Rana A., Habib F.K., Halliday P., Ross M., Wild R., Elton R.A., Chisholm G.D. (1995). A case for synchronous reduction of testicular androgen, adrenal androgen and prolactin for the treatment of advanced carcinoma of the prostate. Eur J Cancer **31**:871-875

132.Reddy E.K., Mebust W.K., Weigel J.W., Giri S., Mansfield C.M. (1984). Incidence of lymph node involvement in localized carcinoma of the prostate. J Natl Med Assoc. **76(5)** : 463-466

133.Reiter E., Lardinois S., Klug M., Sente B., Hennuy B., Bruyninx M., Closset J., Hennen G. (1995). Androgen-independent effects of prolactin on the differents lobes of the immature rat prostate. Mol. Cell. Endocrinol. **112** : 113-122

134.Robaire B., Ewing D., Irby C., Desjardins C. (1979). Interactions of testosterone and estradiol-17β on the reproductive tract of the male rat. Biol. Reprod. **21** : 455-463

135.Robinette C. (1988). Sex-hormone-induced inflammation and fibromuscular proliferation in the rat lateral prostate. The Prostate. **12** : 271-286

136.Rouzaire-Dubois B., Dubois J.M. (1991). A quantitative analysis of the role of K+ channels in mitogenesis of neuroblastoma cells. Cell Signal. **3(4)** : 333-339

137.Rouzaire-Dubois B., Dubois J.M. (1998). K^+ channel block-induced mammalian neuroblastoma cell swelling : a possible mechanism to influence proliferation. **510** : 93-102

138.Rui H., Lebrun J.J., Kirken R.A., Kelly P.A., Farrar W.L. (1994). Endocrinology. **135** : 1299-1306

139.Schacht M.J., Niederberger C.S., Garnett J.E. Sensibar J.A., Lee C., Grayhack J.T. (1992). A local direct effect of pituitary graft on growth of the lateral prostate in rats. The Prostate. **20** : 51-58

140.Schachter B.S., Durgerian S., Harlan R.E., Pfaff D.W., Shivers B.D. (1984). Proalctin mRNA exists in rat hypothalamus. Endocrinology. **114** : 1947-1949

141.Schally A.V., Reeding T.W., Arimura A., Dupont A., Linthicum G.L. (1977). Isolation of gamma-amino-butyric acid from pig hypothalami and demonstration of its prolactin release-inhibiting (PIF) activity in vivo and in vitro. Endocrinology. **100** : 681-691

142.Schramme C., Denef C. (1983). Stimulation of prolactin release by angiostin II in in superfused rat anterior pituitary cell aggregates. Neuroendocrinology. **36** : 483-485

143.Sentman C.L., Shetter J.R., Hockenberry D., Kanagawa O., Korsmeyer S.J. (1991). bcl-2 inhibits multiple forms of apoptosis but not negative selection in thymocytes. Cell. **67** : 879-888

144.Shabisgh A., Chang D.T., Heitjan D.F., Kiss A., Olsson C.A., Puchner P.J., Buttyan R. (1998). Rapid reduction in blood flow to rat prostate ventral gland after castration : preliminary evidence that androgens influence prostate size by regulating blood flow to the prostate gland and prostatic endothelial cell survival. The Prostate. **36(3)** : 201-206

145.Shabisgh A., Tanji N., D'Agati V., Burchardt M., Rubin M., Goluboff E.T., Heitjan D., Kiss A., Buttyan R. (1999). Early effects of castration on the vascular system of the rat ventral prostate gland. Endocrinology. **140(4)** : 1920-1926

146.Shirota M., Banville D., Ali S., Jolicoeur C., Boutin J.M., Edery M., Djiane J., Kelly P.A. (1990). Expression of two forms of prolactin receptor in rat ovary and liver. Mol. Endocrinol. **4** : 1136-1143

147.Schlichter L., Sidell N., Hagiwara S. (1986). Potassium channels mediate killing by human natural killer cells. Proc Natl Acad Sci USA. **83(2)** : 451-5

148.Shin S.H. (1979). Estradiol generates pulses of prolactin secreteion in castrated male rats. Neuroendocrinology. **29** : 270-275

149.Sinha Y.N. (1995). Structural variants of prolactin : occurence and physiological significance. Endocrine Reviews. **16(3)** : 354-369

150.Sitsapesan R., Williams A.J. (1997). Regulation of current flow trough ryanodine receptors by luminal Ca^{2+}. J. Membrane Biol. **159** : 179-185

[151] Skryma R., Prevarskaya N., Dufy-Barbe L., Dufy B. (1997). Novel potassium conductance in androgen-sensitive prostate cancer cell line, LNCaP : involvement in cell proliferation. The Prostate, **42** N4

[152] Skryma R, Van Coppenolle F, Dufy-Barbe L, Dufy B and Prevarskaya N (1999). Characterization of Ca^{2+}-inhibited potassium channels in the LNCaP human prostate cancer cell line. Receptors and Channels. **6** : 241-253

153. Smith C., Assimos D., Lee C., Grayhack J.T. (1985). Metabolic action of prolactin in regressing prostate : independent of androgen action. Prostate. **6** : 49-59

154. Sorin B., Goupille O., Vacher A.M., Paly J., Djiane J., Vacher P. (1998). Distinct cytoplasmic regions of prolactin receptor are required for prolactin-induced calcium entry. J. Biol. Chem. **273(43)** : 28461-28469

155. Spielberg H., June C.H., Blair O.C., Nystron-Rosander C., Cereb N., Deeg H.J. (1991). UV irradiation of lymphocytes triggers an increase in intracellular Ca^{2+} and prevents lectin-stimulated Ca^{2+} mobilization : evidence for UV-and nifedipine-sensitive Ca^{2+} channels. Exp. Hematol. **19** : 4742-4748

156. Stone K.R., Mickey D.D., Wunderlin H., Mickey G.H., Paulson D.F. (1978). Isolation of a human prostate carcinoma cell line (DU 145). Int J Cancer. **21(3)** : 274-281

157. Stricker P., Grueter F. (1928). Action du lobe antérieur de l'hypophyse sur la montée laiteuse. C.R. Soc. Biol. **99** : 1978-1980

158. Syms A.J., Harper M.E., Griffiths K. (1985). The effect of prolactin on human BPH epithelial cell proliferation. Prostate. **6(2)** : 145-153

159. Tasar C., Akdas A., Kirkali Z. (1986). The effect of ergobromocriptine on serum testosterone and prolactin levels in patients with carcinoma of the prostate. Int. Urol. Nephrol. **18(1)** : 71-74

160.Thomas J.A., Manandhar M. (1974). Effect of prolactin and/or testosterone on cyclic AMP in the rat prostate gland. Horm Metab Res. **6(6)** : 529-530

161.Tritsch D., Chesnoy-Marchais D., Feltz A. (1999). Physiologie du neurone. Editions Doin.

162.Vacher P. (1995). Gn-RH agonists in the treatment of prostatic carcinoma. Biomed. Pharmacother. **49** : 325-331

163.Valatx J.L., Paut-Pagano L., Fevre-Montagano M., Dumas Milne Edwards J.B., Jouvet M. (1992). Demonstration of prolactin messenger RNA after amplification in the brain in rats . CR Acad. Sci. [III] **315** : 295-301

164.Van Poppel H., Boeckx G., Westelink K.J., Vereeken R.L., Baert L. (1987). The efficacy of bromocriptine in benign prostatic hypertrophy. A double blind study. Br. J. Urol. **60** : 150-152

165.Vaur S., Bresson-Bepoldin L., Dufy B., Tuffet S., Dufy-Barbe L. (1998). Potassium channel inhibition in the GH3 pituitary cell line. J. Cell. Physiol. **177(3)** : 402-410

166.Vekemans M., Robyn C. (1975). Influence of age in serum prolactin levels in women and men. Br. Med. J. **4**: 738-739

167.Walsh P.C. (1984). Benign prostatic hyperplasia: etiological considerations. In Kimball et al. eds: New approaches to the study of benign prostatic hyperplasia. Alan R. Liss, Inc, New York 1-25

168.Wang Y.F., Jia H., Walker A.M., Cukierman S. (1992). K-current mediation of prolactin-induced proliferation of malignant (Nb2) lymphocytes. J. Cell Physiol. **152(1)** : 185-189

169.Wang H.F., Pathan N., Ethell I.M., Krajewski S., Yamaguchi Y., Shibasaki F., McKeon F., Bobo T., Franke T.F., reed J.C. (1999). Ca2+-induced apoptosis trough calcineurin dephosphorylation BAD. Science. **284** : 339-343

170.Wennbo H., Kindblom J., Isaksson O.G.P., Tornell J. (1997). Transgenic mice overexpressing the prolactin gene develop dramatic enlargement of the prostate gland. Endocrinology. **138** : 4410-4415

171.White E. (1996). Life, death, and the pursuit of apoptosis. genes & Dev. **10** : 1-15

172.Williams D.A., Fay F.S. (1990). Intracellular calibration of the fluorescent calcium indicator fura-2. Cell Calcium. **11** : 75-83

173.Wyllie A.H., Kerr J.F., Currie A.R. (1980). Cell death : the significance of apoptosis. Int Rev Cytol. **68** : 251-306

174.Wilson III D.M., Emanuelle N.V., Jurgens K.L., Kelley M.R. (1992). Prolactin message in brain and pituitary of adult male rats is identical : PCR cloning and suequencing of hypothalamic prolactin cDNA from intact and hypophysectomized adult male rats. Endocrynology. **131** : 2488-2490

175.Wonderlin W.F., Strobl J.S. (1996). Potassium channels, proliferation and G1 progression. J. Membrane Biol. **154** : 91-107

176.Xu B., Wilson B.A., Lu L. Induction of human myeloblastic ML-1 cell arrest by suppression of K+ channel activity. Am J Physiol. **271** : C2037-2044

177.Yazigi R.A., Quintero C.H., Salameh W.A. (1997). Prolactin disorders. Fertility and Sterility. **67(2)** : 215-225

178.Yatani R., Kusano I., Shiraishi T., Miura S., Takanari H., Liu P.I. (1987). Elevated prolactin level in prostates with latent carcinoma. Ann. Clin. Lab. Sci. **17(3)** : 178-182

179.Zhu N., Wang Z. (1999). calreticulum expression is associated with androgen regulation of the sensitivity to calcium ionophore-induced apoptosis in LNCaP prostate cancer cells. Cancer Res. **59(8)** : 1896-1902

180.Zhu N., Pewitt E.B., Cai X., Cohn E.B., Lang S., Chen R., Wang Z. (1998). Calreticulin : an intracellular Ca++-binding protein abundantly expressed and regulated by androgen in prostatic epithelial cells. Endocrinology. **139** : 4337-4344

RESUME

Les hyperplasies bénignes et les cancers de la prostate sont des maladies des plus fréquentes. La plupart des traitements hormonaux de ces pathologies se base sur la diminution des taux d'androgènes circulants, mais malgré des concentrations très basses les tumeurs persistent. Cela signifie que d'autres facteurs interviennent dans la physiopathologie prostatique et notamment la prolactine, une hormone peptidique d'origine hypophysaire.

Le rôle de la prolactine dans la prostate a été abordé sous deux angles : *in vivo* et *in vitro*. Nous avons établi un modèle animal d'hyperplasie prostatique induite par l'hyperprolactinémie, chez le rat, au moyen d'antagonistes du tonus dopaminergique (sulpiride). Nous avons, d'une part, caractérisé l'effet trophique de la prolactine et d'autre part, réalisé des tests pharmacologiques de médicaments utilisés en clinique humaine (Permixon® et Finastéride). L'hyperplasie prostatique induite par la prolactine peut être la conséquence de deux mécanismes : la stimulation de la prolifération cellulaire ou la diminution de l'apoptose. Ces deux hypothèses ont été étudiées, *in vitro*, principalement grâce à l'emploi des techniques électrophysiologiques (patch-clamp), à la microspectrofluorimétrie et à l'imagerie calcique sur des cellules cancéreuses prostatiques humaines, ainsi que sur des cellules normales de prostate de rat. Nous avons démontré que dans ces deux modèles cellulaires, la prolactine stimule le fonctionnement des canaux potassiques dépendants du voltage en augmentant leur probabilité d'ouverture. L'activation de ces canaux, par la prolactine, constitue l'un des événements précoces menant à la prolifération. Nous avons également mis en évidence le rôle du calcium, et plus particulièrement celui des réserves calciques intracellulaires dans le contrôle de l'apoptose. La prolactine, en modulant le contenu de ces stocks, pourrait inhiber les processus apoptotiques et ainsi induire le développement des tumeurs prostatiques.

Mots clés : prolactine, prostate, prolifération, apoptose, conductance potassique, calcium intracellulaire.